UNCLASSIFIED

AD NUMBER

AD822949

NEW LIMITATION CHANGE

TO

Approved for public release, distribution unlimited

FROM

Distribution authorized to U.S. Gov't. agencies and their contractors; Administrative and Operational Use; Sep 1967. Other requests shall be referred to the Air Force Materials Laboratory, Attn: MATF-Manufacturing Technology Division, Wright-Patterson AFB, OH 45433.

AUTHORITY

USAFSC, per ltr dtd 26 May 1972

THIS PAGE IS UNCLASSIFIED

AFML-TR-67-305
Volume I

AD822949

DEVELOPMENT OF JOINING PROCESSES FOR TITANIUM FOILS

C. E. Smeltzer
R. K. Malik
A. N. Hammer
W. A. Compton
Solar Division of International Harvester Company

TECHNICAL REPORT AFML-TR-67-305

September 1967

This document is subject to special export controls and each transmittal to foreign governments or foreign nationals may be made only with prior approval of the Manufacturing Technology Division, MATF, Air Force Materials Laboratory, Wright-Patterson Air Force Base, Ohio 45433

Air Force Materials Laboratory
Research and Technology Division
Air Force Systems Command
Wright-Patterson Air Force Base, Ohio

DDC
RECEIVED
NOV 29 1967
B



NOTICE

When Government drawings, specifications, or other data are used for any purpose other than in connection with a definitely related Government procurement operation, the United States Government thereby incurs no responsibility nor any obligation whatsoever; and the fact that the Government may have formulated, furnished, or in any way supplied the said drawings, specifications, or other data, is not to be regarded by implication or otherwise as in any manner licensing the holder or any other person or corporation, or conveying any rights or permission to manufacture, use, or sell any patented invention that may in any way be related thereto.

Copies of this report should not be returned unless return is required by security considerations, contractual obligations, or notice on a specific document.

AFML-TR-67-305
Volume I

DEVELOPMENT OF JOINING PROCESSES FOR TITANIUM FOILS

C. E. Smeltzer
R. K. Malik
A. N. Hammer
W. A. Compton
Solar Division of International Harvester Company

TECHNICAL REPORT AFML-TR-67-305

September 1967

This document is subject to special export controls and each transmittal to foreign governments or foreign nationals may be made only with prior approval of the Manufacturing Technology Division, MATF, Air Force Materials Laboratory, Wright-Patterson Air Force Base, Ohio 45433

Air Force Materials Laboratory
Research and Technology Division
Air Force Systems Command
Wright-Patterson Air Force Base, Ohio

FOREWORD

This final technical report covers all work performed under Contract AF33(615)-3137 from 1 August 1965 to 31 May 1967. The manuscript was released by the authors on 10 August 1967 for publication as an FML Technical Report. For convenience, the report was published in two volumes. Volume I covers the seven Tasks of Phase I. Volume II covers the five Tasks of Phase II.

This contract with the Solar Division of International Harvester Company was initiated under Manufacturing Methods Project No. 8-315, "Development of Joining Processes for Titanium Foils". It was accomplished initially under the technical direction of Mr. T. L. Campbell of the Manufacturing Technology Division, Advanced Fabrication Techniques Branch (MATF), Wright-Patterson Air Force Base, Ohio. Technical direction was later transferred to Mr. Frederick R. Miller of the same branch.

The program was initially organized at Solar by Mr. W. A. Compton, Assistant Director of Research who acted as Project Director throughout the program. Mr. C. E. Smeltzer, Research Staff Engineer, acted as the Principal Investigator for the program and principal author of the final report.

This project has been accomplished as part of the Air Force Manufacturing Methods Program, the primary objective of which is to develop, on a timely basis, manufacturing processes, techniques and equipment for use in economical production of USAF materials and components.

This technical report has been reviewed and is approved.

JACK R. MARSH, Chief
Advanced Fabrication Techniques Branch
Manufacturing Technology Division
Air Force Materials Laboratory

ABSTRACT

An investigation was conducted of special joining processes and techniques for titanium alloy foils and thin-wall tubing in the thickness range of 2 to 10 mils. (Foil alloys were Ti-6Al-4V (ELI), Ti-5Al-2.5Sn (ELI), and Ti-8Al-1Mo-1V. Tube alloy was Ti-3Al-2.5V). Process development was concentrated upon new Ti-Zr braze systems, designed to circumvent problems of foil corrosion, erosion, and beta-embrittlement characteristics of preexisting braze alloys recommended for titanium. A limited number of diffusion bonding experiments also were carried out which indicated only marginal adaptability to thin-wall tube structures.

Phase I of the program was concerned principally with the development, evaluation, and selection of braze alloys most suitable for titanium foil joining. Over 100 ternary, quaternary, and quinary braze alloy modifications of the basic systems Ti-Zr-Be and Ti-Zr-Ni-Be were evaluated in T joint and lap-joint tests through the required service range of -320 to 1000 F. Emphasis was placed on assessing brazing performance, brazement structural analysis, joint strength, bend toughness, braze-line peel resistance, strain accommodation capability, stress rupture, and fatigue strengths of candidate alloy brazements. The influence on strength and stability of 100-hour simulated service exposure in salt-spray (200 F) as well as static exposure for 100 hours at the maximum service temperature (1000 F, both in air and in high vacuum) were determined. Hot-salt corrosion tests were programmed (1000 F). Post-braze heat treatments were developed to provide braze structures of improved toughness and reliability. Safe maximum process parameters (time and temperature) were established for each program foil alloy.

Upon completion of Phase I studies, the four best braze alloys of the group that successfully passed all test phases were selected for application in Phase II.

oy Designation	Nominal Composition (Wt %)	Minimum Flow Temperature (F)	Density (gm/cc)
RM8	Ti-43.0Zr-12.0Ni-2.0Be	1470	5.46
RM12	Ti-45.0Zr-8.0Ni-2.0Be	1660	5.33
CS217	Ti-(47.2-47.5)Zr-(5.0-5.6)Be	1620 to 1640	4.83
CS217C	Ti-45.1Zr-4.8Be-5.0Al	1700	4.67

The objective of Phase II of the program was to demonstrate the applicability of the braze joining processes developed in Phase I to high performance, titanium foil structures. Honeycomb panels, plate-and-fin heat exchanger modules, and the matrix of a tube-and-shell type heat exchanger were selected as test structures. Preliminary efforts were conducted using subscale modules of each foil structure to develop required component manufacturing, fixturing, and brazing techniques. Mechanical and pressure tests of subscale structures enabled final selection of the titanium braze alloy and technique for each structure type.

The full-scale heat exchanger modules, both plate-and-fin and tube-and-header types, were subjected to similar test programs which included cyclic pressurization, proof pressurization, steady-state flow, thermal shock, resonant frequency vibration, and pressure burst. Both types of structures were shown to have useful engineering properties over the temperature range -320 to 800 F.

The feasibility of brazing large scale titanium honeycomb panels with the developed alloys was established. Honeycomb panels were tested in tension, bending, compression, and shear, over the temperature range of -320 to 800 F, before and after 100 hours exposure to 800 F air, and thermal shock regimes between -320 and 800 F. Subscale specimens demonstrated room temperature strengths in tension over 130,000 psi (core stress) and in shear of 40,000 psi.

Advanced methods were developed for the production of high-purity braze alloy powders used in Phase II work. Special techniques included levitation melting of braze alloy ingots and subsequent crushing of the ingot to powder at cryogenic temperatures.

This abstract is subject to special export controls and each transmittal to foreign governments or foreign nationals may be made only with prior approval of the Manufacturing Technology Division, MATF, Air Force Materials Laboratory, Wright-Patterson Air Force Base, Ohio 45433.

CONTENTS

Section			Page
I	INTRODUCTION		1
II	PROGRAM SCOPE AND OBJECTIVES		3
III	PHASE I - DEVELOPMENT OF JOINING METHODS FOR TITANIUM ALLOY FOIL		9
	3.1	Task I - Selection of Materials	9
		3.1.1 Alloys for Corrugated Sandwich Structures	9
		3.1.2 Alloys for Honeycomb Sandwich Structures	11
		3.1.3 Alloys for Tube-and-Header Structures	13
		3.1.4 Procurement of Foil and Tubing Materials	13
		3.1.5 Baseline Tests of Program Foil and Tube Alloys	17
	3.2	Task II - Effect of Simulated Braze Cycle Exposure Upon Foil	27
	3.3	Task III - Selection of Candidate Bonding and Braze Alloy Systems	41
		3.3.1 Corrosion Resistance of Joints	41
		3.3.2 Joint Strength and Toughness	41
		3.3.3 Dimensional and Metallurgical Stability	42
		3.3.4 Weight and Process Considerations	43
		3.3.5 Analysis of Foil Brazing Problems	45
		3.3.6 Proposed Approach to Problem Solutions	47
		3.3.7 Selection of Braze Systems for Foil Joining Studies	52
	3.4	Task IV - Development and Optimization of Braze Alloy Systems	65
		3.4.1 Experimental and Test Procedures	65
		3.4.2 Test Equipment and Procedures (Tasks IV and V)	72
		3.4.3 Initial Braze Screening Tests	73
		3.4.4 Advanced Braze Optimization Studies	92
		3.4.5 Summary of Task IV - Braze Optimization Studies	104
	3.5	Task V - Evaluation of Braze Systems	135
		3.5.1 Thermal Stability Testing	136
		3.5.2 Reliability Tests	139
		3.5.3 Tensile Tests of Brazements	144

CONTENTS (Cont)

Section			Page
III	PHASE I - DEVELOPMENT OF JOINING METHODS FOR TITANIUM ALLOY FOIL (Cont)		
	3.5.4	Cyclic Annealing Studies	146
	3.5.5	Environmental Stability Tests	153
	3.5.6	Stress-Rupture Tests of Brazements	165
	3.5.7	Fatigue Tests of Brazements	165
	3.5.8	Summary of Task V, Braze Systems Evaluation	167
	3.5.9	Selection of Braze Alloys for Phase II	173
3.6	Task VI - Exploratory Efforts to Optimize Braze Materials and Testing Methods		225
	3.6.1	Effect of Melt Stock Purity (Ti, Zr, Be)	225
	3.6.2	Effects of Braze Hording Time and Cooling Rate	230
	3.6.3	Effect of Braze Process Over-Temperature	232
	3.6.4	Study of Microstructural Components	234
	3.6.5	Braze Particle Size Effects	238
	3.6.6	Homogenization of Braze Alloy Powders Through Heat Treatment of Button Ingots	240
	3.6.7	Preliminary Studies of Cyclic Annealing	242
	3.6.8	Effect of Salt Spray Environment Upon Braze Joint Strength	242
	3.6.9	Preliminary Assessment of Elevated Temperature Brazement Strength	245
	3.6.10	Strain Accommodation Ability of Braze Alloys	270
3.7	Task VII - Diffusion Bonding Development		281
	3.7.1	Diffusion Bonding Parameters	281
	3.7.2	Electrode Sticking Problem	286
	3.7.3	Generation of Baseline Data	288
	3.7.4	Selection of Joint Pressurization Technique	290
	3.7.5	Experimental Heating Methods	293
	3.7.6	Joint Design and Surface Cleanliness	295
	3.7.7	Bonding Tests and Results	295
	3.7.8	Summary	301

ILLUSTRATIONS

Figure		Page
1	Dimples and Wrinkles in As-Received Ti-5Al-2.5Sn Alloy Foil	22
2	Corrugations in As-Received Ti-8Al-1Mo-1V Alloy Foil	23
3	Foil Tensile Test Specimens	24
4	Central-Sheared Notch Tensile Specimen	24
5	Ultimate Tensile Strength of Titanium Alloy Foils	25
6	Hypothetical Safe Limits of Bond Process Time Versus Temperature	33
7	Effects of Simulated Braze Cycles on Strength Properties of 0.006-Inch Ti-5Al-2.5Sn Foil	34
8	Effects of Simulated Braze Cycles on Strength Properties of 0.010-Inch Ti-6Al-4V Foil	35
9	Tube Specimen and End Fittings for Tensile Testing	36
10	Room Temperature Mechanical Properties of Titanium Alloy Foils	37
11	Room Temperature Notch Strength Ratios of Titanium Alloy Foils	38
12	Ultimate and Notched to Plain Ultimate Strength Ratios of Titanium Foils	39
13	Ultimate Strengths of Ti-3Al-2.5V Tubing	40
14	Typical Ti-6Al-4V Foil T-Joint Brazements Made With Silver-Base Braze Alloy	55
15	Typical Honeycomb Core-To-Face Sheet Joints	56
16	Typical Corrugated Fin-To-Plate Sheet Joints	56
17	T-Joint Specimen Used for Braze Evaluation	56
18	Double-Lap Joint Specimen Used for Braze Evaluation	57
19	Typical Eutectic Structure in an Arc-Melted Ingot of Ti-47.2Zr-5.6Be Alloy	58
20	Brazed T-Joints of Ti-6Al-4V Foils After a 96-Hour Salt Spray Exposure	59
21	Progressive Dissolution and Erosion of Ti-5Al-2.5Sn Foil T-Joints With Increasing Braze Time	61
22	Typical Ti-6Al-4V Foil T-Joint Brazed With Zr-6.0Be Eutectic Alloy	62

ILLUSTRATIONS (Cont)

Figure		Page
23	Typical Ti-6Al-4V Foil T-Joint Brazed With Ti-47.2Zr-5.6Be Eutectic Alloy	62
24	Effect of Increasing Braze Time on Ti-5Al-2.5Sn Foil T-Joints	63
25	Typical T-Joint Specimen for Metallography and Bend Tests	107
26	Typical T-Joint Specimen for Tensile Tests	107
27	Typical Lap-Joint Specimen for Shear Tests	107
28	Typical Double Lap-Joint Specimen for Peel Tests	108
29	Typical Strain Accommodation Specimen	108
30	Braze Alloy Charge-Loaded in Melting Facility	109
31	Arc-Melting Facility in Operation	109
32	Analytical Balance for Weight Determination of Braze Alloy Elements	110
33	Titanium-Base Braze Alloy Melts	111
34	Titanium Foil T-Joint Specimens for Braze Alloy Screening Tests	111
35	T-Joint Specimen Before Braze	112
36	T-Joint Specimen After Braze	112
37	Laboratory Brazing Furnace	113
38	Schematic Diagram of the Laboratory Brazing Furnace	113
39	Elevated Temperature Tensile Test Equipment	114
40	Cryogenic Temperature Tensile Test Equipment	114
41	Typical Ti-5Al-2.5Sn Foil T-Joint Brazed in Vacuum With Ti-9.57Cu-5.6Be Alloy	115
42	Typical Ti-5Al-2.5Sn Foil T-Joint Brazed in Vacuum With Ti-8.6Mn-5.6Be Alloy	116
43	Typical Ti-5Al-2.5Sn Foil T-Joint Brazed in Vacuum With Ag-5Al-0.2Mn Alloy	116
44	Melting Temperature Versus Weight Percent Zirconium in Ti-x-7.2Zr-5.6Be Braze Alloy	116
45	Typical Ti-5Al-2.5Sn Foil T-Joints Brazed in Vacuum With Candidate Braze Alloys	117

ILLUSTRATIONS (Cont)

Figure		Page
46	Braze Screening Test With CS217 Braze Alloy	120
47	Braze Screening Test With CS217C Braze Alloy	121
48	Braze Screening Test With CS217G Braze Alloy	121
49	Braze Screening Test With CS217I Braze Alloy	122
50	Braze Screening Test With CS217E Braze Alloy	122
51	Braze Screening Test With CS217F Braze Alloy	122
52	Braze Screening Test With RM1 Braze Alloy	123
53	Braze Screening Test With RM8 Braze Alloy	123
54	Braze Screening Test With RM12 Braze Alloy	123
55	Braze Screening Test With RM28 Braze Alloy	124
56	Braze Screening Test With RM40 Braze Alloy	124
57	Braze Screening Test With RM26 Braze Alloy	124
58	Braze Screening Test With 0.075-MIL, Ni-10P Plated Specimen	125
59	Braze Screening Test With 0.15-MIL, Ni-10P Plated Specimen	126
60	T-Joint Bend Test, Brazed With RM44 Alloy	127
61	T-Joint Bend Test, Brazed With RM23 Alloy	127
62	T-Joint Bend Test, Brazed With RM26 Alloy	127
63	T-Joint Bend Test, Brazed With CS217E Alloy	128
64	T-Joint Bend Test, Brazed With CS217F Alloy	128
65	T-Joint Bend Test, Brazed With RM40 Alloy	128
66	T-Joint Bend Test, Brazed With RM40 Alloy; After 100-Hour Salt Spray Exposure	129
67	T-Joint Bend Test, Brazed With CS217I Alloy	129
68	T-Joint Bend Test, Brazed With CS217I Alloy; After 100-Hour Salt Spray Exposure	129
69	T-Joint Bend Test, Brazed With CS217 Alloy	130
70	T-Joint Bend Test, Brazed With CS217 Alloy; After 100-Hour Salt Spray Exposure	130

ILLUSTRATIONS (Cont)

Figure		Page
71	T-Joint Bend Test, Brazed With RM8 Alloy; After 100-Hour Salt Spray Exposure	130
72	T-Joint Bend Test, Brazed With CS217C Alloy; After 100-Hour Salt Spray Exposure	131
73	T-Joint Bend Test, Brazed With CS217G Alloy; After 100-Hour Salt Spray Exposure	131
74	Distribution of Brazed T-Joint Tensile Strength	132
75	Strain Accommodation Test, Brazed With RM8 Alloy	133
76	Strain Accommodation Test, Brazed With CS217 Alloy	133
77	Thermal Stability Tests on CS Series Braze Alloys; Lap-Shear Tests	175
78	Thermal Stability Tests on RM Series Braze Alloys; Lap-Shear Tests	176
79	T-Joints Brazed With CS217 Alloy	177
80	T-Joints Brazed With CS217F Alloy	177
81	T-Joints Brazed With CS217C Alloy	178
82	T-Joints Brazed With CS217C Alloy, Cyclic Annealed Condition	179
83	Spheroidized Eutectic Berylides in Cyclic Annealed, CS217C Alloy Brazement	180
84	Fine Lamellar Structure of Ti-$TiBe_2$ Eutectic, CS13-5 Alloy Brazement	181
85	Spheroidized Eutectic Berylides in Cyclic Annealed CS13-5 Alloy Brazement	183
86	Hardness Survey of Cyclic Annealed CS217C/Ti-5Al-2.5Sn Brazement	184
87	Base Metal/Diffusion Zone Interface of Cyclic Annealed CS217C/Ti-5Al-2.5Sn Brazement	185
88	Diffusion Zone/Braze Matrix Interface of Cyclic Annealed CS217C/Ti-5Al-2.5Sn Brazement	186
89	Hardness Survey of Cyclic Annealed CS217C/Ti-6Al-4V Brazement	187
90	Martensitic (Widmanstatten) Structure in Cyclic Annealed CS217C/Ti-6Al-4V Brazement	187

ILLUSTRATIONS (Cont)

Figure		Page
91	Lap-Shear Tests on Braze Alloys/Ti-5Al-2.5Sn, As-Brazed	188
92	Lap-Shear Tests on Braze Alloys/Ti-6Al-4V, As-Brazed	189
93	Lap-Shear Tests on Ag-5Al-0.2Mn Braze Alloy, Baseline	190
94	Ultimate Tensile Strength Versus Temperature of Ti-5Al-2.5Sn and Ti-6Al-4V Foils	191
95	Salt Spray Corrosion Tests on Cyclic Annealed CS Series Alloys/Ti-6Al-4V Foil Brazements	192
96	Salt Spray Corrosion Tests on Cyclic Annealed CS Series Alloys/Ti-5Al-2.5Sn Foil Brazements	193
97	Strength of Cyclic Annealed CS Series Alloys/Ti-8Al-1Mo-1V Brazements	194
98	Strength of RM Series/Ti-8Al-1Mo-1V Brazements	195
99	Cyclic Annealed CS217F/Ti-8Al-1Mo-1V Brazement	196
100	Salt Spray Corrosion Test Results, Candidate Alloys/Ti-5Al-2.5Sn Brazements	197
101	Salt Spray Corrosion Test Results, Candidate Alloys/Ti-6Al-4V Brazements	198
102	Diffusion Bonding of Titanium Alloy Foils	199
103	Thermal Stability Test Results, Candidate Alloys/Ti-5Al-2.5Sn Brazements	200
104	Thermal Stability Test Results, Cyclic Annealed Candidate Alloys/Ti-5Al-2.5Sn Brazements	201
105	Thermal Stability Test Results, Candidate Alloys/Ti-6Al-4V Brazements	202
106	Brazements of CS217 Oxidized at 1000 F for 100 Hours in Air	203
107	Brazements of CS217C Oxidized at 1000 F for 100 Hours in Air	204
108	Brazements of CS217F Oxidized at 1000 F for 100 Hours in Air	205
109	Brazements of CS217G Oxidized at 1000 F for 100 Hours in Air	206
110	Brazements of RM8 Oxidized at 1000 F for 100 Hours in Air	207
111	Cyclic Annealed Brazements of CS217 Oxidized at 1000 F for 100 Hours in Air	208

ILLUSTRATIONS (Cont)

Figure		Page
112	Cyclic Annealed Brazements of CS217C Oxidized at 1000 F for 100 Hours in Air	209
113	Cyclic Annealed Brazements of CS217F Oxidized at 1000 F for 100 Hours in Air	210
114	Hot-Salt Stress Rupture Test Specimens	210
115	Hot-Gas Stress Rupture Test Rig	211
116	Hot-Salt Corrosion Test Rig	212
117	Hot-Salt Stress Rupture Test in Progress	213
118	Self-Diffusion Bonded Ti-5Al-2.5Sn Specimens After Hot-Salt Corrosion Testing at 1000 F	214
119	CS Series/Ti-5Al-2.5Sn Brazements After Hot-Salt Corrosion Testing at 1000 F	215
120	RM Series/Ti-5Al-2.5Sn Brazements After Hot-Salt Corrosion Testing at 1000 F	216
121	Cyclic Annealed CS217/Ti-5Al-2.5Sn Brazement After Stress Rupture Test at 1000 F	217
122	Cyclic Annsaled CS217C/Ti-5Al-2.5Sn Brazement After Stress Rupture Test at 1000 F	21
123	Cyclic Annealed RM8/Ti-5Al-2.5Sn Brazement After Stress Rupture Test at 1000 F	218
124	MTS Fatigue Testing Machine	218
125	Specimen Holding Fixture (Hole-and-Pin) in MTS Fatigue Testing Machine	219
126	Room Temperature Fatigue Curve, Self-Diffusion Bonded Ti-5Al-2.5Sn Specimens	220
127	Room Temperature Fatigue Curve, CS Series/Ti-5Al-2.5Sn Brazements	221
128	Room Temperature Fatigue Curve, RM Series/Ti-5Al-2.5Sn Brazements	222
129	Fatigue Strength Versus Brazement Strength, Candidate Alloys and Self-Diffusion Bonded Ti-5Al-2.5Sn Specimens	223

ILLUSTRATIONS (Cont)

Figure		Page
130	Effect of Carbon, Oxygen, and Nitrogen on the Vickers Hardness of Titanium	249
131	Effect of Total Interstitial Content on the Vickers Hardness of Titanium	250
132	Free Energy of Formation of Phases at 1500 F	251
133	Typical Microstructures of Ti-5Al-2.5Sn T-Joints Brazed in Argon With Ti-5.6Be Braze Alloy	253
134	Typical Microstructures of Ti-5Al-2.5Sn T-Joints Brazed in Vacuum With Ti-5.6Be Braze Alloy	255
135	Typical Microstructures of Ti-5Al-2.5Sn T-Joints Brazed in Argon With Ti-47.2Zr-5.6Be Braze Alloy	257
136	Typical Microstructures of Ti-5Al-2.5Sn T-Joints Brazed in Vacuum With Ti-47.2Zr-5.6Be Braze Alloy	259
137	Typical Microstructures of Ti-5Al-2.5Sn T-Joints Brazed in Vacuum With Ti-5.6Be Alloy at 2000 F	261
138	Typical Microstructures of Ti-5Al-25Sn T-Joints Brazed in Vacuum With Ti-47.2Zr-5.6Be Alloy at 1700 F	263
139	CS13-5 Braze Joint; 1825 F for 60 Minutes	265
140	RM8 Braze Joint; 1825 F for 60 Minutes	266
141	RM1 Braze Joint; 1825 F for 60 Minutes	266
142	CS13-5 Braze Joint; 1700 F for 30 Minutes	266
143	RM8 Braze Joint; 1700 F for 30 Minutes	267
144	RM8 Braze Joint; 1600 F for 30 Minutes	267
145	RM8 Braze Joint; 1500 F for 30 Minutes	267
146	Typical Eutectic Structures in Argon Arc-Cast Ingots of Ti-5.6Be Alloy	268
147	Typical Eutectic Structures in Argon Arc-Cast Ingots of Ti-47.2Zr-5.6Be Alloy	269
148	Foil T-Joints Made With Various Particle Size of Heat 13-4; Vacuum Brazed, 1700 F - 5 Minutes	270
149	Foil Dissolution and Erosion Obtained With Particle Size -100/+200 Mesh Ti-47.2Zr-5.6Be Alloy	272

ILLUSTRATIONS (Cont)

Figure		Page
150	Relative Mesh Particle Sizes in a Cast Structure; Heat No. 13-5	273
151	Foil T-Joint Structures Obtained With -100/+200 Mesh Particles	274
152	Typical Foil Braze Structure Obtained With -200/+400 Mesh Particles	275
153	Homogenized RM40 Alloy Button Ingot	275
154	Arc-Melted RM40 Alloy Button Ingot	276
155	Typical Arc-Brazed Structure, CS13-5 Homogenized Alloy	276
156	Braze Structure After Cyclic Anneal, CS13-5 Homogenized Alloy	276
157	Structure of Ti-6Al-4V T-Joint After 112.5 Hours Salt Spray Exposure	277
158	Cleavage Cracks in Massive Beryllide Particles Within the Braze	278
159	Tapered Tensile Specimen With Groove	279
160	Crack Pattern In Ti-47.2 Zr-5.6 Braze Alloy After Tensile Loading	279
161	Cross Section of Crack in Braze Alloy; Strain Approximately 6700 Microinches/Inch	280
162	Cross Section of Crack in Braze Alloy and Parent Metal; Stress of 120,000 psi	280
163	Diffusion Bonder	303
164	Solid-State Diffusion Bonded Joint, Ti-5Al-2.5Sn/Ti-5Al-2.5Sn	304
165	Solid-State Diffusion Bonded Joint, Ti-6Al-4V/Ti-6Al-4V	304
166	Diffusion Bonded Joint, Ti-8Al-1Mo-1V/Ti-8Al-1Mo-1V	305
167	Diffusion Bonded Joint, Ti-8Al-1Mo-1V/Ti-6Al-4V	305
168	Diffusion Bonded Joint, Ti-6Al-4V/Ti-5Al-2.5Sn	305
169	Diffusion Bonded Joint, Ti-6Al-4V/Ti-6Al-4V	306
170	Diffusion Bonded Joint, Ti-8Al-1Mo-1V/Ti-8Al-1Mo-1V	306
171	Diffusion Bonded Joint, Ti-6Al-4V/Ti-3Al-2.5Sn/Ti-3Al-2.5V	306
172	Tapered Lap-Joint	307
173	Diffusion Bonded Joint, Ti-8Al-1Mo-1V/Ti Interleaf/Ti-6Al-4V	307
174	Elevated Temperature Foil Tester	308

ILLUSTRATIONS (Cont)

Figure		Page
175	Stress Decay Versus Time, Ti-6Al-4V Foil	309
176	Solid Plug Design	310
177	Hollow Plug Design	310
178	Encapsulated Liquid Metal Plug Design	311
179	Steel Encapsulated Lead Plugs	311
180	Welding the Lead-Filled Plugs in a Copper Block Cooled With Liquid Nitrogen	312
181	Lead-Filled Plug in Bottom Die of Swaging Tool	313
182	Swaging Lead-Filled Plug With Pneumatic Hammer	313
183	Pneumatic Expansion Plug Design and System	314
184	Pneumatic Expansion Plug	315
185	Typical Tube and Header Test Specimen	315
186	Beveled Edge of Header Hole	315
187	Assembling the Tube-Header Joint	316
188	Vacuum Furnace and Controls Used for Electrical Resistance Heating of Expansion Plugs	316
189	Eutectic Melting of Resistance-Heated Tube and Plug	317
190	Cold-Wall Vacuum Furnace	317
191	Tube-To-Header Joint Produced in Specimen L4	318
192	Tube-To-Header Joint Produced in Specimen L11	319
193	Tube-To-Header Joint Produced in Specimen L7	319
194	Tube-To-Header Joint Produced in Specimen L10	319
195	Tube-To-Header Joint Produced in Specimen L9	320
196	Tube-To-Header Joint Produced in Specimen L8	320
197	Pneumatic Pressurization Equipment	321
198	Pneumatic Bonding Cycle of Sample P2; Pressure Applied and Released at Temperature	322
199	Pneumatic Bonding Cycle of Sample P3; Cooled Under Pressure	322

ILLUSTRATIONS (Cont)

Figure		Page
200	Pneumatic Bonding Cycle of Sample P6; Heated Under Pressure	323
201	Diffusion Bond Produced in Sample P6 by Pneumatic Pressurization	323
202	Diffusion Bond in Specimen P7	324
203	Diffusion Bond in Specimen P8	324
204	Diffusion Bond in Specimen P10	324

TABLES

Table		Page
I	Phase II Structures	5
II	Proposed Evaluation Tests for Heat Exchangers	6
III	Proposed Evaluation Tests for Brazed Honeycomb Structures	7
IV	Proposed Evaluation Tests for Tube and Header Heat Exchangers	8
V	Selected Properties of Annealed Alloys	10
VI	Heat Treatments and Beta Transus Temperatures of Program Alloys	14
VII	Foil Materials for Phase I	15
VIII	Foil Materials for Phase II - Rodney Metals Inc.	17
IX	Properties and Analyses of Titanium Alloy Foils - Rodney Metals Inc.	18
X	Tensile Test Schedule	19
XI	Average Tensile Strength Results for As-Received Titanium Alloy Foils	21
XII	Effect of Foil Thickness on Mechanical Properties of Titanium Alloy Foils (Ref. 42)	22
XIII	Tensile Test Data for Titanium Alloy Foils Following Simulated Braze Cycles	29
XIV	Properties and Analysis of Ti-3Al-2.5V Titanium Alloy Tubing	30
XV	Ultimate Strengths of Ti-3Al-2.5V Alloy Tubing	32
XVI	Standard Oxidation - Reduction Potentials of Candidate Braze Bases	48
XVII	Candidate Alloying Elements for Producing Titanium - And Zirconium-Base Braze Alloys	49
XVIII	Influence of Melt Stock Purity on Interstitial Contaminent Levels	67
XIX	Variation of Weight Percent Beryllium in CS13-6 Braze Alloy	69
XX	Candidate Ternary Braze Alloys of the Ti-X-Be System	74
XXI	Candidate Ternary Braze Alloys of the Ti-Zr-Be System	75
XXII	RM Series Alloys Based on Ti-Zr-Ni and Ti-Ni Eutectics	77
XXIII	Results of Braze Studies on the Ternary Braze Alloy Ti-X-Be	79

TABLES (Cont)

Table		Page
XXIV	Results of Braze Studies on the Ternary Braze Alloy Ti-Zr-Be	80
XXV	Modifications of the Basic CS13-5 Braze Alloy	82
XXVI	Modified CS217 Series Braze Alloys	84
XXVII	Strength and Strain Accommodation Testing of CS217 Series Braze Alloys at Room Temperature	85
XXVIII	Effect of Addition of 10 Percent Silver on RM Series Alloys	87
XXVIX	Braze Alloys Evaluated in Task IV	93
XXX	Results of Room Temperature T-Joint Tensile Tests	94
XXXI	Flow Characteristics and Mechanical Properties of Candidate Braze Alloys	97
XXXII	Strain Accommodation Test Results	100
XXXIII	Double Lap-Joint Peel Test Results	102
XXXIV	Lap-Shear Test Results	103
XXXV	Alloys Selected for Study and Evaluation in Task V	135
XXXVI	Thermal Stability Test Results, Lap-Shear Tests	137
XXXVII	Microhardness Determination of Braze Alloys, Thermal Stability Tests	139
XXXVIII	Reliability Testing of Braze Alloys, Lap-Shear Specimens	140
XXXIX	Effects of Cyclic Annealing on CS217C Alloy	142
XL	Foil Strain for Failure of CS217C Braze Alloy	143
XLI	Average Strength of Braze Alloys/Ti-5Al-2.5Sn Foil	145
XLII	Average Strength of Braze Alloys/Ti-6Al-4V Foil	146
XLIII	Average Strength of CS Series Braze Alloys/Ti-6Al-4V Foil	149
XLIV	Average Strength of CS Series Braze Alloys/Ti-5Al-2.5Sn Foil	150
XLV	Lap-Shear Test Results, Ti-6Al-1Mo-1V Brazements	151
XLVI	Summary of Cyclic Annealing Effects on CS Series Braze Alloy/Foil Combinations	153
XLVII	Results of Lap-Shear Tests of Candidate Alloy/Ti-5Al-2.5Sn Self-Diffusion Bonded Specimens	158

TABLES (Cont)

Table		Page
XLVIII	Results of Lap-Shear Tests of Candidate Alloy/Ti-6Al-4V Self-Diffusion Bonded Specimens	159
XLIX	Microhardness Determination of Candidate Alloy Brazements	160
L	Hot-Salt Corrosion Test Data	164
LI	Fatigue Strength of Candidate Alloys and Self-Diffusion Bonded Ti-5Al-2.5Sn Specimens	166
LII	Reliability Tests on Candidate Braze Alloys/Titanium Foils	169
LIII	Effect of Braze Purity on Braze Temperature and Brazing Characteristics (Ti-5.6Be Alloy)	227
LIV	Effect of Braze Purity on Braze Temperature and Brazing Characteristics (Ti-47.2 Zr-5.6Be Alloy)	229
LV	Chemical Analyses of Arc-Melted and Arc-Melted Plus Homogenized CS13-5 and RM8 Braze Alloys	241
LVI	Change in Mechanical Properties of Brazed T-Joints Effected by Aging	243
LVII	Room Temperature Tensile Strength of Ti-6Al-4V T-Joints Before and After Salt Spray Exposure	244
LVIII	Elevated Temperature Strength of Ti-47.2Zr-5.6Be Brazements	246
LIX	Complet ist of Diffusion Bonded Joints	282
LX	Minimum Diffusion Bonding Process Parameters	285
LXI	Results of Diffusion Bonding Using 0.3-Mil Titanium Foil Interleaf	286
LXII	Tensile Data of Ti-6Al-4V Foil	288
LXIII	Creep Relaxation Data for Ti-6Al-4V Foil	289
LXIV	Test Results of Electrical Resistance Heating of Plugs for Differential Thermal Expansion	296
LXV	Test Results for Furnace Heating of Solid Plugs for Differential Thermal Expansion	297
LXVI	Test Results of Furnace Heating Lead-Filled Plugs for Differential Thermal Expansion	298
LXVII	Test Results of Pneumatic Pressurization Plugs	299

SECTION I

INTRODUCTION

Thin foils of titanium alloys, which offer significant design advantages in density, strength-to-weight, and modulus-to-weight from cryogenic temperature to 1000 F, are becoming available in increasing quantities from American producers. Commercial alloys such as Ti-5Al-2.5Sn, Ti-6Al-4V, and Ti-8Al-1Mo-1V are potentially useful in 2- through 10-mil foil forms as materials from which to make critical high-performance aerospace structures (e.g., tube-and-shell as well as plate-and-fin heat exchangers, honeycomb and corrugated sandwich panels). In addition to strength and modulus considerations, titanium alloys provide unique combinations of corrosion resistance, oxidation resistance, notch toughness, and structural stability over the temperature range of -400 to 1000 F. Hence, titanium foil structures theoretically lend themselves well to heat transfer systems involving cryogenic fuels, oxidizers, and air fractioning equipment.

Unfortunately, these titanium foil alloys have not received as much attention as they have deserved during the past ten years because of fabrication and joining difficulties and cost. Today, the lack of suitable joining techniques remain the greatest single deterrent to their more general use. Advanced aerospace vehicles currently under consideration by the USAF require extensive efforts in fabrication techniques to develop joining and forming methods for titanium alloy foils. In particular, advancements are necessary in high-performance heat transfer systems and honeycomb type structures where 2- through 10-mil foils are employed to maximum advantage.

The intricacy and complexity of the large numbers of joints required in the lightweight foil structures under consideration restrict joining techniques to brazing and solid state diffusion bonding. Honeycomb panels, for example, must be fabricated by brazing or diffusion bonding to obtain highest structural efficiency and reliability. The heat transfer systems being considered are normally composed of many thousands of thin-walled tubes and channels, making brazing or diffusion bonding the only practical processes to consider.

The braze alloys and processes heretofore developed for joining titanium are not considered satisfactory for joining titanium foils, principally because of erosion and corrosion effects. The need to braze at a relatively low temperature (below the foil's beta-transus) has led to the selection primarily of silver-base braze alloys. The interfacial formation of brittle Ti-Ag intermetallic upon the titanium substrate and crevice corrosion have proven serious disadvantages, thus the need to consider approaches that may avoid these problems. The Ti-Be and Ti-Zr-Be base braze alloys recently developed at Solar have shown promise of solving these problems and were investigated further in the subject program.

SECTION II

PROGRAM SCOPE AND OBJECTIVES

The overall purpose and objective of this program has been to develop and establish improved processes to join titanium alloy foils and thin-wall tubing by brazing and diffusion bonding, which would, in turn, provide stable, corrosion-resistant joints suitable for operation in the temperature range of -400 to 1000 F.

The subject program was designed to accomplish these objectives in two phases. Phase I was concerned with the development of titanium-base and titanium-zirconium-base braze alloys and diffusion bonding techniques for titanium alloy foils (≤ 0.010 inch thick). Phase II was concerned with the demonstration and application of the developed joining methods to high-performance structures. Honeycomb panels, corrugated heat exchanger panels, and tube-and-shell heat exchanger matrices were the structural shapes chosen to be fabricated and tested with boundary test conditions which simulate high-performance aerospace applications.

Phase I work was further divided into seven consecutive tasks. Tasks I through IV were concerned with the logical selection and screening of materials and over 100 braze alloy modifications with potential for titanium foil joining.

Special test procedures to evaluate the relative merits of different braze systems were developed. They included:

- Braze Screening Tests. To appraise braze flow and filleting behavior on foils, measure erosion characteristics with different braze cycles, and determine brazement microstructure and microhardness.
- Corrosion Tests. To detect susceptibility of specific foil brazements to general or crevice corrosion in long-term, salt-spray environment.
- Mechanical Tests. To measure, in foil configurations, the braze tensile and shear strengths; peel resistance and strain accommodation of brazements under a variety of test conditions and prior thermal histories.
- Thermal Stability Tests. To detect possible degradation of brazement structure and/or mechanical properties during simulated service regimes in both vacuum and air.

The number of candidate braze materials was reduced to eight at the end of Task IV on the basis of room temperature test data comparisons.

Tasks V and VI were designed to provide a much broader evaluation of the remaining eight candidate braze materials. The test regimes covered the range of probable operating temperatures (-320 to 900 F) and included:

- Statistical survey of T-joint and lap-joint strength data (-320 to 900 F) as a measure of design strength reliability.
- Effects of long-term, salt-spray exposure (100 hours, 200 F) on lap-joint strength (-320 to 900 F).
- Effect of thermal aging (100 hours, 1000 F in both air and high vacuum environment) on lap-joint strength (-320 to 800 F).
- Stress-rupture tests of lap-joint specimens (~100 hours, 1000 F) both in oxidizing, jet-fuel exhaust gas and in molten hot salt (NaCl).
- Tension-tensile fatigue tests of lap-joint specimens ($^{SA}/_{SM} = 1.0$) at room temperature.

At the conclusion of Task VI, the number of braze alloy candidates was narrowed to four for final evaluation in fabrication and testing of Phase II structures.

The feasibility of self-diffusion bonding tube-to-header joints was investigated in Task VII, with chief process criteria of:

- Joint Quality (joints metallurgically sound and leak-tight)
- Joint Reproducibility (high probability of constant quality)
- Equally Competitive Process (braze process versus diffusion bonding process)

The charter of Phase II was to construct and test a prescribed number of full-scale foil structures using a single recommended braze alloy and/or joining process for each of the three structure types. The structure types and quantities of each are listed in Table I.

Subscale modules of each structure type were initially fabricated, bonded, and tested to yield information on the relative merits of the remaining braze alloys and joining techniques thereby enabling the ultimate selection of an optimum joining process for each full-scale structure. The detailed format of the full-scale test program is shown in Tables II, III, and IV along with the kinds of data generated for analysis.

TABLE I

PHASE II STRUCTURES

Task	Structure-Type	Design and Dimensional Requirements	Number of Modules to be Constructed (Minimum)
I	Multilayer, corrugated, sandwich structure	Six-inch cube, external. Corrugation pitch and height, 0.050 to 0.100 inch. Foil materials in the thickness range of 0.002 to 0.006 inch. Simple cross flow or counter-cross flow design.	2
II	Honeycomb core sandwich structure	Panel size: 0.375 to 0.500 inch thick by 12 inches square. Core cell size: 0.25-inch square cell, 0.002 inch thick core ribbon Face sheet thickness: 0.010 inch.	6
III	Tube-to-header matrix	Number of tubes in module: 50 to 100. Tubing dimensions: 0.125-inch OD by 0.002 to 0.006 inch wall thickness by 12 inches long. Header thickness: 0.015 to 0.030 inch. Tube spacing in the headers to be on a pitch to tube diameter ratio of 1.07 longitudinally and 1.25 transverse direction.	2

Key tests of the three types of foil structure were as follows:

Structure	Test Program
Corrugated Sandwich	Pressure cycling Pressure burst [illegible]al shock [illegible]ation
Honeycomb Sandwich	Flatwise tension and compression Edgewise compression Panel (beam) flexure Block shear Thermal cycling and aging effects on above tests
Tube-and-Header Matrix	Vibration Pressure cycling Proof pressure Thermal shock Steady-state flow

TABLE II

PROPOSED EVALUATION TESTS FOR HEAT EXCHANGERS

Test Number	Type of Test	Test Temperature (F)	Number of Specimens*	Specimen Size (Inches)	Purpose
P-1	Pressure cycling (Up to 50 cycles of 150% of expected service pressure)	-320	2	2 x 2 x 2	To verify the capability of the brazed structure to withstand typical cyclic pressure fluctuation over the range of operating temperatures.
P-1		-260	2	2 x 2 x 2	
P-2		RT	2	2 x 2 x 2	
P-3		500	2	2 x 2 x 2	
P-3		1000	2	2 x 2 x 2	
P-4	Pressure burst	RT	1	2 x 2 x 2	To verify the design strength of the brazed structure and to determine the safe limits of internal pressurization.
			1	6 x 6 x 6	
P-5	Thermal shock (100 cycles) and steady state flow thermal gradient	-320 to 1000	2 (1)	6 x 6 x 6	To affirm the ability of the brazed structure to withstand severe thermal gradients and strains during transient and steady flow conditions.
P-6	Vibration (with and without internal pressurization)	RT	2 (1)	6 x 6 x 6	To confirm resonant frequencies of module design experimentally and to determine kind and degree of vibration damage resulting from vibration in the 50 to 2000 cps frequency range.

*Tests shall be sequenced such that one full-scale unit will be exposed to all tests.

(1)Specimen destruction not anticipated.

TABLE III

PROPOSED EVALUATION TESTS FOR BRAZED HONEYCOMB STRUCTURES

Test Number	Type of Test	Test Temperature (F)	Number of Specimens	Specimen Size (Inches)	Purpose
H-1	Flatwise Tension and/or Compression	-320 -100 RT 300 500 1000	3 3 3 3 3 3	1 x 1 1 x 1 1 x 1 1 x 1 1 x 1 1 x 1	(a) Tensile and compressive strengths of core/face sheet joint versus test temperature. (b) Failure mode versus temperature.
H-2	Edgewise Compression	RT RT	3 (longitudinal) 3 (transverse)	3 x 4 3 x 4	(a) Compressive edge loading versus compressive strain. (b) Facing modulus of elasticity. (c) Conditions of onset of buckling and catastrophic panel failure. (d) Effective elastic limit of panels in edge loading.
H-3	Panel Flexure (2-point, 1/3-span loading)	RT	3 (longitudinal) 3 (transverse)	3 x 8	(a) Midspan deflection versus load. (b) Core shear modulus. (c) Effective panel facing strength in flexure.
H-4	Block Shear (30 degree deflection)	-320	3 (As-brazed) +3 (After 100 hr Aging;500-1000F)	(longitudinal) 1 x 1	(a) Shear load versus core deflection (toughness rating).
		RT	3 (As-brazed) +3 (After 100 hr. Aging;500-1000F)	1 x 1	(b) Effect of test temperature on panel toughness and failure mode.
		300	3 (As-brazed) +3 (After 100 hr Aging;500-1000F)	1 x 1	(c) Effect of simulated service aging upon panel toughness and failure mode.
		500	3 (As-brazed) +3 (After 100 hr Aging;500-1000F)	1 x 1	
		1000	3 (As-brazed) +3 (After 100 hr Aging;500-1000F)	1 x 1	
H-5	Thermal Cycling Tests (Repetition of several of the preceding test regimes following thermal cycling of panels between -300F and 1000F; 10 cycles)				
	(a) Flatwise Tension	-320 RT 500 1000	3 3 3	1 x 1 1 x 1 1 x 1	As before
	(b) Edgewise Compression	RT	3	3 x 4	As before
	(c) Panel Flexure	RT	3	3 x 8	As before

Tasks IV and V of Phase II were concerned with post braze heat treating and high purity braze alloy production, respectively.

TABLE IV

PROPOSED EVALUATION TESTS FOR TUBE AND HEADER HEAT EXCHANGERS

Test Number	Type of Test	Test Temperature (F)	Number of Specimens	Specimen Size	Purpose
T-1	Vibration	RT	1 (Normal to tube axis (1) 1 (Parallel to tube axis) (1)	Full-Size Module	To determine fundamental resonant frequency and vibration tolerance of the brazed structures.
T-2	Pressure cycling (up to 200 pressure cycles at each test temperature)	-320	1 and 1 (1)	Subscale and Full-Size Module	To verify the capability of the brazed structures to withstand typical cyclic pressure fluctuations over the range of operating temperature.
		RT	1 and 1 (1)	Subscale and Full-Size Module	
		500	1 and 1 (1)	Subscale and Full-Size Module	
		1000	1 and 1 (1)	Subscale and Full-Size Module	
T-3	Pressure test (Up to 150% of expected service pressure)	RT	2 (1)	Full-Size Module	Conducted on modules before and after vibration to assess the ability of brazed structure to withstand high internal pressure.
			2	Subscale Module	
		500	2 (1)	Full-Size Module	
			2	Subscale Module	
		1000	2 (1)	Full-Size Module	
			2	Subscale Module	
T-4	(a) Thermal shock	-320 to 500 or 1000	2 (1)	Full-Size Module	To evaluate the ability of both as-brazed and vibrated structures to withstand severe thermal gradients, and sustained periods of temperature differential.
	(b) Steady state flow	Service	2 (1)	Full-Size Module	

(1) Specimen destruction not anticipated.

SECTION III

PHASE I - DEVELOPMENT OF JOINING METHODS FOR TITANIUM ALLOY FOIL

As discussed in Section II, Phase I was divided into seven individual tasks. These tasks are discussed in this section.

3.1 TASK I - SELECTION OF MATERIALS

The primary intent of foil alloy selection was to match desired metallurgical properties and degree of fabricability for each candidate foil alloy against specific, usually controlling material requirements of each of the three different foil structures to be bonded in Phase II. Candidate titanium foil alloys were restricted to those commercial sheet and foil alloys in general usage throughout the aerospace industry, and commonly available as foil in the required 2- through 10-mil range of thickness. (This stipulation was held advisable to ensure maximum utilization and adaptability for industry of the bonding methods developed.) Foil alloys considered were Ti-6Al-4V (AMS-4907), Ti-5Al-2.5Sn (AMS-4909), and Ti-8Al-1Mo-1V (AMS-4916). The only high-strength, thin-wall tubing alloy commercially available was Ti-3Al-2.5V (0.125-inch OD by 0.002 to 0.006-inch wall thickness). To ensure starting foil materials with the lowest available levels of interstitial element contaminants (carbon, oxygen, and nitrogen) and a minimum amount of surface contamination, extra low interstitial (ELI) grades were procured wherever applicable. (Hard layers of surface contamination are often detrimental to formability and restrict joining processes.) The Ti-6Al-4V and Ti-5Al-2.5Sn alloys were available in ELI grades (AMS-4907 and AMS-4909, respectively), and were used exclusively in Phase II and in much of Phase I work.

3.1.1 Alloys for Corrugated Sandwich Structures

The corrugated sandwich structures for countercrossflow heat-exchanger applications were required to operate over a wide range of temperatures and different fluid media from -425 F up to 1000 F in air. The foil materials had to be weldable to facilitate post-braze assembly of the foil structure to accessory components, such as inlet and outlet gas ducts and header reinforcements. Another critical requirement was excellent cold formability; first to permit precision rolling to 2- to 4-mil foils, and

TABLE V

SELECTED PROPERTIES OF ANNEALED ALLOYS

	Annealed Alloy					
	Ti-6Al-1Mo-1V	Ti-6Al-4V	Ti-6Al-4V ELI	Ti-6Al-2.5Sn	Ti-6Al-2.5Sn ELI	Ti-3Al-2.5V
Typical Tensile Properties at Room Temperature						
Elastic Modulus (10^6 psi)	18.0[1]	16.5	16.5	16.0	16.0	15.5
Ultimate Strength (ksi)	150	128	135	125	110	100
Yield Strength (ksi)	142	120	127	117	95	85
Elongation (%)	13	12	15	16	20	20
600 F						
Elastic Modulus (10^6 psi)	---	15.5	13.5	13.4	13.4	13.0
Ultimate Strength (ksi)	107[2]	106	105	82	78	70
Yield Strength (ksi)	85[2]	96	96	65	60	50
Elongation (%)	19[2]	11	12	19	20	25
Extreme Temperature						
Temperature (F)	1000[3]	800	-320	100	-423	---
Ultimate Strength (ksi)	80[2]	90	230	75	220	---
Yield Strength (ksi)	72[2]	78	205	56	205	---
Elongation (%)	20[3]	10	13	18	15	---
Creep						
Temperature (F)	1000	800	---	800	---	---
Stress (ksi)	10	70	---	45	---	---
Time (hr)	100	1000	---	100	---	---
Total Plastic Deformation (%)	0.15	0.10	---	0.10	---	---
Stress Rupture K_T = 1						
Temperature (F)	---	850	---	800	---	---
Stress (ksi)	---	65	---	52	---	---
Time (hr)	---	100	---	1000	---	---

1. Duplex
2. Bar annealed 1650 F, 1 hr, AC + 1100 F, 4 hr, AC (air cooled)

secondly to enable die-forming these thin foils into high-density, miniature corrugations for heat exchangers of desired high-compactness ratio and high thermal transfer efficiency. In the subject work, sine wave corrugations with the corrugation pitch and height of ~ 0.070-inch and bend radii of 1T to 4T were desirable.

The Ti-5Al-2.5Sn (ELI) alloy was selected for the corrugated structure (with Ti-6Al-4V alloy as the backup). In sheet form, this material is weldable without appreciable loss in strength and ductility. As shown in Table V (Ref. 1), the material has good low-temperature toughness and strength in the -423 F range, has good creep strength in the 600 to 800 F range, and has usable short time strength to 1000 F. The ELI grade sheet material has guaranteed room temperature ultimate and yield strengths of 100,000 and 90,000 psi compared to 120,000 and 115,000 psi for the non-ELI grade.

Therefore, for non-cryogenic applications, the non-ELI grade could have a strength advantage, although it would be more difficult to form. The ELI grade was preferred for formability in this situation inasmuch as foil strength was not a controlling factor.

The Ti-5Al-2.5Sn is an alpha-type alloy with a high aluminum content that stabilizes the alpha phase and shifts the beta transus into the 1900 F range. Tin is a neutral element having appreciable solubility in both alpha and beta phases of titanium, but adds considerably to the strength without changing the ductility. The alloy is not heat treatable: therefore, annealing is achieved in the 1325 to 1550 F range, followed by slow cooling. Stress relief annealing is in the 1000 to 1200 F range, followed by slow cooling.

The high beta transus of the Ti-5Al-2.5Sn alloy also has a favorable attribute as it allows brazing without danger of beta embrittlement in the range of 1600 to 1750 F, where most applicable braze systems for titanium are processed. The high beta transus and single-phase character of Ti-5Al-2.5Sn also promote structural stability of this alloy in the proposed range of operating temperatures (-425 F to 1000 F).

3.1.2 Alloys for Honeycomb Sandwich Structures

The paramount requirements for high-strength, high-rigidity beams made of honeycomb sandwich panels are highest possible foil strength and modulus values over the normal range of operating temperatures (RT to 1000 F). High creep and rupture strengths become important for long-term structural stability above about 600 F. The high strength and high modulus criteria are most vital for the face sheet alloy (10-mil maximum thickness), permitting the honeycomb core to be made of a weaker, more workable alloy (2 to 4-mil thickness). Both foil alloys thus serve to enhance strength/weight and modulus/weight ratios. Cold formability of face sheet foils and honeycomb core ribbon is not a critical requirement inasmuch as no plastic deformation of foils is necessary to make either the face sheet or core components (i.e., for required flat, closed-face panels with 0.25 inch square, unit cell dimension). Weldability is of minor importance for initial bonding of core node joints because the weld-backed node joints are ultimately supplanted by larger and stronger braze joints.

In view of the above emphasis upon highest possible strength and modulus values, the following alloys were selected:

Component	First Choice	Backup
Face Sheet	Ti-8Al-1Mo-1V	Ti-6Al-4V (ELI)
Honeycomb Core	Ti-6Al-4V (ELI)	Commercially Pure Ti (A-70)

For highest strength values, both the Ti-6Al-4V and Ti-8Al-1Mo-1V alloys require rather complex heat treatments above 1500 F (Table VI). Quite probably such high-temperature heat treatment of foil structures following brazing or diffusion bonding would be inadvisable because of the extreme dangers of warpage and progressive foil contamination. Consequently, candidate foil alloys were compared in the fully annealed condition; and as shown in Table V, the Ti-8Al-1Mo-1V alloy still retains a strength and modulus advantage.

Ti-8Al-1Mo-1V Face Sheets

The Ti-8Al-1Mo-1V alloy was selected for the honeycomb face sheets on the basis of high strength and modulus, good elevated temperature properties to 1000 F, high toughness, ability to withstand the brazing cycle, and, as reported in Reference 2, has an alpha-rich microstructure. Because of the weakly stabilized beta phase, the alloy is not considered heat treatable in the strengthening sense; the good strength and high creep resistance at room and elevated temperature are obtained mainly through solid solution alloying, particularly in the alpha phase matrix as manifested by the 8 percent aluminum addition. The weaker beta phase stabilization is attained by the molybdenum and vanadium additions. The beta transus temperature is 1900 F.

The Ti-8Al-1Mo-1V alloy develops its best combination of properties in the triplex annealed conditions: anneal at 1450 F for 8 hours, solution treat in the alpha-beta phase field (1850 F), air cool, stabilize at 1100 to 1400 F, followed by air cool (Ref. 3). The heat treating cycle (latter portion ≤1400 F) and high beta transus appeared to be ideally matched to the brazing cycles anticipated in the foil joining program.

On the debit side, the Ti-8Al-1Mo-1V alloy has a history of experiencing serious stress corrosion problems (Ref. 4 through 7). In addition, it was recognized that difficulties such as severe texturing and cracking might be experienced in the foil rolling processes due to the great strength and stiffness of the high-aluminum, alpha-phase matrix.

Ti-6Al-4V Core

Because a material less strong than the face sheet material was suitable, the more readily available Ti-6Al-4V (Ref. 8) was selected for the 0.002-inch thick core material on the basis of its attractive annealed strength (Table V), good corrosion resistance, and adequate formability and weldability. For the same reasons, this alloy was selected as a backup for the Ti-8Al-1Mo-1V face sheet material.

Ti-6Al-4V is a heat treatable, alpha-beta alloy. The aluminum addition stabilizes the alpha phase, increases the beta transus of the alloy to 1820 F, and significantly increases the elevated temperature strength level of the alloy (when compared with Ti-5Al-2.5Sn at 600 F - Table V.)

3.1.3 Alloys for Tube-and-Header Structures

The Ti-3Al-2.5V alloy (Ref. 9) was the only high-strength titanium alloy commercially available in thin-wall tube form (Tables V and VI). The Ti-6Al-4V alloy was selected as a metallurgically compatible header material.

The Ti-3Al-2.5V is an alpha-beta type alloy, stabilized by the aluminum addition. The low aluminum content places the beta transus at 1725 ± 25 degrees F, a situation which should permit brazing and diffusion bonding up to the 1650 to 1700 F range. The alloy is also reported to be weldable (Ref. 9).

The Ti-3Al-2.5V alloy is structurally stable and does not respond to hardening by heat treatment. Stress relief and annealing treatments are usually accomplished at 1300 F for one hour followed by slow cooling.

3.1.4 Procurement of Foil and Tubing Materials

Procurement of Phase I Material

The alloys procured for Phase I are listed in Table VII. The foil thicknesses selected are representative of current practices for the types of foil structures used on this program (Ref. 10 through 12). The 0.002-inch foil thicknesses of the honeycomb core (Ti-6Al-4V) and heat exchanger corrugation (Ti-5Al-2.5Sn) were chosen as the minimum available and usable without excessive complications to the program. The Ti-8Al-1Mo-1V alloy was used only in the 0.010-inch thickness as thinner material was considered developmental at time of ordering.

TABLE VI

HEAT TREATMENTS AND BETA TRANSUS TEMPERATURES OF PROGRAM ALLOYS

Alloy	Beta Transus Temperature (F)	Heat Treatment Conditions	Heat Treatment Objective
Ti-8Al-1Mo-1V	1900	Anneal: 1450 F, 8 hr, FC	Simplest treatment; optimum ductility and impact resistance; good tensile strength and structural stability.
Ti-8Al-1Mo-1V	1900	Triplex Annealed: 1450 F, 8 hr, FC + 1850 F, 5 min, AC + 1375 F, 15 min, AC	Best combination of engineering properties including optimum creep rupture strength to 1000 F, and excellent notch toughness.
Ti-6Al-4V	1820	Solution Treatment: 1550 to 1750 F, 5 min to 1 hr, WQ age, 900 to 1000 F, 4 to 8 hr, AC	Unstable until aged. After aging, best combination of engineering properties including optimum levels of tensile and creep rupture strengths, good impact resistance and notch toughness.
Ti-6Al-4V ELI	1820	Anneal: 1300 to 1550 F, 1 to 8 hr, SC to 1050 F, AC	Maximum toughness to -425 F.
Ti-5Al-2.5Sn ELI	1910	Anneal: 1325 to 1550 F, 10 min to 4 hr, AC	Optimum properties, non-heat treatable alloy with good weldability.
Ti-8Al-2.5V	1715	Anneal: 1300 F, 1 hr, AC	Optimum properties, solution treatment and aging not recommended. Readily formed alpha/beta alloy.

AC = Air cooled
FC = Furnace cooled
SC = Slow cool
WQ = Water quench
ELI = Extra low interstitial contaminants

As there were long lead times for the rerolled material (≤ 0.010-inch), 0.006 inch thick Ti-5Al-2.5Sn and 0.010-inch thick Ti-6Al-4V were procured from material suppliers for interim use on Phase I studies. Although these materials likely did differ somewhat in strength properties from the rerolled foils, they were deemed suitable for initial braze evaluation studies until the rerolled foils were received.

Rerolled alloy foils were readily available from only one supplier, Rodney Metals, Inc., in widths up to 12 inches with delivery times ranging from 12 to 16 weeks. An alternate foil supplier, Hamilton Watch Co., agreed to reroll two of the foil alloys for interim use (Table VII), but would not accept further orders until additional experience was gained.

TABLE VII

FOIL MATERIALS FOR PHASE I

Alloy	Thickness (Inches)	Phase I Delivery Date	Price/ Pound (Dollar)	Application	Supplier
Ti-8Al-1Mo-1V (AMS-4916)	0.010	10-1-65	54.90	Honeycomb Face Sheets	Rodney Metals, Inc.
Ti-6Al-4V (AMS-4911)	0.010	10-1-65	45.25	Alternate Honeycomb Face Sheets	Rodney Metals, Inc.
Ti-6Al-4V (AMS-4911)	0.002	2-15-66 11-29-65	128.25	Honeycomb Core	Rodney Metals, Inc. Hamilton Watch Co. (Cancelled)
Ti-6Al-4V (AMS-4911)	0.016	10-1-65	37.12	Tube and Header Headers	TMCA
Ti-3Al-2.5V	0.002[1]	10-31-65		Tube and Header Tubes	Superior Tube Co.
	0.006[1]	10-1-65	0.68[2]		
	0.031[1]	10-31-65			
	0.004[1]	3-15-66			
Ti-5Al-2.5Sn ELI (AMS-4909)	0.006	10-1-65	42.25	Corrugated Structure Separators	Rodney Metals, Inc.
Ti-5Al-2.5Sn ELI (AMS-4909)	0.002	2-10-66	83.25	Corrugated Structure Corrugations	Rodney Metals, Inc. Hamilton Watch Co. (Cancelled)

[1] 0.125 OD Tubes (wall thickness indicated)

[2] Price foot

The Ti-3Al-2.5V was the only titanium alloy available in thin-wall tube form, and Superior Tube Co. was the only supplier. The 0.031-inch thick tube was to be employed for tensile testing of the tube/header joints; the thinner wall tubes were expected to fail in the tubes rather than at the joint under tensile loading, hence the need for the thicker-walled tubing to force failure through the joints.

The 0.010-inch thick Ti-6Al-4V alloy was ordered as a ready alternate to the Ti-8Al-1Mo-1V alloy for honeycomb face sheets because the Ti-8Al-1Mo-1V alloy had experienced serious stress corrosion problems which might preclude its eventual use on the program (Ref. 4 through 7).

The extra low interstitial (ELI) grade of the Ti-6Al-4V (AMS-4967) would have been preferable to the standard grade ordered; however, the extra time required to procure the ELI grade material for Phase I effort could not be tolerated because of tight scheduling. ELI grades were used exclusively in Phase II work.

The prices shown in Table VII are those quoted in June 1965 and are given as a guide to the relative costs of the materials. These prices are dependent on the overall demand for the materials and the size of the orders, which affect the type of facility doing the rerolling and annealing operations, and the relative setup cost for each foil order. An example of the effect demand has on the cost of materials is the titanium composite price index for sheet, strip, bar, and billet. The index was $15.25 per pound in 1965. In 1963, after the use of titanium was well established, it was $5.50 per pound (Ref. 13 and 14).

The 0.006-inch thick Ti-5Al-2.5Sn and the 0.010-inch thick Ti-8Al-1Mo-1V alloy foils from Rodney Metals contained distortion imperfections (Fig. 1 and 2). Although the material was usable for the small specimens of the Phase I program, fabrication of actual structures in Phase II would undoubtedly be difficult. According to the supplier, the imperfections in the form of dimples and corrugations are typical of the shape problems encountered in the processing of very hard-to-work alloys in short strip lengths. These distortion problems were expected to be minimized when the raw material for rerolling became available in coil form rather than in the (small-order) sheet form of the Phase I materials. This proved to be the case, as no such problems were encountered in filling the larger orders for Phase II materials.

It developed ultimately that Hamilton Watch Company was unable to complete the processing of the 0.002-inch thick Ti-6Al-4V and Ti-5Al-2.5Sn alloys; they, therefore, recommended that the order with them be terminated. Although the order was cancelled, personnel at Hamilton indicated continuing interest in developing titanium-alloy foil rolling capability.

Procurement of Phase II Materials

During the latter half of Phase I work, when it became evident that promising braze systems were available for titanium foil structures, procurement orders were placed (with sponsor approval) for sufficient foil materials to accomplish Phase II objectives.

TABLE VIII

FOIL MATERIALS FOR PHASE II - RODNEY METALS INC.

AMS Specification	Material	Thickness (in.)	Width (in.)	Length[1] Total (ft)	Application	Approximate Weight (lb)	Cost ($)	Total Cost ($)
4816	Ti-6Al-1Mo-1V	0.010	12	40	Honeycomb face sheets	10	600.00 lot	600
4907	Ti-6Al-4V ELI	0.010	12	40	Backup honeycomb face sheets	10	600.00 lot	600
4907	Ti-6Al-4V ELI	0.002	2	460	Honeycomb core	7	145.75/lb	1020
4907	Ti-6Al-4V ELI	0.002	8	650	Backup material for heat exchanger corrugations	20	144.25/lb	2890
4909	Ti-5Al-2.5Sn ELI	0.006	8	325	Heat exchanger separators	30	74.00/lb	2220
4909	Ti-5Al-2.5Sn ELI	0.002	8	650	Heat exchanger corrugations	20	145.50/lb	2910
							Total	10,240

1. Random lengths at least 3 feet long

16-week delivery conditional on fabricability of 0.002-inch material and availability of ELI grades.

Inquiries were sent to the following manufacturers for titanium alloy foils in the quantities required for Phase II of the program.

- Du Pont Metal Products Division
- Hamilton Watch Company
- Reactive Metals, Inc.
- Rodney Metals, Inc.
- Techalloy, Inc.
- Titanium Metals Corporation of America
- Wah Chang Corporation

The only manufacturer to respond affirmatively was Rodney Metals, Inc. A typical delivery time of 16 weeks, and a total estimated cost of $10,240 was quoted. The detailed cost figures are shown in Table VIII.

3.1.5 Baseline Tests of Program Foil and Tube Alloys

Mechanical tests to gage tensile strength and toughness levels of as-received (mill-annealed) program foils were conducted to provide baseline information for later test comparisons with actual bonded foils and also foils subjected to thermal cycles simulating bond processing. A description of the program foils tested is shown in Table IX. Testing included unnotched tensile tests of program foils and tubing in liquid N_2 or air environment through the temperature range of -320 to 900 F (Table X) and in both the parallel and transverse rolling directions. The designs of the notched

TABLE IX

PROPERTIES AND ANALYSES OF TITANIUM ALLOY FOILS - RODNEY METALS INC.

Alloy	Ti-5Al-2.5Sn ELI		Ti-6Al-4V		Ti-8Al-1Mo-1V
Size	0.003 inch x 6 inch		0.010 inch x 6 inch		0.010 inch x 6 inch
Specification	AMS4909		AMS4911A		Mil-T-9046D Type II Composition F
Mechanical Properties (Annealed)	Longitudinal	Transverse	Longitudinal	Transverse	Longitudinal
Ultimate Tensile Strength	117,800 psi	119,500 psi	151,000 psi	149,850 psi	152,000 psi
Yield Strength, 0.2% Offset	107,000 psi	108,500 psi	128,500 psi	135,750 psi	139,000 psi
Elongation, 2 inch	13.1%	13.3%	9.6%	7.8%	11.3%
Bend Test	Passed	Passed	Passed	Passed	Passed
Rockwell Hardness	C33		C34		C31
Ladle Analysis	Heat Number D4203		Heat Number D8941		Heat Number D8141
Al	5.0%		6.0%		7.8%
Mo	--		--		1.0%
Sn	2.4%		--		--
V	--		4.1%		0.9%
O	0.06%		0.12%		0.07%
H	0.010%		0.008% to 0.010%		0.011%
N	0.011%		0.014%		0.014%
Fe	0.14%		0.08%		0.06%
C	0.022%		0.025%		0.023%
Mn	0.010%		--		--
Ti	Balance		Balance		Balance

and unnotched tensile specimens are shown in Figure 3. The notched tensile test was employed to determine the relative notch-toughness level of foils, employing the ratios of notched ultimate strength to unnotched ultimate strength, and notched ultimate to yield strength as indicators. The higher the ratios (especially desirable above 1.0), the greater a material's relative resistance to notch or crack propagation and the higher its notch toughness rating.

Tensile testing of sheets and foils containing notches or other stress raisers has merited wide discussion in recent literature (Ref. 15 through 40), and was recommended for toughness testing by the ASTM Committee on Fracture Testing of High

TABLE X

TENSILE TEST SCHEDULE

(Numbers in Table Refer to Number of Specimens to be Tested)

Material Condition			As Received							After Simulated Braze Cycles						
Test Temperature			-320 F		Room Temperature		Elevated(1) Temperature			-320 F		Room Temperature		Elevated(1) Temperature		
Specimen Type			P	N	P	N	P	N		P	N	P	N	P	N	
No.	Material	Rolling Direction							Totals							Totals
1	Ti-8Al-1Mo-1V 0.010 inch	Transverse	3	3	3	3	3	3	18	3	3	3	3	3	3	18
		Parallel	3	3	3	3	3	3	18							
2	Ti-6Al-4V 0.010 inch	Transverse	3	3	3	3	3	3	18	3	3	3	3	3	3	18
		Parallel	3	3	3	3	3	3	18							
3	Ti-5Al-2.5Sn 0.006 inch	Transverse	3	3	3	3	3	3	18	3	3	3	3	3	3	18
		Parallel	3	3	3	3	3	3	18							
4	Ti-3Al-2.5V 0.006 inch wall 0.125 inch OD	Parallel	3		3		3		9	3		3		3		9
5	Ti-3Al-2.5V 0.002 inch wall 0.125 inch OD	Parallel	3		3		3		9	3		3		3		9
		Totals	24	18	24	18	24	18	126	15	9	15	9	15	9	72

Totals: As Received — N - Notched 3 x 6 x 3 = 54; P - Plain 3 x 8 x 3 = 72

Simulated Braze — N - Notched 3 x 3 x 3 = 27; P - Plain 3 x 5 x 3 = 45

Total Specimens = 126 + 72 = 198

(1) Elevated Temperatures Test

Ti-8Al-1Mo-1V = 900 F

Ti-6Al-4V = 800 F

Ti-5Al-2.5Sn = 800 F

Ti-3Al-2.5V = 600 F

Strength Sheet Materials (Ref. 18 and 19). The method has been subjected to considerable stress analyses which can aid in interpreting the results (Ref. 41 and 20). Since the notch tensile testing method appeared to be adaptable to the testing of foils in the 0.010-inch thick range (Ref. 21 and 22), it was adopted for the brazing program. (preliminary work with bend testing of foils proved insensitive and inadequate for gaging differences in foil toughness.)

Some investigators favor specimens with sharper notches which give high stress concentrations (Ref. 25); however, at the higher stress concentrations, the measured toughness values tend to be less dependent upon the stress concentration factor itself (Ref. 26) and more sensitive to the actual toughness characteristics of the material. Although the fatigue crack is reported to be one of the best stress concentrators, some investigators favor the machined notch or sheared notch (as adopted here) with a radius less than 0.001-inch because of cost considerations and better uniformity of notches.

The sheared notch was selected as the method which would give the highest stress concentration without excessive complications. It was reasoned that machined notches would be easier to fabricate, but they would produce a relatively low stress concentration factor in the foil sized specimens, even with tip radii in the 0.001-inch range. The low stress concentration factor would cause a loss in toughness test sensitivities.

The edge-sheared notch produced with a precision shear, was selected rather than a central-sheared notch (Fig. 4) as the lateral deformation and buckling problems of the central notch configuration are accentuated in foil materials. The ratio of notch depth to specimen width of 0.1875 (edge notch) fell within the limits suggested by the ASTM Fracture Toughness Committee (Ref. 18).

The specimen width to thickness ratio varied between 25 and 125 for the foil thicknesses used in the brazing program. It was suggested by the ASTM Committee that the width to thickness ratio be kept below 45 as lateral warping and buckling might occur, especially with pin-loaded specimens. However, if the thinner specimens had been made narrower to comply, the effective notch stress concentration would have been reduced, seriously affecting the test sensitivity. Therefore, the specimen configuration was maintained as shown in Figure 3 for all foil thicknesses tested.

TABLE XI

AVERAGE TENSILE STRENGTH RESULTS FOR AS-RECEIVED TITANIUM ALLOY FOILS

Material	Parallel (P) Transverse (T) To Rolling Direction	Temperature (F)	Yield Strength (psi)	Ultimate Strength (psi)	Ultimate Modulus (psi x 10^{-6})	Notch To Avg Yield Strength Ratio	Notch To Avg Ultimate Strength Ratio
Ti-5Al-2.5Sn ELI (0.0062 Inch Thick)	T	75	110,000	119,000	15.8	1.47	1.36
	P	75	111,000	119,000	16.3	1.51	1.38
	T	-320	171,000	177,000		1.16	1 13
	P	-320	173,000	180,000		1.16	1.12
	T	800	63,000	73,000		1.49	1.27
	P	800	56,000	72,000		1.60	1.29
Ti-6Al-4V (0.0099 Inch Thick)	T	75	135,000	149,000	15.5	1.01	0.91
	P	75	129,000	150,000	14.7	1.19	1.03
	T	-320	217,000	223,000		0.89	0.88
	P	-320	213,000	227,000		0.89	0.86
	T	800	107,000	109,000		1.25	1.24
	P	800	100,000	113,000		1.18	1.04
Ti-8Al-1Mo-1V (0.0100 Inch Thick)	T	75	142,000	157,000	17.6	0.96	0.87
	P	75	140,000	163,000	16.2	1.08	0.90
	T	-320	207,000	217,000		0.68	0.65
	P	-320	219,000	231,000		0.66	0.62
	T	900	105,000	114,000		1.33	1.22
	P	900	106,000	118,000		1.20	1.08

Tensile test data related to foils in the as-received (mill-annealed) condition are listed in Table XI and plotted in Figure 5. In general, the actual values of foil strength and the variation with test temperature follow very closely the published data (Table XII) for thicker foils and sheet stock of the same alloys. As shown in Figure 5, foil tensile strengths increased roughly two- to three-fold from 800 to 900 F down to -320 F, along with decreasing notch/smooth strength ratios. These trends were anticipated from published data on annealed sheet stock. The Ti-5Al-2.5Sn alloy exhibited the best notch toughness behavior, especially at -320 F.

Notch/smooth strength ratios considerably less than unity were obtained for the two strongest alloys (Ti-8Al-1Mo-1V and Ti-6Al-4V) at -320 F and occasionally

TABLE XII

EFFECT OF FOIL THICKNESS ON MECHANICAL PROPERTIES OF TITANIUM ALLOY FOILS (Ref. 42)

Grade	Gage (in.)	Tensile Strength (psi)	Yield Strength (psi)	Elongation (%)
C120AV Ti-6Al-4V	0.002	152,000	125,000	10
	0.004	149,000	125,000	10
	0.006	148,000	125,000	10
	0.008	145,000	125,000	10
	0.010	142,000	125,000	10
A55 Commercially Pure	0.002	82,000	65,000	18
	0.004	80,000	62,000	20
	0.006	78,000	60,000	22
	0.008	78,000	60,000	24
	0.010	77,000	59,000	26
A70 Commercially Pure	0.002	99,000	75,000	18
	0.005	95,000	74,000	20
	0.008	93,000	74,000	23
	0.010	90,000	74,000	25

at room temperature. It was felt that the practical significance of this trend toward increasing notch sensitivity with decreasing test temperature would be revealed in Phase II foil component testing.

Some minor variations in strength and notch toughness were recorded with differences in test direction (i.e., transverse versus parallel orientation to rolling direction). However, elastic moduli (RT) definitely were greater in the transverse direction in all cases due to anisotropy effects. Possible future advantages might be taken of this directional behavior in component assembly for highest possible rigidity.



0.006 inches thick x 6 inches wide
Rodney Metals Mill Order

FIGURE 1.

DIMPLES AND WRINKLES IN AS-RECEIVED Ti-5Al-2.5Sn ALLOY FOIL



0.010 inches thick x 6 inches wide
Rodney Metals Mill Order

FIGURE 2.

CORRUGATIONS IN AS-RECEIVED Ti-8Al-1Mo-1V ALLOY FOIL

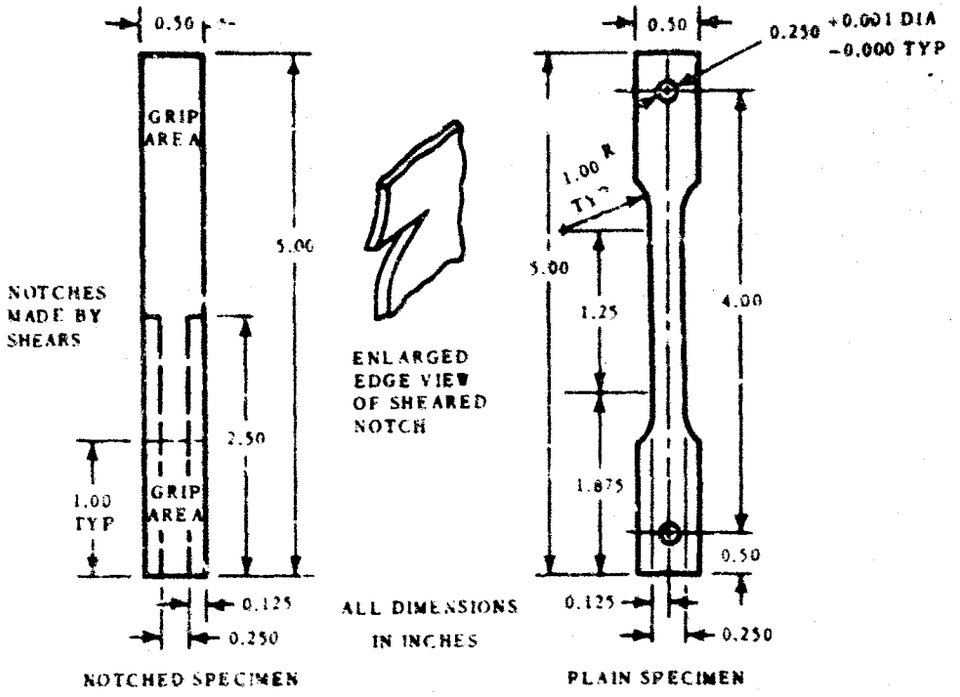


FIGURE 3. FOIL TENSILE TEST SPECIMENS

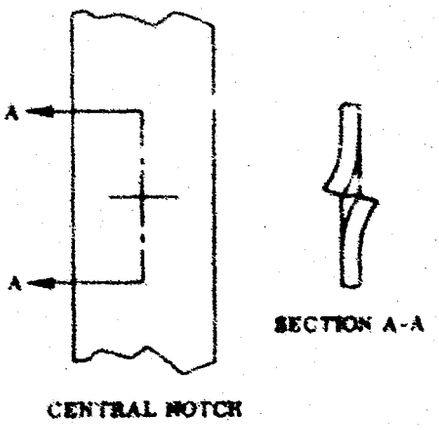


FIGURE 4. CENTRAL-SHEARED NOTCH TENSILE SPECIMEN

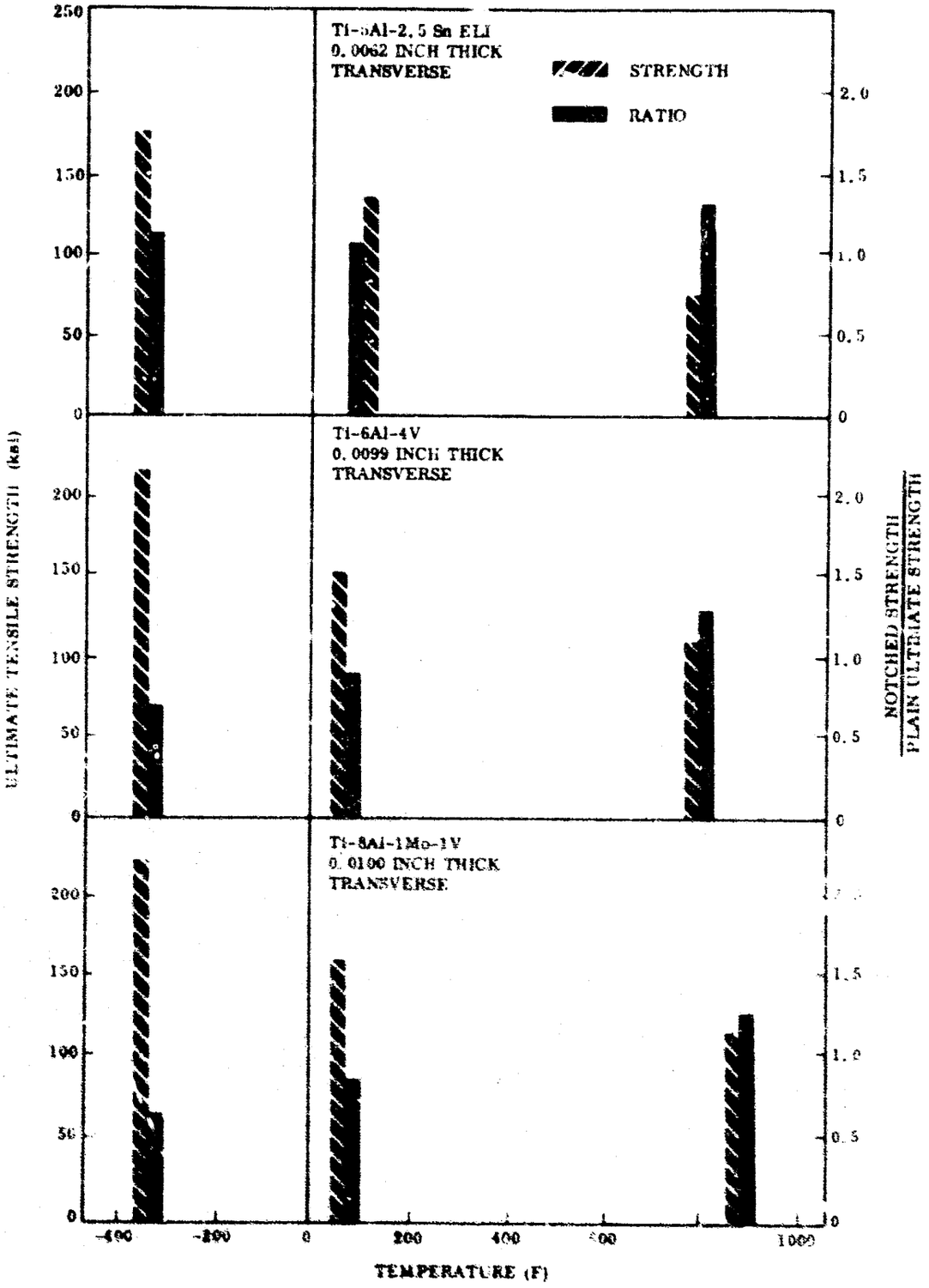


FIGURE 5. ULTIMATE TENSILE STRENGTH OF TITANIUM ALLOY FOILS

3.3 TASK II - EFFECT OF SIMULATED BRAZE CYCLE EXPOSURE UPON FOIL

The original intent of Task II was to determine the degree of degradation in foil strength and toughness levels caused by the thermal cycling associated with typical brazing and diffusion bonding processes. In this way, it was hoped that practical limits could be placed upon bond process time and temperature parameters to ensure adequate retention (75 to 80 percent) of original foil strength and toughness levels for each foil alloy in the main body of the foil structure. It was anticipated that charts similar to the hypothetical one shown in Figure 6 could be developed from test data to indicate safe limits of bond-process temperature and time. (Gradual deterioration of foil properties was expected during thermal cycling due to progressive foil contamination from process environment, recrystallization, grain growth effects, and beta embrittlement at temperatures above each foil alloy's beta transus.)

Early work was carried out to establish safe process limits along these lines of thought. Unnotched tensile specimens of 0.006-inch Ti-5Al-2.5Sn and 0.010-inch Ti-6Al-4V foils were subjected to simulated vacuum braze cycles in the temperature range of 1700 to 1900 F for times of 5 to 30 minutes. The minimal effects of these simulated high-temperature braze cycles (very near the beta-transus temperatures) upon yield strength and tensile strength levels are shown in Figures 7 and 8.

About the same time, it was learned in concurrent work evaluating candidate braze systems that the joint structures and mechanical properties of program foils are vulnerable to much more severe and rapid degradation by the action of the liquid braze materials alone. These factors, including progressive erosion and dissolution of foils and beta-embrittlement of braze-affected foils, were observed to occur in the lower range of process temperatures (~ 1600 to 1700 F), becoming serious problems for process times ≥ 10 to 20 minutes. The threshold temperature of the undesirable braze/foil reactions, several hundred degrees below the foil alloys' beta transus temperatures, were well below the process temperatures which might reasonably be expected to cause significant thermal degradation of foil properties.

In view of the preceding discussion, it became evident that:

- Extensive study of bonding process time-temperature effects on foils would not be pertinent because of more serious limitations on bonding parameters imposed by the more promising candidate braze materials themselves (viz., through foil erosion and chemical-structural modification of foils).

- Curves of the effect of high process temperatures and extended process time on the mechanical properties of program foils were no longer of primary importance to optimize eventual joining processes.

Therefore, the test program for Task II was modified to the schedule shown in Table X. The program was designed to complement the evaluation of the as-received mechanical strength and toughness properties of the program foils, and to compare these properties with the properties after simulated brazing at probable safe maximum process temperatures (based on aforementioned braze evaluation studies).

Test specimens of all foil and tube alloys were mechanically tested at three temperatures, both before and after a simulated braze cycle. The braze-cycled foils were tested in tension (notched and unnotched) in direction transverse to the direction of rolling (Fig. 3). Testing temperatures were -320 F, ambient temperature, and an elevated temperature listed in Table X. The procedure for tensile testing tubes was similar to that used for testing foils, but with loading only in the direction of the axis and without notches (Fig. 9).

The braze cycles were simulated by heating tensile test specimens in a cold-wall vacuum furnace (1.0×10^{-5} Torr) at a rate of 100 degrees F/minute from 1000 F to the braze temperature, holding 20 minutes, then cooling at a rate of 50 degrees F/minute to 1000 F. The simulated braze temperatures chosen for test were approximately 50 degrees F below the beta transus temperatures for each program alloy foil or tube. These simulated braze temperatures were:

Program Alloy	Simulated Brazing Temperature (F)
Ti-5Al-2.5Sn (0.006 in.)	1850
Ti-6Al-4V (0.010 in.)	1775
Ti-8Al-1Mo-1V (0.010 in.)	1850
Ti-3Al-2.5V (0.002 in. wall)	1675
Ti-3Al-2.5V (0.006 in. wall)	

TABLE XIII

TENSILE TEST DATA FOR TITANIUM ALLOY FOILS FOLLOWING SIMULATED BRAZE CYCLES

Material	Simulated Braze (F)	Test Temp. (F)	Yield Strength (psi)	Ultimate Strength (psi)	Elastic Modulus (psi x 10^{-6})	Notch To Avg Yield Strength Ratio	Notch To Avg Ultimate Strength Ratio
Ti-5Al-2.5Sn ELI (0.0062 Inch Thick)	1850	75	109,000	119,000	16.4	1.54	1.41
	1850	-320		199,000			1.12
	1850	600		70,000			
	1850	800		70,000			1.19
Ti-6Al-4V (0.0099 Inch Thick)	1775	75	122,000	134,000	16.6	1.26	1.14
	1775	-320		207,000			0.85
	1775	800		106,000			1.09
Ti-8Al-1Mo-1V (0.0100 Inch Thick)	1850	75	134,000	139,000	18.0	1.28	1.23
	1850	-320		220,000			0.79
	1850	900		91,000			1.18

All values are for specimens cut transverse to rolling direction

The tensile test results are summarized in Table XIII and graphically compared with test data for program foils in the as-received (mill-annealed) condition in Figures 10, 11, and 12. All room and elevated temperature tests were conducted in air atmosphere.

The results for the Ti-5Al-2.5Sn alloy show very little change in strength properties or notch sensitivity due to the simulated braze cycle, as anticipated for this alloy. One exception is the -320 F strength, which was increased from an average 177,000 psi to 199,000 psi (Fig. 12). Both the Ti-6Al-4V and the Ti-8Al-1Mo-1V heat treatable alloys experienced minor decrease in strength and notch sensitivity of room temperature following the simulated braze cycle. These changes were expected due to the effective annealing of the alloys at the simulated braze temperatures. Also, both the Ti-6Al-4V and Ti-8Al-1Mo-1V showed improvement in elastic modulus at room temperature following the simulated braze cycle (Fig. 10). A possible explanation for modulus increase in the transverse direction might be the more pronounced α-phase texturing due to annealing effects at the braze temperature, hence intensified anisotropy. As-received foils all have exhibited higher elastic modulii in the transverse test direction.

TABLE XIV

PROPERTIES AND ANALYSIS OF Ti-3Al-2.5V TITANIUM ALLOY TUBING

Alloy	Ti-3Al-2.5V	Ti-3Al-2.5V	
Form	Seamless Tubing	Seamless Tubing	
Size	0.125 inch O.D. x 0.003 inch wall	0.125 inch O.D. x 0.006 inch wall	
Ultimate Tensile Strength	93,200 psi 83,300 psi	94,700 psi	
Elongation, 2 inch	14% 16%	12%	
Chemical Analysis	**Heat Number 30095**	**Heat Number 30095**	
Al	3.1%	3.1%	
V	2.5%	2.5%	
O_2	0.11%	0.11%	
H_2	16 ppm	16 ppm	
N_2	0.01%	0.01%	
C	0.05%	0.05%	
Ti	Balance	Balance	

The decrease in strength and notch sensitivity following braze cycling of the Ti-6Al-4V alloy extended to -320 F. At 800 F, strength and notch sensitivity remained essentially unchanged. No change in strength was noted for the Ti-8Al-1Mo-1V alloy at -320 F but a slight gain in notch toughness was effected by the braze cycle. At 900 F, average foil strength dropped from 114,000 psi to 91,000, although notch sensitivity did not change.

It should be noted that the modest improvements in foil notch toughness at room and cryogenic temperatures due to the braze thermal cycles more than compensates for the rather minor losses in foil strength. In general, it can be concluded that the braze cycles tested, representing safe maximum process limits, do not significantly impair foil strengths or notch toughness levels in braze unaffected zones.

Tensile tests were performed on Ti-3Al-2.5V titanium alloy tubes obtained from Superior Tube Company (Table X). The objectives of the tests were to determine the baseline strength of the tubes and the change in strength caused by the safe maximum braze time-temperature cycles. The chemical compositions and tensile strengths of the Ti-3Al-2.5V tubing, as certified by the supplier, are given in Table XIV.

The average cross-sectional (load carrying) areas of the tubes were calculated from precision weight and length measurements using a density value of 0.162 pound/cubic inch as given in Reference 43.

The tubes when subjected to a simulated braze cycle, were heated at a controlled rate of 100 degrees F/minute to a temperature of 1675 F, held at this temperature for 20 minutes, cooled at a rate of 50 degrees F/minute to 1000 F, and then furnace cooled to room temperature. The cycles were performed in a cold wall vacuum furnace with typical vacuums of 5×10^{-6} Torr.

The tubes were gripped with Swagelock stainless steel tube fittings as shown in Figure 9. Solid end plugs (also shown in Figure 9) were inserted into the tubes in the region of the fittings to prevent the fittings from collapsing the tubes. During loading, the tendency of the tubes to reduce in diameter caused the plugs to carry some of the end load, thereby assuring that all ultimate tube failures would occur near the center of the tube test section.

The ultimate strengths were determined at three test temperatures: -320 F, room temperature, and 600 F: and the results are shown in Table XV and in Figure 13. All failures occurred in the center section of the tube specimens. Also shown in Figure 13 for comparison are typical tube strength data obtained from DMIC Memorandum 171 (Ref. 43).

At room temperature, the as-received 0.006-inch thick tubes were 26 percent stronger than the 0.002-inch thick tubes. At -320 F, the strength differential amounted to 11.0 percent; at 600 F, 52 percent; indicating significantly greater recovery response to mill-annealing by the more heavily worked 0.002-inch thick wall tubing. The 0.002-inch thick tube strength at room temperature was closest to the typical value given in DMIC Memorandum 171 (Ref. 43).

The simulated brazing cycles had only a small effect on the ultimate strengths of the tubes, as was expected with this non-heat treatable alloy. The strengths of the 0.002-inch thick tubes were improved slightly by the simulated braze cycle, compared to a slight decrease in strength for the 0.006-inch thick tubes.

TABLE XV

ULTIMATE STRENGTHS OF Ti-3Al-2.5V ALLOY TUBING

Specimen No.	Condition As Rec'd (R) Simulated Braze (S)	Wall Thickness (Inches)	Test Temp. (F)	Ultimate Strength (psi)	Average Ultimate Strength (psi)
T-1	R	0.0017	75	92,000	
T-2	R	0.0017	75	92,000	92,000
T-3	R	0.0017	75	92,000	
T-10	R	0.0017	-320	168,000	
T-11	R	0.0017	-320	170,000	170,000
T-12	R	0.0017	-320	173,000	
T-16	R	0.0017	600	49,000	
T-17	R	0.0017	600	53,000	48,000
T-18	R	0.0017	600	46,000	
T-7	S	0.0018	75	98,000	
T-8	S	0.0017	75	95,000	96,000
T-9	S	0.0017	75	95,000	
T-13	S	0.0016	-320	180,000	
T-14	S	0.0017	-320	182,000	182,000
T-15	S	0.0017	-320	182,000	
T-19	S	0.0017	600	52,000	
T-20	S	0.0016	600	50,000	52,000
T-21	S	0.0017	600	55,000	
T-4	R	0.0057	75	120,000	
T-5	R	0.0057	75	114,000	116,000
T-6	R	0.0057	75	113,000	
T-27	R	0.0056	-320	188,000	
T-28	R	0.0057	-320	188,000	188,000
T-29	R	0.0056	-320	187,000	
T-33	R	0.0057	600	73,000	
T-34	R	0.0056	600	74,000	73,000
T-35	R	0.0057	600	73,000	
T-24	S	0.0057	75	109,000	
T-25	S	0.0057	75	110,000	109,000
T-26	S	0.0056	75	107,000	
T-30	S	0.0057	-320	184,000	
T-31	S	0.0057	-320	185,000	185,000
T-32	S	0.0056	-320	187,000	
T-36	S	0.0056	600	66,000	
T-37	S	0.0057	600	67,000	66,000
T-38	S	0.0056	600	66,000	

Superior Tube Company - No. 3 Temper

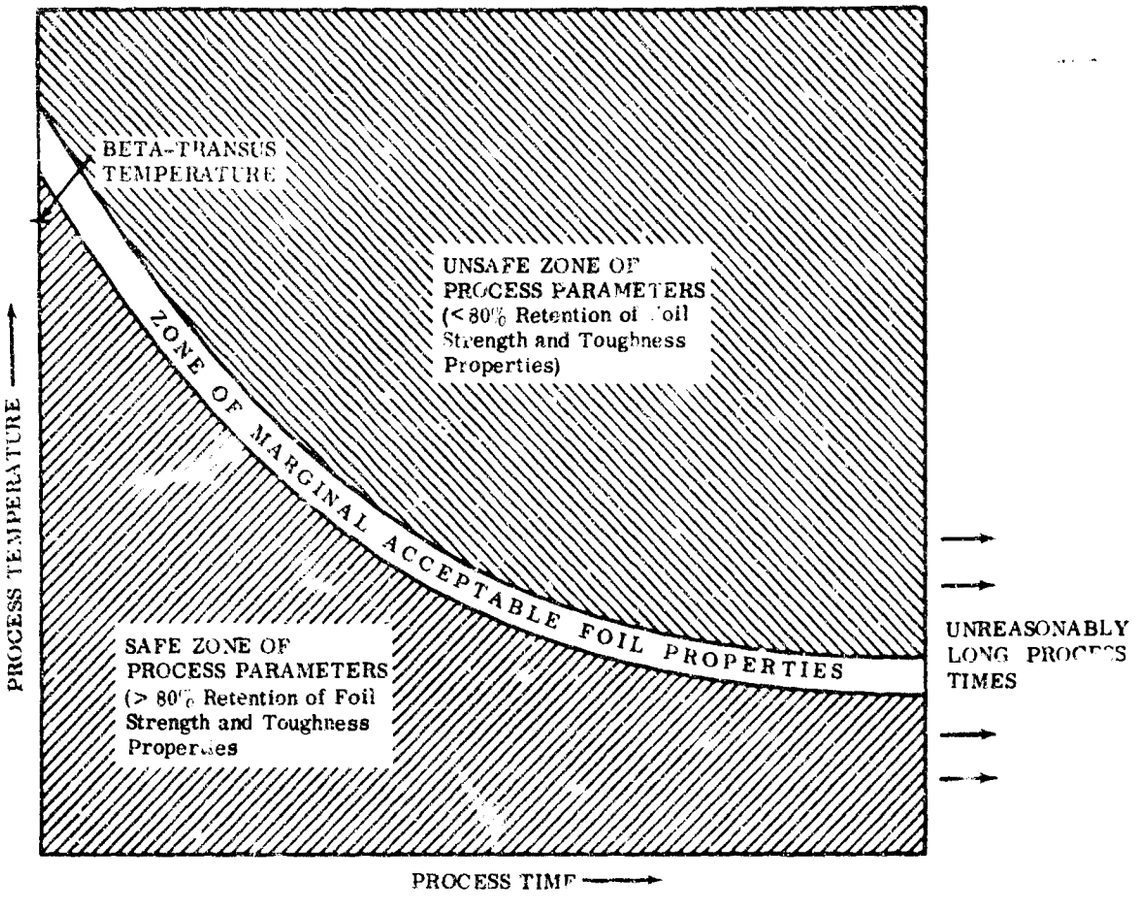


FIGURE 6. HYPOTHETICAL SAFE LIMITS OF BOND PROCESS TIME VERSUS TEMPERATURE

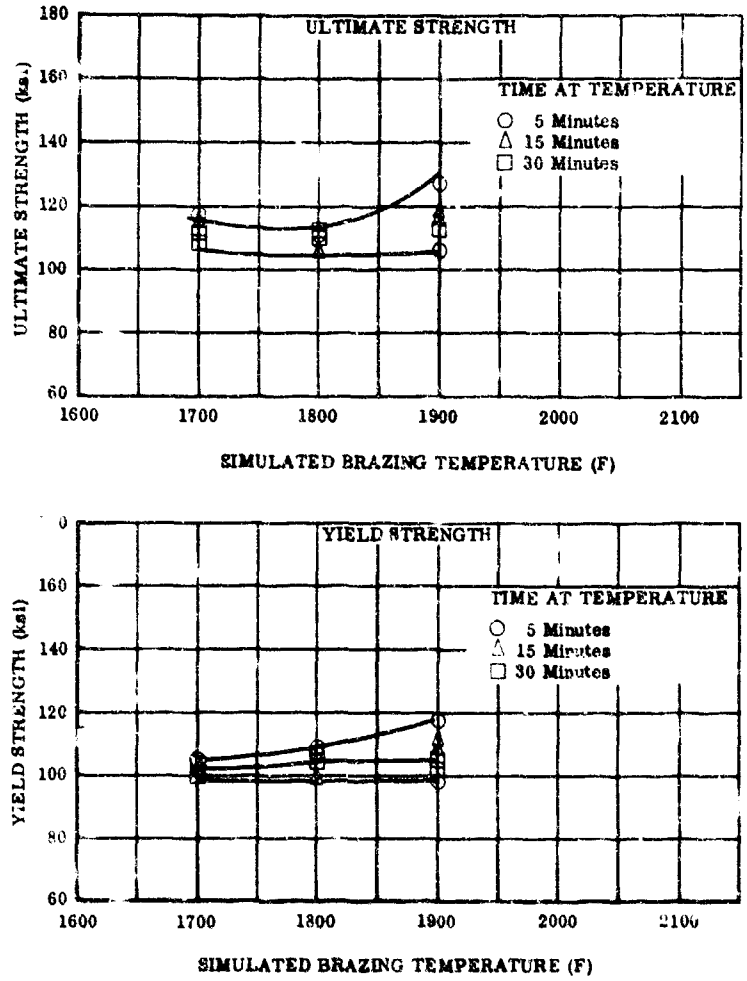


FIGURE 7. EFFECTS OF SIMULATED BRAZE CYCLES ON STRENGTH PROPERTIES OF 0.006-INCH Ti-5Al-2.5Sn FOIL

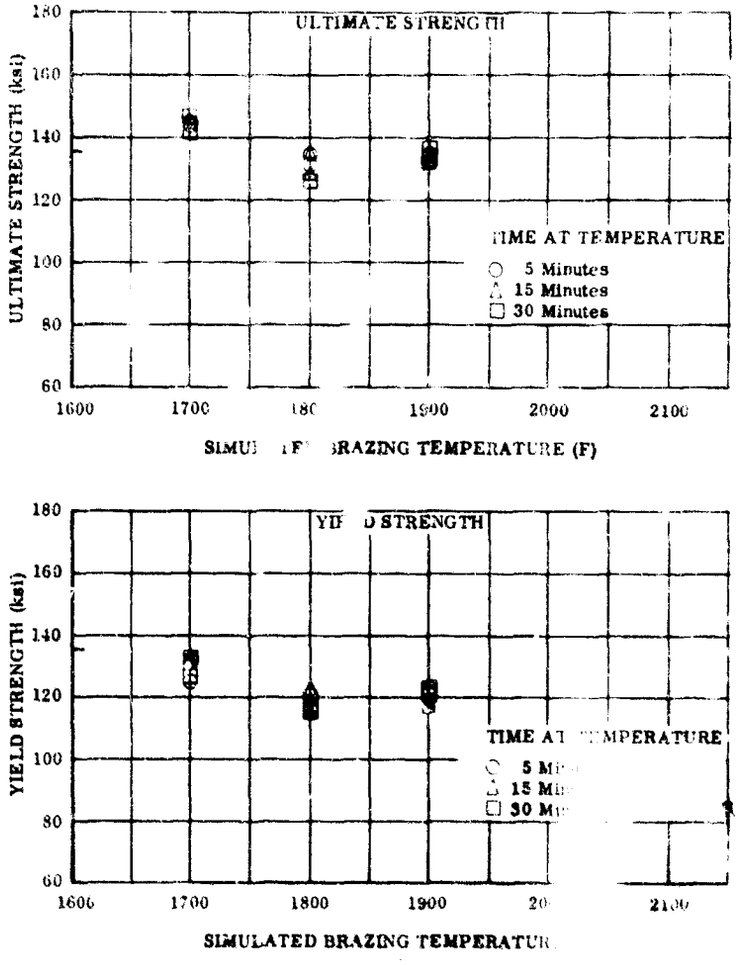
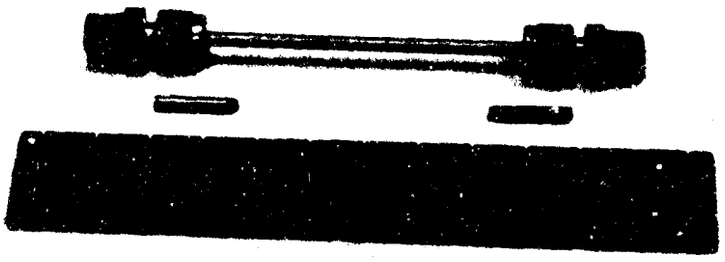


FIGURE 8. EFFECTS OF SIMULATED BRAZE CYCLES ON STRENGTH PROPERTIES OF 0.010-INCH Ti-6Al-4V FOIL



PLUGS FOR CENTER OF TUBES ARE SHOWN NEXT TO THE GRIPS

FIGURE 9. TUBE SPECIMEN AND END FITTINGS FOR TENSILE TESTING

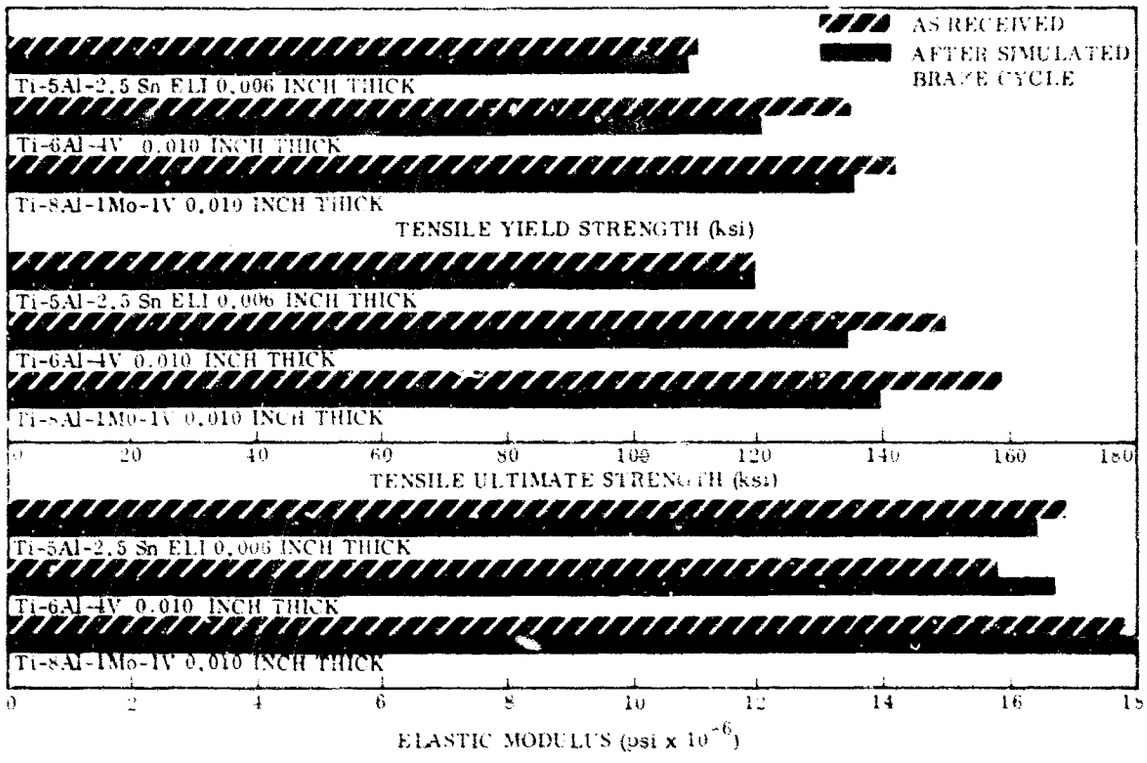


FIGURE 10. ROOM TEMPERATURE MECHANICAL PROPERTIES OF TITANIUM ALLOY FOILS

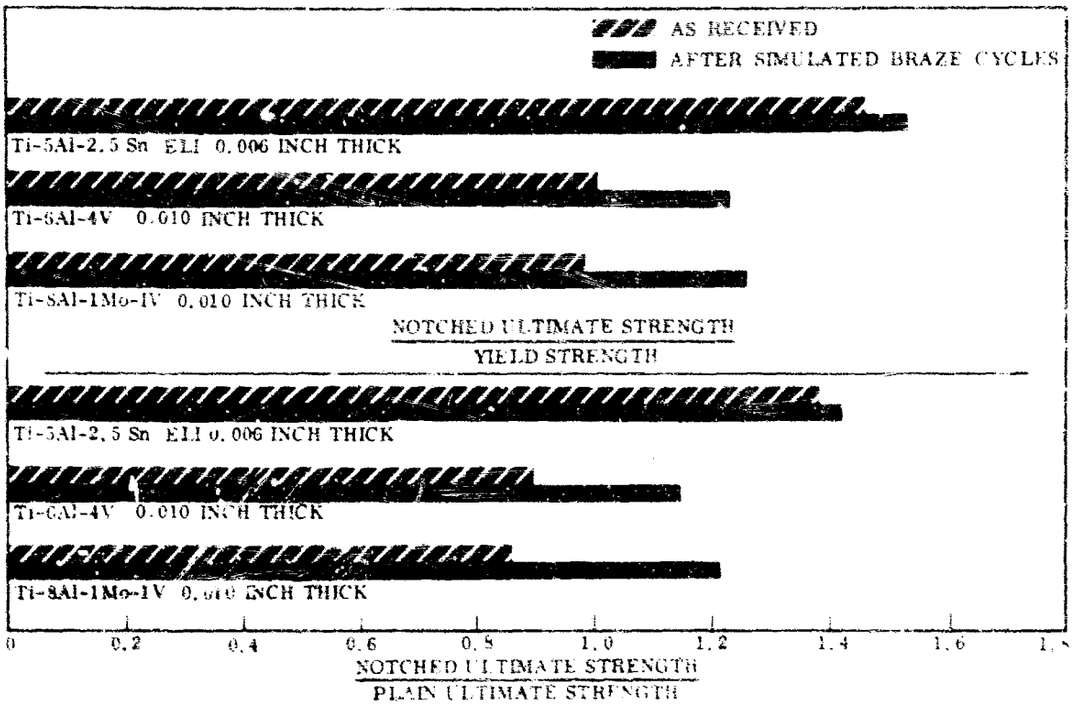


FIGURE 11. ROOM TEMPERATURE NOTCH STRENGTH RATIOS OF TITANIUM ALLOY FOILS

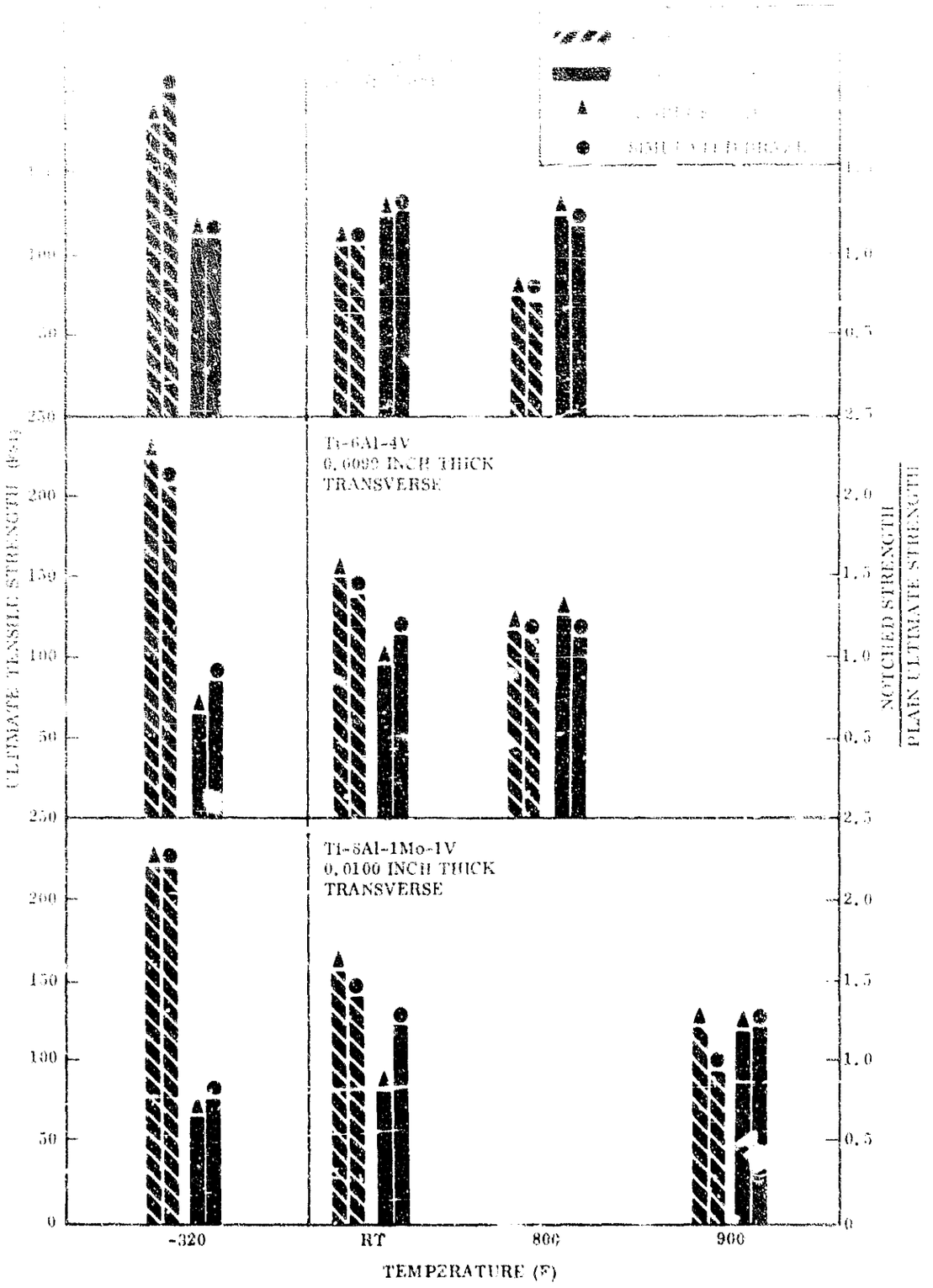


FIGURE 12. ULTIMATE AND NOTCHED TO PLAIN ULTIMATE STRENGTH RATIOS OF TITANIUM FOILS

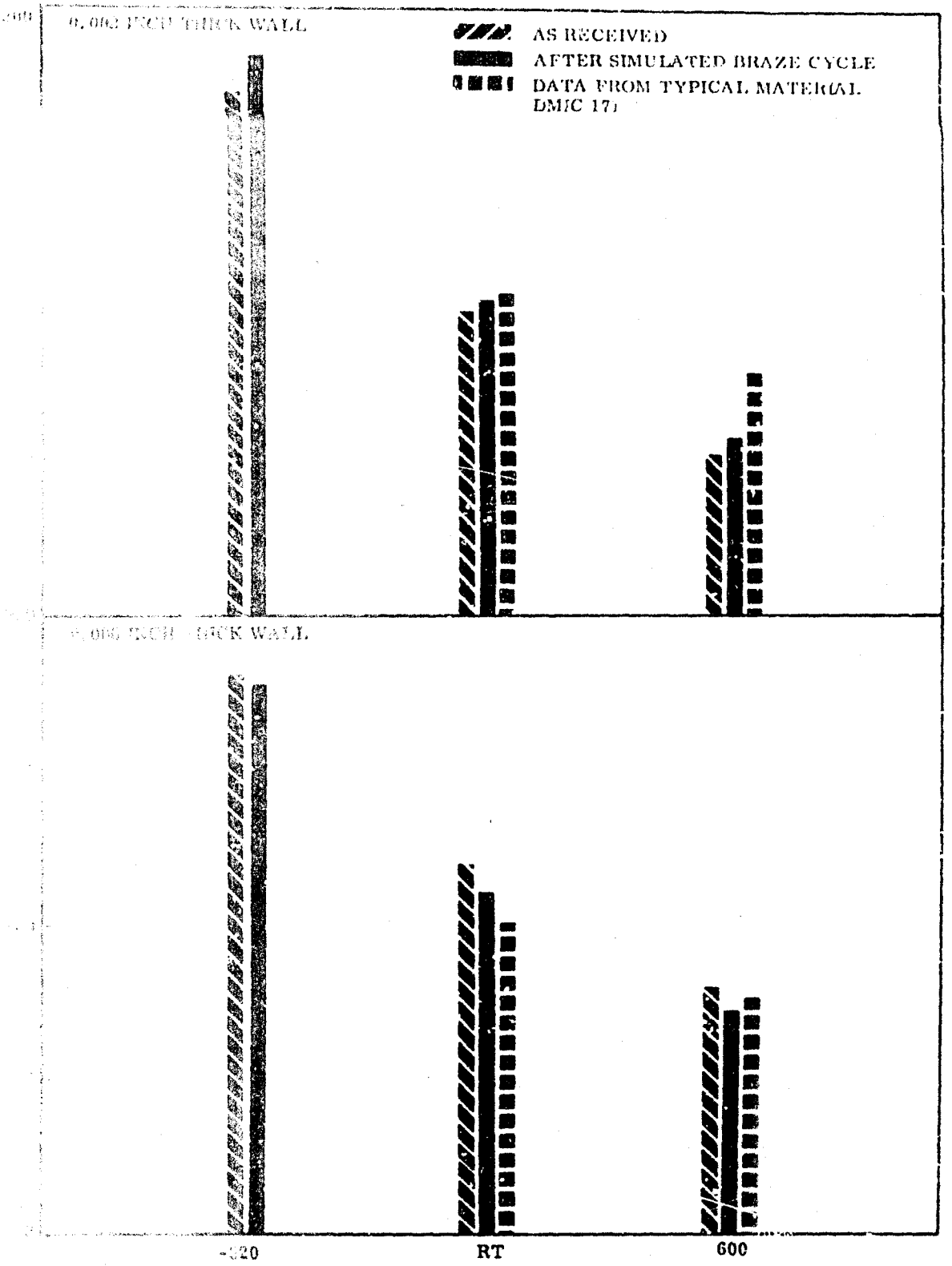


FIGURE 13. ULTIMATE STRENGTHS OF Ti-3Al-2.5V TUBING

3.3 TASK III - SELECTION OF CANDIDATE BONDING AND BRAZE ALLOY SYSTEMS

Ideally, every titanium-foil structure should be made integrally from a single piece of foil (or other metal shape) thereby eliminating the need for artifically produced joints. However, since this concept is still beyond the state of the art for such complex aerospace structures as thin foil heat exchangers and honeycomb panels, it is necessary for joining methods to be developed which can tie together the required foil components in such a manner as to approximate an integral structure. The study of joint structural requirements, therefore, is really the logical study and evaluation of permissible compromises made in component strength, stability, toughness, and corrosion-resistance for the sole purpose of permanently bonding an assemblage of foils into a single unit. The proper balance of compromises produces the optimum fabricated structure. In general, the categories of joint strength, toughness, dimensional and metallurgical stability, corrosion resistance, and weight penalties are of prime importance to titanium foil structures.

3.3.1 Corrosion Resistance of Joints

Severe corrosive attack of titanium alloys by aerosol or fused salt media containing halide salts or dissolved halogens is undoubtedly the most serious problem threatening the general application of brazed titanium foil structures. Little is known of the corrosion mechanism except that it is essentially galvanic by nature. However, practical experience has shown that dissimilar metal joints, especially those brazed with the currently popular silver-base alloys, are particularly susceptible to crevice-type corrosion (RT to 200 F). Silver-brazed titanium T-joints commonly fail catastrophically after 10 to 15 hours exposure to 200 F salt spray (unstressed condition) and, as shown in Figure 14, crevice-corrosion failure normally occurs along the Ti/TiAg interface. This degree of joint deterioration would be intolerable in both the heat exchanger and honeycomb structures. Rather, the joints must remain sound and leak-tight for extended periods of operation. This structural requirement is of extreme importance.

3.3.2 Joint Strength and Toughness

The nominal design stresses imposed upon joints in typical foil heat exchangers (through internal pressurization or pressure differentials) and honeycomb panels (chiefly through flexure) are quite low. However, very high transient stresses of indeterminate magnitude can be experienced in localized joint regions due to severe

Best Available Copy

thermal gradients and/or aerodynamic shock loads encountered in normal service. The effect of such transient stresses can be intensified by virtue of the natural stress concentrations imposed by the typical (angular) joint geometries and their intrinsic rigidity (Fig. 15 and 16), and by internal stress concentration due to microcracks formed at moderate stress levels in relatively hard, high-modulus, secondary phases of filler materials (e.g., the TiAg phase encountered with silver-base braze alloys or beryllides in Ti-Zr-Be braze alloys).

Consequently, it becomes imperative that joint matrices achieve a proper balance between strength and toughness. High strength, approaching that of the parent foil, is desirable to resist permanent joint deformation and resultant component distortion during periods of high transient stress and also to better combat thermal fatigue failure. A good matrix toughness rating is equally desirable to minimize the likelihood of stress concentration cracking and premature joint failure. Solar's concern with joint strength and toughness was reflected in the choice of the test specimen types to screen candidate bonding systems; the T-joint tensile test specimen (Fig. 17) and the double-lap joint peel test specimen (Fig. 18). Both tests measure relative joint strength and toughness under conditions simulating the stress fields and natural geometric stress concentration found in foil structures.

3.3.3 Dimensional and Metallurgical Stability

Honeycomb panels and heat exchanger structures are required to have precisely controlled external dimensions. Therefore, it follows that suitable joining methods must be perfectly adaptable to the exact fit-ups and carefully tailored dimensions of a precision assembly. To avoid progressive thermal distortion and joint-mismatch in the making of thousands of interconnected and interrelated joints, it becomes advisable to accomplish all of the joints simultaneously. This is feasible on a large scale only through brazing and, in certain instances, diffusion bonding. Even these joining techniques may contribute to dimensional instability if process heating and cooling rates cannot be made uniform throughout the foil structure. As a result of this situation, dimensional control can readily be lost through non-simultaneous joining and by thermal distortion or warpage of the erratically joined integral structure. Excessive liquid braze erosion of foil faying surfaces can also create problems of dimensional stability by consuming variable amounts of foil length, thereby disrupting or weakening joint areas and changing critical component dimensions.

Metallurgical instability is a different problem which arises from undesirable foil structural changes occuring during heat treatment associated with the joining process or due to foil/braze (or foil/interleaf) interaction. A good example of metallurgical instability derived from process heat treatment is beta embrittlement of foils, related to beta-phase grain growth and second-phase dissolution and subsequent reprecipitation effects in the all-beta field (e.g., > 1850 F for Ti-6Al-4V foil or > 1900 F for Ti-8Al-1Mo-1V, and Ti-5Al-2.5Sn foils). The braze cycle simulation work previously described was designed to characterize this problem. Foil instability arising from foil/braze interaction may be evidenced by regions of high hardness and embrittlement in the braze-affected foil resulting from undesirable beta transformation products on cooling (e.g., omega, alpha-prime, or equilibrium alpha phase extensively hardened by interstitial element absorption). The Ti-8Al-1Mo-1V alloy is also susceptible to an alpha-ordering phenomenon, particularly intense when contaminated with alpha-stabilizing interstitials picked up during joining, leading to losses of strength and ductility and increased susceptibility to salt corrosion. It follows, therefore, that the joining process itself must not act to induce instability of either kind.

3.3.4 Weight and Process Considerations

The task of making foil joints incurs a penalty in the form of braze alloy weight or interleaf material weight (diffusion bonding). The single possible exception is self-diffusion bonding which appears feasible only for tube-to-header joints, characteristically possessing large, well-supported faying areas. (Honeycomb core-to-face sheet joints, as well as plate-to-fin joints do not adapt well to diffusion bonding parameters of high stress-temperature because of the extreme flexibility and low buckling resistance of these structures.)

Typical weight penalties range from 0.5 to 1.0 percent of total structure weight for diffusion bonding or in-situ brazing, and up to as much as 3.0 to 5.0 percent of total weight for conventional powder or foil-type braze loading. The objective in all cases is to provide 100 percent bonding of all faying surfaces with the formation of the smallest useful fillet (i.e., minimal fillet brazing). The overly large fillet in foil joints is usually superfluous from a design standpoint, yet contributes most to braze weight.

In-situ brazing requires the best fit-ups (as precise as for diffusion bonding) but definite advantages accrue in weight saving. Ideally, the in-situ braze process puts a thin layer of braze alloy solely on the faying surfaces in sufficient quantity to just bridge the fit-up gap with minimal flow and filleting. Examples could include Ni-P eutectic braze alloys plated (Kanigen plating process) upon faying surfaces (0.0001 inch thick) or very fine powders of friable braze alloys slurry-coated upon faying surfaces (0.0001 inch thick). Additional processing advantages of in-situ brazing are:

- Heating rate of the brazing temperature is not usually cricital inasmuch as only short-path braze flow and negligible filleting are required. This situation eases the normally difficult process and equipment requirement for rapid heating, and thereby minimizes the likelihood for thermal distortion. (The in-situ process guide line is most applicable to plate-and-fin heat exchanger technology where heating rates are naturally and unavoidably slow, and faying surface fit-ups have to be near perfect regardless of brazing technique.)

- Further weight savings can be achieved in the case of honeycomb brazing inasmuch as node flow can be avoided entirely through minimal braze loading. Normally, diffusion bonded or resistance welded node joints require no further reinforcement by brazing.

Conventional braze loading consists simply of placing braze alloy powder or wire immediately adjacent to the joint faying surfaces. Normal liquid flow and filleting carries the braze material into the joint area. Obvious advantages of conventional braze loading are:

- High precision fit-ups are not mandatory, although usually desirable to minimize distortion.

- Loading technique is relatively simple and inexpensive, contrasted with the in-situ loading technique.

- Conventional nondestructive inspection methods can be used to ensure quality.

A less obvious, but very real, advantage of conventional loading is that the large fillets produced help to lower applied stress levels (buttressing effect) and reduce stress concentrations in braze joints. For example, in a honeycomb panel, both core-face sheet joints and node joints would be benefitted by the heavier flow. This advantage can be beneficial to brazement reliability, especially in braze systems characterized by potentially embrittling interfacial compound formation (e.g., the TiAg intermetallic in silver-base systems) or random occurrence of massive intermetallic phases (e.g., titanium beryllides in the TiBe system).

The weight problem and associated bond process problems of variably "precise" fit-ups, heating-rate sensitivity, and braze loading techniques (with their individual advantages and disadvantages) had to be considered in selecting the most promising bonding systems for study. A distinct advantage resides with the more versatile braze alloys which can operate well in either in-situ or conventional braze situations, and are relatively insensitive to normal (design-imposed) variations in heating rate, braze loading, and degree of fit-up. Such versatility permits wider tolerances for process parameters, a larger measure of bond process control, and more reliable foil joints. Varying the braze load also permits some control over the weight penalty. Additional advantages in weight reduction accrue to the less dense braze alloys, such as the newer varieties of Ti- or Zr-base, as contrasted with those of Ag- or Pd-base. The relative densities of these elements are:

Element	Density (gm/cc)
Ti	4.51
Zr	6.49
Ag	10.49
Pd	12.02

3.3.3 Analysis of Foil Brazing Problems

The currently available braze systems used to join titanium suffer from the fact that they were not devised specifically for the unique metallurgical problems of titanium alloys. For example, braze alloys based upon the two eutectics in the Ti-Ni binary system, Ti-66Ni (2040 F) and Ti-28Ni (1725 F), have been evaluated by industry (Ref. 44). The high titanium levels ensure good self-fluxing ability and fluidity. The principal problem with the high-nickel variety is rapid and severe erosion of the titanium alloy foils (>2050 F) due to the tendency of the liquid braze to dissolve foil to more closely approach thermodynamic equilibrium. This tendency has been observed to be aggravated at brazing temperatures ≥ 1750 F for similar nonequilibrium systems. The lower temperature Ti-28Ni eutectic braze alloy shows much reduced erosion tendency because the liquid braze can coexist under quasi-equilibrium conditions with the terminal titanium solid solution at or just above the eutectic temperature (1750 to 1775 F). However, upon braze solidification, the preponderant phase in volume percent is the brittle intermetallic Ti_2Ni, which creats a poor engineering structure.

To minimize brittle intermetallics and erosion problems, most investigators have resorted to silver-base braze alloys with doubtful success (Ref. 45 and 46). Typical silver-base braze alloys used in production brazing of titanium are Ag-5Al-0.2Mn (1650 F), Ag-2Li (1400 F), Ag-10Sn (1700 F), and Ag-28Cu-0.2Li (1500 F). In high vacuum or gettered argon atmosphere, these silver-base alloys flow well on titanium surfaces without flux. The rapid formation of the semi-ductile intermetallic, TiAg, at the braze/substrate interface acts as a physical barrier to titanium erosion. The TiAg phase has quite good adhesion, but a lower coefficient of expansion than either braze or foil. Consequently, on cooling, cleavage cracks frequently form within the interface region. An even more serious problem has been crevice corrosion cracking in marine atmosphere and industrial environments (requiring several weeks or months to be evidenced at ambient temperature). Crevice corrosion cracking along the Ti/TiAg interface takes place in silver alloy brazements (frequently in an insidious manner) that are difficult to detect without handling the parts. The interface corrosion can be accelerated by salt spray testing (5%NaCl, 200 F), requiring 10 to 15 hours of spray exposure. Apparently, the problem arises from a strong surface electromotive force potential generated between the TiAg/Ag or TiAg/Ti couples (Fig. 14)

Another metallurgical problem to consider in titanium foil brazing is that of preventing beta embrittlement. Prolonged heating above the beta transus temperatures[1] of most commercial titanium alloys gives rise to a matrix structural change termed "beta embrittlement", characterized by low ductility and low notch toughness levels. The coarse-grained Widmanstatten structures generated are somewhat harder and considerably less ductile than the former equilibrium or heat treated structures. They are caused by a combination of beta grain growth, absorption and redistribution of interstitial element contaminants, and formation of nonequilibrium beta transition products on cooling. Prevention is the best remedy for beta embrittlement. Therefore, it is imperative that titanium foil brazing be conducted well below each foil alloy's beta transus temperature and that the effective beta transus of braze-affected foil not be lowered significantly (by progressive absorption of beta-stabilizing elements from the braze; e.g., by zirconium, nickel, or silver).

---

1. Approximate beta transus temperatures:

Ti-8Al-1Mo-1V	1990 F
Ti-5Al-2.5Sn	1900 F
Ti-6Al-4V	1850 F

It should be emphasized that the four principal metallurgical problems consisting of crevice corrosion, liquid-metal erosion, beta embrittlement, and undesirable intermetallic compound formation are valid for titanium joining per se, but are greatly magnified for the condition of joining foils. This is true because of the enlarged faying surface (i.e., reaction surface) to bulk volume ratios for foils; making foil joints much less able to accommodate the adverse effects of corrosion, erosion, contamination, and unfavorable structural changes than similar joints in heavier sheet and plate.

3.3.6 Proposed Approach to Problem Solutions

The rationale supporting the development of improved braze systems for titanium alloys was directed primarily at solving the two most serious problems of joint corrosion and erosion. To combat corrosion, it was reasoned that the braze material and the titanium foils should have surface electromotive force potentials as closely matched as possible. This situation would reduce the likelihood of dissimilar metal couples developing electromotive forces of sufficient magnitude to drive potentially corrosive reactions. Consequently, to minimize the surface electromotive force differences between braze microconstituents and titanium foil members, it was decided (in pre-contract work at Solar) to select braze alloy bases that are chemically similar to the foils themselves. This, of course, narrowed the candidate elemental bases to titanium, zirconium, and possibly hafnium. The standard oxidation-reduction potentials of candidate braze bases are shown in Table XVI.

To counteract erosion, it was felt that the liquid braze metal should be in thermodynamic phase equilibrium (or at least approximate equilibrium) with the solid titanium-base foil alloy. To accomplish this end, and also to lower the base alloy braze temperature to decelerate the rate of any liquid/solid interaction, it was decided to evaluate eutectic braze systems of Ti-Be, Zr-Be, and Ti-Zr-Be. These systems were chosen using the criteria of melting point depression, the matched oxidation-reduction potentials, and the likelihood of forming compatible liquid systems which can coexist in a state of actual or quasi-thermodynamic equilibrium with foils. The candidate elements considered are included in Tables XVI and XVII. Beryllium proved to be a nearly ideal melting point depressant for these bases. The first eutectics formed with beryllium for the titanium, zirconium, and Ti-Zr bases - 3.6 to 6.0 weight percent beryllium (Ref. 47 and 48) - provided superior brazing characteristics on foils at process temperatures ≤ 2000 F. The standard surface electromotive

TABLE XVI

STANDARD OXIDATION - REDUCTION POTENTIALS OF CANDIDATE BRAZE ALLOYS

Most Common Valencee	Voltage (v)
$Ti = Ti^{++} + 2e^-$	+1.63
$Ti = Ti^{+4} + 4e^-$	+1.90
$Zr = Zr^{+4} + 4e^-$	+1.53
$Hf = Hf^{+4} + 4e^-$	+1.70
$Be = Be^{++} + 2e^-$	+1.85
$Al = Al^{+++} + 3e^-$	+1.66
$Ni = Ni^{++} + 2e^-$	+0.25
$Cu = Cu^{++} + 2e^-$	-0.34
$Ag = Ag^{+} + e^-$	-0.80
$Pd = Pd^{++} + 2e^-$	-0.83
$Au = Au^{+} + e^-$	-1.68

force of elemental beryllium indicated a suitability for diffusion alloying with both the foil alloys and the titanium or titanium-zirconium terminal solid solutions of the braze (with which the liquid eutectic braze alloys approach thermodynamic equilibrium). Not only are the beryllium solubilities low (≤ 1.0 percent) in the corresponding terminal solid solutions of the solid braze (to ensure minimal changes in chemical activity), but beryllium is only a weak β-phase stabilizer (minimizing the probability of beta transus temperature reduction in braze-affected foil). The effect of the more potent beta stabilizer, zirconium, in braze-affected foil was determined to be minor so long as braze temperatures are maintained ≤ 1700 F. The solid eutectic structures themselves consist of approximately 35 volume percent $TiBe_2$ and/or $ZrBe_2$ arranged in fir-tree dendritic patterns within a continuous matrix phase of the titanium, zirconium, or Ti-Zr terminal solid solution (Fig. 19). It was subsequently shown in prior work at Solar that the eutectic braze structures characterized by continuous, preponderant (65 volume percent) matrices, and an absence of interfacial beryllide films ensure a good measure of braze toughness. The beryllides themselves demonstrated

TABLE XVII

CANDIDATE ALLOYING ELEMENTS FOR PRODUCING TITANIUM - AND ZIRCONIUM-BASE BRAZE ALLOYS

Alloying Element	Melting Point Depression (degree F per 1%)	Maximum Depression (F)	Maximum Depression (% Alloying Element)	Remarks
Titanium-Base				
Aluminum	12.0	468	39	α stabilizer
Beryllium	255.0	1402	5.5	β stabilizer
Cobalt	46.7	1260	27	β stabilizer
Chromium	12.7	594	47	β stabilizer
Copper	31.3	1314	42	β stabilizer
Iron	36.1	1153	32	β stabilizer
Germanium	67.4	1483	22	Mild α stabilizer
Manganese	23.1	981	42.5	β stabilizer
Nickel	48.3	1378	28.5	β stabilizer
Silicon	82.7	702	8.5	Mild β stabilizer
Silver	8.1	558	69	β stabilizer (soluble in α)
Tin	5.9	208	35	Mild α stabilizer
Zirconium	4.0	200	50	β stabilizer
Zirconium-Base				
Aluminum	82.0	902	11	α stabilizer
Beryllium	285.0	1568	5.5	Weak β stabilizer
Cobalt	101.0	1566	15.5	Weak β stabilizer
Chromium	55.1	992	18	Weak β stabilizer
Copper	77.1	1541	20	β stabilizer
Iron	103.0	1644	16	β stabilizer
Germanium	73.7	568	7.7	Mild α stabilizer
Manganese	57.3	1289	22.5	β stabilizer
Nickel	94.4	1604	17.0	β stabilizer
Silicon	149.5	434	2.9	Mild β stabilizer
Silver	36.4	1082	12	β stabilizer
Tin	20.0	470	23.5	α stabilizer

to be corrosion-resistant in the eutectic mix, presumably because of their chemical inertness or matched electromotive forces. Brazements of all eutectic alloys withstood 100 hours of salt-spray exposure (5%NaCl, 200 F) without apparent structural change in prior work at Solar (Fig. 20).

Erosion problems were still apparent with the binary titanium- and zirconium-base alloys in initial brazing experiments. For example, the Ti-5.6Be eutectic alloy gave evidence of progressive foil erosion at the minimum brazing temperature of 2000 F (Fig. 21). Although 2000 F is only 50 degrees F greater than the apparent eutectic temperature (a measure of thermodynamic imbalance), the reaction kinetics are sufficiently rapid at this high process temperature to severely erode and structurally modify the 10-mil Ti-5Al-2.5Sn foils within 5 to 25 minutes at temperature. In addition, the braze-affected foils suffered complete beta embrittlement at the 2000 F process temperature. The lower melting Zr-6.0Be eutectic alloy exhibited a different kind of erosion problem with foils. In just 30 seconds of braze process time at the eutectic temperature of 1810 F, the titanium alloy foils underwent severe liquid metal erosion (Fig. 22). In this case, the underlying cause proved to be related to the liquidus-temperature minimum occurring in the Ti-Zr binary at 50 weight percent Zr (Ref. 47). Experiments at Solar with Ti-Zr-Be ternary alloys (with varying Ti/Zr ratios but constant 5.6 percent Be level) revealed that the minimum in the liquidus temperature (1625 F) for the ternary alloys also occurs at a Ti/Zr ratio of 1.0. Hence, liquid zirconium-rich braze alloy and solid titanium-rich foil are too far removed from thermodynamic equilibrium at 1810 F, and cannot coexist without initially strong interaction and modification (foil erosion).

Reflection upon the methods available to control erosion led to an eventual solution. There are five general methods for controlling erosion:

1. Keep temperature and time to the absolute minimums required for brazing.
2. Use low melting braze alloys to reduce rates of liquid metal attack.
3. Use a minimum quantity of braze alloy.
4. Form continuous interfacial compound with slow diffusion rate at the interface.
5. Use a braze alloy that approaches thermodynamic equilibrium with base metal substrate.

The use of rapid process cycles (Method 1) can be considered in special cases, but was unacceptable as a complete solution for the "heat-shield" type of structure required in this program. Reduction of the melting point of the braze alloy (Method 2) does reduce the erosive rate of attack. However, the strength versus temperature curve for a braze alloy is generally related to the melting point so that a braze alloy melting at 1250 F (braze flow temperature may be 1350 F) cannot be expected to have much strength at 1000 F. Therefore, this approach offered a very limited solution to the problem. (However, the high 2000 F flow temperature of the Ti-Be eutectic represents the other extreme and was equally unsuitable.)

The use of a minimum quantity of braze alloy (Method 3) is required by other factors, including:

- Minimum weight structure
- Efficiency of heat exchanger structure
- Control of braze alloy flow (e.g., node flow in honeycomb sandwich)

Therefore, Method 3 could not be considered an independent variable to control erosion, because the quantity of braze alloy was already controlled for these other reasons.

Method 4 (formation of a compound at the interface) is used in many practical cases. The formation of TiAg at the titanium-silver braze alloy interface has already been discussed. The problem with this type of approach is to find compounds with a modicum of ductility. For this reason, it does not represent a versatile approach.

Method 5 has been used by Solar in the development of nonerosive alloys for brazing refractory metals and titanium. The ideal situation is to braze a solid solution alloy (foil or sheet) with a eutectic braze alloy composed of the same or closely related solid solution plus another component or components in thermodynamic equilibrium. The trouble with the Zr-Be eutectic is that Zr, although chemically similar to Ti, does not provide the required thermodynamic equilibrium between liquid and solid phases.

These early metallurgical studies at Solar led to the obvious solution to both problems occurring with the binary Ti-Be and Zr-Be braze alloys. The problem of erosion due to thermodynamic imbalance of chemical species (Zr/Ti ratios) was solved by employing the balanced ternary eutectic alloy, Ti-47.2Zr-5.6Be. (The absence of the foil erosion tendency is shown in Figure 23.) In addition, the

problem of minor thermodynamic imbalance caused by the typical temperature differential between actual eutectic temperature and minimum flow temperature (normally ~ 50 degrees F) was alleviated by employing the same ternary eutectic alloy. At the quite low minimum brazing temperature of 1650 F, the reaction rate of liquid/solid was shown to be appreciably slower than at 2000 F, so that rapid foil erosion ceased to be a problem. Metallographic examination indicated that neither erosion nor beta embrittlement of program alloy foils occurred to any appreciable degree at 1650 to 1700 F for process times up to 25 minutes (Fig. 24). On the strength of these promising structural and behavioral characteristics, the ternary Ti-Zr-Be eutectic alloy was chosen as the principal base for further alloy studies aimed at optimizing foil joining capabilities.

3.3.7 Selection of Braze Systems for Foil Joining Studies

To obtain the proper background information from which to select the candidate braze alloys with best potential for the subject program, a comprehensive literature survey was made of all published titanium brazing experience to date (Ref. 49 through 92).

This survey revealed that published information on titanium brazement strength, toughness, corrosion resistance, and general metallurgy was quite sketchy and frequently vague for most braze systems; indicating that very little concerted effort has been made to develop titanium brazing alloys using sound metallurgical approaches. Thus, the braze alloys reported by manufacturers of titanium-braze structure usually represented existing braze alloys not specifically designed for joining titanium, but apparently suitable on a cut-and-try basis. The silver-base family of braze alloys falls into this category. Reported attempts at developing braze alloys specifically for (and metallurgically compatible with) titanium had been carried out normally as laboratory efforts, with little application or service experience yet available.

The three probable exceptions which warranted attention in this program are described in the following paragraphs.

Palladium-Containing Braze Alloy

For brazing titanium to stainless steel, a new alloy (Ref. 79) containing 81.1 palladium, 14.3 silver, and 4.6 silicon in percent by weight had been developed under a NASA contract. The homogeneous solid was reported inert to nitric acid

attack. The ultimate tensile strength of the joint was approximately 75,000 psi. The alloy was reported to form a metallurgical bond, with alloy interfacial penetration of 0.0015 inch into the titanium substrate and 0.003 inch into the stainless steel. The alloy reportedly exhibited excellent flow characteristics at a brazing temperature in the range of 1395 to 1450 F.

This palladium-base alloy provided a novel approach to a low-temperature braze alloy for titanium. However, it was decided to eliminate this alloy as a candidate because of:

- The wide difference in surface electromotive potentials for Pd (-0.83 volts) and Ti (+1.63 volts)
- The high densities of both Pd and Ag
- The high intermetallic content

Nickel-Phosphorous Braze Alloys (Kanigen Process)

Nickel-base braze alloys containing phosphorous (Ref. 81) have been developed for use in the nuclear energy industry where the presence of boron (even in small quantities) cannot be tolerated. This type of alloy does not erode stainless steel and, therefore, has found acceptance for joining thin gage material. It does, however, tend to be brittle. Most of the alloys are available as powder; an exception is the Ni-P eutectic alloy which can be applied by the Kanigen electroless plating technique.

A suitable filler metal for producing sound, corrosion-resistant joints in zirconium alloy tubing operating in high-pressure, high-temperature (~ 680 F) water was reported to be Ni-7 to 10P (Ref. 49). Because of the metallurgical similarity of titanium and zirconium, it was decided to screen Ni-10P plated by the Kanigen electroless process on titanium foils for possible in-situ braze application. A typical use of an in-situ process is the joining of flat plate and corrugated fin components of thin foil heat exchangers.

Titanium and Titanium-Zirconium Base Alloys

The promising characteristics of Ti- and Ti-Zr-base braze alloys, employing beryllium as the major melting point depressant were discussed previously. These eutectic bases were selected for further study and development, with the hope of evolving a suitable braze material for foil joining.

Plans were drawn for minor chemical modification of the basic Ti-5.6Be and Ti-47.2Zr-5.6Be eutectic alloys, with the primary objectives of:

- Lowering the flow temperature of the Ti-base alloy from ~ 2000 F to ~1600-1700 F, to minimize foil erosion tendency for Ti-8Al-1Mo-1V, Ti-6Al-4V, and Ti-5Al-2.5Sn foils. (Modifiers included Al, Co, Cr, Fe, Cu, Ni, Ge, Mn, Si, Ag, and Sn.)

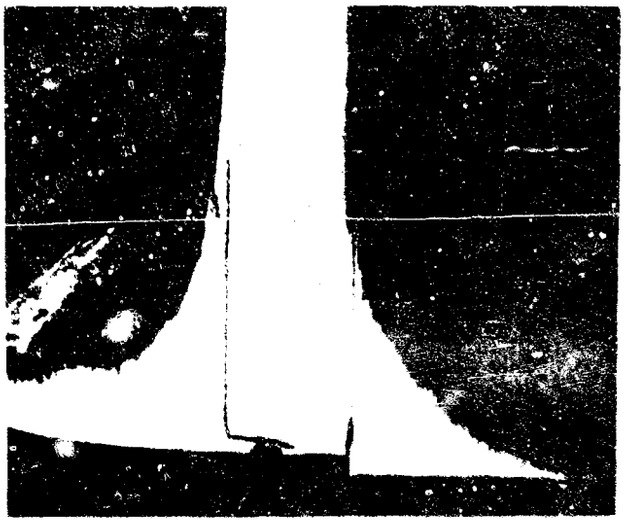
- Lowering the flow temperature of the Ti-Zr base alloy from 1625 to 1400 or 1500 F; principally to permit safe brazing of the Ti-3Al-2.5V tube alloy below its beta transus (1715 F) and to enable safe, long-term brazing periods for all the program foil alloys. A secondary objective was to reduce the beryllide content of the basic braze structure by partial or total substitution of other melting point depressants for Be. (Modifiers included Ni, Mn, Sn, Fe, Cu, Pd, Si, Ge, Ag, and Al.)

The selection of alloying additives and the quantities of additives used were based upon the stated objectives of lowering the effective melting points of the braze alloys some 200 to 400 F. The candidate alloying elements and their relative potentials for melting point depression in binary alloy systems (both Ti- and Zr-bases) are listed in Table XVII.



Braze Alloy: Ag-5Al-0.2Mn
Braze Temperature: 1790 F
Etchant: Kroll's
Magnification: 60X

Note the thin TiAg film



Braze Alloy: Ag-5Al-0.2Mn
Braze Temperature: 1790 F
Etchant: Kroll's
Magnification: 60X

Crevice corrosion destroyed the foil/braze interface joint after a 96-hour exposure to salt spray

FIGURE 14. TYPICAL Ti-6Al-4V FOIL T OINT BRAZEMENTS MADE WITH SILVER-BASE BRAZE ALLOY

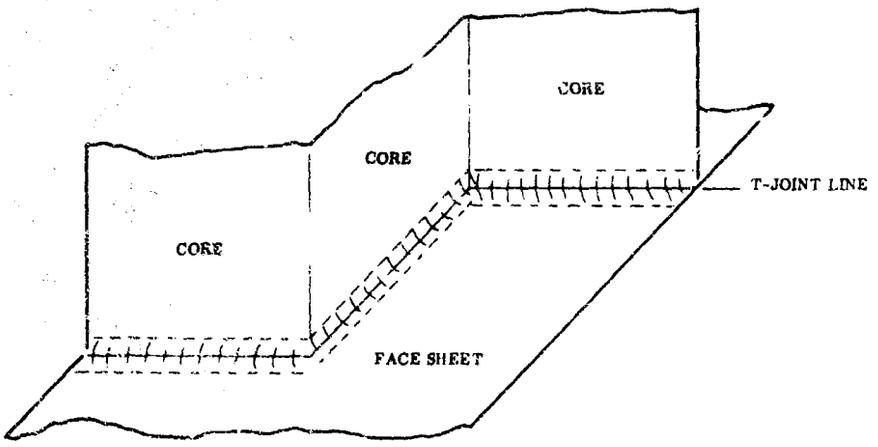


FIGURE 15. TYPICAL HONEYCOMB CORE-TO-FACE SHEET JOINTS

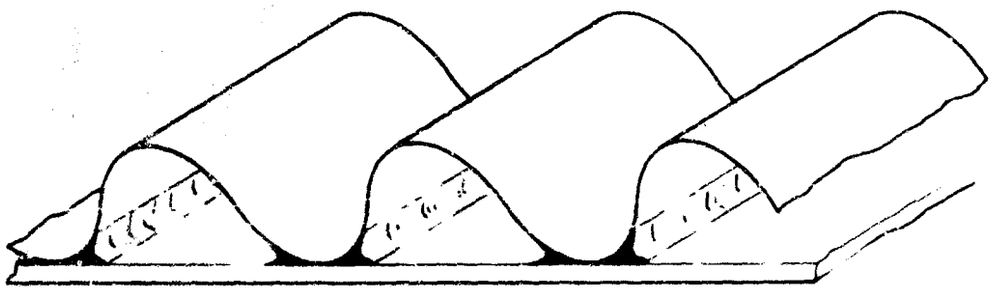


FIGURE 16. TYPICAL CORRUGATED FIN-TO-PLATE SHEET JOINTS

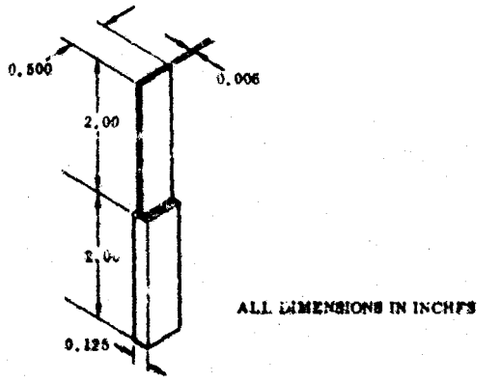


FIGURE 17. T-JOINT SPECIMEN USED FOR BRAZE EVALUATION

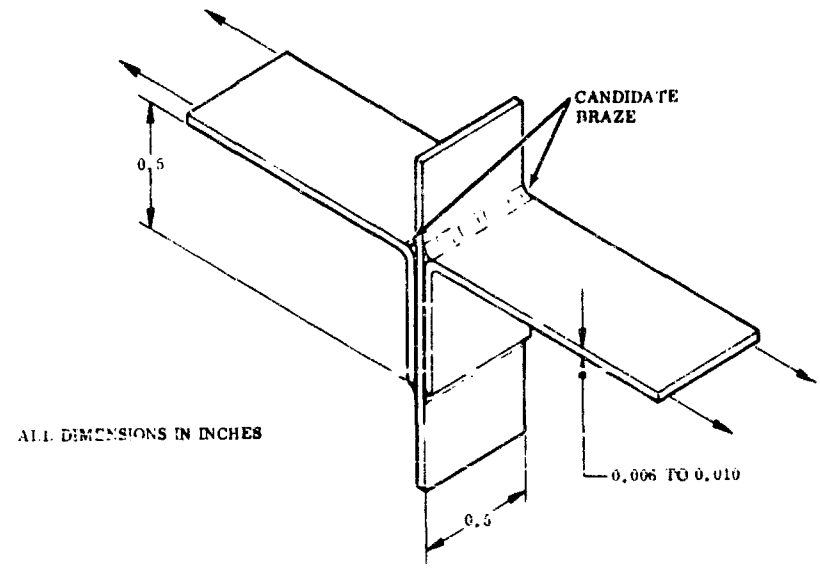
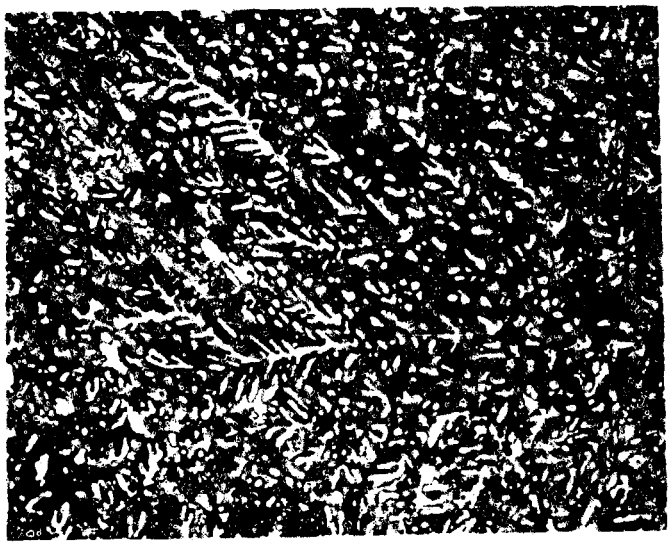


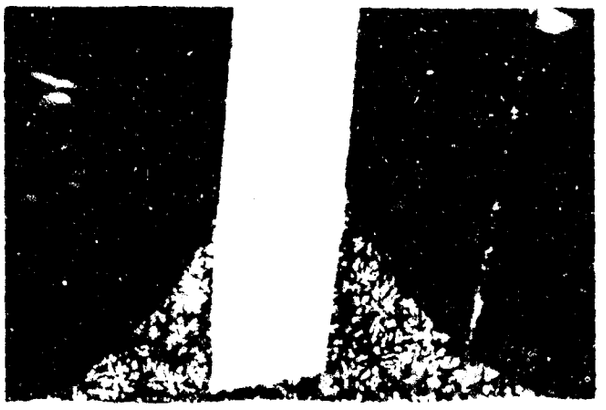
FIGURE 18. DOUBLE-LAP JOINT SPECIMEN USED FOR BRAZE EVALUATION



Etchant: Kroll's
Magnification: 100X

FIGURE 19.

TYPICAL EUTECTIC STRUCTURE IN AN ARC-MELTED INGOT OF Ti-47.2Zr-5.6Be ALLOY



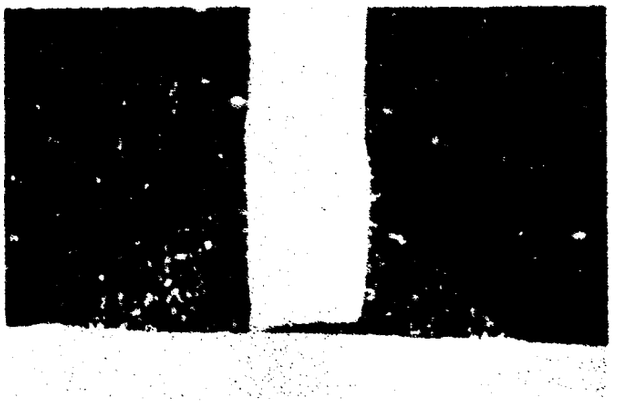
Alloy: Ti-5.6Be
Etchant: Kroll's
Magnification: 60X

Absence of corrosive attack



Alloy: Ti-6Ni-5.3Be
Etchant: Kroll's
Magnification: 60X

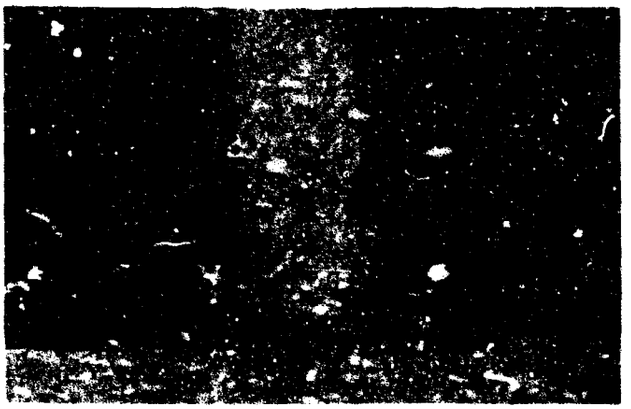
Absence of corrosive attack



Alloy: Ti-2.8Al-[illegible]Be
Etchant: Kroll's
Magnification: 60X

Absence of corrosive attack

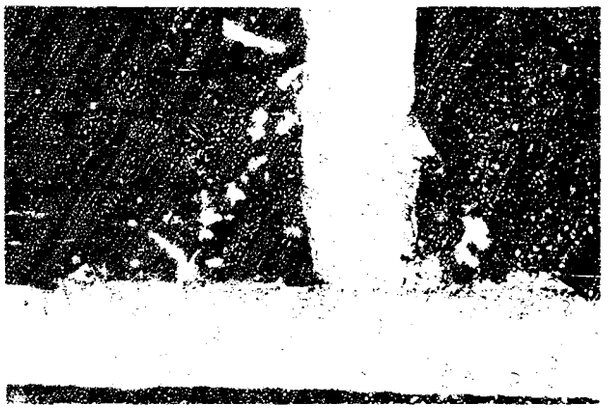
FIGURE 20. BRAZED T-JOINTS OF Ti-6Al-4V FOILS AFTER A 96-HOUR SALT SPRAY EXPOSURE (Sheet 1 of 2)



Alloy: Ti-6Al-4V-5.6Be
Etchant: Kroll's
Magnification: 60X

Absence of corrosive attack

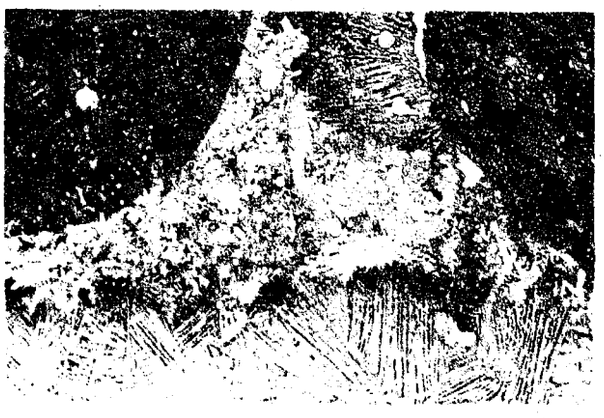
FIGURE 20. BRAZED T-JOINTS OF Ti-6Al-4V FOILS AFTER A 96-HOUR SALT SPRAY EXPOSURE (Sheet 2 of 2)



Braze Alloy: Ti-5.6Be
Braze Time: 1 Minute
Braze Temperature: 2000 F
Etchant: Kroll's
Magnification: 100X

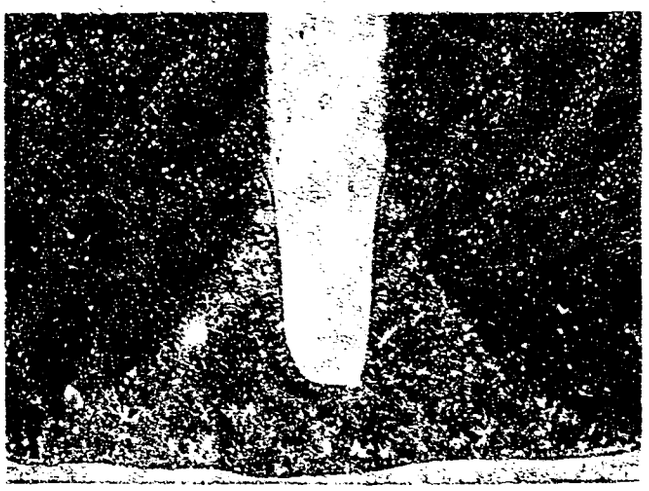


Braze Alloy: Ti-5.6Be
Braze Time: 5 Minutes
Braze Temperature: 2000 F
Etchant: Kroll's
Magnification: 100X



Braze Alloy: Ti-5.6Be
Braze Time: 25 Minutes
Braze Temperature: 2000 F
Etchant: Kroll's
Magnification: 100X

FIGURE 21. PROGRESSIVE DISSOLUTION AND EROSION OF Ti-5Al-2.5Sn FOIL T-JOINTS WITH INCREASING BRAZE TIME



Braze Alloy: Zr-6.0Be
Braze Time: 30 Seconds
Braze Temperature: 1810 F
Etchant: Kroll's
Magnification: 60X

Note foil erosion. This alloy proved unacceptable for foil brazing.

FIGURE 22.

TYPICAL Ti-6Al-4V FOIL T-JOINT BRAZED WITH Zr-6.0Be EUTECTIC ALLOY

Braze Alloy: Ti-47.3Zr-5.6Be
Braze Time: 5 Minutes
Braze Temperature: 1650 F
Etchant: Kroll's
Magnification: 60X

Note absence of foil erosion through adoption of thermodynamic and metallurgical principles in braze alloy design.

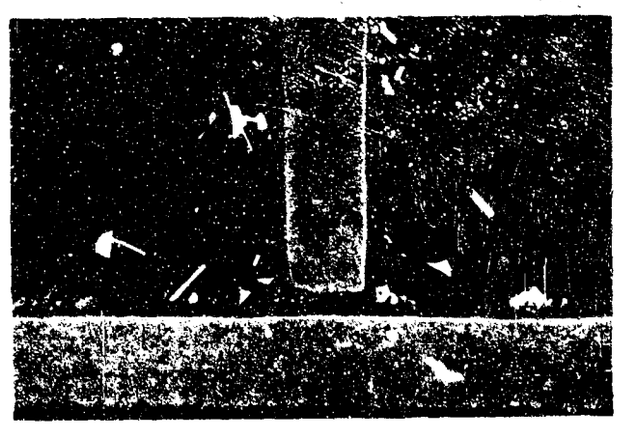


FIGURE 23.

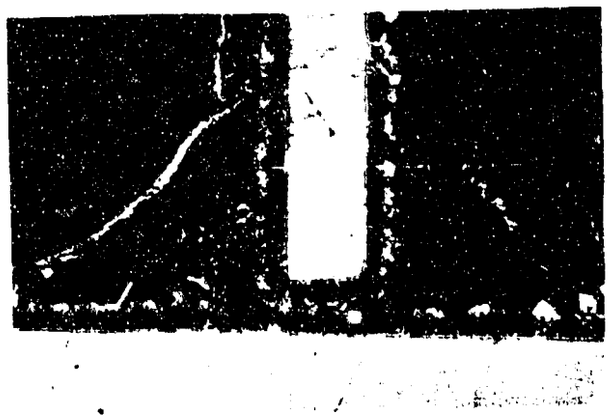
TYPICAL Ti-6Al-4V FOIL T-JOINT BRAZED WITH Ti-47.2Zr-5.6Be EUTECTIC ALLOY



Braze Alloy: Ti-47.2Zr-5.6Be
Braze Time: 1 Minute
Braze Temperature: 1700 F
Etchant: Kroll's
Magnification: 100X



Braze Alloy: Ti-47.2Zr-5.6Be
Braze Time: 5 Minute
Braze Temperature: 1700 F
Etchant: Kroll's
Magnification: 100X



Braze Alloy: Ti-47.2Zr-5.6Be
Braze Time: 25 Minutes
Braze Temperature: 1700 F
Etchant: Kroll's
Magnification: 100X

FIGURE 24. EFFECT OF INCREASING BRAZE TIME ON Ti-5Al-2.5Sn FOIL T-JOINTS

3.4 TASK IV - DEVELOPMENT AND OPTIMIZATION OF BRAZE ALLOY SYSTEMS

It was the intent of this portion of the program to develop and modify existing braze alloy systems to fit the special requirements of titanium foil brazing. To this end, a series of subtasks was programmed to aid in the comparative evaluation of braze alloys. These subtasks included:

- The formulation of candidate braze compositions.
- The melting and comminution of candidate braze alloys preparatory to brazing tests.
- Brazing tests upon titanium foils to assess brazing characteristics and relative applicabilities of candidate braze alloys to titanium foil joining.
- Salt spray corrosion tests of alloy brazements.
- Mechanical tests at room temperature to appraise relative strength and toughness levels of candidate alloy brazements.
- Metallographic structural examination of candidate alloy brazements, before and after corrosion and mechanical tests, to detect zones of potential weakness. This information (in total) was then used to re-modify braze composition, braze cycle, and heat treatment to further optimize each braze alloy system.

The ultimate objective of this braze alloy study was the establishment of an optimum braze system for each of the foil structure types to be evaluated in Phase II (viz., corrugated sandwich structure, honeycomb sandwich structure, and tube-to-header matrix structure).

3.4.1 Experimental and Test Procedures

Testing Format

The test program of Phase I was divided into two consecutive tasks (Tasks IV and V). Task IV was concerned primarily with the (compositional) optimization of braze alloy systems to maximize corrosion and erosion resistance and to obtain the best combination of brazing characteristics and processing flexibility along with joint toughness and strength properties. Adaptability to all program alloy foils was stressed[1]. Eighteen of the most brazeable alloys, screened by foil brazing performance and microstructure from over 100 chemical modifications of the basic Ti-Be and Ti-Zr-Be

---

1. Ti-6Al-4V, ELI (AMS-4907)2-10 mil foils
   Ti-5Al-2.5Sn, ELI (AMS-4909)2-10 mil foils
   Ti-3Al-1Mo-1V (AMS-4918)10 mil foil
   Ti-3Al-2.5V tubing (0.125 inch OX by 0.006 inch wall thickness)

braze alloys were comparatively tested in an evaluation program involving simple T-joint (Fig. 25 and 26) and lap-joint brazements (Fig. 27). The T-joint configuration was chosen to simulate the critical core/face sheet joints of honeycomb panels. Lap-joint specimens effectively simulated other important foil joints, typified by node joints in honeycomb core and corrugated fin-to-plate joints in heat exchangers.

T-joint tensile and bend tests and lap-joint shear tests were conducted principally at room temperature, both in the as-brazed condition and after 100 to 238 hours exposure to salt spray (200 F, 5 percent NaCl). Special tests were also conducted to gage braze-line peel resistance, using the double lap-joint specimen shown in Figure 28 and to measure the strain-accommodation ability of thin films of braze alloy upon a thicker substrate of stressed alloy foil (Fig. 29). This latter test was important to evaluate braze adaptability to thin foil structures where local and general surface strains can be quite high as a result of combinations of flexure and vibration and pronounced thermal differentials. At the conclusion of Task IV, the list of 18 candidate alloys was reduced to six for further evaluation in Task V.

Braze Alloy Production

Button ingots of 5.0 or 10.0 grams of each candidate braze alloy were argon arc-melted in the water-cooled copper crucible shown in Figures 30 and 31. Elemental melting stock used to prepare alloy charges were drawn initially from sources of commercial purity. However, the advantage of using higher purity melt stock was revealed early in the program. As shown in Table XVIII, significantly lower levels of interstitial element contaminants were obtained using electrolytic titanium and electrolytic zirconium in combination with ingot sheet beryllium. As a result, the high-purity heats permitted reliably lower braze temperatures, improved and more consistent brazing characteristics, as well as lower braze matrix hardness levels. Unmelted braze residues were virtually eliminated.

All candidate braze alloys were prepared in either 5- or 10-gram melt charges (usually 5-gram charges). Alloying elements for every heat were first weighed separately to the nearest milligram, then totaled; secondly, each heat charge was weighed as a unit to obtain a check upon total charge weight. For each heat, the total charge weight was compared to button ingot weight after melting to detect possible weight gain or loss attributible to the melting practice. The heat was considered acceptable if the weight change was calculated to be $\leq(\pm)$ 0.005-gram for

TABLE XVIII

INFLUENCE OF MELT STOCK PURITY ON INTERSTITIAL CONTAMINENT LEVELS

Heat Number	Nominal Composition	Titanium	Zirconium	Berrylium	Total Oxygen Concentration (ppm-wt)
CS1-1	Ti-5.6Be	Commercial Purity (A55 wire)		Commercial Purity (QMV)	2200
CS1-23	Ti-5.6Be	Commercial Purity (A55 wire)		High Purity Ingot Sheet(1)	1430
CS1-24	Ti-5.6Be	High Purity Electrolytic Titanium(2)		High Purity Ingot Sheet(1)	260
CS13-1	Ti-47.2Zr-5.6Be	Commercial Purity (A55 wire)	Commercial Purity	Commercial Purity (QMV)	2200
CS13-3	Ti-47.2Zr-5.6Be	Commercial Purity (A55 wire)	Commercial Purity	High Purity Ingot Sheet(1)	1430
CS13-4	Ti-47.2Zr-5.6Be	High Purity Electrolytic Titanium(2)	Commercial Purity	High Purity Ingot Sheet(1)	850
CS13-5	Ti-47.2Zr-5.6Be	High Purity Electrolytic Titanium(2)	High Purity Electrolytic(3) Zirconium	High Purity Ingot Sheet(1)	2[illegible]0

1. High Purity Beryllium Ingot Sheet (Type I, S-2) (Beryllium Corp., Reading, Pa.)

   Typical Interstitial Levels (ppm-wt)

C	O	N
400.0	100.0	-

2. High Purity Electrolytic Titanium (Donated by the U.S. Bureau of Mines, Reno Metallurgy Research Center, Boulder City, Nevada.)

   Interstitial Levels (ppm-wt); Lot Analysis

C	O	N
60.0	270.0	30.0

3. High Purity Electrolytic Zirconium (Wah Chang Metallurgical Co., Albany, Ore.)

   Interstitial Levels (ppm-wt); Lot Analysis

C	O	N
13.0	50.0	10.0

5-gram heats or ≤ (±) 0.010-gram for 10-gram heats. These figures correspond to a maximum weight change of ± 0.1 percent. The normal weight change proved to be much smaller, usually ≤ (±) 0.001 to 0.002-gram. Semiautomatic precision balances of the type shown in Figure 32 were employed exclusively.

The arc-melter consisted of a sealed Vycor glass melt-chamber (approximately 12 inches high with a 6-inch ID) with a water-cooled copper crucible for the heat charge (Fig. 31). Heat for melting the charge was provided by an argon arc which was established between a nonconsumable tungsten electrode and the charge itself. The

tungsten electrode was controlled manually through a sliding O-ring seal in the top of the chamber. Power for the arc was provided by a low-voltage, dc, welding unit (selenium-rectified, portable).

In a typical melting operation, the heat charge was positioned in the crucible cavity together with a premelted 5-gram button of pure titanium. High-purity titanium-gettered argon was allowed to flow through the chamber for about 30 minutes to establish a suitable protective environment for melting. To check the purity of the resultant argon atmosphere and to getter any residual gaseous contaminants in the chamber, the pure titanium button was first remelted and held molten for about 1 minute. If the surface of the solidified button remained bright metallic after cooling to approximately 500 F, the atmosphere was assumed to be sufficiently clean for melting the charge. (The interstitial element contaminant level of the atmosphere at this point can be assumed ≤ 10.0 ppm.)

The heat charge was then arc-melted three separate times, the solid button being turned over between each melting operation. After cooling to room temperature, the button ingot was removed from the chamber and weighed to the nearest milligram to detect possible weight change.

All braze alloy buttons used in Phase I work were made in the manner described. Braze alloy button ingots used to supply braze powders for Phase II work (particularly full-scale component brazing) were further refined by levitation melting procedures prior to crushing.

Button ingots were prepared for brazing by mechanical crushing and sieve grading of resultant powders to sizes suitable for use (e.g., -24/+35 mesh for conventional brazing or -100/+200 mesh for in-situ brazing). A study of braze particle size effects (Ti-Zr-Be base) showed that normal ingot comminution procedures cause a mechanical segregation of the beryllium-rich berylides to the finer particle fractions (Table XIX). The fine mesh sizes, adaptable to in-situ brazing of foils (e.g., -100/+200 or -200/+400 mesh), were found to be strongly hypereutectic with respect

TABLE XIX

VARIATION OF WEIGHT PERCENT BERYLLIUM IN CS13-5 BRAZE ALLOY

Mesh Size	Weight Percent Beryllium in CS13-5	
	Arc Melted	Homogenized[1]
+12	4.90	5.90
-12/+24	5.30	6.20
-24/+35	5.55	6.35
-35/+48	5.70	6.40
-48/+100	5.50	6.45
-100/+200	6.60	6.50
-200/+400	8.00	6.30
-400 (fines)	13.40	---

1. At 1450 F for 40 hours.

to beryllium, resulting in severe foil erosion at usual brazing temperatures. To counteract mechanical segregation, two different solutions were determined to be effective:

- Hydriding of button ingots in dry hydrogen (1300 F) prior to crushing to render all braze components equally susceptible to fragmentation upon ingot crushing, followed by a vacuum dehydriding treatment of braze powders (1400 F) prior to brazing. This procedure worked well where very fine powders were desired (-200 mesh). Hydriding was not adopted as standard procedure.

- Thermal annealing treatment of ingots prior to comminution so as to spheroidize and break up the pattern of beryllide dendrites and render them less susceptible to consolidation in the fines. Ingot annealing treatments were adopted as standard procedure for all candidate braze alloys because of the uniform beryllium levels obtained in all powder fractions (Table XIX). The CS series alloys were vacuum annealed (homogenized) at 1450 F for 40 hours; RM series alloys were vacuum annealed at 1200 F for 65 hours.

Braze Screening Tests

Specimen Preparation. All candidate braze alloys were first screened through a simple T-joint brazing test to determine general applicability for titanium foil brazing. Typical of the all-foil titanium alloy T-joint used for braze screening is shown in Figure 25. Figures 33 and 34 show the large number of T-joints required to

effectively screen candidate braze systems and their many possible variations in composition, braze cycle, and braze particle size. The braze production and screening tests not only yielded useful information related to brazing characteristics (e.g., minimum melt and flow temperatures, wettability, braze fluidity and filleting behavior, and erosion tendency), but they also gave a good indication of the braze alloys' ability to be arc-melted, its relative toughness (gaged in terms of resistance to comminution procedure), and its microstructural components in the braze condition. (Salt spray corrosion tests also were conducted using the T-joint brazements produced.) Consequently, the T-joint braze screening test was deemed a valuable tool for quickly eliminating the candidate braze alloys with little promise as well as in providing an introduction to those braze systems which did possess potential for foil joining.

The preparation of foil T-joint specimens for braze screening was a simple, though delicate, operation. Wafers (0.5-inch square) of 0.006-inch thick program alloy foils were cut using precision shears. Two such wafers were then assembled, as in Figures 35 and 36, to form a T-joint. The two sections were held together by the use of 0.5-mil titanium foil straps, tack welded to the 0.006-inch foils. A nearly constant fitup or gap width of 0.50- to 0.75-mil was typical between faying surfaces of the foil T-joint. Before assembling, the foil wafers were cleaned in an aqueous solution of 15 percent HNO_3 - 2 percent HF acids (room temperature) followed by distilled water and acetone rinses. This cleaning procedure was standard for all foil specimens.

Preparation of the T-joint specimens (Fig. 26) adaptable to tensile testing was carried out in a similar manner. The upper foil member was precision sheared to size and positioned against the flat, faying surface of the heavier bottom member (1/8-inch thick sheet stock of the desired program alloy) to form a T-joint. Again, the foil member was held permanently in place for brazing by the use of 0.5-mil titanium foil straps, tack welded to both top and bottom members of the specimen.

Specimen Braze Procedure. All specimen brazing was carried out using the laboratory brazing furnace shown in Figure 37 and 38. The furnace chamber was enclosed in clear, heavy-wall Vycor glass tubing so that the braze specimen could be viewed at all times during heating, brazing, and cooling cycles. The hot zone of the furnace consisted of a wholly enclosed, pure columbium cylindrical susceptor (approximately 1.0 inch ID by 3.0 inches high by 1/16-inch wall) which provided radiant heating to the braze specimen inside. (The susceptor was heated inductively through coils

external to the Vycor tube.) The top cap of the susceptor contained a hole for viewing the performance of the candidate braze material upon the specimen. There was also a hole in the side of the susceptor for measuring specimen temperature continuously using a microoptical pyrometer. Pyrometer readings were calibrated initially against thermocouples attached to dummy specimens. The braze specimen rested upon a bed of low-mass columbium alloy honeycomb, which raised the specimen to midheight of the susceptor heater.

The furnace was rigged to permit brazing in either high-vacuum environment or an atmosphere of titanium-gettered argon. A 4-inch diameter vacuum diffusion pump rapidly pumped the Vycor chamber to a vacuum of 1.0×10^{-4} Torr or better for brazing studies. Almost all preliminary brazing studies were conducted in high vacuum because it is freer of potential interstitial contaminants (e.g., the best argon atmosphere contains ~ 1.0 to 2.0 ppm interstitial element contaminants; whereas a vacuum of 1.0×10^{-5} Torr has only ~ 10^{-2} ppm contaminants based upon equivalent volumes). However, brazing environments of argon and vacuum frequently were employed interchangeably with no significant differences in braze behavior or results.

In a typical brazing run, the foil T-joint specimen was positioned inside the columbium susceptor at an angle to permit gravity feeding of the liquid braze into the joint capillary. Normally, the candidate braze was loaded on only one side of the joint to gain a better appraisal of braze fluidity. A typical braze load was 4.0 to 6.0 milligrams of -12/+24 or -24/+35 mesh powder for both Ti-Be and Ti-Zr-Be system modifications. The braze particles were loaded in the conventional manner adjacent to the joint surfaces using polybutene organic binder. After establishment of an acceptable vacuum, the specimen was heated gradually to ~ 800 to 1000 F to slowly drive off the binder without scattering the braze load. Once this was accomplished, the specimen was heated rapidly to within 200 F of the anticipated braze temperature, then held 1.0 to 3.0 minutes for temperature equalization prior to heating at a controlled rate to discover the minimum brazing temperature (e.g., 10 degrees F/minute to 300 degrees F/minute typically, 100 F/min.). After the braze was seen to flow and form a braze joint, the specimen was then cooled naturally at a rapid rate (~ 1000 degrees F/minute) or more slowly at a preselected, controlled rate. Minimum brazing temperatures were invariably selected to minimize the degree of braze/foil interaction.

Similar procedures were employed to braze all test specimens for Phase I work.

Evaluation of Braze Alloy Performance and Structure. Evaluation of candidate braze performance began during each braze run when the degrees of braze fluidity, filleting behavior, and residue formation were noted visually (through the Vycor tube), in addition to the apparent melting temperature and minimum actual flow temperature. The variation in the aforementioned brazing characteristics (fluidity, filleting, residue) with systematic increase in brazing temperature also was determined visually. After brazing, every specimen was examined with a 10X magnifying lens to search for signs of surface porosity, cracking, foil erosion (undercut fillets), variable size fillets, and residue. The next step was metallographic examination of random sections cut through test brazements. Thorough metallographic studies and microhardness surveys helped to reveal not only the microstructural components of the braze and braze-affected foils, but the character of braze residues, foil erosion, primary solidification structures and segregation products in the braze. Occasionally, undesirable transformation products in the foil were detected as well as regions of high hardness or marked hardness gradients which might prove embrittling.

3.4.2 Test Equipment and Procedures (Tasks IV and V)

T-joint tensile tests, double-lap peel tests, strain accommodation tests, and lap-shear tests at room temperature and above were executed with a Hounsfield Tensometer (Fig. 39). Tests in the range of 300 to 900 F were carried out in argon atmosphere. Cryogenic temperature tests were conducted with a Riehle Universal Testing Machine (Fig. 40), employing test environments of dry ice and acetone (-100 F) or liquid nitrogen (-320 F). A moderate strain rate of approximately 0.01 min^{-1} was employed overall. Bend tests of foil T-joint specimens were carried out manually by exerting pressure upon the vertical foil member, one-half inch above the joint, and bending the vertical foil slowly in an arc of 90 degrees. Cracking, if it occurred, was detected both audibly and metallographically.

Salt spray conditioning of selected specimens prior to test was carried out in accordance with ASTM-B117 using a 5 percent NaCl aqueous solution at a chamber temperature of 200 F. Stress rupture tests and hot-salt corrosion tests were conducted upon lap-joint specimens dead-weight loaded in a closed chamber. Heating

and test environments were provided by the oxidizing exhaust gases of a JP-4 burner rig. Special foil enclosures were affixed to the hot salt specimens to maintain molten salt within the joint areas. Fatigue excitation of lap-joint specimens (RT) was provided by a Materials Testing Systems (MTS) Fatigue Tester, Model 901.37

3.4.3 Initial Braze Screening Tests

The Ti-Be and Ti-Zr-Be Systems (CS Series)

The basic Ti-5.6Be eutectic alloy was modified chemically for study with the hope of reducing the minimum flow temperature (~ 2000 to 2050 F) to a more favorable level (≤1850 F) as indicated advisable by data from the braze-cycle simulation work. It was felt that the braze temperature reduction would not only benefit retention of foil properties, but would minimize the likelihood of foil erosion during extended process cycles. Additionally, should third-element alloying produce the desired reduction in flow temperature, it might be feasible to partially substitute the third element for beryllium, thereby decreasing the beryllide content of the braze alloy.

The third elements selected for alloying studies are those listed in Table XVII and XX. With respect to their binary constitution diagrams with titanium, many of these elements accomplish appreciable melting point depression without the associated production of a titanium intermetallic phase during solidification, unlike beryllium (e.g., aluminum, cobalt, chromium, iron, copper, nickel, germanium, manganese, silver, and zirconium). Silicon and tin are the two exceptions. Therefore, it seemed likely at the outset that significant reduction in gross intermetallic content should result from this study (especially beryllide content) if desired melting and flow point depressions were achieved.

Three levels of third-element additions were programmed. On the basis of the liquidus-temperature depression noted for the titanium binaries, the smallest third-element addition was calculated to decrease the ternary alloy liquidus 100 degrees F (~ 1950 F); the next level, 200 degrees F (~ 1850 F); and the largest addition, 300 degrees F (~ 1750 F). The possible influence of beryllium and complex beryllide formation tendencies were discounted in the first consideration. Modifications of the Ti-5.6Be braze alloy selected for braze screening test are listed in Table XX.

TABLE XX

CANDIDATE TERNARY BRAZE ALLOYS OF THE Ti-X-Be SYSTEM

Braze Alloy Composition (wt %)			Anticipated Melting Point Depression (F)	Anticipated Minimum Braze Temperature (F)
Titanium	Beryllium	X		
(1) Balance	5.6	—	0 (binary base)	2050
(2) Titanium	Beryllium	Aluminum		
Balance	5.6	8.3	100	1950
Balance	5.6	16.6	200	1850
Balance	5.6	24.9	300	1750
(3) Titanium	Beryllium	Cobalt		
Balance	5.6	3.14	100	1950
Balance	5.6	4.28	200	1850
Balance	5.6	6.42	300	1750
(4) Titanium	Beryllium	Chromium		
Balance	5.6	7.9	100	1950
Balance	5.6	15.8	200	1850
Balance	5.6	23.7	300	1750
(5) Titanium	Beryllium	Iron		
Balance	5.6	8.77	100	1950
Balance	5.6	8.54	200	1850
Balance	5.6	8.31	300	1750
(6) Titanium	Beryllium	Copper		
Balance	5.6	3.19	100	1950
Balance	5.6	6.38	200	1850
Balance	5.6	9.57	300	1750
(7) Titanium	Beryllium	Nickel		
Balance	5.6	2.07	100	1950
Balance	5.6	4.14	200	1850
Balance	5.6	6.21	300	1750
(8) Titanium	Beryllium	Germanium		
Balance	5.6	1.48	100	1950
Balance	5.6	2.96	200	1850
Balance	5.6	4.44	300	1750
(9) Titanium	Beryllium	Manganese		
Balance	5.6	4.33	100	1950
Balance	5.6	8.66	200	1850
Balance	5.6	12.99	300	1750
(10) Titanium	Beryllium	Silicon		
Balance	5.6	1.21	100	1950
Balance	5.6	2.42	200	1850
Balance	5.6	3.62	300	1750
(11) Titanium	Beryllium	Silver		
Balance	5.6	3.4	100	1950
Balance	5.6	34.6	200	1850
Balance	5.6	36.2	300	1750
(12) Titanium	Beryllium	Tin		
Balance	5.6	17.9	200	1850
Balance	5.6	34.6	300	1850

TABLE XXI

CANDIDATE TERNARY BRAZE ALLOYS OF THE Ti-Zr-Be SYSTEM

Braze Alloy Composition (wt %)			Anticipated Melting Point Depression (F)	Anticipated Minimum Braze Temperature (F)
Titanium	Zirconium	Beryllium		
Balance	0	5.6	0 (binary base)	2050
Balance	9.5	5.6	86	1964
Balance	18.9	5.6	172	1878
Balance	28.4	5.6	258	1792
Balance	37.9	5.6	344	1706
Balance	47.2	5.6	430	1620 (based upon prior work)
Balance	61.4	5.6	Unknown	Unknown

Special attention was given to studying zirconium as a ternary alloying agent. Because zirconium has a potent effect in depressing the flow temperature of the Ti-5.6Be base without incurring problems of crevice corrosion (due to its chemical similarity to titanium), it was planned to evaluate systematic additions of zirconium to the basic Ti-5.6Be alloy. All precontract work had been carried out using the Ti-47.2Zr-5.6Be alloy, which corresponds to the Ti/Zr ratio (50/50) showing a minimum melting point in the Ti-Zr binary. Therefore, the interval between zero percent and 47.2 percent zirconium was divided into five equal segments (including one additional segment beyond 47.2 percent), each corresponding to a braze alloy candidate (Table XXI). It was hoped that this preliminary investigation would lead to an optimum composition in the Ti-Zr-Be ternary system, with the best combination of brazing characteristics, minimum flow temperature, and resistance to corrosion and erosion phenomena. In all cases, the beryllium concentration was fixed at 5.6 percent inasmuch as prior work at Solar has established the eutectic beryllium concentrations in both Ti-Be and Zr-Be binary systems at 5.6 weight percent.

The Ti-Zr-Ni System (RM Series)

The RM series of alloys (developed initially during Phase I work) was based on a combination of three potential braze systems - the eutectics of Ti-24.5 atomic percent Ni and Zr-24.0 atomic percent Ni, combined with the minimum melting point existing at Ti-50 weight percent Zr for the Ti-Zr binary system. These alloys were suggested by the literature survey which revealed prior work on Ti-Ni braze systems (Ref. 72). The basic RM1 alloy (Ti-41.0Zr-18.0Ni) was arc-melted and found to possess excellent brazing characteristics on titanium foils at 1650 F.

In spite of the low braze temperature and promising brazeability of RM1, it was recognized that modification would be necessary to limit the heavy formation of Zr_2Ni and Ti_2Ni intermetallic compounds and to improve brazement toughness. Structural optimization was attempted through variation of Zr and Ni levels, fourth element additions, and post-braze heat treatment. The programmed chemical modifications are itemized in Table XXII.

Results of Braze Screening Studies

Ti-X-Be Systems. The effects of each candidate alloying agent (termed "X") used to make up the ternary braze alloy, Ti-X-5.6 Be, are discussed separately for each alloying element evaluated. Aluminum additions (in the range 8.3 to 24.9 percent aluminum) and tin additions (in the range 17.0 to 34.0 percent tin) had an adverse effect upon braze wetting and fluidity; i.e., no braze joint formation was evident for trial braze temperatures up to 2050 F (Ti-5Al-2.5Sn foils). In the case of aluminum, the problem was believed caused by transient Al_2O_3 or TiAl formation at the braze/foil interface which effectively blocked the braze wetting mechanism. Apparently the wetting problem was restricted to the higher aluminum concentrations, inasmuch as a Ti-2.3Al-5.6Be alloy had exhibited excellent brazing characteristics with Ti-6Al-4V foils in prior work at Solar (braze temperature = 1950 F). Therefore, any concept to stabilize α-Ti in future titanium or Ti-Zr braze alloys by small to moderate additions of aluminum need not be abandoned. The difficulty caused by tin additions was not identified, but very probably it was related to the high vapor pressure of tin at anticipated braze temperatures. (This also could have been the problem with germanium, which, as shown in Tables XX and XXIII, exhibited a disappointingly small and constant effect upon melting point depression. Rapid evolution of an alloying agent can have a disruptive effect upon any candidate's braze performance.

TABLE XXII

RM SERIES ALLOYS BASED ON Ti-Zr-Ni AND Ti-Ni EUTECTICS

RM Number	Braze Alloy Composition (at %) Ti	Zr	Ni	X	Melt (F)	Flow (F)	Flow	Fillet	Residue	Microstructure	Hardness R_C (a)	(b)	(c)	(d)	Remarks
1	41.0	41.0	18.0	--	1650	1650	G	F	R	Minimal erosion and 0.5 mil thick intermetallic layer.	62.0 to 64.7	48.0	80.0 to 88.0	31.2 to 37.9	Pool test - 5.5 lb/in. and after 116 hours salt spray. As-brazed. Pool test 104 lb/in.
2	37.5	37.5	18.0	7.0Mn	1700	1750	-	-	-	Considerable erosion and 0.5-mil thick intermetallic layer.	[illegible] 5	--	69.0	34.5	--
3	41.0	--	7[illegible].9	18.0Mn	1960	/050	P	F	M		--	--	--	--	Poor flow.
	42.0	42.0	16.0	--	1650	1700	F	-	L	Minimal erosion and 1/2-mil thick intermetallic layer.	48.0	--	86.0	31.0	--
5	40.0	40.0	13.5	6.5Mn	1610	1640	-	-	-	Minimal erosion and 1/2-mil thick intermetallic layer.	48.5	--	61.7 to 61.8	30.8 to 35.0	30% RM 4 - 70 Zr
6	43.[illegible]	42.0	--	14.0Fe	1750	1850	P	F	L	[illegible]onsiderable erosion, extensive intermetallic compound formation (1.5-mil thick layer). Poor flow.	48.0	48.0	88.0	30.0	--
											48.0	48.0	86.0	30.0	
7	42.0	43.0	11.5	[illegible]	1640 1650 1685	1670 1800 1870	F	G	L	Minimal erosion and 1/2-mil thick intermetallic layer (similar to RM 4 and RM 9).	50.0	--	83.0 to 73.0	28.0	--
8	43.0	43.0	12.0	2.[illegible]Zr	1670	1675	G	G	M	Very little erosion. Very little intermetallic compounds. Excellent flow.	--	--	82.3 to 80.0	29.0 to 28.[illegible]	Pool test 215 lb/in. as-brazed - excellent braze characteristics.
10	43.5	43.5	12.0	1.0Mn	1680	1680	G	G	L	Considerable erosion; about 0.25-mil thick intermetallic layer. Heavy intermetallic compounds internally. Very good flow.	--	--	81.0	28.0	--
11	46.0	46.0	8.0	1.0Be	1660	1850	F	G	L	Minimal erosion; about 0.5-mil thick intermetallic layer and internal intermetallic compounds. Transformation in titanium foil observed.	--	--	--	--	--
12	45.0	45.0	8.0	2.0Mn	1630	1670	G	G	M	Very little erosion, no intermetallic layer formed. Some intermetallic compounds.	--	--	68.0 to 68.0	28.0 to 33.5	Pool test - 170 lb/in. as-brazed 170 lb/in after 114 hours salt spray.
13	45.5	45.5	8.0	1.0Be	1650	1650	G	G	M	Considerable erosion; about 0.25-mil thick intermetallic layer and intermetallic compounds internally.	--	--	66.0	26.0	--
14	46.0	46.	6.0	2.0Be	1660	1700	F	G	L	--	-	--	--	--	--
15	42.0	42.0	8.0	8.0Mn	--	--	-	-	-	--	--	-	--	--	Does not melt until 1900 F
16	40.0	40.0	12.0	8.0Mn	--	--	-	-	-	--	--	--	--	--	Does not melt until 1900 F
17	42.0	42.0	12.5	3.5Mn	1650	1850	-	-	-	--	--	--	--	--	--
18	41.5	43.0	86.0	8.4Pd	1640	--	-	-	-	--	--	--	--	--	Poor flow @1750 F
19	17.0	17.0	28.4	38.6Pd	1730	1730	-	-	-	--	--	--	--	--	Highly erosive. Erodes hole in foil during brazing.
20	45.0	45.0	3.2 Ni	4.8Pd + 2.0Be	1650	1670	G	G	M	--	--	--	--	--	Pool test as brazed 180 lb/in. after salt spray 113 hours - 60 lb/in.
21	45.0	45.0	6.0 Ni	1.2Pd + 2.0Be	1690	1640	G	G	M	--	--	--	--	--	Pool test as brazed 196 lb/in. after salt spray 113 hours - 50 lb/in.

(a) Intermetallic layer at braze/foil interface
(b) Matrix of braze alloy
(c) Intermetallic compounds interior of braze
(d) Titanium foil

F - Fair
G - Good
L - Large
M - Minimum
N - None
P - Poor

Of the remaining candidate alloying [illegible]ly copper (9.57 percent copper) and manganese (8.66 percent manganese) were shown capable of depressing the flow temperature to, or below the maximum permissible braze temperature of 1850 F. The Ti-9.57Cu-5.6Be alloy demonstrated good brazing characteristics at 1800 F but, as shown in Figure 41, left a moderate unmelted residue indicating the beryllium level required some adjustment. The Ti-8.66Mn-5.6Be alloy brazed well at 1850 F on Ti-5Al-2.5Sn foils, but also left a moderate residue (Fig. 42). Only slight erosive tendencies were noted for either alloy. Both of these candidate alloy brazements

TABLE XXII (Cont)

RM SERIES ALLOYS BASED ON Ti-Zr-Ni AND Ti-Ni EUTECTICS

RM Number	Brass Alloy Composition wt % Ti	Zr	Ni	Be	X	Melt (F)	Flow (F)	Flow	Fillet	Reaction	Microstructure	Hardness R_C (a)	(b)	(c)	(d)	Remarks
22	37.5	37.5	21.0	3.0	--	1580	1580	G	G	M	Good flow but excessive erosion.	--	--	--	--	Alloy is brittle
23	70.0	--	17.5	4.0	--	1670	1700	G	G	N	Good flow, no erosion, and no intermetallic layer.	37.0	--	41.5	39.5 to 31.0	Pool test at ... ...ed - 400 lb/in
24	94.5% RM 23 + 5.5% ...					1594	1662	G	G	M	--	--	--	--	--	Alloy is very brittle
25	...	42.5	15.5	4.0	--	1602	1695	G	G	N	--	--	--	--	--	Flow temperature higher than RM 8.
26	95.0% RM 22 + 5.0% ...					1690	1690	G	G	M	Good flow, no erosion, but 1/8-mil thick intermetallic layer.	--	--	33.0	30.0	Pool test as brazed - 90 lb/in. Not well brazed
27	90.0% RM 22 + 5.0% ...					1773	1760	G	G	M	--	--	--	--	--	--
28	80.0% RM + 10.0% ...					1606	1693	G	G	P	Excellent flow, no erosion and only 1/4 mil thick intermetallic layer formed.	--	--	--	--	--
29	35.0	35.0	15.0	--	15.0Ag	1660	--	-		-	--	--	--	--	--	--
30	74.0	--	18.0	4.0	4.0Ag	1700	1780	G	G	M	--	--	--	--	--	--
31	90.0% ... 5.0 + 10.0% ...					1560	1797	G	G	L	--	--	--	--	--	Flow temperature higher than RM 8.
32	90.0% RM 4 + 10.0% ...					1660	1729	G	G	M	Good flow, little erosion and only 1/8-mil thick intermetallic layer formed.	--	--	--	--	--
33	90.0% RM 12 + 10.0% ...					1564	1680	G	G	M	--	--	--	--	--	--
34	90.0% RM 23 + 10.0% ...					1580	1680	G	G	M	--	--	--	--	--	Melts at a higher temperature than RM 32.
35	Ti - 5.0% ... 5.0%					>1870	--	-	-	-	--	--	--	--	--	Tough alloy
36	95.0% RM 16 + 5.0% ...					1626	1660	G	G	M	Flow is not as good as RM 8, no erosion.	--	--	--	--	--
37	90.0% RM 1 + 5.0% ...					1780	1730	G	G	M	--	--	--	--	--	--
38	90.0% RM 12 + 5.0% ...					1660	1710	G	G	L	--	--	--	--	--	Joint broke away during ... ing dur... ...erature
39	38.0	39.0	5.0	4.0	--	1630	1695	P	P	L	--	--	--	--	--	Tough alloy
40	87.0	80.0	6.0	5.0	--	1748	1790	G	G	P	Good flow and fillet. No erosion. β bridges.	--	--	47.0	--	Tough alloy
41	80.0	80.0	12.0	2.0	--	1680	1760	G	G	M	--	--	--	--	--	Tough alloy
42	64.0	80.0	12.0	4.0	--	1700	1790	G	G	M	Good flow and fillet. No erosion. β bridges.	--	--	51.5	--	Tough alloy
43	48.0	35.0	13.0	5.0	--	1646	1680	G	G	P	Joint broke away during machining.	--	--	--	--	Tough alloy. Excellent braze.
44	RM 43 + 5% ...					1700	1780	G	G	P	β bridges. Good flow and fillet - no erosion.	--	67.0	66.0 to 68.0	--	Tough alloy. Excellent braze.
45	80.0	30.0	15.0	4.0	5.0Ag	1650	1795	G	G	P	β bridges. Good flow and fillet - moderate erosion.	--	66.0	66.0 to 66.0	--	Tough alloy. Excellent braze.
46	80.0	30.0	15.0	4.0	5.0%	1752	1790	G	G	M	--	--	--	--	--	--

(a) Intermetallic compound matrix of braze
(b) Interfacial layer
(c) Braze matrix
(d) Titanium foil

G - Good
L - Large
M - Medium
N - None
P - Poor

displayed notable resistance to crevice corrosion, having withstood 72 hours exposure to salt spray without apparent attack. In contrast, control specimens brazed with Ag-5Al-0.2Mn suffered extensive damage by corrosion (Fig. 43).

However, because significantly lower brazing temperatures had been observed in the Ti-Zr-Be system with equivalent salt spray corrosion resistance, the alloying agents copper and manganese appeared at this point more applicable as additives to Ti-Zr-Be braze alloys. It was reasoned that those Ti-Zr-Be eutectic alloys, already possessing flow temperatures in the range 1600 to 1760 F, might well benefit from

TABLE XXIII

RESULTS OF BRAZE STUDIES ON THE TERNARY BRAZE ALLOY Ti-X-Be

Braze Alloy Composition (wt)			Anticipated Melting Point Depression (F)	Anticipated Minimum Braze Temperature (F)	Actual Minimum Braze Temperature (F)	Actual Melting Point Depression (F)	Brazing Characteristics Upon Ti-6Al-4V Alloy Foils		
Titanium	Beryllium	X					Braze Fluidity	Fillet Formation	Diffusion (rate)
Balance	5.6	---	0 (binary base)	2000	2000	---	G	G	M-H
Titanium	Beryllium	Aluminum							
Balance	5.6	8.3	100	1900	No braze flow 2000 F	---	P	---	---
Balance	5.6	16.6	200	1800	No braze flow 2000 F	---	P	---	---
Balance	5.6	24.9	300	1700	No braze flow 2000 F	---	P	---	---
Titanium	Beryllium	Cobalt							
Balance	5.6	2.14	100	1900	1970	30	G	G	M
Balance	5.6	4.29	200	1800	1850	150	G	G	M
Balance	5.6	6.43	300	1700	2000	30	G	G	M
Titanium	Beryllium	Chromium							
Balance	5.6	7.9	100	1900	1900	100	G	G	M
Balance	5.6	15.8	200	1800	1900	100	G	G	M
Balance	5.6	23.7	300	1700	1900	100	G	G	M
Titanium	Beryllium	Iron							
Balance	5.6	2.77	100	1900	1930	100	G	G	M
Balance	5.6	5.54	200	1800	1900	100	G	G	M
Balance	5.6	8.31	300	1700	1970	30	G	M	M
Titanium	Beryllium	Copper							
Balance	5.6	3.19	100	1900	1970	30	G	G	M
Balance	5.6	6.38	200	1800	1915	115	G	G	M
Balance	5.6	9.57	300	1700	1900	200	G	G	M
Titanium	Beryllium	Nickel							
Balance	5.6	2.97	100	1900	1990	90	G	G	M
Balance	5.6	4.14	200	1800	1950	150	G	M	M
Balance	5.6	6.21	300	1700	1903	103	G	M	L
Titanium	Beryllium	Germanium							
Balance	5.6	1.48	100	1900	1970	30	G	G	L
Balance	5.6	2.96	200	1800	1970	30	G	G	L
Balance	5.6	4.44	300	1700	1970	30	G	G	L
Titanium	Beryllium	Manganese							
Balance	5.6	4.39	100	1900	1940	130	G	M	M
Balance	5.6	8.68	200	1800	1800	200	G	G	M
Balance	5.6	13.00	300	1700	1800	300	G	G	L
Titanium	Beryllium	Silicon							
Balance	5.6	1.2	100	1900	1890	170	G	G	M
Balance	5.6	2.4	200	1800	1830	130	G	G	M
Balance	5.6	3.60	300	1700	1970	30	G	G	M
Titanium	Beryllium	Silver							
Balance	5.6	12.3	100	1900	1930	70	G	G	M
Balance	5.6	24.6	200	1800	1870	80	G	G	M
Balance	5.6	36.9	300	1700	1830	170	G	M	L
Titanium	Beryllium	Tin							
Balance	5.6	17.6	100	1900	No braze flow 2000 F		P	---	---
Balance	5.6	35.2	200	1800	No braze flow 2000 F	---	P	---	---

G - Good, C - Good, M - Some
S - Sluggish, M - Medium, M - Medium
P - Poor, P - Poor, L - Large

TABLE XXIV

RESULTS OF BRAZE STUDIES ON THE TERNARY BRAZE ALLOY Ti-Zr-Be

Braze Alloy Composition (wt)			Anticipated Melting Point Depression (F)	Anticipated Minimum Braze Temperature (F)	Actual Minimum Braze Temperature (F)	Actual Melting Point Depression (F)	Brazing Characteristics Upon Ti-6Al-5.6Be Foils		
Titanium	Zirconium	Beryllium					Braze Fluidity	Fillet Formation	Unmelted Residue (size)
Balance	0	5.6	0 (binary base)	2050	~1760	---	G	G	N-M
Balance	9.3	5.6	86	1964	1820	230	G	G	M
Balance	18.9	5.6	172	1878	1840	210	G	G	M
Balance	28.4	5.6	258	1792	1800	250	S	M	M
Balance	37.9	5.6	344	1706	1750	320	S	G	M
Balance	47.2	5.6	430	1620 (based upon prior work)	1700	430	G	G	N-M
Balance	61.4	5.6	---	---	1660	460	G	G	N

G - Good, S - Sluggish, P - Poor; G - Good, M - Moderate, P - Poor; N - None, M - Moderate, L - Large

minor additions of manganese or copper to further depress flow temperatures. The same reasoning held true for the alloying agents, silicon, iron, cobalt, and nickel. In the systems, Ti-X-Be, minor additions of these elements brought about marked reductions in flow temperatures (although not of sufficient magnitude to be interesting in the Ti-X-Be system itself). For example, just 4.28 percent cobalt reduced the flow temperature 130 degrees F; 2.76 percent iron reduced the flow temperature 160 degrees F; 4.14 percent nickel reduced the flow temperature 150 degrees F; and only 1.21 percent silicon reduced the flow temperature 170 degrees F. Such reductions would be most desirable for Ti-Zr-Be braze alloys which themselves already possess nominally acceptable flow temperatures in the range of 1600 to 1700 F. Consequently, the effects of controlled alloying with the elements copper, manganese, silicon, iron, cobalt, and nickel were studied on the most promising alloys of the Ti-Zr-Be system.

The Ti-Zr-Be System. Progressive additions of zirconium to the Ti-Zr-5.6Be ternary (starting at zero percent zirconium) resulted in a systematic decrease in braze flow temperature from 2050 F to a minimum of 1620 F at 47.2 percent zirconium (Tables XXI, XXIV, and Fig. 44). The minimum in flow temperature occurs at the same Ti/Zr ratio (50.0/50.0 weight percent) as that which produces the minimum liquidus temperature in the Ti-Zr binary system. Since the first eutectics in both the Ti-Be and Zr-Be systems occur at 5.6 percent beryllium (Solar determination), the minimum at Ti-47.2Zr-5.6Be was not surprising. Typical braze structures for all six zirconium levels are shown in Figure 45. All candidate brazements passed a 72-hour salt-spray corrosion test without apparent structural damage.

An apparent anomaly in the mode of liquidus depression was observed in the first run of tests at the 9.5 percent zirconium and 18.9 percent zirconium levels (Fig. 44). At 9.5 percent zirconium, the depression was approximately 140 degrees F lower than expected; at 18.9 percent zirconium, about 40 degrees F. Initially, it was suspected that another low-beryllium eutectic or minimum in the Ti-Zr-Be system was being evidenced, possibly occurring at a high Ti/Zr ratio. Such a eutectic or other low-melting phenomenon might have proven desirable as a braze alloy base by inhibiting the erosion and corrosion tendencies (i.e., the inhibition of both is favored by high Ti/Zr ratios at equivalent braze temperatures). Unfortunately, the anomalously low braze temperatures could not be reproduced in second and third attempts to confirm first run data. The most logical explanation was that random Zr segregation in the button ingots caused the sporadic low melting behavior.

The most important result of this screening study, however, was that the Ti-47.2Zr-5.6Be braze appeared to be the most promising base for further study and optimization. The flow temperature was the lowest recorded at the 5.6 percent beryllium level (1620 F); consequently, foil erosion was minimal. The alloy exhibited excellent brazing characteristics in a high-vacuum environment and in argon. Particularly attractive were its outstanding fluidity in capillaries and its smooth filleting behavior. Both were consistent in any one specimen and reproducible from specimen to specimen. In spite of its high fluidity characteristic, it showed no inclination towards deleterious "super-fluidity" or "sweating" as do most silver-base alloys. Finally, the crevice corrosion resistance of Ti-47.2Zr-5.6Be brazements in salt spray tests appeared equivalent to the best titanium-base brazements evaluated to date (Fig. 45F).

Because the Ti-47.2Zr-5.6Be looked so promising as a candidate braze material, additional studies (other than the standard braze screening tests) were felt warranted to better gage its potential for foil joining. This work took the form of:

- Mechanical tests, as-brazed and with post-braze heat treatment, to more completely appraise brazement strength, toughness and effects of corrosion.
- Additional foil brazing and structure studies to determine the critical elements of braze alloy preparation and safe limits of braze cycling.

This additional study resulted in the high-purity compositions, CS13-4 and CS13-5, both nominally Ti-47.2Zr-5.6Be (Table XVIII). As a final system modification, the Ti/Zr ratio was varied simultaneously with reduction in beryllium concentration in

TABLE XXV

MODIFICATIONS OF THE BASIC CS13-5 BRAZE ALLOY

Braze Alloy Designation	Composition High Purity Melt Stocks (wt %)			Solidus Temperature (F)	Minimum Flow Temperature (F)	Fluidity	Fillet Formation	Unmelted Residue
	Ti	Zr	Be					
101	Balance	5.0	5.6	1930	1930	G	F	N
102	Balance	10.0	5.6	1850	1890	G	G	L
103	Balance	15.0	5.6	1780	1790	F	F	M
201	Balance	45.0	5.6	1640	1640	G	G	N
202	Balance	47.5	5.6	1625	1625	G	G	N
203	Balance	50.0	5.6	1620	1620	G	G	N
204	Balance	47.5	5.6	1640	1645	G	G	N
205	Balance	47.7	5.6	1650	1650	G	G	N
206	Balance	46.0	5.0	1630	1630	G	G	N
207	Balance	50.0	5.0	1640	1640	G	G	N
208	Balance	46.0	4.0	1630	1640	G	F	L
209	Balance	48.0	4.0	1615	1630	G	P	L
210	Balance	50.0	4.0	1630	1640	G	G	L
211	Balance	48.3	3.5	1625	1635	G	F	L
212	Balance	48.5	3.0	1630	1650	G	F	L
213	Balance	47.0	3.0	1630	1650	G	F	L
214	Balance	45.0	3.0	1620	1650	G	F	L
215	Balance	45.3	5.0	1620	1620	G	G	M
216	Balance	45.5	4.5	1635	1650	G	G	M
217	Balance	47.5	5.0	1640	1640	G	G	N
218	Balance	47.8	4.5	1660	1675	G	G	M

F - Fair
G - Good
L - Large
M - Moderate
N - None
P - Poor

the hope of lowering the beryllide content to the lowest level without appreciably changing braze characteristics. The objective was to produce a tougher (hypoeutectic) braze alloy with eutectic braze characteristics. The alloy modifications examined in the T-joint screening tests are listed in Table XXV. The 50Ti/50Zr ratio ultimately was considered most beneficial to retain inasmuch as lower Ti/Zr ratios resulted in more pronounced erosion tendency while higher Ti/Zr ratios resulted in higher braze temperatures and unmelted residue. The optimum beryllium level, however, proved to

be only 5.0 percent beryllium, which favored significantly less beryllide formation. (This hypoeutectic alloy modification was labeled CS217.) Beryllium levels below 5.0 percent created problems of braze sluggishness and heavy unmelted residue because of their very hypoeutectic nature. The two best CS alloys, CS13-5, (eutectic and low interstitial content) and CS217 (hypoeutectic), were chosen for optimization through fourth element additions and heat treatment.

The Ti-Zr-X-Be System (CS Series). Previous work had established the optimum beryllium concentration (5.0 percent) and Ti/Zr ratio (50/50 weight percent) for braze alloys of the Ti-Zr-Be ternary system. The resultant alloy (labeled CS217, an obvious derivation of CS13-5) brazed well at 1640 F with minimal foil erosion and negligible alteration of foil structure and hardness (Fig. 46). The chief concerns at this point over braze structures in general for the CS series alloys were:

- An occasional tendency to form massive beryllide particles (R_C 65 to 70) in the as-brazed condition.
- A moderately hard eutectic structure (~R_C 50 to 55) which constituted the bulk of the braze volume.
- A tendency to form retained β or partially transformed β "bridges" on faying surfaces upon prolonged holding (> 5 minutes) at the braze temperature (~R_C 35 to 40 with Ti-5Al-2.5Sn foils). The primary beta formation tendency was relatable to foil assimilation of the beta stabilizers, zirconium and beryllium, from the braze. An example of the surface buildup of beta is shown in Figure 45C and F.

None of these structural characteristics were definitely known to impair brazement strength, toughness, or stability. The concern was that they might well influence braze properties or stability. A more favorable braze structure doubtless would be devoid of massive beryllide; would possess a softer eutectic (~R_C 35 to 45) comprised of fully (i.e., equilibrium) transformed titanium matrix enclosing spheroidized, uniformly distributed beryllides; and would possess interlocking bridges of primary solids (fully transformed beta at R_C 30 to 35). All of these desirable alterations in braze structure might be accomplished by one or more of the following:

- Controlled minor alloying additions (substitute partially for beryllium as a melting point depressant).
- Controlled braze cycle (controlled braze solidification).
- Heat treatment post brazing (primarily to achieve equilibrium products of β transformation).

TABLE XXVI

MODIFIED CS217 SERIES BRAZE ALLOYS

	Nominal Alloy Composition (wt %)	Melting Point (F)	Flow Temperature (F)	Flow	Fillet	Reaction	Microstructure	Hardness R_C (a)	(b)	(c)	(d)	Remarks
	[illegible] CS 217 + 10% Ag	1650	1670	G	G	N	Good flow and no erosion. Massive beryllides near the foil interface.	65 to 67	-	49 to 51.5	33	Peel test as brazed = 253 lb/in.
	[illegible] CS 217 + 5% Ag	1650	1680	G	G	M	Good flow and no erosion. Massive beryllides near the foil interface.	64 to 66	-	51 to 52.5	33	
	[illegible] CS 217 + 0.5 Al	1700	1700	E	E	N	Excellent Flow. Beryllides are small. No erosion.	-	-	52	36	Peel test as brazed = 246 lb/in.
	[illegible] CS 217 + 5% Fe	1700	1720	G	G	L	---					
	[illegible] CS 217 + 5% Ni	1690	1690	G	G	N	Good flow and fillet. Small beryllides and uniformly distributed.					
	CS 217 + 5% Co	1680	1670	E	E	N	Excellent flow and fillet. Small beryllides and uniformly distributed.					Excellent braze
	CS 217 + 2% Si	1665	1680	G	G	N	Good flow and fillet. Massive beryllides.	64 to 67	-	49 to 52	35	
	CS 217 + 1.2% Ge	1650	1650	G	F	N	Fair fillet. Beryllides small.					
	CS 217 + 9.6% Cu	1625	1660	E	E	N	Excellent flow and fillet. Beryllides are small, spheroidized and uniformly distributed	64 to 68	-	50 to 52	34	Alloy appears very tough in comminution of button ingot.
	CS 217 + 13% Mn	1580	1630	P	P	N	Poor fillet. Moderate erosion. Beryllides are variable in size (a few are massive).					Alloy appears brittle in comminution of button ingot.

(a) Intermetallic compound
(b) Intermetallic layer
(c) Ductile matrix
(d) Titanium foil

E - Excellent
F - Fair
G - Good
L - Large
M - Moderate
N - None
P - Poor

Work was concentrated upon minor alloying additions, based largely upon the encouraging results of similar additions to the Ti-5.6Be binary alloy. It was anticipated that the alloy additions would (in general) tend to lower the braze flow temperature of the base alloy, CS217. However, it was felt that as long as the braze temperatures of CS217 modifications remained ≤1700 F, no problems of excessive foil erosion or beta embrittlement (foil) would be experienced. The actual effects of controlled additions of silver, aluminum, iron, nickel, cobalt, silicon, germanium, copper, and manganese upon braze characteristics and braze structure are listed in Table XXVI. The method of alloying consisted of adding a given weight percent of a fourth element (silver, silicon, nickel, etc.) to the CS217 base so that the Ti/Zr ratio remained constant (50/50), but the beryllium level was reduced by the amount of the fourth element addition (4.4 to 4.9 percent beryllium).

On the nonberyllide formers (silver, aluminum, silicon, and germanium), only aluminum and silicon exhibited promise. In T-joint braze tests with CS217C

Best Available Copy

TABLE XXVII

STRENGTH AND STRAIN ACCOMMODATION TESTING OF CS217 SERIES BRAZE ALLOYS AT ROOM TEMPERATURE

Alloy	Stress in foil component (psi) to cause joint failure in T-joint tests. (Ti-6Al-4V) Foil Area = 0.5 x 10 x 10^{-3} sq in.	Threshold foil stress and strain levels for first crack in tapered tensile specimen (Ti-5Al-2.5Sn) 6 mils thick	
		Minimum Stress (ksi)	Strain (micro in./in.)
CS217	105,000, 93,000	103	6438
CS217A : + 10% Ag	108,000, 40,000	109	6812
CS217C : + 5% Al	142,000, 137,000	132	8250
CS217E : + 5% Ni	105,000, 49,000	120	7500
CS217F : + 5% Cu	137,000, 74,000	95	5800
CS217G : + 2% Si	139,000(1), 139,000(1)	98	6100
CS217H : + 1.2% Ge	81,000, 90,000	103	6400
CS217I : + 9.6% Cu	52,000, 49,000	81	5000
Ti-6Al-4V foil (0.006 in.)	135,000, 157,000	~100 (Yield Stress)	~6700 (Yield Stress)

1. Parent metal failures.

(5 percent aluminum) and CS217G (2 percent silicon) alloys, very good brazing characteristics were evident at the somewhat elevated flow temperatures of 1700 and 1380 F, respectively (Fig. 47 and 48). The aluminum-containing alloy (CS217) showed no massive beryllide formation, but neither braze alloy eutectic structure revealed any softening trend (Table XXVI). The important advantages afforded by these two alloys ultimately lay in the areas of high and reproducible brazement strength (T-joint tensile) and, in the case of CS217C (Table XXVII), good strain accommodation (tapered foil tensile specimen covered with thin surface film of braze). In duplicate T-joint tensile tests on CS217C, T-joint failures occurred in the braze, but very near the fracture strength of the Ti-6Al-4V foils. In similar tests upon CS217G, failure did occur in the foil members at high stress levels (139,000 psi foil stress). Strain accommodation tests also revealed that cracks did not develop in thin surface braze films (CS217C) until a foil strain higher than that equivalent to the foil yield strain was developed.

These test values showed a marked improvement over those for the CS217 base, and helped to indicate the CS217C braze modification as the most promising braze candidate to this point. T-joint strength values for CS217G (2 percent silicon) were equally promising in spite of the massive beryllides in the braze structure and lower strain accommodation values.

Of the beryllide formers, copper, nickel, and cobalt additives appeared to have good potential (Table XXVI). Brazing characteristics were uniformly good to excellent, and lower braze temperatures were possible, e.g., 1520 F with CS217I (3.6 percent copper); 1600 F with CS217E (5 percent nickel); and 1620 F with CS217F (5 percent cobalt). As shown in Figures 49, 50, and 51, alloys showed a tendency to form small, uniformly dispersed beryllides, with negligible massive beryllide formation. The copper-containing alloy (CS217I) appeared especially good in this structural aspect, which may account for its high level of toughness as gaged by its resistance to ingot crushing. However, the T-joint tensile strength of CS217I proved much inferior to the CS217 base (Table XXVII). The nickel- and cobalt-containing braze alloys yielded erratic strength data with low strength levels. Strain accommodation tests on those modifications showed that the nickel-containing alloy (CS217E) was the only one capable of being strained above the yield strain of the substrate foil.

It was decided at this point to select the following CS series alloys for more thorough evaluation in Task IV of Phase I:

Alloy	Basis for Selection
CS217, Eutectic (CS13-5) and CS217	Baseline for comparison
CS217C and CS217G	Highest strength, good to moderate strain accommodation (respectively)
CS217E	Moderate strength, good strain accommodation
CS217F	Excellent braze characteristics, moderate strength and strain accommodation
CS217I	Excellent braze characteristics and braze structure, good toughness level indicated, fair strength and strain accommodation

The Ti-Zr-Ni System (RM Series). Modification of the basic RM1 alloy was undertaken to obtain greater toughness and to evaluate and improve corrosion resistance. The details of this initial investigation for the variations of the RM series (RM1 to RM21) are included in Table XXII. The modifiers were manganese, copper, tin, beryllium (which form eutectics with titanium, zirconium, and nickel), and palladium (which forms a continuous solid solution with nickel with a minimum melting point at

TABLE XXVIII

EFFECT OF ADDITION OF 10 PERCENT SILVER ON RM SERIES ALLOYS

RM Number	Alloy Composition	Flow Point (F)	Strain Accommodation Tests (Ti-5Al-2.5Sn Tapered Foil, 0.500 Inch Thick)		T-Joint Tensile Test (0.010 inch thick Ti-6Al-4V foils)	
			Foil Stress at Initial Braze Cracking (ksi)	Foil Strain at Initial Braze Cracking (micro in./in.)	Foil Stress at Component Failure (ksi)	
1	Ti-41Zr-18Ni	1650	91.5, 95.6	5820, 5975	81	65
26	RM1 + 10%Ag	1620	98.5	6160	---	--
4	Ti-42Zr-14Ni	1750	--- ---	--- --	---	--
32	RM4 + 10%Ag	1720	90.7	5670	61	56
12	Ti-Zr-8Ni-2Be	1670	80.7, 108.0	5040, 6750	110	58
33	RM12 + 10%Ag	1580	110.0	6960	78	61

60 weight percent palladium). For various reasons detailed in Table XXII, manganese, copper, tin, and palladium additions did not improve braze characteristics. Principal problems were:

- Continuous, intermetallic layer formation at braze/foil interface
- Excessive erosion
- Low peel test values (< 100 lb/in.)
- Poor flow ≤ 1750 F and heavy unmelted residues

Beryllium was found to depress the melt and flow temperatures considerably and allowed the selection of three possible alloys for second step evaluation studies. Three alloys were found satisfactory from evaluation of flow characteristics, foil erosion, microstructure, and corrosion resistance (examined metallographically after 114 hours in salt spray). These alloys are:

- RM1: Ti-41Zr-18Ni (flow point - 1650 F)
- RM8: Ti-43Zr-12Ni-2.0Be (flow point - 1670 F)
- RM12: Ti-45Zr-8Ni-2.0Be (flow point - 1650 F)

The microstructures (after 114 hours salt spray exposure) of titanium foil T-joints brazed with the above alloys are shown in Figures 52, 53, and 54.

These RM alloys not only possessed very good brazing characteristics with titanium foils (similar to the CS series of Ti-Zr-Be alloys), but also illustrated the potential for providing significantly lower brazing temperatures (<1600 F) with less

beryllium content. As the next step, several other alloying agents (silicon, germanium, silver, and aluminum) as well as more nickel and/or beryllium content were evaluated with the intent of finding even lower melting braze compositions. The details of this investigation are also included in Table XXII. From the flow-temperature standpoint, the following alloys appeared interesting, though extremely brittle:

Designation	Composition (wt %) Titanium	Zirconium	Nickel	X	Flow Temperature (F)	Remarks
RM22	37.5	37.5	21.0	(4.0Be)	1380	Very brittle ingot
RM24	(94% RM1) + (4Be+2Si)				1550	Very brittle ingot
RM25	42.0	42.0	12.0	(4.0Be)	1500	Brittle ingot
RM34	(85% RM22) + (15% Ag)				1550	Brittle ingot

However, on the combined bases of brazing characteristics, apparent toughness in ingot comminution, and favorable joint microstructure (minimal erosion and low intermetallic content), the following RM modifications with silver showed considerably more promise.

Designation	Composition	Flow Temperature (F)
RM28 (Fig. 55)	90% RM1 + 10% Ag	1620
RM32	90% RM4 + 10% Ag	1720
RM33	90% RM12 + 10% Ag	1580

As shown in Table XXVIII, the preliminary test results on the above alloys indicated fair to good strain accommodation levels with only fair braze joint strengths in T-joint tensile tests.

A good possibility existed that improvements in braze toughness, strength, and stability would result from lowering the zirconium content of the RM alloys making

them essentially titanium-based. This was reasonable in light of the following influences attributable to zirconium:

- Zirconium tends to stabilize the β phase and may promote undesirable β transformation products in RM series matrices and braze-affected foils.
- Zirconium tends to restrict the solid solubility of nickel in the terminal solid solution, which acts to increase the $(Ti, Zr)_2Ni$ intermetallic concentration.

One or both of the above tendencies might explain the uniformly easier comminution (as a measure of relative toughness) of RM alloys versus the CS series alloys.

Therefore, a group of RM alloys with just 20 percent zirconium was formulated with the hope of obtaining improved stability and toughness (RM39 to RM46). In comminution, marked improvement in ingot toughness was observed; however, higher beryllium levels were required to maintain braze temperatures ≤1700 F. The RM40 (Fig. 56), RM42, and RM44 alloys displayed best brazing characteristics. Two alloys with no zirconium (RM23 and RM26 - Fig. 57) also appeared interesting from the toughness standpoint and were included in the group for further study.

On the basis of initial screening tests, the following RM-series alloys were chosen for more thorough evaluation in Task IV of Phase I:

Alloy	Basis of Selection
RM1	Baseline
RM8, RM12	Good brazing characteristics and structure, corrosion resistance, and low flow temperatures (1470 and 1650 F, respectively). Moderate strength and strain accommodation.
RM28, RM32, RM33	Superior brazing characteristics ≤1720 F with the 10% Ag addition. Moderate strength and strain accommodation levels. Good toughness levels.
RM23, RM26, RM40, RM42, RM44	Best toughness gaged by resistance to comminution, due to reduced Zr contents. Good brazing Characteristics ≤ 1700 F.

Ni-10P Plating (In-Situ Braze Candidate). To screen Ni-10P, several flat and corrugated pieces of 0.006-inch, Ti-5Al-2.5Sn foil were Kanigen plated on both sides. The plan was to simulate in-situ brazing of a plate-and-fin heat exchanger section.

One series was plated to 0.075 mil and the other to 0.150 mil, with the assumption that some influence of thickness could be measured. First trial brazing temperature of 1825 F for thirty minutes in vacuum was selected to correspond with the most successful previous experience (Ref. 93). As shown in Figure 58A and B, the microstructure of the brazed area and the braze affected center foil was composed of the beta-embrittled ($\alpha + \beta$) Widmanstatten-type structure while the areas adjacent were only affected next to the plating. The normal α structure away from the Ni-10P layer was very clear, indicating that the Kanigen plating can be detrimental as a braze material in lowering the effective beta transus.

Results from salt spray exposure of one hundred hours on the joints were sufficient to show definite corrosion effects and substantial degradation in joint strength and peel resistance (based upon manual bend and peel tests). Evidently, sufficient quantities of nickel and/or phosphorus diffused into the previously all-alpha foils during brazing (1825 F, 0.5 hour) to lower the beta transus from 1900 to <1825 F, resulting in a coarse Widmanstatten precipitate of acicular alpha within untransformed beta upon cooling. Such structures are normally associated with beta embrittlement phenomena. To minimize Ni/Ti/P interdiffusion, lower braze temperatures and shorter braze times were investigated. A braze cycle of 1725 F for 5 minutes apparently left the beta transus >1725 F, but did produce a 1.2-mil thick layer of hard intermetallic phase (Ti_2Ni) adjacent to the braze, leaving just 3.0 mils of unaltered foil (Fig. 58C). Braze flow and fillet formation also proved marginal at 1725 F due to the proximity to the Ni-P eutectic temperature (1700 F).

Subsequent brazing tests conducted at intermediate temperature (1750, 1775, and 1800 F) revealed a logical transition in the foil structures. Foil brazed at 1750 F for 5 minutes exhibited a 1.2-mil thick layer of a coarse Widmanstatten pattern (acicular α and untransformed β) adjacent to the braze alloy coating (Fig. 59A). At 1775 F (5 minutes), the Widmanstatten structure increased to 1.8 mils thick (Fig. 59B). At 1800 F, the entire Ti-5Al-2.5Sn foil was comprised of the coarse Widmanstatten structure and significant grain growth was observed (Fig. 59C).

Because the Ni-10P coating strongly promoted a beta-embrittlement condition at the lowest possible braze temperature, and because foil brazements were found to be susceptible to salt corrosion, it did not appear that the Ni-P system had sufficient merit for titanium foil joining. Therefore, no further investigation was programmed.

Summary of Braze Screening Results

Work began with braze screening tests on some 40 candidate braze alloys using foil T-joint specimens to assess minimum flow temperatures and brazing characteristics. By selective third-element alloying of the Ti-5.6Be eutectic base with minor additions of aluminum, cobalt, chromium, iron, germanium, manganese, copper, nickel, silicon, silver, and tin, attempts were made to reduce the ~2000 to 2050 F binary eutectic braze temperature to ≤1750 F. The main objectives were to minimize the high-temperature foil erosion tendency and to favor retention of foil properties by brazing below the foil alloys' beta transus temperature. Generally, excellent brazing characteristics were obtained, but the lowest braze temperature recorded was 1800 F (with 9.57 percent copper). Fortunately, the Ti-Zr-Be eutectic braze system was found to provide considerably lower starting flow temperatures (~1620 to 1650 F for Ti-47.2Zr-5.6Be) and the third element additions which had shown most promise with the Ti-Be eutectic, were evaluated further (as fourth element additions) with the Ti-Zr-Be eutectic (aluminum, copper, cobalt, nickel, manganese, and silicon). Although lower flow temperatures were not achieved, several of these quaternary alloys (CS series) developed superior strength and toughness properties in foil brazements. Because they brazed well at intermediate temperatures (1650 to 1700 F), foil erosion was minimal and retention of foil properties excellent.

In the final screening study, the largest number of candidate braze alloys were evaluated for applicability to foil joining: 28 more ternary and quaternary alloys based upon the Ti-Zr-Be eutectic (CS series), and 46 more quaternary and quinary alloys based upon Ti-Zr-Ni, Ti-Zr-Ni-Be, and Ti-Ni-Be eutectics (RM series). The RM series substituted nickel in combination with other melting point depressants for beryllium to reduce the total beryllide content and to obtain braze temperatures <1600 F. (Beryllium concentration was varied from 0.0 to 5.0 weight percent.)

An investigation was made also of thin Ni-10P coatings (plated on program alloy foils by the Kanigen electroless process) for possible in-situ braze application (minimal flow brazing). Trial, short-time brazing runs with simulated plate-and-fin

structures were carried out successfully in the range of 1750 to 1825 F, but two serious problems were encountered:

- A brittle, Widmanstatten structure was developed in braze-affected foils at all braze temperatures because of the strong influence of nickel and phosphorus lowering the foil alloy's beta transus temperatures.
- Salt-spray exposure of 100 hours caused visible joint corrosion and substantial degradation in joint strength and peel resistance.

Because of the unpromising screening results, Ni-10P was dismissed as a candidate braze material.

3.4.4 Advanced Braze Optimization Studies

Work was concentrated on studying, in depth, those candidate braze alloys which evidenced most promise in previous screening tests.

Referenced screening of braze characteristics and braze structures reduced the number of useable compositional modifications to the 18 candidate braze alloys listed in Table XXVIX. The braze alloys were divided into two categories:

- The CS series, dependent upon beryllium (4.5 to 5.6%) as the principal melting point depressant.
- The RM series, using both nickel (7.2 to 18.0%) and typically reduced beryllium (0.0 to 5.0%) as major melting point depressants.

The intent of the RM series was to substitute nickel partially for beryllium as a melting point depressant to reduce the total beryllide content. In general, the beryllide content was decreased in the RM series, but the total volume percent of intermetallics remained approximately the same as the CS series (due to Ti_2Ni and Zr_2Ni formation).

T-Joint Corrosion Tests

Small T-joint brazements of Ti-5Al-2.5Sn foil, 0.006-inch thick were exposed to 100 hours of salt spray environment, then bent manually 90 degrees and examined visually and metallographically. The candidate braze alloys RM1, RM23, RM26, RM28, RM32, RM44, CS217E, and CS217F showed a slight tendency toward braze (not joint interface) cracking on bending before the salt spray test; and as shown in Figure 60 through 64, the salt spray environment did not aggravate this tendency. Only RM40 and CS217I appeared somewhat more prone to in-braze cracking following salt spray exposure and, as shown in Figures 65 through 68, there was no evidence of interface corrosion.

TABLE XXVIX

BRAZE ALLOYS EVALUATED IN TASK IV

Alloy No.	Braze Alloy Designation	Nominal Composition (wt %)									Minimum Flow Temperature (F)
		Ti	Zr	Ni	Be	Al	Co	Si	Cu	Ag	
1	CS13-5	Bal	47.2	—	5.60						1620
2	CS217[1]	Bal	47.5	—	5.00						1640
3	CS217C[2]	Bal	45.1	—	4.75	5.0					1700
4	CS217E	Bal	45.1	5.0	4.75						1600
5	CS217F	Bal	45.1	—	4.75	—	5.0				1610
6	CS217G	Bal	46.6	—	4.90	—	—	2.0			1680
7	CS217I	Bal	42.9	—	4.50	—	—	—	9.6		1520
8	RM8[3]	Bal	43.0	12.0	3.00						1470
9	RM12[4]	Bal	45.0	8.0	2.00						1660
10	RM1	Bal	41.0	18.0	—						1650
11	RM33	Bal	40.5	7.2	1.80	—	—	—	—	10.0	1580
12	RM32	Bal	38.7	12.6	—	—	—	—	—	10.0	1720
13	RM28	Bal	36.9	16.2	—	—	—	—	—	10.0	1620
14	RM23	Bal	—	17.2	4.00						1700
15	RM26	Bal	—	16.9	3.90	—	—	2.0			1660
16	RM40	Bal	20.0	8.0	5.00						1700
17	RM42	Bal	20.0	12.0	4.00						1700
18	RM44	Bal	18.0	7.2	4.50	—	—	—	—	10.0	1700

1. Density = 4.63 gm/cc
2. Density = 4.67 gm/cc
3. Density = 5.46 gm/cc
4. Density = 5.33 gm/cc

The remainder of the candidate braze alloys exhibited no cracking tendency either before or after salt spray exposure; and as shown in Figures 69 through 73, there was no evidence of interface (crevice-type) corrosion or general corrosion on any candidate brazement.

T-Joint Strength Tests

T-joint tensile tests were carried out on candidate alloy brazements in both the as-brazed condition and after 100 hours exposure to salt spray (0.010-inch thick Ti-6Al-4V foils). Inasmuch as the great majority of failures occurred in the braze

TABLE XXX

RESULTS OF ROOM TEMPERATURE T-JOINT TENSILE TESTS

Braze Alloy	Foil Stress at Failure - T-Joint Tensile Specimens (ksi)	
	As-Brazed Condition	After 100 Hours Salt Spray
CS13-5	147.8, 47.0	60.0, 47.0
CS217	154.5[1](PM), 145.6, 105.3, 93.2	118.5, 49.2
CS217C	141.1, 136.8, 112.0, 111.5	129.0, 87.8
CS217E	105.3, 82.0, 49.3, 41.0	40.5, 40.0
CS217F	136.8, 83.0, 73.9, 63.0	117.5, 100.0
CS217G	138.9[1](PM), 138.9(PM), 129.0, 60.0	148.0, 100.5, 125.2[1]
CS217I	60.5, 60.5, 51.5, 49.3	41.0, 40.3
RM8	119.0, 83 0, 74.0, 70.0, 62.0	82.0, 41.0
RM12	118.0, 108.0, 62.0, 60.0	94.0, 56.0
RM1	82.0, 76.0, 64.0, 40.0	92.3, 76.0
RM33	80.0, 61.0, 40.0, 30.0	15.0
RM28	40.0, 30.0	58..., 36.0
RM23	74.0, 60.0, 30.0, 25.0	77.0, 36.0
RM26	108.0, 47.0	76.0
RM40	112.0, 105.3, 80.0	87.8, 37.0
RM42	67.0, 62.0, 27.0, 40.0	95.5, 37.0
RM44	130.0, 30.0	44.8, 25.0
Ag-5Al	56.0, 28.0	---

1. Same T-joint specimen exposed in salt for 100 hours, then retested.
PM - specimen failed in foil component.

metal, a relative assessment of braze strength and resistance to corrosion effects was possible. The results of the T-joint tensile tests are tabulated in Table XXX and the flow characteristics and mechanical properties of the candidate braze alloys are summarized in Table XXXI. The CS series of braze alloys showed the highest strength potential (Fig. 74). Maximum as-brazed strengths in the range of 105 to 155 ksi (foil stress) were quite common. However, the variation of strength for a given alloy brazement was seen to be great also; in many cases the minimum strengths were only 50 percent or less of the maximum values (e.g., CS13-5, CS217E, CS217F, and CS217G). The wide scatter of strength values very likely reflects the marginal

notch toughness of the high-beryllium CS series. In this regard, the candidates CS217C with 5 percent aluminum and CS217G with 2 percent silicon appeared most promising, using the double criteria of highest strength levels and most consistent strengths. This observation was valid both as-brazed and after salt spray. The braze alloy CS217I also gave consistent strength values, quite possible due to its naturally spheroidized as-brazed structure. Strength values of CS217I were the lowest of the CS series, however.

With the limited number of test results, it was difficult to assess the effect of salt spray environment on joint strength of the CS series braze alloys. However, for the CS series as a whole, the very general observation could be made that the minimum strengths following salt spray are the highest (> 85,000 psi) for the candidates CS217C, CS217F, and CS217G. However, the wide scatter of as-brazed strength values for the CS217F and CS217G alloys, with values as low as 60,000 to 63,000 psi, reduced the importance of the preceding observation. For cases where data scatter were not appreciable, no definite strength degradation was observed (single exception: CS217I). Hence, the corrosion effect tentatively was assumed negligible to minor. The big problem again appeared to be marginal notch toughness of the braze materials, leading to widespread scatter of strength values.

The same general observations regarding the broad scatter of strength data and vagueness of a corrosion effect held true for the RM series of braze alloys. The braze alloys RM8, RM12, and RM40 showed most promise on the basis of consistently providing minimum braze strengths ≥ 60,000 psi (as-brazed condition). This criterion ensured an as-brazed strength superior to that afforded by Ag-5Al alloy. In general, the better RM series alloys exhibited lower potential for T-joint tensile strength than the better CS series alloys. Surprisingly, the high toughness RM series alloys containing lower zirconium content (e.g., RM40, 42, 44) and no zirconium (e.g., RM23, 26) exhibited just as much scatter in strength data as the less tough, high-zirconium heats. The problem likely stemmed from the higher beryllium (and beryllide) levels required to maintain flow temperatures ≤ 1700 F.

TABLE XXXI

FLOW CHARACTERISTICS AND MECHANICAL PROPERTIES OF CANDIDATE BRAZE ALLOYS

Braze Alloy and Composition	CBBA-6 Ti-47.5Zr-5.0Be	CBB17 Ti-47.5Zr-5Be	CBB17C Ti-40.1Zr-4.7Be-5Al	CBB17E Ti-40.1Zr-4.7Be-5Mn	CBB17F Ti-40.1Zr-4.7Be-5Cu	CBB17G Ti-40.4Zr-4.9Be-5Ni	
Resistance to Cracking	A	A	B	B	B	A	
Flow Point (F)	1650	1640	1700	1660	1650	1690	
Microstructural Details	Excellent flow and fillet. No erosion but massive beryllides.	Excellent flow and fillet No erosion but some massive beryllides.	Good flow and fillet. No erosion. Small beryllides which are uniformly distributed.	Excellent flow and fillet. No erosion. Many beryllides, small and uniformly distributed.	Very good flow and fillet. Similar to CBB17E.	Good flow and fillet. No erosion. Some massive beryllides.	
Fluidity	A	A	A	A	A	B	
Hardness Values R_C							
Matrix	40 to 46	38.0 to 41.0	36 to 39	40 to 43	46 to 50.0	36.5 to 38	
Composite	66 to 70	70.7	66 to 70	66 to 70	67.5	68.2	
Strain Accommodation (micro in. /in.)	5545	5904	5478	5900	5850	5830	
T-joint Tensile Test, Stress at Failure (ksi)							
Arc-Melted Ingot	107.5, 97.0	154.5(PSB), 146.4 100.0, 95.2	141.1, 136.0 113.0, 111.5	136.0, 82.0 40.0, 41.0	135.5, 88.0 72.0, 83.0	136.5(PSB)[1], 130.0(PSB) 129.0, 90.0	
Homogenized Ingot	107.5, 107.0	140.0, 91.5	136.0, 136.0	--	--	150.0, 113.0	
After 100-hour salt spray	90.0, 97.0	116.5, 98.5	120.5, 97.5	40.0, 40.0	117.0, 100.0	123.2, 108, 100.5	
Double Pull Lap Joint Pull Test (lb/in.), Fuse Blist[1]	744, 650[1]	0.0, 500[1]	890, 880	906, 781	1161, 430[1]	868, 487[1]	
Lap Shear Test: Ult stress at failure (ksi)	85.5	91.6	106.0	97.0	90.2	86.8	

Braze Alloy and Composition	CBB17I Ti-42.5Zr-4.8Be-3.0Cu	Ag-4Al	Zr-Be Ti-40Zr-12Be-5Ni	BM18 Ti-45Zr-5Be-5Ni	BM1 Ti-41Zr-10Be	BM33 Ti + 40.5Zr + 7.5Be + 1.5Fe + 10Ag	
Resistance to Cracking	B	--	F	B	F	B	
Flow Point (F)	1690	1750	1670	1660	1650	1680	
Microstructural Details	Excellent flow and fillet. No erosion. As-brazed structure is spheroidized.	Good flow and fillet. No erosion.	Excellent flow and fillet. No erosion.	Average flow and fillet. No erosion.	Average flow and fillet. No erosion.	Average flow and fillet. No erosion.	
Fluidity	A	A	A		C	B	
Hardness Values R_C							
Matrix	38.5 to 41.5	--	38.0	60 to 62	56.0 to 62.0	38.0	
Composite	60	--	--	--	43 to 45	--	
Strain Accommodation (micro in. /in.)	7035	--	6400	9864	6650	9864	
Arc-Melted Ingot	60.5, 60.5 51.5, 60.5	86.0, 86.0	118.0, 80.0, 74.0 70.0, 82.0	118.0, 108.0 62.0, 60.0	82.0, 76.0 64.0, 60.0	90.0, 81.0 60.0, 50.0	
Homogenized Ingot	--	--	90.0, 65.0	134.0, 90.0	--	--	
After 100-hour Salt Spray	41.0, 60.0	--	88.0, 61.0	94.0, 90.0	92.0, 76.0	15.0	
Double Pull Lap Joint Pull Test (lb/in.) Fuse Blist[1]	1160, 827	1250, 1220	670, 690, 680	710, 690	872, 314[1]	827, 464[1]	
Lap Shear Test: Ult stress at failure (ksi)	90.5	78.0	97.0	100.1	--	73.0	

Braze Alloy and Composition	BM28 Ti-60.7Zr-13.4Be-10Ag	BM29 Ti-66.9Zr-13.2Be-10Ag	BM23 Ti-17.2Be-4Cu	BM26 Ti-16.9Be-8.9Be-5Ni	BM40 Ti-60Zr-30Be-5Be	BM42 Ti-60Zr-12Be-4Be	P2644 Ti-16Zr-7.2Be- 4.5Be-10Ag
Resistance to Cracking	B	C	B	B	A	A	A
Flow Point (F)	1750	1650	1700	1660	1700	1700	1700
Microstructural Details	Good flow and fillet. Little erosion.	Good flow and fillet. No erosion.	Good flow and fillet. No erosion.	Very good flow and fillet. No erosion.	Very good flow and fillet. No erosion. Formation of β-beryllide. Com-	Very good flow and fillet. No erosion. Formation of β+eutectic. Com-	Very good flow and fillet. No erosion. Formation of β-beryllide.

Double Fillet Lap Joint Proof Test (lb/in.). Plate Failure[1]	744, 696[1]	840, 884[1]	864, 880	936, 76[illegible]	1161, 686[1]	885, 687[1]	
Lap Shear Test, fail stress at failure (ksi)	88.8	91.6	108.6	97.8	96.2	96.6	
Braze Alloy and Composition	**CB81[2]** Ti-40.4Zr-4.8Mo-0.6Cb	**Ag-4Al**	**B268** Ti-40Zr-12Mn-8Be	**B3612** Ti-44Zr-6Mn-8Be	**B361** Ti-41Zr-19Mn	**B3629** Ti + 40.8Zr + .9Mn + 1.8Mo + .04Ag	
Resistance to Cracking	B	--	B	B	B	B	
Flow Point (F)	1850	1700	1470	1660	1350	1530	
Microstructural Details	Excellent flow and fillet. No erosion. Ag-bronze eutectic in splines/matrix.	Good flow and fillet. No erosion.	Excellent flow and fillet. No erosion.	Average flow and fillet. No erosion.	Average flow and fillet. No erosion.	Average flow and fillet. No erosion.	
Fluidity	A	A	A	C	C	B	
Hardness Values R_C							
Matrix	39.5 to 44.5	--	38.0	[illegible] to 43	46.5 to 52.0	35.9	
Component	60	--	--	--	43 to 45	--	
Strength Accommodation on Failure (ksi)	[illegible]	--	6000	6000	6000	6000	
As-Welded Ingot	60.5, 60.5 51.5, 48.5	56.0, 48.0	118.0, 88.0, 74.0 70.0, 62.5	118.5, 106.0 62.0, 60.0	82.0, 76.5 64.0 40.0	60.5, 61.0 40.0, 30.0	
Homogenized Ingot	--	-	86.5, 66.5	1[illegible]0, 90.0	-	--	
Alkar 100-hour Salt Spray	41.9, 40.3		53.0, 41.0	84.0, 86.2	96.3, 76.0	[illegible].0	
Double Fillet Lap Joint Proof Test (lb/in.). Plate Failure[1]	1160, 880	1660, 1320	690, 690, 660	710, 690	673, 314[1]	927, 604[1]	
Lap Shear Test, fail stress at failure (ksi)	85.3	78.0	87.8	102.1	--	72.2	
Braze Alloy and Composition	**B3628** Ti-50.7Zr-13.6Mn-16Ag	**B3636** Ti-36.9Zr-16.8Mn-10Ag	**B3633** Ti-17.2Al-4Be	**B3626** Ti-[illegible].8Mn-8.9Be-2Al	**B3640** Ti-50Zr-6Mn-5Be	**B3642** Ti-[illegible]Zr-12Mn-4Be	**B3644** Ti-16Zr-7.2Al-4.5Be-10Ag
Resistance to Cracking	B	C	B	B	A	A	A
Flow Point (F)	1750	1800	1760	1660	1700	1760	1700
Microstructural Details	Good flow and fillet. Limit[illegible] erosion.	Good flow no fillet. No erosion.	Good flow and fillet. No erosion.	Very good flow and fillet. No erosion.	Very good flow and fillet. No erosion. Formation of β-bridges. Compounds massive and uniformly distributed.	Very good flow and fillet. No erosion. Formation of β-bridges. Compounds massive and uniformly distributed.	Very good flow and fillet. No erosion. Formation of β-bridges. Compounds massive and uniformly distributed.
Fluidity	C	C	C	A	A	A	A
Hardness Values R_C							
Matrix	87 to 88	84 to 90	41.6	--	47 and 36	51.5 and 35	54 to 63
[illegible]ponent	Intermetallic Layer - 48 to 47	--	87	--	--	--	67.6
Strength Accommodation (psi/in./in.)	[illegible]800	4500	8500	7217	8675	7199	9325
T-joint Tensile Test, Stress at Failure (ksi)							
As-Welded Ingot	61.8, 80.9	40.0, 32.0	76.6, 80.0 80.6, 83.6	100.[illegible], 41.0	112.0, 106.3, 80.0	67.9 62.0 60.5, 87.0	130.0 39.0
Homogenized Ingot	--	--	--	--	86.3, 81.8	--	--
Alkar 100-hour Salt Spray	--	86.2, 81.0	71.6, 86.8	76.8	87.6, 87.9	86.5 87.6	44.8, 25.0
Double Fillet Lap Joint Proof Test (lb/in.). Plate Failure[1]	--	--	798, 878[1]	886, 836	909, 780	546, 186[1]	878, 836
Lap Shear Test, fail stress at failure (ksi)	--	--	96.6	86.0	89.8	86.8	70.8

A - Good
B - Fair
C - Poor

Strain Accommodation Tests

To gage the relative strain accommodation capability of each candidate braze alloy, a very thin layer of braze alloy (< 0.001-inch thick) was spread and brazed discontinuously along the centerline surfaces of tensile specimens of Ti-6Al-4V (0.010-inch thick) with tapered section. Each specimen was pulled in tension at room temperature to a maximum stress of 135,000 psi[1], then examined for cracks in and along the surface braze film. In many cases, no cracks were discernible and the specimens were pulled to failure and reexamined. The width of foil at the last crack was measured with an ST Optical Comparator and this figure was then related to the minimum strain and stress (in the titanium foil) at which cracking started. These strain data are recorded in Tables XXXI and XXXII and typical transverse crack patterns in the braze are shown in Figures 75 and 76. Since brazements in service are not usually subjected to a foil stress above the 0.2 percent yield strength (~ 135,000 psi for Ti-6Al-4V), braze alloys which tend to crack only at foil stress ≥130,000 psi were considered satisfactory from strain accommodation considerations. Those which crack at lower stresses and corresponding strains were screened out as marginal.

The marginal alloys are contained in the following list.

Braze Alloy	Minimum Foil Stress For Braze Film Failure (ksi)
RM1	97.3
RM28	72.0
RM32	120.6
RM42	114.9
RM2S	117.8
CS217I	125.2

Fortunately, all of the candidate braze alloys which exhibited best potential in the preceding corrosion and strength tests also developed satisfactory strain accommodation values (viz. CS217, CS217C, CS217F, CS217G, RM8, RM12, and RM40).

---

1. Stress corresponding to average 0.2 percent yield strength of Ti-6Al-4V foil (braze-cycled condition)

TABLE XXXII

STRAIN ACCOMMODATION TEST RESULTS

Braze Alloy	Thickness in Mils		Specimen Width at Last Crack (in.)	Maximum Load (lb)	For Start of Cracking	
	Foil	Foil + Braze Alloy			Minimum Stress (ksi)	Minimum Strain (micro in./in.)
CS13-5	9.0	9.7	0.270	405	154.5	9650
CS217	9.5	9.6	0.294	410	145.0	9060
CS217C	9.3	10.0	0.299	415	135.6	8475
CS217E	9.5	9.7	0.269	375	143.5	9000
CS217F	9.3	10.0	0.294	390	132.5	8290
CS217G	9.3	10.3	0.296	405	133.0	8320
CS217I	9.1	9.4	0.334	405	125.2	7825
RM8	9.1	10.3	0.289	385	129.5	8090
RM12	9.4	10.0	0.283	420	148.1	9260
RM33	9.3	9.8	0.289	420	147.4	9260
RM23	9.0	9.4	0.302	380	134.0	8380
RM26	9.4	10.0	0.365	430	117.8	7375
RM40	9.1	10.0	0.282	400	142.0	8875
RM42	9.4	10.2	0.324	380	114.9	7190
RM44	9.4	9.6	0.319	408	133.1	8325
RM1					97.3	6080
RM32					120.6	7500
RM28					72.0	4500

Double Lap-Joint Peel Tests

The lap-joint peel tests were conducted on specimens made of 0.010-inch thick Ti-6Al-4V alloy and the results are included in Tables XXXI and XXXIII. Significantly lower values of load for peel failure were obtained when a poor fillet was formed; otherwise, the data obtained are considered satisfactory for evaluation of braze-line peel resistance (a measure of toughness) of the candidate braze alloys.

The Ag-5Al braze joint was found to require the highest average load (1390 lb/in.) for peel-type failure, followed closely by CS217I (9.6 percent copper), CS217E, RM44, CS217C, and CS217F (with average values of 1043, 873, 860, 840 and 794 lb/in. respectively). The alloy CS217F was quite interesting as it exhibited a high tensile strength potential (up to 137,000 psi) as determined by T-joint tensile testing, as well as good strain accommodation and insensitivity to corrosion effects. Curiously, it was occasionally prone to in-braze cracking in manual bend tests. Many of the RM series alloys (RM33, RM12, RM26, RM40, and RM44) possessed about the same maximum peel values as the CS series alloys (except CS217F and CS217I). The promising braze alloys RM8, RM12, RM40, and CS217C, all showed high and consistent T-joint strengths and also exhibited consistently good peel test properties. The CS217G alloy was considered to have satisfactory peel resistance, inasmuch as the one poor test result was attributed to marginal fillet formation.

Lap Shear Strength Tests

The lap shear test consisted of brazing together two 0.010-inch thick by 0.5-inch wide foils (Ti-6Al-4V) with an average overlap of about 0.030 inch, holding at the flow point for 5 minutes, and then testing the resultant specimen in a tensometer to obtain failure by shear through the braze joint. This test was conducted with an idea of determining shear strength of the various braze alloys, but it was found that the joint failure by shear occurred at about the same tensile load regardless of the exact overlap area (except when the overlap was > 0.040 inch, the failure invariably occurred in the titanium foil). This led to the tentative interpretation that failure by shear always occurs by the start of a braze crack or other structural defect at a certain foil stress (or strain) in the fillet area. The inference was that this threshold stress is characteristic of the braze alloy and does not depend primarily on the overlap area. However, when the overlaps exceed 0.040 inch, failure occurs in the titanium foil rather than the joint due to reduced shear strain along the joint interface.

TABLE XXXIII

DOUBLE LAP-JOINT PEEL TEST RESULTS

Alloy	Pounds/Inch (of Braze Line) at Failure (Actual Data)	Average Value
CS13-5	744, 468	606
CS217	840, 550	695
CS217C	860, 820	840
CS217E	985, 761	873
CS217F	1151, 436	794
CS217G	865, 457	661
CS217I	1160, 927	1043
RM1	672, 314	493
RM8	690, 690, 650	677
RM12	710, 690	700
RM33	927, 404	666
RM23	726, 270	498
RM26	838, 650	744
RM40	800, 730	765
RM42	645, 180	412
RM44	878, 838	860
Ag-5Al-.2Mn	1560, 1220	1390

and correspondingly less susceptibility of the braze to notch-induced cracking. The shear strength data obtained at overlap ≤ 0.040 inch are included in Tables XXXI and XXXIV. The values for most braze alloys are in good agreement. Thus, the lap shear test data were considered reproducible in terms of the stress in the foil at incipient shear failure.

The candidate braze alloys CS217C (5 percent aluminum) and RM12 showed the highest lap-shear strengths (related to foil stresses of 106,000 psi and 102,000 psi, respectively). The corresponding average shear stresses based upon the lap-joint area were 39,200 psi and 43,200 psi, respectively. These are quite respectable values of shear strength for titanium foil braze joints and undoubtedly reflect both the influence of intermetallic strengthening and the buttressing effect of the braze fillet at small

TABLE XXXIV

LAP-SHEAR TEST RESULTS

Alloy	Mean Overlap Width (mil)	Exact Thickness of Foil (mil)	Load at Shear Failure (lb)	Stress in Foil at Shear (ksi)	Mean Overlap Width (mil)	Exact Thickness of Foil (mil)	Load at Shear Failure (lb)	Stress in Foil at Shear (ksi)	Average or Most Representative Stress in Foil at Shear (ksi)
CS13-5	28.5	10.6	495.0	93.5	21.5	10.6	493.0	93.1	93.3
CS217	24.5	10.7	482.0	90.1	26.5	11.3	526.0	93.1	91.6
CS217C	28.0	10.3	549.0	106.6	41.0	10.8	639.0	118.3(PM)	106.6
CS217E	22.0	11.1	449.0	81.0	19.0	10.4	492.0	94.5	87.8
CS217F	30.0	11.5	540.0	94.0	25.0	10.6	482.0	93.4	93.2
CS217G	41.0	10.5	505.0	96.4	27.5	10.6	505.0	95.3	95.8
CS217I	15.0	10.7	515.0	96.1	15.0	10.4	470.0	90.5	93.3
RM8	36.0	11.3	347.2	61.5	27.0	10.6	392.0	74.1	67.8
RM12	20.5	10.4	515.0	99.0	30.5	10.4	549.0	105.2	102.1
RM33	20.5	10.45	358.0	68.6	29.5	10.3	392.0	75.8	72.2
RM23	2[illegible](1)	10.4	257.6	49.4	33.5	11.1	369.6	66.6	66.6
RM26	17.5	11.0	348.0	63.4	16.6	11.1	381.0	68.6	66.0
RM40	22.5	10.6	374.0	70.5	22.0	10.7	370.0	69.2	69.8
RM42	16.5	11.0	392.0	71.2	20.5	10.8	336.0	62.4	66.8
RM44	34.5(1)	10.7	224.0	42.7	25.5	10.4	372.0	70.8	70.8
RM22	28.5	10.6	328.0	61.9	31.5	10.6	310.0	59.6	60.7
Ag-5Al	20.0	12.0	425.6	70.9	20.0	11.5	459.0	79.9	75.0

1. Marginal fillet formation.

overlaps. The other CS series alloys developed slightly lower foil stresses at shear failure in the range of 87,800 to 95,800 psi, but substantially greater values than the standard silver braze (75,000 psi) and the other RM series alloys (60,700 to 72,200 psi). The RM22 alloy, with the lowest observed flow temperature (1380 F), actually had the lowest foil stress for failure by shear (60,700 psi).

Selection of Most Promising Candidates

Viewing all of the candidate braze alloys and screening tests in perspective, two alloys appeared outstanding on the combined bases of the highest and most consistent test values for all tests. They were CS217C and RM12. The following eight braze alloys, also showing considerable promise, were transferred as candidates for Task V testing.

- CS217
- CS217C
- CS217F
- CS217G
- RM8
- RM12
- RM26
- RM40

3.4.5 Summary of Task IV - Braze Optimization Studies

Effect of Salt Spray Exposure Upon T-Joint Bend Toughness (RT)

Because of the overriding importance of corrosion resistance, 0.006-inch foil (Ti-5Al-2.5Sn) T-joint brazements of the candidate alloys were subjected initially to salt-spray conditioning (5% NaCl, 200 F, 100 hours). Braze joints made of RM1, RM23, RM26, RM28, RM32, RM44, CS217E, and CS217F exhibited tendencies toward braze cracking during bend toughness tests prior to salt spray. The salt spray conditioning did not aggravate these tendencies. Only RM40 and CS217I brazements appeared more prone to in-braze cracking following salt-spray exposure. The remainder of the candidate braze alloys:

- CS13-5
- CS217
- CS217C
- CS217G
- RM8
- RM12
- RM33
- RM42

showed no cracking tendency in the bend toughness testing (i.e., neither as-brazed nor after salt spray exposure). Of equal significance, no metallographic evidence of braze/foil interface corrosion (crevice-type) or general braze corrosion was observed within any of the candidate alloy brazements.

In contrast, T-joints braze with Ag-10Sn and Ag-5Al-0.2Mn (baseline specimens) fell apart on removal from the salt spray cabinet following exposure times as short as 15 hours.

Effect of Salt Spray Exposure Upon T-Joint Strength (RT)

Tensile tests of braze T-joints at room temperature (both as-brazed and after 100 hours salt spray exposure) developed promising results for most corrosion-resistant braze candidates. The highest strengths (range of ~ 50 to 150 ksi) were generated consistently by CS13-5, CS217, CS217C, CS217F, CS217G, RM8, RM12, RM26, and RM40. Data scatter in this range, both before and after salt spray, was, in many cases, widespread due to the marginal notch toughness of the as-brazed structures and the natural geometric stress raisers inherent in the T-joint specimen

design. Specimens failed predominantly within the braze. In spite of these factors, the better candidate braze alloys exhibited more than double the average T-joint strength of the baseline silver-base braze specimens (as-brazed condition). After salt-spray conditioning, the silver-brazed specimens were so badly corroded that testing was impossible.

Single Lap-Joint Tensile Tests (RT)

The 2t to 4t overlap, lap-joint specimens also produced interesting strength data at room temperature. It was found that overlaps exceeding 4t (i.e., >0.040 inch) invariably resulted in base-metal foil failure. At controlled overlaps, in the range 2t to 4t, specimen failure occurred by tensile shear through the braze. However, it was found that braze fracture was initiated at a near constant foil stress value (regardless of overlap area) rather than at a constant shear stress value. The inference drawn was that fracture initiates at a limiting stress in the braze fillet or braze affected foil immediately adjacent to the joint, triggering subsequent notch-induced shear failure through the braze joint interface. Hence, lap shear test data were recorded in terms of foil stress at specimen failure.

The candidate braze alloys CS217C and RM12 developed the highest average lap-shear strengths (viz., 39,200 and 43,200 psi, respectively, related to foil stresses of 106,000 and 102,000 psi respectively). These levels of shear strength were considered adequate for titanium foil brazements, and undoubtedly reflect both the influence of braze intermetallic strengthening and the buttressing effect of the braze fillets at small overlaps. The baseline silver braze strength was 75,000 psi (foil stress).

Peel Resistance and Strain Accommodation Tests

Special screening tests to appraise the interface peel resistance and strain accommodation capability of candidate braze alloys showed the good applicability of titanium-zirconium base systems. In the double-lap joint peel tests, the soft, tough silver-base braze alloy and two CS series alloys with naturally spheroidized beryllides (as-brazed) exhibited the highest potentials of peel resistance (viz., Ag-5Al-0.2Mn with an average failure load of 1390 pounds/inch of braze line; and CS217F and CS217I with maximum failure loads of 1151 pounds/inch and 1160 pounds/inch, respectively). However, the following alloys with (previously determined) superior corrosion resistance, strength and bend toughness yielded good average values of peel resistance of

650 pounds/inch or greater, many with better reproducibility: viz., CS217, CS217C, RM8, RM40 and RM12. The CS217C alloy with an average peel resistance level of 840 pounds/inch gave the best performance of this latter group.

The strain accommodation test was unique, in that it was developed specifically to determine whether or not braze alloys with a high proportion of high-modulus second phase ca wil stand strains equivalent to the yield strains of the substrate foils. A thin veneer (< 0.001-inch thick) of each candidate alloy was brazed discontinuously along the centerline surface of the 10-mil, Ti-6Al-4V foil tensile specimens of varying (tapered) width. The foil and braze-interface strains on subsequent tensile loading then were inversely proportional to the specimen width, so that the minimum actual strain at which braze or braze/foil interface cracking occurred could be determined through microscopic examination. The best strain accommodation was provided by those braze alloys which cracked only at the highest levels of strain.

Fortunately, almost all the better braze alloy candidates in previous tests showed capabilities of accommodating total strains higher than that corresponding to the 0.2 percent yield strain for the base foils (i.e., approximately 8,400 micro in./in. at 135,000 psi). Assuming a predominantly elastic stress/strain relation, the better candidate alloys for strain accommodation are listed below:

Alloy Designation	Minimum Strain at Incipient Braze Cracking (micro in./in.)
CS13-5	9650
RM12	9260
CS217	9060
RM40	8875
CS217C	8475
CS217G	8320
CS217F	8290
RM8	8090

Overall Performance in Screening Tests

Two candidate braze alloys (CS217C and RM12) consistently warranted superior ratings on all screening tests of Task IV. The braze alloys, CS217, CS217F, CS217G, as well as RM8, RM26, and RM40 also displayed good to superior ratings on most screening tests and, together with RM12 and CS217C, were selected for more advanced testing in Task V.

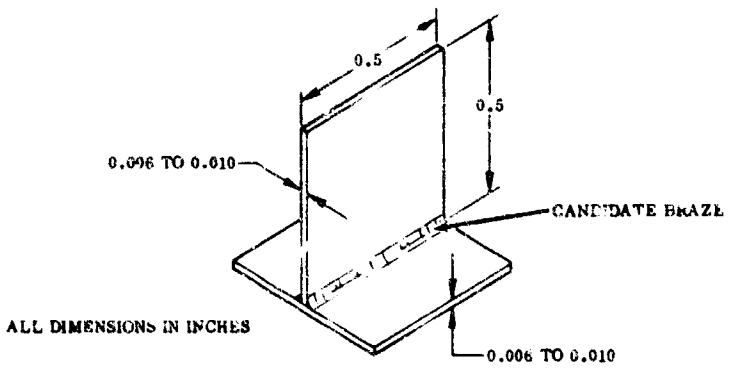


FIGURE 25. TYPICAL T-JOINT SPECIMEN FOR METALLOGRAPHY AND END TESTS

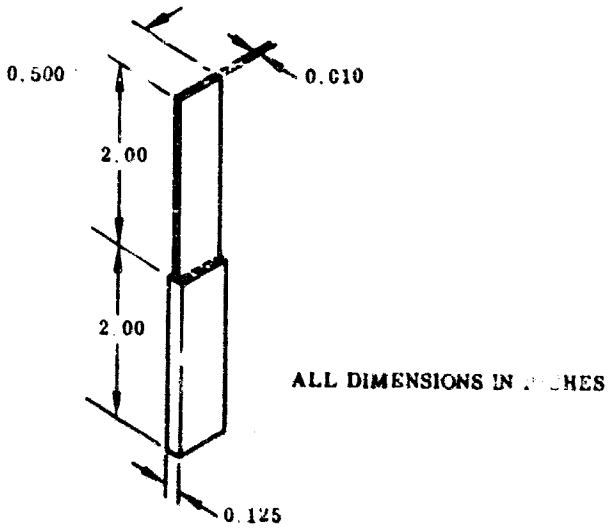
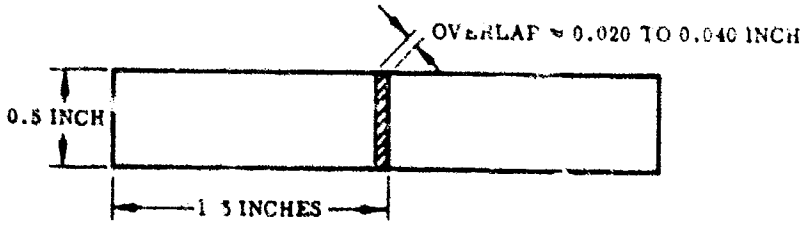


FIGURE 26. TYPICAL T-JOINT SPECIMEN FOR TENSILE TESTS



MATERIAL: Program alloy foils; 0.010-inch thick

FIGURE 27. TYPICAL LAP-JOINT SPECIMEN FOR SHEAR TESTS

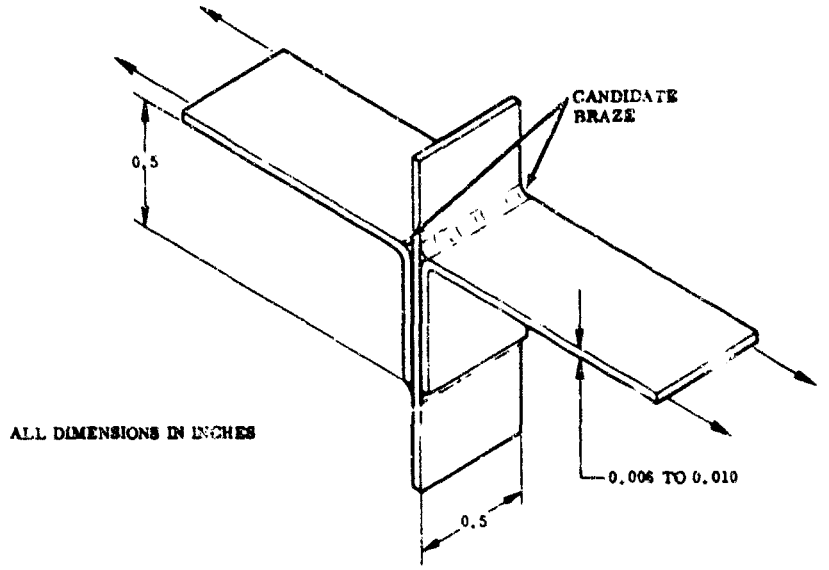


FIGURE 28. TYPICAL DOUBLE LAP-JOINT SPECIMEN FOR PEEL TESTS

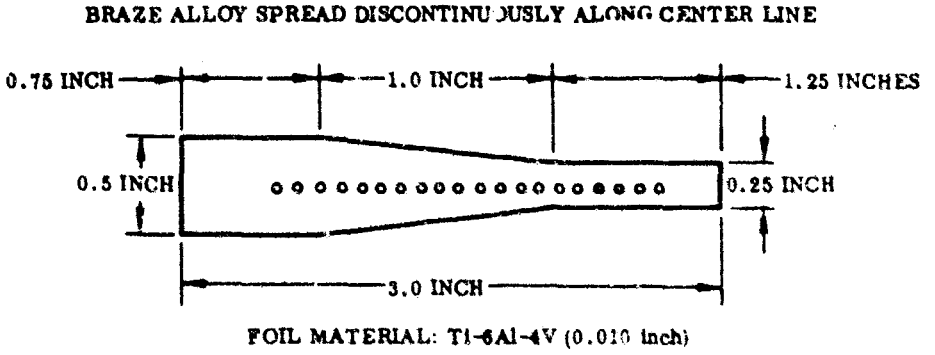


FIGURE 29. TYPICAL STRAIN ACCOMMODATION SPECIMEN

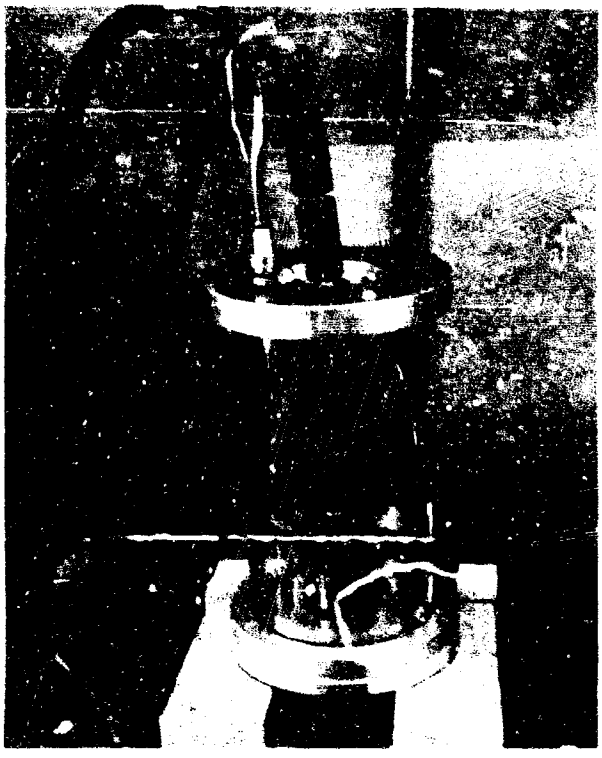


FIGURE 30.

BRAZE ALLOY CHARGE-LOADED IN MELTING FACILITY

Braze alloys are melted in a small arc melting facility. The unit contains a water-cooled copper crucible and an arc electrode contained within a pyrex tube. Purified argon is passed through the pyrex tube.

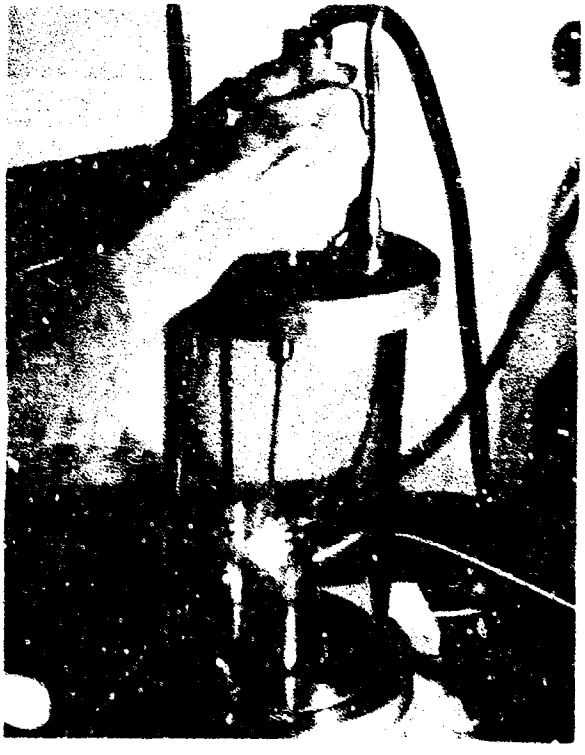


FIGURE 31.

ARC MELTING FACILITY IN OPERATION

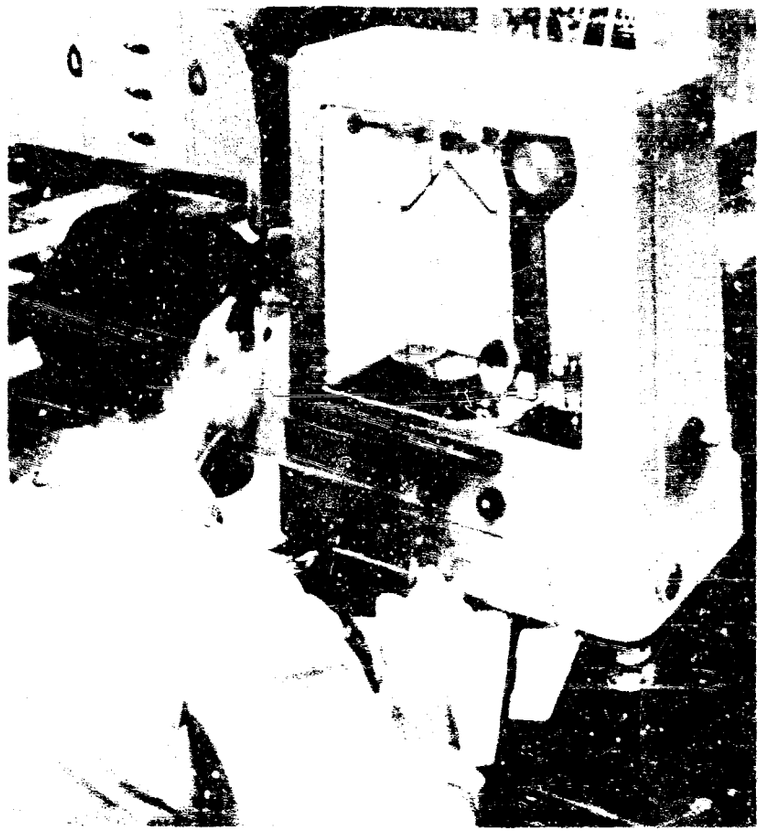
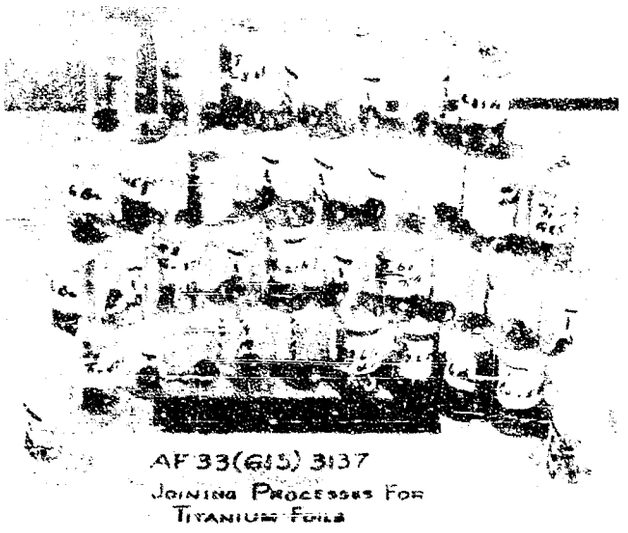


FIGURE 32. ANALYTICAL BALANCE FOR WEIGHT DETERMINATION OF BRAZE ALLOY ELEMENTS



Titanium-base braze alloys prepared for preliminary braze screening tests. The braze alloy "heat" button is crushed to provide a small sample for flow test.

FIGURE 33.

TITANIUM-BASE BRAZE ALLOY MELTS

Titanium foil T-joints used for braze alloy screening tests. Characteristics which are identified include wetting, flow, filleting behavior, structural compatibility and substrate metal erosion.

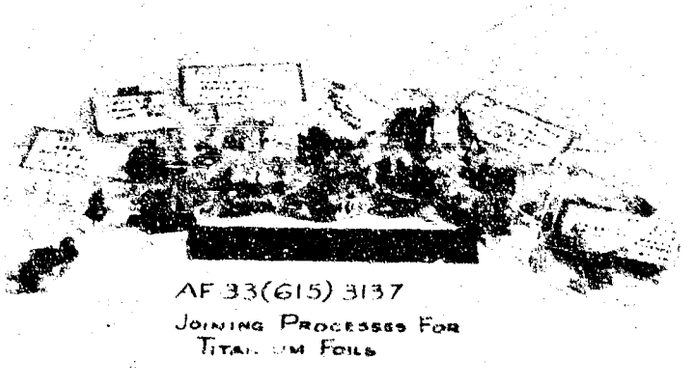
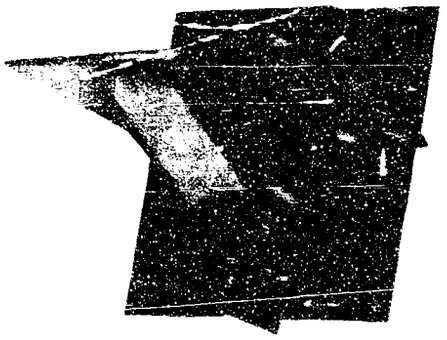


FIGURE 34.

TITANIUM FOIL T-JOINT SPECIMENS FOR BRAZE ALLOY SCREENING TESTS

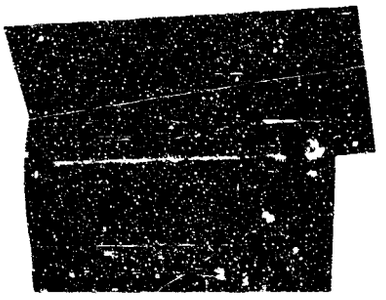


Note the [illegible] titanium foil used to hold assembly in place during braze run.

Magnification: 3X

FIGURE 35.

T-JOINT SPECIMEN BEFORE BRAZE



Magnification: 3X

FIGURE 36.

T-JOINT SPECIMEN AFTER BRAZE



FIGURE 37. LABORATORY BRAZING FURNACE

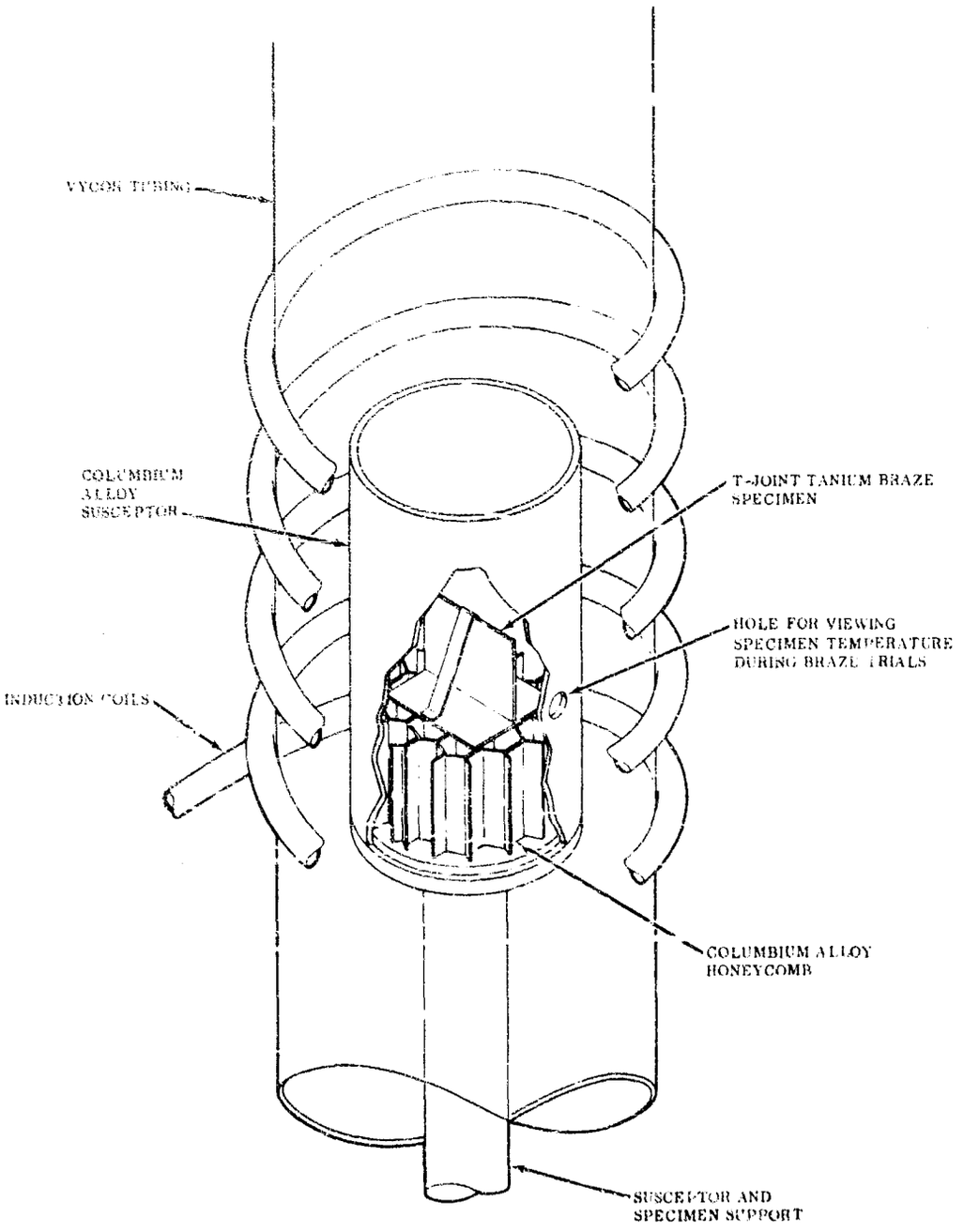


FIGURE 38. SCHEMATIC DIAGRAM OF THE LABORATORY BRAZING FURNACE

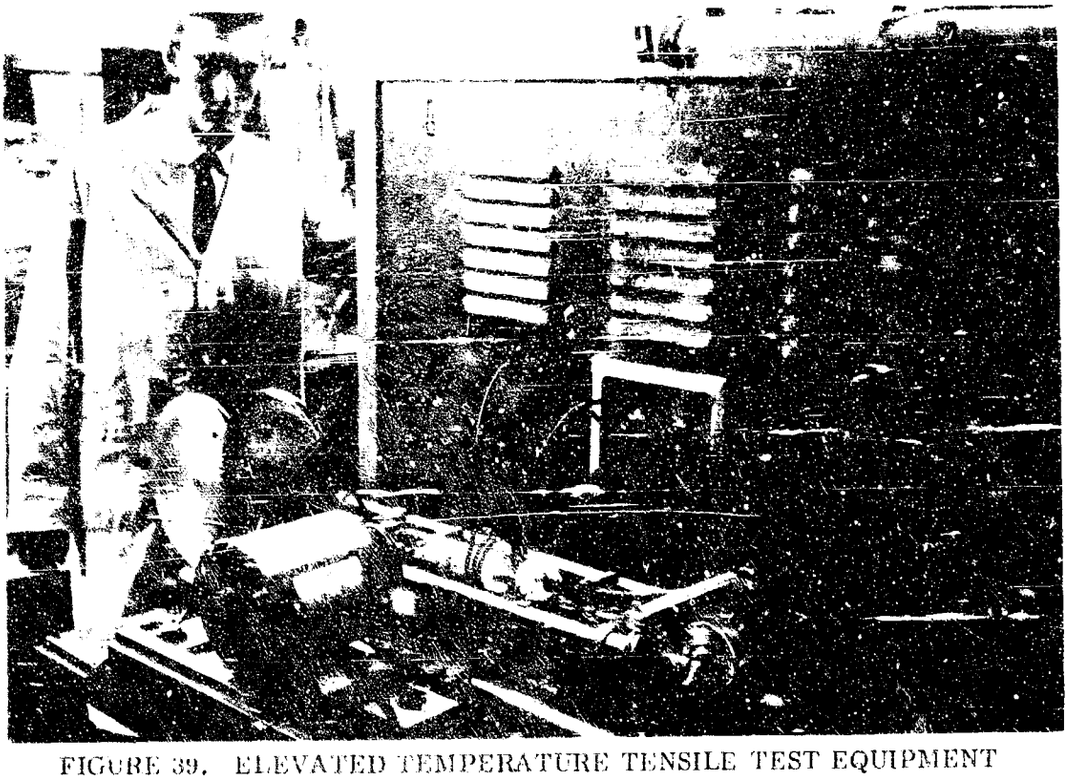


FIGURE 39. ELEVATED TEMPERATURE TENSILE TEST EQUIPMENT



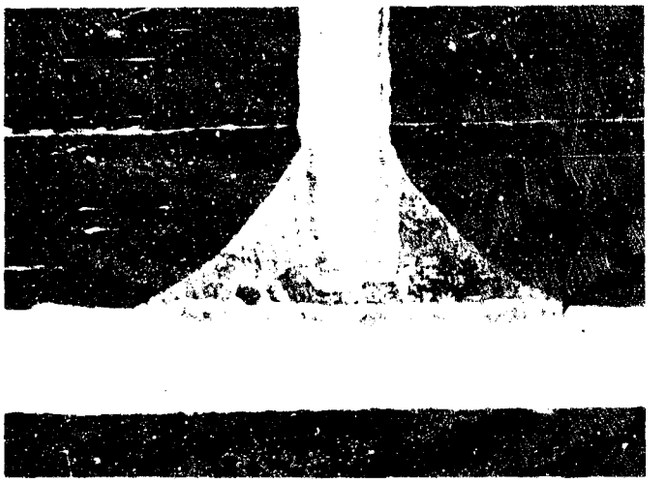
FIGURE 40. CRYOGENIC TEMPERATURE TENSILE TEST EQUIPMENT



Braze Alloy: Ti-9.57Cu-5.6Be
Braze Temperature: 1800 F
Etchant: Kroll's
Magnification: 100X

FIGURE 41.

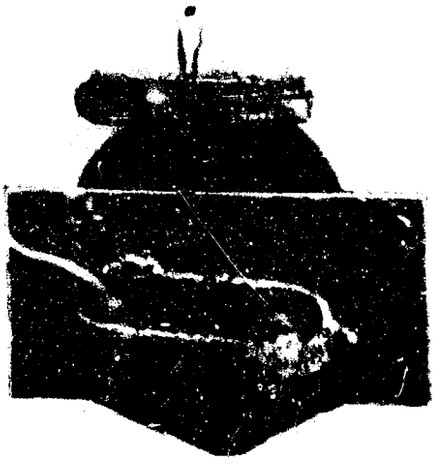
TYPICAL Ti-5Al-2.5Sn FOIL T-JOINT BRAZED IN VACUUM WITH Ti-9.57Cu-5.6Be ALLOY



Braze Alloy: Ti-8.66Mn-5.6Be
Braze Temperature: 1850 F
Etchant: Kroll's
Magnification: 0X

Figure 42.

TYPICAL Ti-5Al-2.5Sn FOIL T-JOINT BRAZED IN VACUUM WITH Ti-8.66Mn-5.6Be ALLOY



Braze Alloy: Ag-5Al-0.2Mn
Braze Temperature: 1700 F
Salt Spray Exposure: 72 Hours
Magnification: 2.5X

Extensive crevice corrosion resulted in complete separation of the foil components. Corrosion was concentrated along the interface between the braze and the bottom foil surface.

FIGURE 43.

TYPICAL Ti-5Al-2.5Sn FOIL T-JOINT BRAZED IN VACUUM WITH Ag-5Al-0.2Mn ALLOY

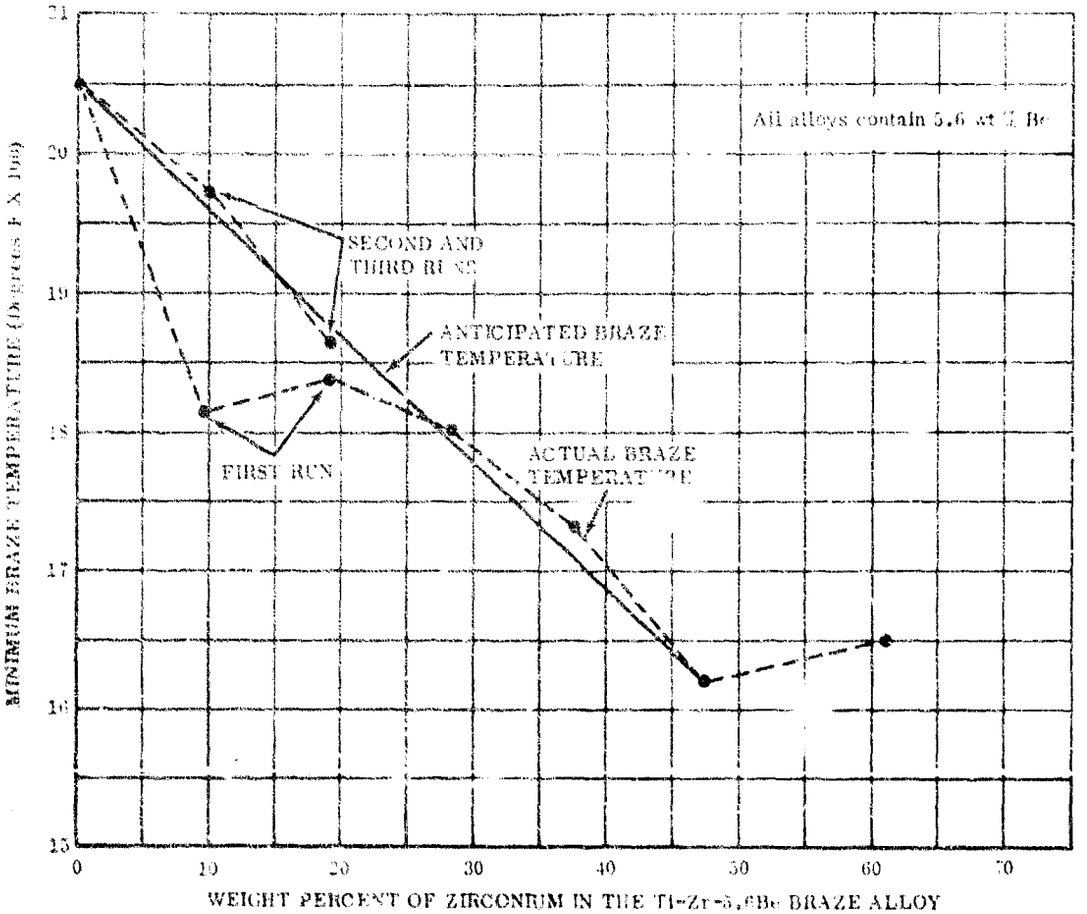
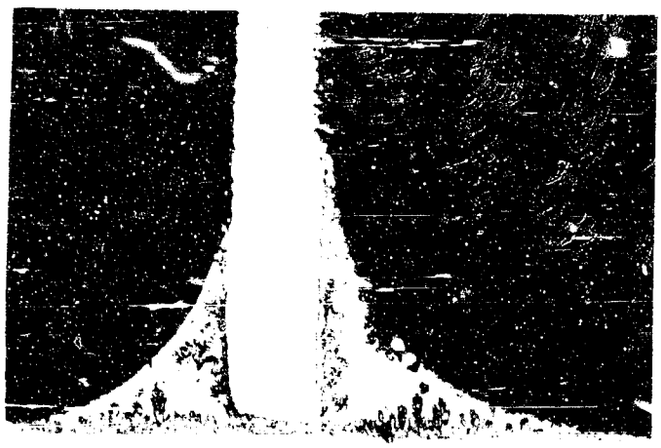
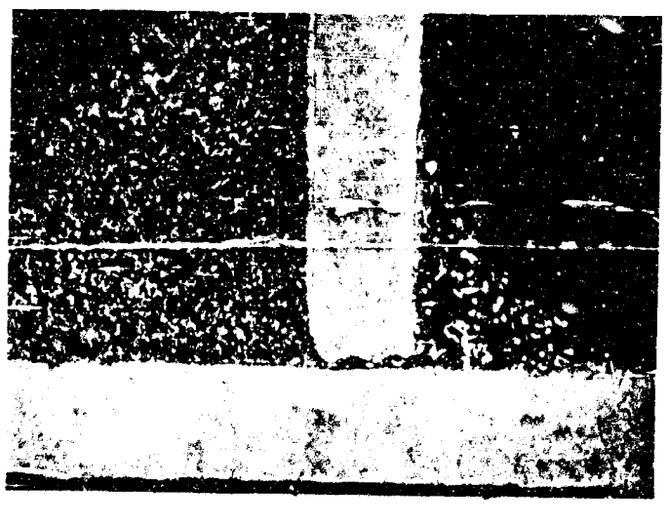


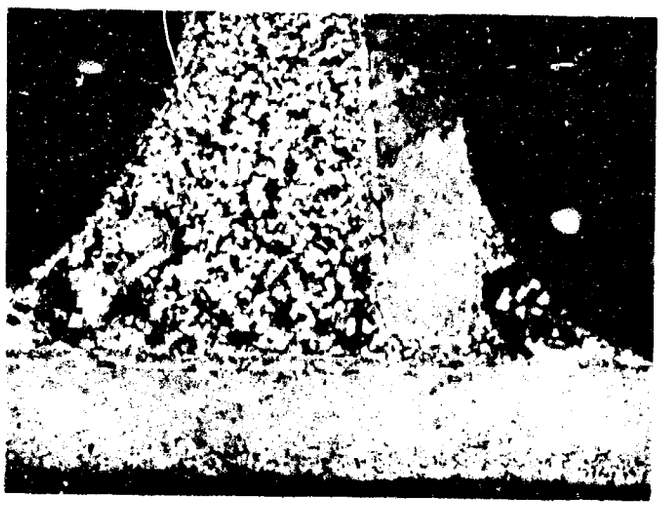
FIGURE 44. MELTING TEMPERATURE VERSUS WEIGHT PERCENT ZIRCONIUM IN Ti-47.2Zr-5.6Be BRAZE ALLOY



A.
Braze Alloy: Ti-5, 2Sn
Braze Temperature: 2050 F
Salt Spray Exposure: 72 Hours
Etchant: Kroll's
Magnification: 100 X



B.
Braze Alloy: Ti-9, 5Zr-5, 6Be
Braze Temperature: 1820 F
Salt Spray Exposure: 72 Hours
Etchant: Kroll's
Magnification: 100 X



C.
Braze Alloy: Ti-18, 9Zr-5, 6Be
Braze Temperature: 1840 F
Salt Spray Exposure: 72 Hours
Etchant: Kroll's
Magnification: 100 X
Section Through Residue

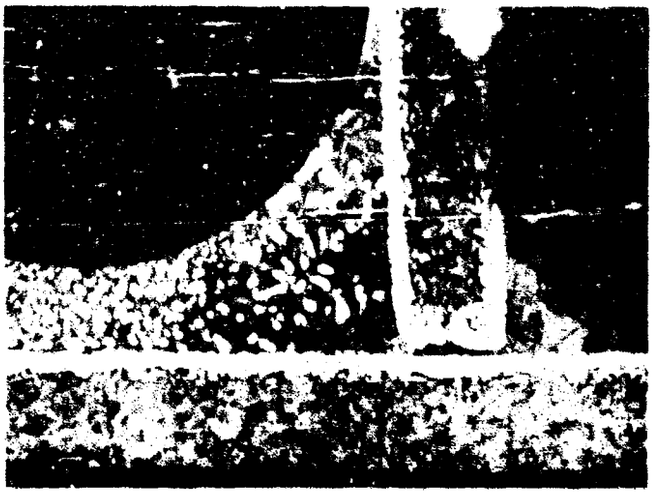
FIGURE 45. TYPICAL Ti-5Al-2.5Sn FOIL T-JOINTS BRAZED IN VACUUM WITH CANDIDATE BRAZE ALLOYS (Sheet 1 of 3)



D.
Braze Alloy: Ti-28.1Zr-5.6Be
Braze Temperature: 1850 F
Salt Spray Exposure: 72 Hours
Etchant: Kroll's
Magnification: 100 X

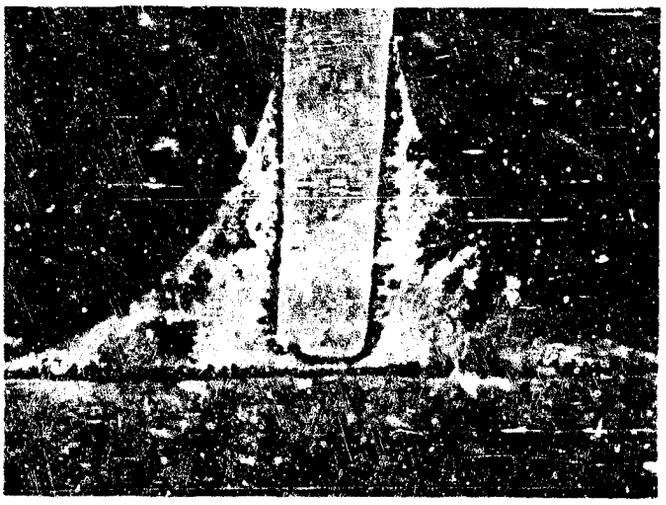


F.
Braze Alloy: Ti-37.9Zr-5.6Be
Braze Temperature: 1630 F
Salt Spray Exposure: 72 Hours
Etchant: Kroll's
Magnification: 100 X
Section Through Residue



E.
Braze Alloy: Ti-47.2Zr-5.6Be
Braze Temperature: 1650 F
Salt Spray Exposure: 72 Hours
Etchant: Kroll's
Magnification: 100 X
Section Through Residue

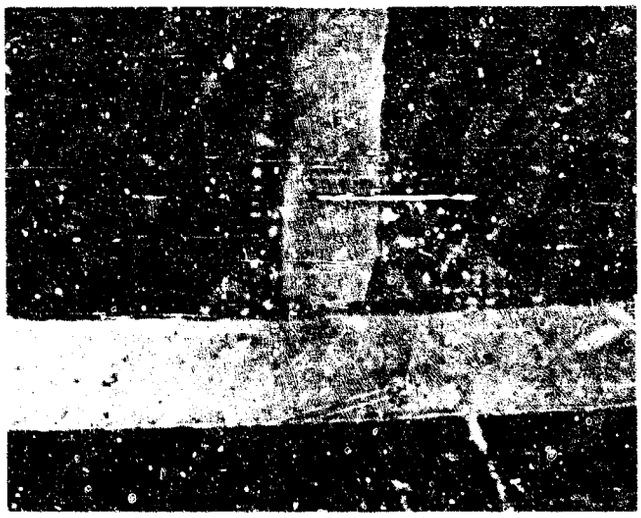
FIGURE 15. TYPICAL Ti-5Al-2.5 FOIL T-JOINTS BRAZED IN VACUUM WITH CANDIDATE BRAZE ALLOYS (Sheet 2 of 3)



G
Braze Alloy: Ti-6Al-4V - 5.0Be
Braze Temperature: 1650 °F
Salt Spray Exposure: 72 Hours
Etchant: Kroll's
Magnification: 100 X

...ndition: All brazements (A through G) exposed 72 hours in salt spray post brazing. Note absence of corrosion effects.

FIGURE 45. TYPICAL Ti-6Al-4V-2.5Sn FOIL T-JOINTS BRAZED IN VACUUM WITH CANDIDATE BRAZE ALLOYS (Sheet 3 of 3)



Magnification: 100X

FIGURE 46.

BRAZE SCREENING TEST WITH CS217 BRAZE ALLOY



Braze Alloy: CS 217C (5% Al)
Braze Temperature: 1700 F
Etchant: Kroll's
Magnification: 100 X

FIGURE 47.
BRAZE SCREENING TEST WITH CS217C BRAZE ALLOY

Braze Alloy: CS 217G (2% Si)
Braze Temperature: 1680 F
Etchant: Kroll's
Magnification: 100 X

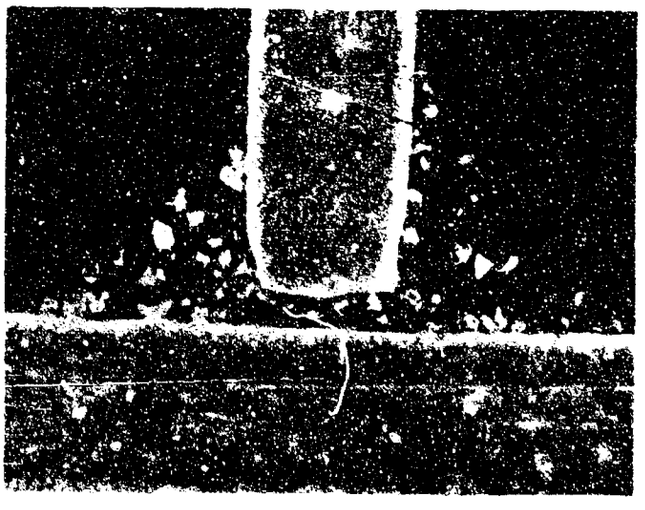
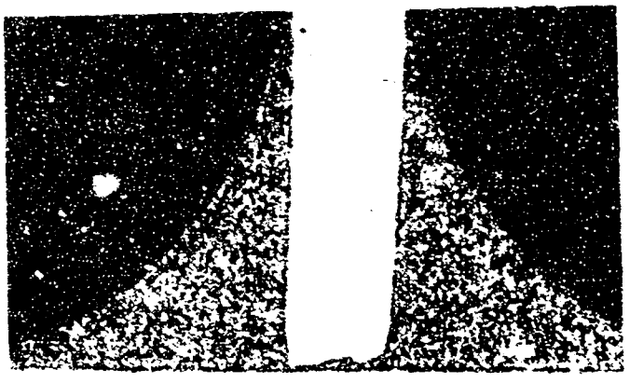


FIGURE 48.
BRAZE SCREENING TEST WITH CS217G BRAZE ALLOY



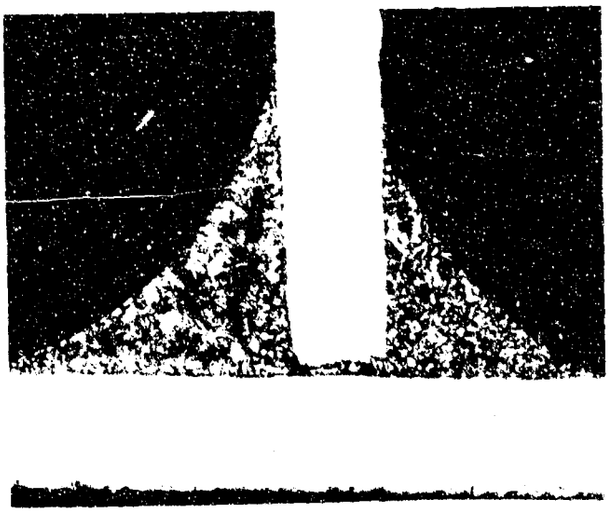
Braze Alloy: CS 217I (9.6% Co)
Braze Temperature: 1520 F
Etchant: Kroll's
Magnification: 100 X

FIGURE 49.
BRAZE SCREENING TEST WITH CS217I BRAZE ALLOY

Braze Alloy: CS 217E (5% Ni)
Braze Temperature: 1600 F
Etchant: Kroll's
Magnification: 100 X



FIGURE 50.
BRAZE SCREENING TEST WITH CS217E BRAZE ALLOY



Braze Alloy: CS 217E (5% Co)
Braze Temperature: 1620 F
Etchant: Kroll's
Magnification: 100 X

FIGURE 51.
BRAZE SCREENING TEST WITH CS217F BRAZE ALLOY



Braze Alloy: RM 1 (Ti-41Zr-1SNi)
Braze Temperature: 1650 F
Salt Spray Exposure: 114 Hours
Etchant: Kroll's
Magnification: 100 X
No apparent corrosion.

FIGURE 52.

BRAZE SCREENING TEST WITH RM1 BRAZE ALLOY

Braze Alloy: RM 8 (Ti-43Zr-12Ni-2Be)
Braze Temperature: 1470 F
Salt Spray Exposure: 114 Hours
Etchant: Kroll's
Magnification: 100 X
No apparent corrosion:
Screening braze joint with RM 8 alloy (Ti-43Zr-12Ni-2Be) after 114 hours in salt spray

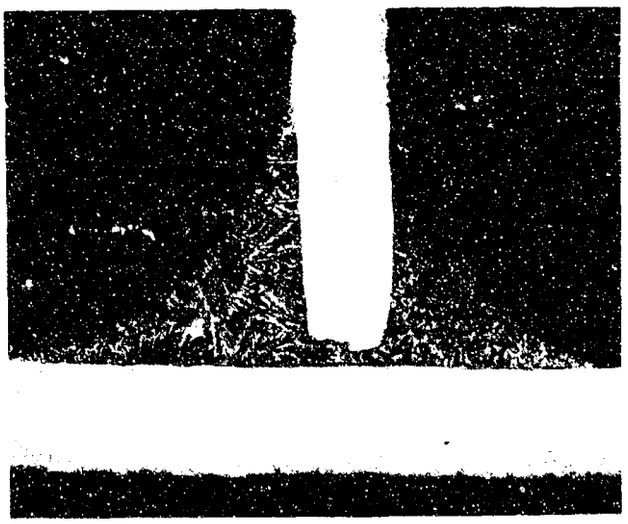
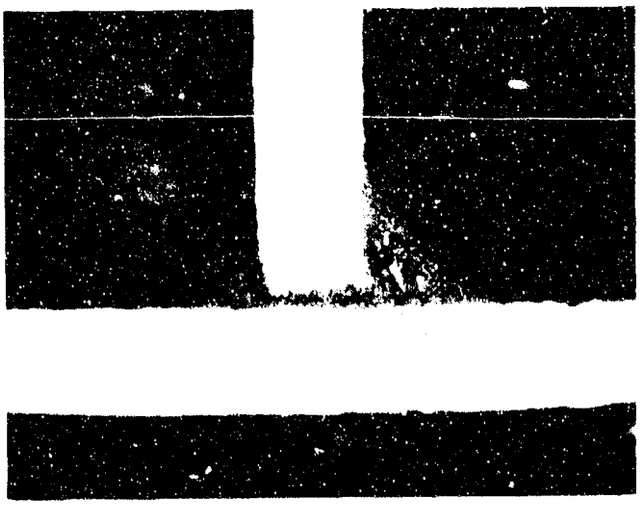


FIGURE 53.

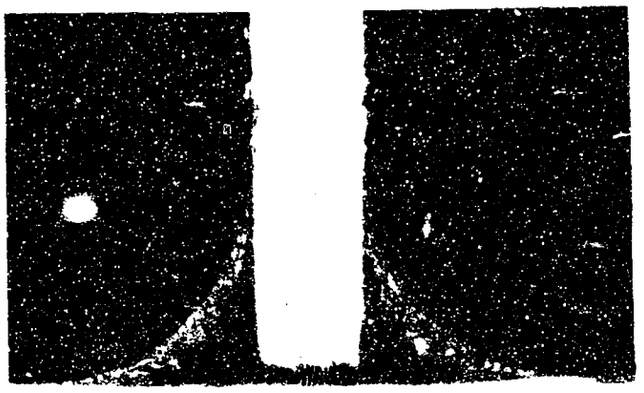
BRAZE SCREENING TEST WITH RM8 BRAZE ALLOY



Braze Alloy: RM 12 (Ti-45Zr-8.0Ni-2.0Be)
Braze Temperature: 1650 F
Salt Spray Exposure: 114 Hours
Etchant: Kroll's
Magnification: 100 X

FIGURE 54.

BRAZE SCREENING TEST WITH RM12 BRAZE ALLOY



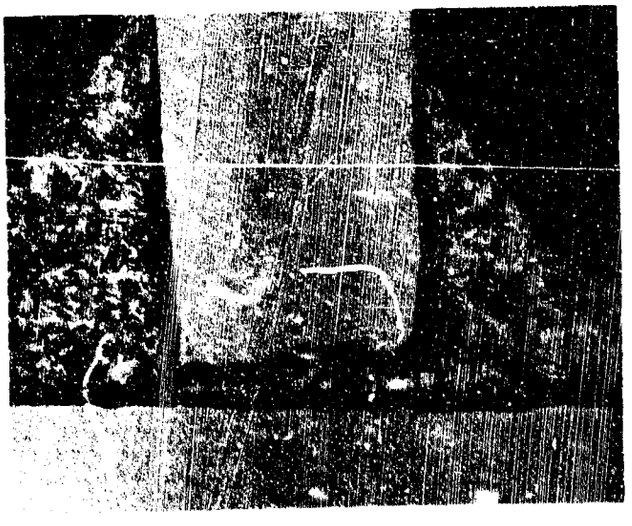
Braze Alloy: RM 28 (Ti-43Zr-13Ni-10Ag)
Braze Temperature: 1620 F
Etchant: Kroll's
Magnification: 100 X

FIGURE 55.
BRAZE SCREENING TEST WITH RM28 BRAZE ALLOY

Braze Alloy: RM 40 (Ti-20Zr-8Ni-5Be)
Braze Temperature: 1700 F
Etchant: Kroll's
Magnification: 100 X

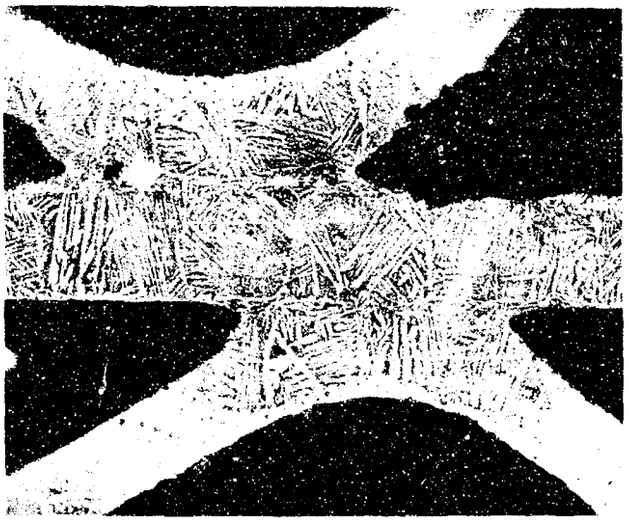


FIGURE 56.
BRAZE SCREENING TEST WITH RM40 BRAZE ALLOY



Braze Alloy: RM 26 (Ti-16.9Ni-3.9Be-2.0Si)
Braze Temperature: 1660 F
Etchant: Kroll's
Magnification: 250 X

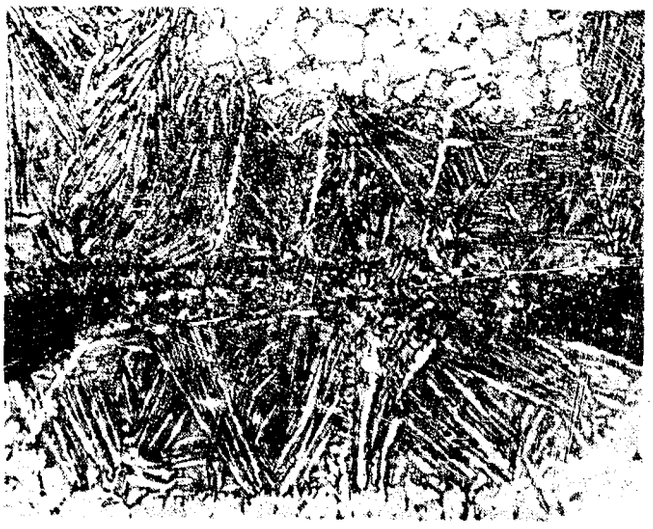
FIGURE 57.
BRAZE SCREENING TEST WITH RM26 BRAZE ALLOY



A.

Center foil only was plated on both sides with 0.065 mil Ni-10P. Test sample was heated for 30 minutes at 1825 F. Note the completely transformed structure in the center foil and the partially transformed structure in the braze affected area.

Magnification: 100 X



B.

Brazing was accomplished at 1825 F for 30 minutes in vacuum of less than 1 x 10^{-4}Torr. Note the duplex structure near the braze joint and the single phase structure in the adjacent area.

Magnification: 250 X



C.

Brazed joint with 0.065 mil Ni-10P coating on center foil only; brazed in vacuum at 1725 F for 5 minutes. Note the formation of a 1.2 mil intermetallic compound layer with no apparent transformation of the structure.

Magnification: 250 X

FIGURE 58. BRAZE SCREENING TEST WITH 0.075-MIL, Ni-10P PLATED SPECIMEN

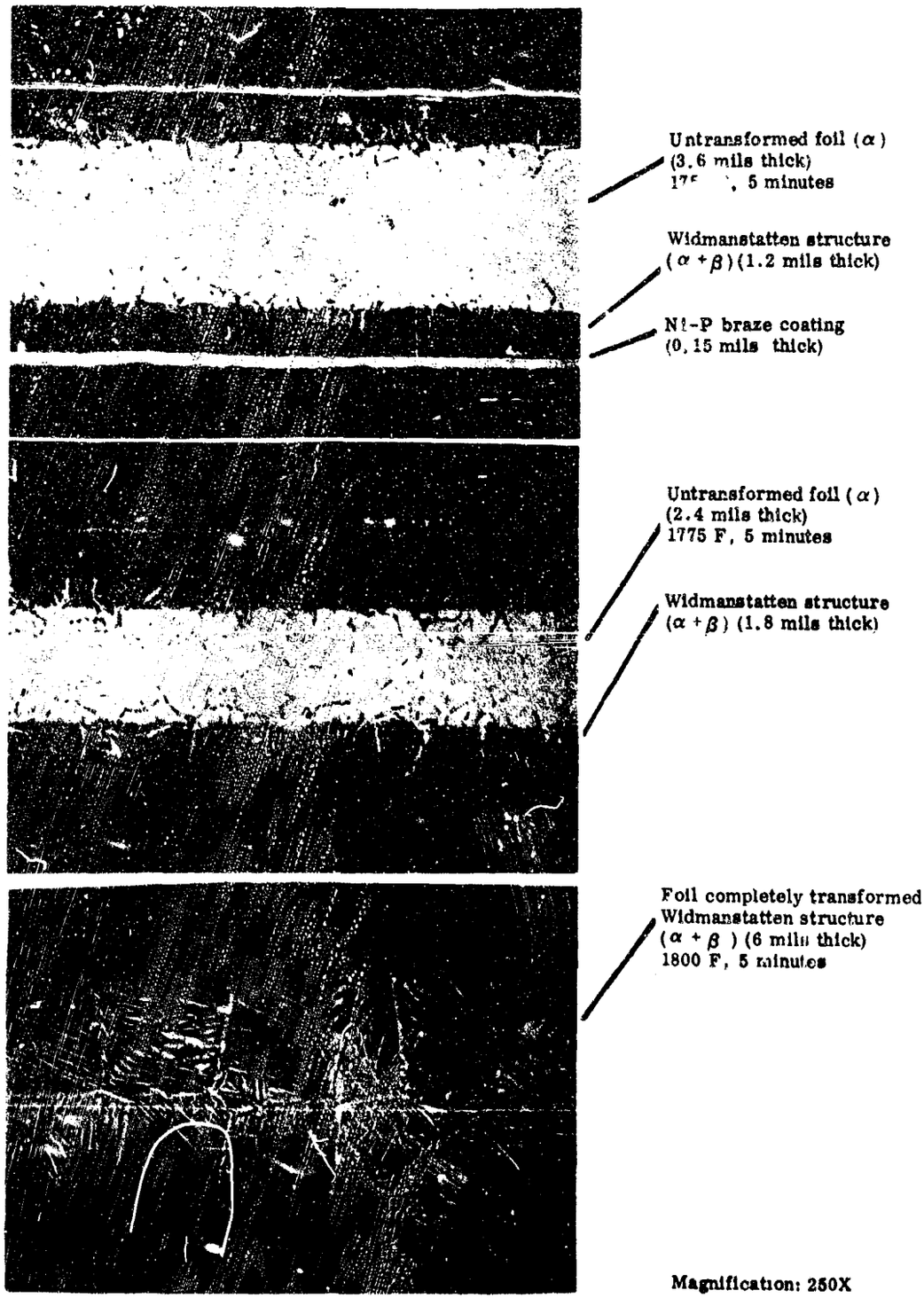
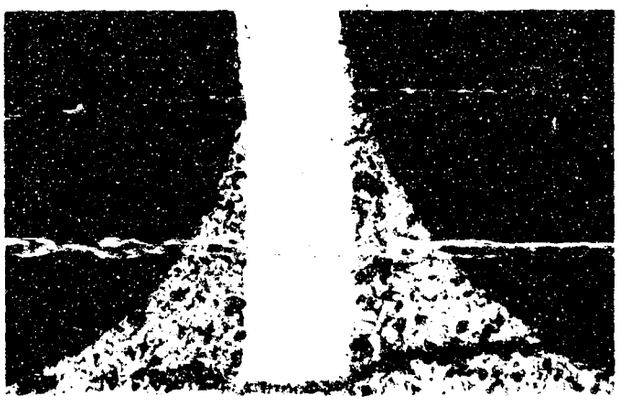


FIGURE 59. BRAZE SCREENING TEST WITH 0.15-MIL, Ni-10P PLATED SPECIMEN



Braze Cracked
Magnification: 100 X

FIGURE 60.

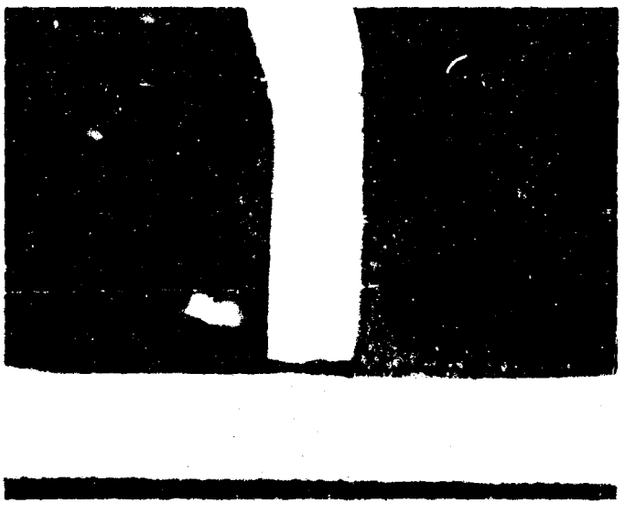
T-JOINT BEND TEST, BRAZED WITH RM44 ALLOY



Braze and Braze Affected Foil Cracked
Magnification: 100 X

FIGURE 61.

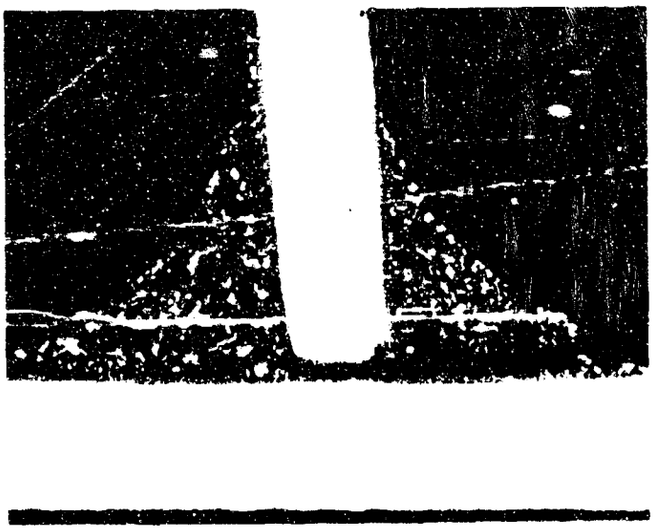
T-JOINT BEND TEST, BRAZED WITH RM23 ALLOY



Small Braze Cracks
Magnification: 100 X

FIGURE 62.

T-JOINT BEND TEST, BRAZED WITH RM26 ALLOY



Braze Cracked
Magnification: 100 X

FIGURE 63.

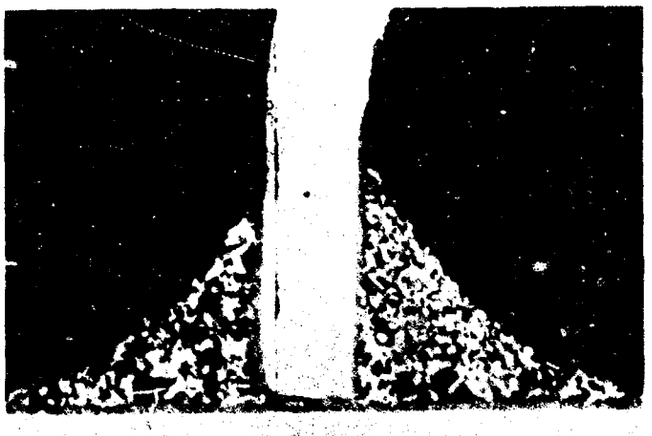
T-JOINT BEND TEST, BRAZED WITH CS217E ALLOY



Small Braze Cracks
Magnification: 100 X

FIGURE 64.

T-JOINT BEND TEST, BRAZED WITH CS217F ALLOY



No Crack
Magnification: 100 X

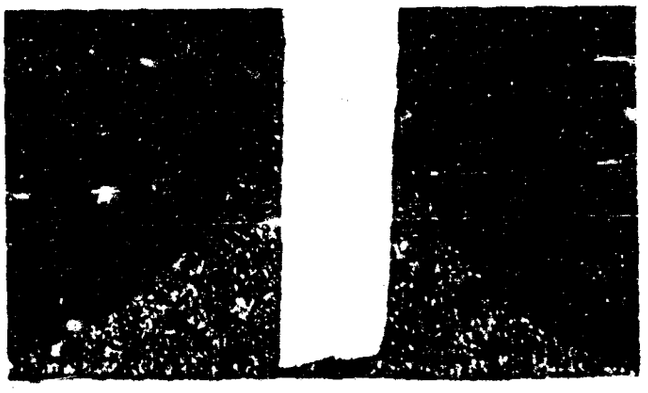
FIGURE 65.

T-JOINT BEND TEST, BRAZED WITH RM40 ALLOY



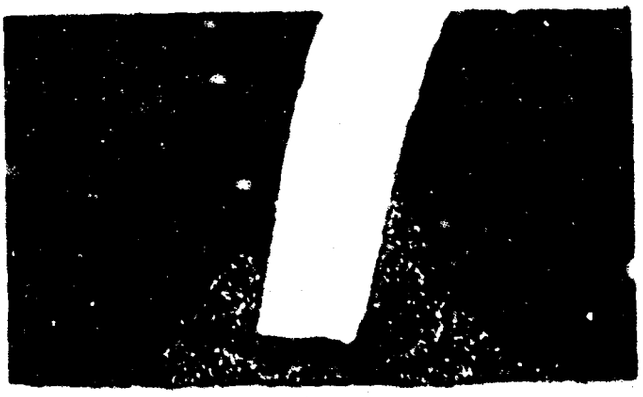
Braze Cracked
Magnification: 100 X

FIGURE 66.
T-JOINT BEND TEST, BRAZED WITH RM40 ALLOY; After 100-Hour Salt Spray Exposure



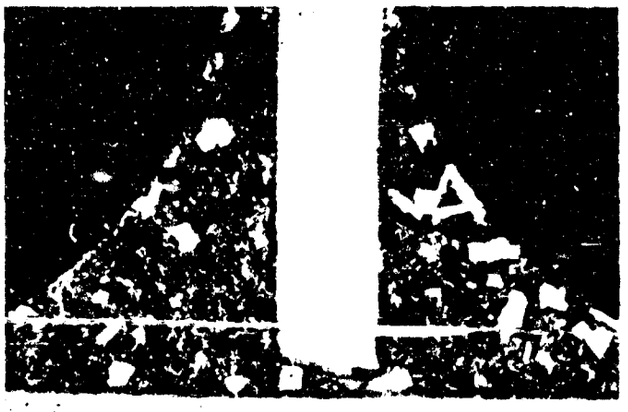
No Crack
Magnification: 100 X

FIGURE 67.
T-JOINT BEND TEST, BRAZED WITH CS217I ALLOY



Braze Cracked
Magnification: 100 X

FIGURE 68.
T-JOINT BEND TEST, BRAZED WITH CS217I ALLOY; After 100 Hour Salt Spray Exposure



No Crack
Magnification: 100 X

FIGURE 69.

T-JOINT BEND TEST, BRAZED WITH CS217 ALLOY



No Crack
Magnification: 100 X

FIGURE 70.

T-JOINT BEND TEST, BRAZED WITH CS217 ALLOY; After 100-Hour Salt Spray Exposure



No Crack
Magnification: 100 X

FIGURE 71.

T-JOINT BEND TEST, BRAZED WITH RMS ALLOY, After 100-Hour Salt Spray Exposure



No Crack
Magnification: 100 X

FIGURE 72.
T-JOINT BEND TEST, BRAZED WITH CS217C ALLOY; After 100-Hour Salt Spray Exposure



No Crack
Magnification: 100 X

FIGURE 73.
T-JOINT BEND TEST, BRAZED WITH CS217G ALLOY; After 100-Hour Salt spray Exposure

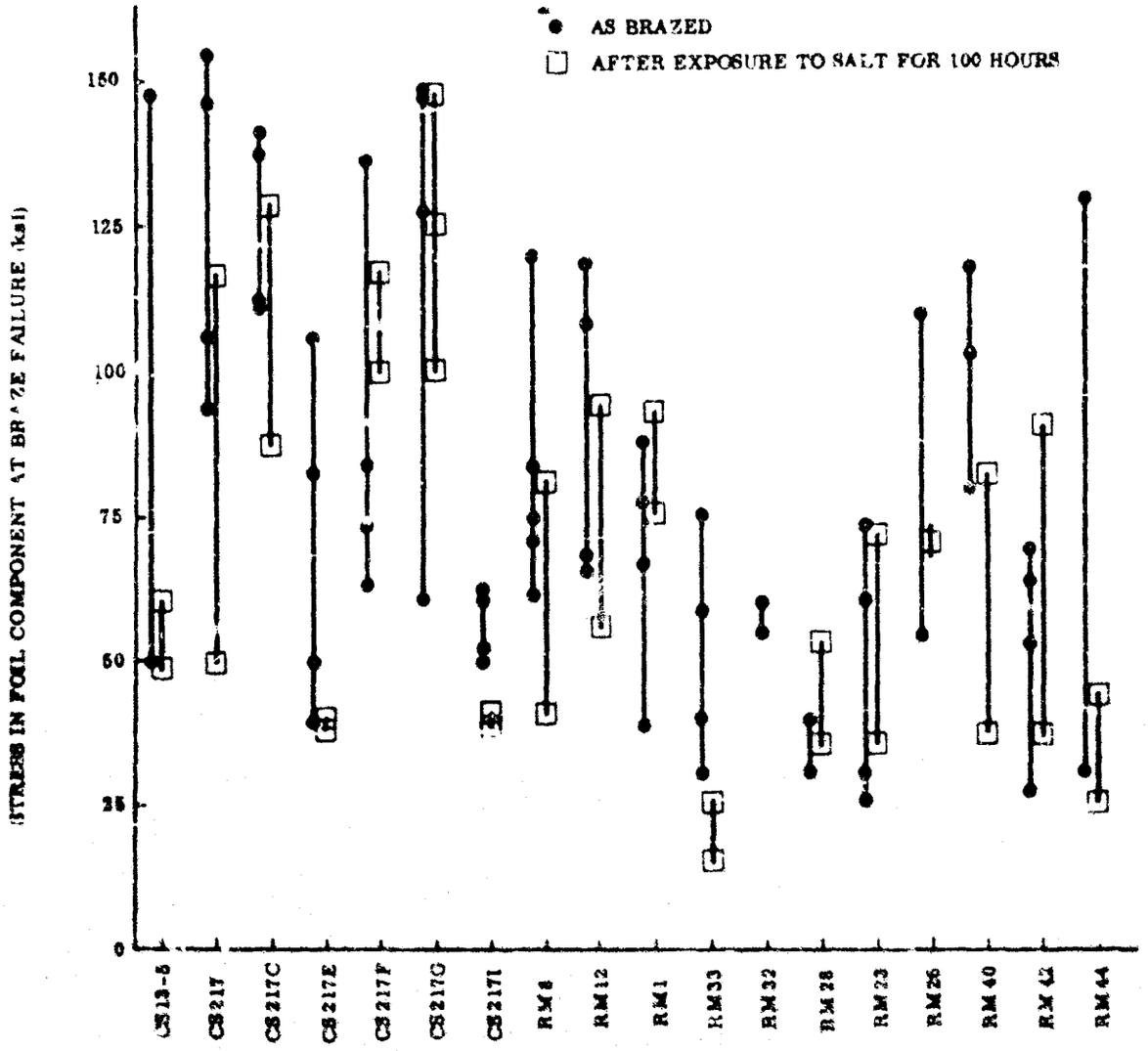
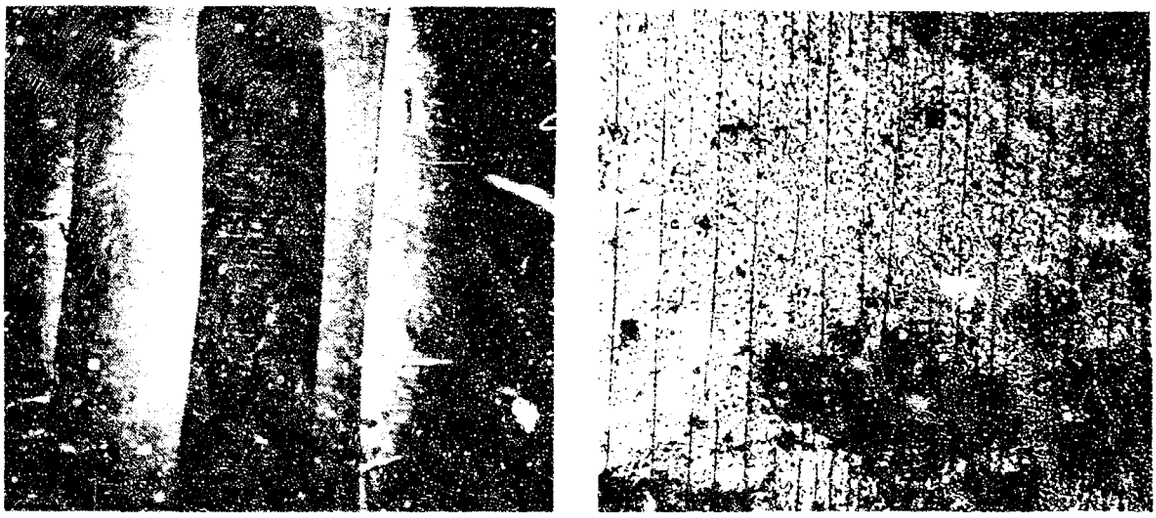


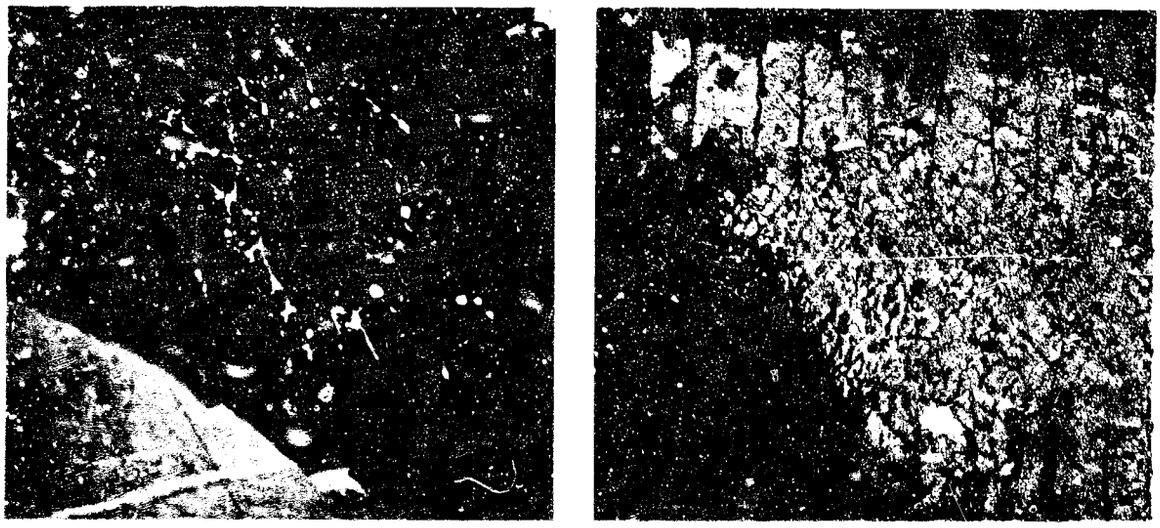
FIGURE 74. DISTRIBUTION OF BRAZED T-JOINT TENSILE STRENGTH



Magnification: 6X

Magnification: 40X

FIGURE 75. STRAIN ACCOMMODATION TEST, BRAZED WITH RM8 ALLOY



Magnification: 10X

Magnification: 40X

FIGURE 76. STRAIN ACCOMMODATION TEST, BRAZED WITH CS217 ALLOY

3.5 TASK V - EVALUATION OF BRAZE SYSTEMS

On the basis of excellent foil brazing characteristics and performance in special brazement strength, toughness, strain accommodation and salt-corrosion tests, the eight braze alloys listed in Table XXXV were selected for further evaluation and study.

TABLE XXXV

ALLOYS SELECTED FOR STUDY AND EVALUATION IN TASK V

Braze Alloy Designation	Nominal Composition (wt %)							Minimum Braze Temperature (F)
	Ti	Zr	Be	Ni	Al	Co	Si	
CS217	Balance	47.5	5.00	--	--	--	--	1640
CS217C	Balance	45.1	4.75	--	5.0	--	--	1700
CS217F	Balance	45.1	4.75	--	--	5.0	--	1620
CS217G	Balance	46.6	4.90	--	--	--	2.0	1680
RM8	Balance	43.0	2.00	12.0	--	--	--	1470
RM12	Balance	45.0	2.00	8.0	--	--	--	1660
RM26	Balance	--	3.90	16.9	--	--	2.0	1660
RM40	Balance	20.0	5.00	8.0	--	--	--	1700

Of these eight alloys, prior screening tests at room temperature showed two braze alloys (CS217C and RM12) to be outstanding from an overall viewpoint (highest and most consistent test results in all tests).

Task V of Phase I was designed to provide a much broader evaluation of the eight best candidate braze alloys screened from Task IV. All program alloy foils were employed. Lap-joint shear tests were conducted (-320 to 800 F) upon candidate alloy brazements initially in the as-brazed condition and following thermal aging periods of 100 hours at 1000 F in high vacuum (1.0×10^{-5} Torr). The objective was to determine thermal stability effects upon structure and degree of strength retention of candidate alloy brazements. A statistical survey was made of both T-joint and lap-joint strengths (room temperature) to measure the joint strength reproducibility (or degree of data scatter) of the marginally tough brazements; especially as influenced by post-braze heat treatments devised to improve toughness and strength reproducibility. Subsequently, lap shear tests were conducted over the broad temperature range of -320 F to 800 F or 900 F on both the as-brazed specimens and specimens

given the best post-braze heat treatment determined above. These tests provided baseline design strength data. Additional stability tests were programmed to evaluate the effects of salt spray exposure (100 hours, 200 F) on lap-joint strengths over the test temperature range of -320 F to 800 F or 900 F. A similar test regime evaluated the effects of air oxidation (100 hours, 1000 F, static air). The air oxidation data were compared directly with the previously mentioned thermal stability data. The advantages of post-braze thermal treatment became very evident by this stage so that post-braze heat treatment became a significant variable in developing these test data. Task V testing was concluded with special lap-joint tests to:

- Gage relative susceptibility of candidate alloy brazements to hot salt stress corrosion (encrusted NaCl in oxidizing atmosphere at 1000 F, constant foil stress levels of 10,000 and 20,000 psi).

- Measure comparative stress-rupture lives of candidate brazements in an oxidizing atmosphere at 1000 F. The 30,000 psi foil stress level employed was selected to yield a minimum 100-hour rupture life (Ti-5Al-2.5Sn foils). Self-diffusion bonded specimens were employed for baseline data.

- Gain information on the relative abilities of candidate alloy brazements to withstand cyclic loading. A series of tension-tension fatigue tests was conducted at room temperature using a sine-wave excitation with frequency of 70 cps and a fixed alternating stress/mean stress ratio of 1.0. Tests were carried out to the range of 10^5 to 10^6 cycles. All lap-joint fatigue specimens were made of 0.010-inch Ti-5Al-2.5Sn foils, with a controlled 0.020- to 0.040-inch overlap, as in all previous lap shear specimens. Self-diffusion bonded specimens were also tested to develop baseline fatigue data.

At the conclusion of this study, the field of candidate braze alloys was narrowed to the four best for final evaluation in fabrication and testing of Phase II structures.

3.5.1 Thermal Stability Testing

The objective of the thermal stability testing was to determine the effects of prolonged service or aging time at the maximum anticipated service temperature (1000 F) on brazement strength and structure. Thermal stability tests were conducted on the eight candidate braze alloys (Ti-6Al-4V foils). Lap shear test specimens of each braze alloy were exposed at 1000 F for 100 hours in high vacuum (1.0×10^{-5} Torr) prior to lap shear testing at -320 F, room temperature, and 800 F. (Tests were conducted at 800 F in argon atmosphere to eliminate possible contamination effects.) Test results were augmented by metallographic examination and microhardness determinations on small Ti-5Al-2.5Sn and Ti-6Al-4V foil T-joints, which were aged similarly.

TABLE XXXVI

THERMAL STABILITY TEST RESULTS, LAP-SHEAR TESTS

Braze Alloy and Composition	As-Brazed (ksi)			After Aging at 1000 F for 100 Hours in Vacuum (ksi) (5×10^{-5} mm Hg)		
	At Room Temperature	At 800 F	At -320 F	At Room Temperature	At 800 F	At -320 F
CS217 Ti-47.5Zr-5Be	104.4, 100.0, 99.2	90.5, 86.4	114.5[1], 82.4	113.3, 97.8	100.0, 96.1	135.2[1], 128.7[1]
Average	101.2	88.5	98.4	105.5	98.0	129.0
CS217C Ti-45.1Zr-4.75Be-5Al	104.7, 86.6	96.8, 93.1	119.0[1], 117.2[1]	93.6, 83.0	90.4, 78.3	122.6[1], 111.5[1]
Average	95.6	95.0	118.1	88.3	84.3	117.0
CS217F Ti-45.1Zr-4.75Be-5Co	96.2, 92.0	73.6, 6[illegible].5	104.2, 103.4	89.1, 96.9	94.3, 81.6	127.9[1], 107.9
Average	93.6	74.0	103.8	88.0	77.9	117.5
CS217G Ti-46.6Zr-4.90Be-2Si	103.5, 97.7	87.4, 82.9	113.6[1], 111.0	103.3, 100.9	96.7, 83.2	117.0[1], 72.0
Average	100.6	85.1	112.3	103.6	90.0	94.5
RM8 Ti-43Zr-12Ni-2Be	88.6, 87.4	83.1, 52.1	110.[illegible]3.6	69.8, 56.0	88.5, 74.6	116.8[1], 102.4
Average	88.0	82.7	109.3	62.9	81.5	109.6
RM12 Ti-46Zr-8Ni-2Be	[illegible], 66.9	97.4, 93.6	116.9[1], 113.5	85.5, 72.4	70.4, 69.9	112.0, 90.7
Average	80.0	93.6	115.2	79.0	70.6	101.3
RM26 Ti-16.8Ni-3.9Be	75.1, 52.2	71.6, 32.4	100.5, 51.6	91.3, 46.0	70.6, 61.2	76.3, 46.2
Average	63.7	51.9	76.1	68.6	65.9	62.2
RM40 Ti-20Zr-6Ni-5Be	73.1, 56.5	47.0, 46.6	35.6, 33.4	66.0, 67.0	67.0, 62.6	73.1, 44.5
Average	64.8	46.8	34.5	76.5	65.3	58.8

1. Signifies failure occurred in braze-affected foil rather than the joint. (In all other instances, failure occured in joint.

The lap shear specimens of Ti-6Al-4V were composed of 0.010-inch thick foils approximately 0.5-inch wide and with a typical overlap of about 0.020-inch. The braze schedule consisted of vacuum brazing twelve such specimens for each of the eight candidate braze alloys and testing as follows:

- Two specimens tested as-brazed at room temperature
- Two specimens tested as-brazed at 800 F in argon
- Two specimens tested as-brazed at -320 F in liquid nitrogen

Six specimens were aged at 1000 F for 100 hours in vacuum (1.0×10^{-5} Torr) and then tested as follows:

- Two specimens tested at room temperature
- Two specimens tested at 800 F in argon
- Two specimens tested at -320 F in liquid nitrogen

Lap Shear Test Results

The data from lap shear testing (Table XXXVI; Figures 77 and 78) indicated that no significant degradation in average strength (-320 F, room temperature, and 800 F) developed as the result of the 1000 F vacuum aging treatment for the following

braze alloys: CS217, CS217C, CS217F, and CS217G. The single exception was a 15 percent reduction in strength for the CS217G alloy at -320 F. In fact, vacuum aging appeared to have improved strength of the CS217 alloy, particularly at -320 F (an average increase of ~ 30 percent) as shown in Figure 77. Maximum strength levels for the CS series alloys were most frequently observed at the lowest test temperature (-320 F).

The RM series alloys reacted somewhat differently to 1000 F vacuum aging (Table XXXVI and Figure 78). Except for a curious drop in room temperature strength post aging (~ 35 percent), the RM8 alloy showed no change in strength at -320 and 800 F resulting from aging. Vacuum aging produced directly the opposite effect on the strength of RM12 alloy. Average room temperature strength of RM12 did not change, but joint strengths at -320 and 800 F dropped 11 percent and 26 percent respectively, after 1000 F aging. Braze strength levels for RM8 and RM12 (i.e., those unaffected by aging) compared favorably with corresponding levels of the CS series alloys. In contrast, the remaining two RM alloys (RM26 and RM40) yielded appreciably lower strength values with generally greater scatter in data for both the as-brazed and the vacuum-aged conditions. Hence, RM26 and RM40, which were included to evaluate effects of the reduced zirconium content, were screened out at this point. It has been hoped that the lowered zirconium content would benefit braze toughness and stability in the RM series through reduction of the intermetallic content and through an increased tendency to form equilibrium beta transformation products on cooling from the braze process.

In summation, the CS217, CS217C, and CS217F braze alloys exhibited best overall strength retention after 100 F aging. The six candidate braze alloys, CS217, CS217C, CS217F, CS217G, as well as RM8 and RM12, were recommended for further study in Task V because of their generally satisfactory performance in thermal stability testing.

Metallography and Microhardness Studies

Small T-joints of Ti-5Al-2.5V and Ti-6Al-4V foils (0.006-inch thick) were brazed in argon by holding at minimum flow temperatures for 5 minutes. They were then aged at 1000 F for 100 hours in vacuum. Minimal foil erosion was found as anticipated from previous tests. Microstructures of brazed joints after 1000 F aging exhibited more uniform distribution of intermetallics due to thermal diffusion and

TABLE XXXVII

MICROHARDNESS DETERMINATION OF BRAZE ALLOYS, THERMAL STABILITY TESTS

Braze Alloy	Hardness As Brazed (R_C)		Hardness After Aging At 1000 F For 100 Hours (R_C)	
	Braze Matrix	Intermetallics	Braze Matrix	Intermetallics
CS217	51.0 to 52.0	71.0	52.0 to 53.0 DZ to 34.0 to 39.0	69.0
CS217C	52.0 to 56.0	--	53.0 to 56.0 DZ 44.0	--
CS217F	46.0 to 51.0	68.0	54.0 DZ to 43.0	66.0
CS217G	51.0 to 53.0	66.0	49.0 to 53.0 DZ to 33.0	--
RM8	53.0	--	15.0 to 56.0 DZ to 38.0	60.0
RM12	60.0 to 62.0	--	44.0 to 60.0 DZ 38.0	--
RM26	--	--	55.0 to 57.0 DZ 31.0	--
RM40	47.0	--	DZ to 37.0	64.0 to 68.0

DZ signifies braze/foil diffusion zone.

homogenization effects. Coalescence and spheroidization of intermetallic particles were apparent for all aged brazes, especially for the CS217 and CS217F alloys shown in Figures 79 and 80. No significant hardness changes in the CS series braze structures were observed after aging at 1000 F for 100 hours (Table XXXVII). A moderate softening of the braze matrix was noted for the RM8 and RM12 alloys resulting from 1000 F vacuum aging.

3.5.2 Reliability Tests

The objective of reliability testing was to obtain a statistical measure of strength data reproducibility for the six remaining candidate braze alloys.

TABLE XXXVIII

RELIABILITY TESTING OF BRAZE ALLOYS, LAP-SHEAR SPECIMENS

Braze Alloy	Foil (10 mil thick)	As-Brazed				As Cyclic Annealed for 4 Hours[1]				Increase in Average Foil Stress at Failure[2] (%)
		Average Foil Stress at Failure (ksi)	Number of Data Points	Standard Deviation	Standard Deviation (%)	Average Foil Stress at Failure (ksi)	Number of Data Points	Standard Deviation	Standard Deviation (%)	
CS217	6Al-4V	95.5	8	6.9	7.2	102.8	5	12.6	12.3	7.7
	5Al-2.5Sn	108.6	5	5.0	4.6	129.1	5	16.1	12.5	18.9
	8Al-1Mo-1V	106.6	5	6.3	5.9	---	-	--	--	--
CS217C	6Al-4V	107.7	6	10.3	9.6	119.8	5	10.4	8.8	11.2
	5Al-2.5Sn	104.0	5	8.3	8.0	120.2	5	8.7	7.3	15.6
	8Al-1Mo-1V	108.3	5	13.6	12.5	---	-	--	--	--
CS217F	6Al-4V	97.8	7	6.3	6.5	113.1	5	4.1	3.6	15.6
	5Al-2.5Sn	99.5	4	3.7	3.7	116.9	4	10.6	9.1	17.5
	8Al-1Mo-1V	98.2	5	4.4	4.5	---	-	--	--	--
CS217G	6Al-4V	100.9	6	3.2	[illegible]	106.0	5	12.2	11.5	5.1
	5Al-2.5Sn	110.5	4	5.5	5.2	115.5	4	16.4	14.2	4.5
	8Al-1Mo-1V	93.9	5	18.6	19.8	---	-	--	--	--
RM8	6Al-4V	85.1	7	3.8	4.5	78.1	4	2.9	3.7	--
	5Al-2.5Sn	84.3	5	6.6	7.9	68.7	3	10.6	15.3	--
	8Al-1Mo-1V	94.7	5	4.2	4.4	---	-	--	--	--
RM12	6Al-4V	130.0	4	6.6	6.6	88.0	4	7.8	8.8	--
	5Al-2.5Sn	94.8	4	4.6	4.9	75.8	4	4.85	6.5	--
	8Al-1Mo-1V	100.3	5	7.0	7.0	---	-	--	--	--
Total Number of Data Points			96				53			

1. Cyclic Annealing Treatment:

For CS Series Braze Alloys	For RM8 and RM12
1550 F - 10 minutes	1400 F - 10 minutes
1300 F - 10 minutes	1200 F - 10 minutes
Repeat for 4 hours	Repeat for 4 hours

2. Due to Cyclic Annealing

Reliability tests were conducted using brazed lap shear specimens of the candidate braze alloys in the as-brazed condition and after experimental cyclic annealing treatment. The six braze alloys evaluated were CS217, CS217C, CS217F, CS217G, RM8 and RM12. Lap shear specimens of Ti-6Al-4V and Ti-5Al-2.5Sn foils (both 0.010-inch thick) were used with a typical overlap of 0.020-inch. Testing was conducted at room temperature. Ten data points for foil stress values at shear failure (five from the Ti-6Al-4V specimens and five from the Ti-5Al-2.5Sn specimens) were obtained for each braze alloy in both the as-brazed condition and after cyclic annealing. This amounted to 20 data points for each braze alloy or a grand total of 120 data points. Later, the Ti-8Al-1Mo-1V foil brazements in the as-brazed condition were tested to bring the grand total to 150 data points. Statistical variance in foil stress values at braze failure was calculated (Table XXXVIII) and found to be within reasonable limits for the as-brazed condition (i.e., standard deviation expressed in percent of the average strength ≤ 10 percent). The only brazements which exceeded the 10 percent figure (as-brazed condition) were the combination CS217C/8Al-1Mo-1V (12.5 percent) and CS217G/8Al-1Mo-1V (19.8 percent). The statistical reliability or

reproducibility of joint shear strength was, for most braze/foil combinations, considered satisfactory. The data obtained were referred to as baseline data for all subsequent subtasks of Task V.

A preliminary investigation of cyclic annealing was carried out on the same six braze alloys by lap shear testing. The CS series alloys first were cyclic annealed in vacuum between 1550 and 1300 F for four hours. Improvement in mean foil stress values due to cyclic annealing was appreciable for the CS series, and included 7.7 to 18.9 percent with CS217, 11.2 to 15.6 percent with CS217C (5 percent Al), and 15.6 to 17.5 percent with CS217F (5 percent Co). The RM8 and RM12 alloys were cyclic annealed in vacuum between 1200 and 1400 F for four hours, but mean strength values dropped. Unfortunately, the primary objective of cyclic annealing (to improve braze strength reproducibility) was not achieved in most cases. The data contained in Table XXXVIII show that in 8 out of 12 instances data scatter and percent standard deviation actually increased because of the specific cyclic anneal used. In just one instance, however, the same cyclic anneal not only reduced percent standard deviation significantly (6.5 to 3.6 percent), but served also to increase average brazement strength by 15.6 percent (viz. Ti-6Al-4V/CS217F). The inference drawn was that a specific foil/braze combination requires a specific cyclic annealing treatment tailored to meet desired property objectives. It was decided, therefore, to explore and evaluate a wide variety of possible cyclic annealing treatments, to define suitable ones empirically. The six vacuum cyclic anneals evaluated with Ti-5Al-2.5Sn foils and CS217C braze alloy, employing T-joint tensile and lap shear tests are listed in Table XXXIX.

As always, the main objective of cyclic annealing was to improve reliability and reproducibility of braze strength through braze structure alteration (i.e., by spheroidization of eutectic and pro-eutectic beryllides and stabilization of the titanium-zirconium terminal solid solutions).

Very promising results were obtained with cyclic anneal "F" (Table XXXIX) for lap-shear and T-joint test configurations and was, therefore, used throughout the program. This cycle produced an increase in average room temperature strength of about 12 percent for braze lap shear joints and about a 22 percent increase for T-joints. It also reduced the values of standard deviation by 30 percent (lap-shear) and 56 percent (T-joints). In previous work, appreciably greater scatter in the foil

TABLE XXXIX

EFFECTS OF CYCLIC ANNEALING ON CS217C ALLOY

	Cycle	Lap Shear Tests			T-joint Tensile Tests		
		Average Stress	Standard Deviation (σ)	Standard Deviation (%)	Average Stress	Standard Deviation (σ)	Standard Deviation (%)
	As Brazed	104.0	8.3	8.0	106.2	11.5	10.8
A	1550 F-10 min 1300 F-10 min 4 hours	120.2	8.7	7.3	-----	----	----
B	1550 F-2 hrs 1300 F-2 hrs	110.7	5.9	5.3	104.5	25.4	24.4
C	1550 F-10 min 1300 F-10 min 1 hour	113.4	8.8	7.7	119.5	19.6	16.3
D	1550 F-10 min 1000 F-10 min 1 hour	111.4	8.8	8.0	109.4	13.4	12.3
E	1550 F-10 min 1300 F-10 min 8 hours	102.6	4.5	4.3	105.6	10.3	9.7
F	1550 F-10 min 1450 F-10 min 1 hour	116.6	5.7	4.9	129.7	6.1	4.7

stress values for specimen failure had been observed with T-joints than with lap-shear joints. However, following cyclic anneal "F", the standard deviations for both joint types were found to be nearly equivalent (viz., 4.7 percent versus 4.9 percent). This relation indicated a marked improvement in joint toughness and reliability. The average foil stress values at failure for both lap-shear and T-joint tests were high (≥ the typical foil yield strength of ~ 115,000 psi) and roughly the same. This suggested that:

- Joint failures in both lap-shear and T-joint tests may be initiated at a minimum foil strain (viz., ~ 6560 micro inch/inch in the as-brazed condition and ~ 7700 micro inch/inch after cyclic anneal "F"). As indicated in Tables XXXI, XXXII, and XL, proper cyclic annealing provides significantly higher strain accommodation ability.

TABLE XL

FOIL STRAIN FOR FAILURE OF CS217C BRAZE ALLOY

	Average foil strain for failure (micro in./in.)		
	Lap Shear Test	T-joint Tensile Test	Average
As brazed with CS217C	6500	6625	6560
Cyclic Annealed 1550F 10 min 1450F 10 min Repeat 1 hour	7300	8100	7700

- The marginally tough braze alloy CS217C (as-brazed condition) is capable of producing very tough and strong titanium foil brazements with proper cyclic annealing treatment (post-braze).

The fact that cyclic anneal "F" required only one hour of heat treatment or furnace time was important from considerations of production feasibility and minimization of interstitial contaminants.

Metallographic examination (optical microscopy) of cyclic annealed braze structures revealed extensive spheroidization of both eutectic and primary beryllides, the apparent reason behind the improvements in braze strength and reliability (Fig. 81 and 82). Subsequent examination using high magnification electron microscopy (Fig. 83) confirmed the indicated spheroidization of beryllides. The best example of the remarkable change in braze structure afforded by cyclic annealing is that of the braze alloy CS13-5 (CS217 eutectic) shown in Figures 84 and 85. (CS13-5 is closely related, both chemically and structurally, to CS217 and CS217C.) The electron micrographs (Fig. 84) reveal the finely spaced, lamellar eutectic structure of the as-brazed condition. Cyclic annealing completely altered the eutectic structure, transforming the beryllide lamellae or plates into finely dispersed spheroids as well as partially spheroidizing massive primary beryllides (Fig. 85). Such a structure change logically should prove beneficial to braze toughness, reliability, and notch insensitivity.

In addition, the structures of the braze-affected zones for the cyclic annealed CS217C brazements were shown to differ, depending upon the program foil alloy used. For Ti-5Al-2.5Sn foils, the structure apparently consists of a very fine dispersion of spheroidal alpha phase in a matrix of metastable beta (Fig. 86, 87, and 88). For Ti-6Al-4V foils, the resultant structure is the Widmanstatten or martensitic type (Fig. 89 and 90). Both braze-affected structures were characterized by rather high hardness levels (R_C 39.0 to 44.0), indicative of undesirable beta transformation products (Fig. 86 and 89). A recommended supplemental study aimed at obtaining stable equilibrium structures in both the braze and braze-affected zones of brazements was directed to the sponsor at this juncture. In essence, the approved study was set up to obtain stronger, tougher, and metallurgically more stable braze structures through determination of optimum post-braze thermal treatments, employing both cyclic annealing and isothermal aging.

3.5.3 Tensile Tests of Brazements

The objective of extensive tensile testing of candidate alloy brazements was to determine:

- The variation of foil stress for failure of lap-shear braze specimens with temperature in the range of -320 to 800 F (Ti-6Al-4V and Ti-5Al-2.5Sn foils)
- The relative scatter of lap-shear strength levels at specific test temperatures in the as-brazed condition

Lap-shear specimens Ti-5Al-2.5Sn, Ti-6Al-4V, and Ti-8Al-1Mo-1V (each 0.010-inch thick) were used with the six candidate alloys. Testing was done in the temperature range of -320 to 800 F as follows:

- At -320 F in liquid nitrogen
- At -100 F in methyl alcohol and dry ice
- Elevated temperature testing at 300, 500, and 800 F in an argon atmosphere

Four data points were obtained at each of the test temperatures for each braze alloy. The actual and average foil stress values at joint failure are plotted in Figures 91 and 92 for each test temperature. The plotted results of testing candidate braze alloys using lap-shear specimens of Ti-5Al-2.5Sn foil and also uniaxial tensile data for the Ti-5Al-2.5Sn foil itself is shown in Figure 91, and Figure 92 shows the plotted results of testing candidate braze alloys using lap-shear specimens of

TABLE XLI

AVERAGE STRENGTH OF BRAZE ALLOYS/Ti-5Al-2.5Sn FOIL

Braze Alloy	Average Foil Stress (for failure in lap shear tests) in ksi at Various Test Temperatures								
	-320F		-100F	75F		300F	500F	800F	
	B	S	B	B	S	B	B	B	S
CS217	98.4	46.5	95.6	108.6	103.8	84.3	74.6	72.6	52.8
CS217C	87.4	72.6	85.4	104.0	107.1	81.4	81.6	72.0	62.8
CS217F	88.3	87.3	81.4	99.5	92.1	79.4	64.3	65.7	68.6
CS217G	98.9	89.3	96.2	110.5	101.3	81.4	73.6	67.5	67.5
RM8	79.0	91.1	78.4	84.3	97.1	66.3	61.9	59.0	86.4
RM12	99.1	105.1	90.9	94.8	90.6	91.1	75.9	68.5	78.8
Ti-5Al-2.5Sn foil	180.0	-	-	119.0	-	-	-	72.0	-

B - As Brazed

S - After 100 hours salt spray exposure

Ti-6Al-4V foil and also uniaxial tensile data for the Ti-6Al-4V itself. Baseline data for Ag-5Al-0.2Mn braze specimens are presented in Figure 93 for comparison purposes.

The average foil stress values (for failure in lap shear tests) at different test temperatures are tabulated in Table XLI (for specimens of Ti-5Al-2.5Sn foil) and Table XLII (for specimens of Ti-6Al-4V foil).

Over the descending temperature range of 800 F to room temperature, all braze specimen strengths generally increased systematically with decreasing temperature: from about 60 to 70 ksi (Ti-5Al-2.5Sn) or 80 to 90 ksi (Ti-6Al-4V) at 800 F to about 95 to 110 ksi (both foil alloys) at room temperature. This pattern of increasing strength with decreasing temperature parallels reasonably well with that exhibited by both base alloy foils in uniaxial tensile tests over the same temperature range.

TABLE XLII

AVERAGE STRENGTH OF BRAZE ALLOYS/Ti-6Al-4V FOIL

Braze Alloy	Average Foil Stress (for failure in lap shear tests) in ksi at Various Test Temperatures								
	-320F		-100F	75F		300F	500F	800F	
	B	S	B	B	S	B	B	B	S
CS217	102.0	107.3	111.6	95.5	77.5	95.3	77.5	92.6	77.0
CS217C	112.0	59.0	94.9	107.7	87.1	98.7	93.5	97.2	76.7
CS217F	97.4	91.6	93.4	97.8	84.4	87.0	85.3	77.8	77.2
CS217G	105.1	79.9	77.6	100.9	79.4	82.4	87.3	79.6	72.3
RM8	110.6	75.6	83.2	85.1	68.3	83.6	77.9	80.7	71.4
RM12	106.6	78.8	54.8	100.0	94.2	83.4	80.4	87.7	76.5
Ti-6Al-4V	207.0	-	-	134.0	-	-	-	106.0	-

B - As Brazed

S - After 100 hours salt spray exposure

Two noteworthy exceptions to the stated strength levels were observed. First, CS217C brazements made with Ti-6Al-4V foils proved strongest at 800 F (~ 97 ksi) while maintaining the best overall profile of strength over the range of room temperature to 800 F. Second RM8 with the lowest braze temperature (1470 F) exhibited the lowest strength profile over the same temperature range, developing only ~85 ksi at room temperature. The Ti-6Al-4V foil specimens brazed with Ag-5Al-0.2Mn yielded strength levels comparable to the better Ti-Zr base braze alloys; however, the braze foil combination Ag-5Al-0.2Mn/Ti-5Al-2.5Sn produced decidedly inferior strengths (Fig. 93).

With but one exception, all braze/foil combinations underwent what appeared to be some form of ductile-brittle transition phenomenon between room temperature and -100 F (between -100 and -320 F for CS217/Ti-6Al-4V). This situation was

evidenced by a definite drop or stabilization in specimen strength with decreasing temperature in the cryogenic temperature range but of varying degree, depending upon both the braze alloy and the foil base alloy. Maximum strength losses (usually between room temperature and -100 F) of 15 to 20 ksi were common with the CS series alloys on Ti-5Al-2.5Sn foils, but this loss was reduced to 5 to 10 ksi on Ti-6Al-4V foils (the single exception being CS217G with a maximum 22 ksi strength drop). The RM series alloys exhibited considerably less tendency toward strength reduction (~3-5 ksi losses with Ti-5Al-2.5Sn foils); in fact, RM8 with Ti-6Al-4V foils experienced progressively increased joint strength below room temperature, as did the base metal foils themselves in uniaxial tests. On the other hand, the RM12 alloy with Ti-6Al-4V foils dropped 10 ksi in joint strength between room temperature and -100 F.

From the viewpoint of minimizing ductile-brittle transition behavior in the as-brazed condition, the following braze alloys appeared most desirable:

- Ti-5Al-2.5Sn foils: RM8, RM12
- Ti-6Al-4V foils: RM8, CS217F, CS217C, RM12

At -320 F, lap-joint specimens brazed with any of the candidate braze alloys failed at a foil stress about half the uniaxial tensile strength of the base metal foil at -320 F (for specimens of both Ti-5Al-2.5Sn and Ti-6Al-4V foils). In addition, the scatter in foil stress values at -100 or -320 F was higher than at room temperature for all six candidate braze alloys. Research efforts, therefore, were directed toward increasing the strength and reliability of brazed joints at cryogenic temperatures, principally through continued cyclic annealing experiments.

The exact cause of the strength reductions and greater data scatter at cryogenic temperatures was not clear, but it was felt that a possible contributory cause might be the lap-shear specimen geometry itself. This was studied by testing self-diffusion bonded, lap-shear specimens (no interleaf or braze). Specimens bonded with a thermal cycle simulating a typical braze cycle (1650 F, 5 min, 5000 psi) showed no signs of ductile-brittle transition and, furthermore, failed at high foil stress levels nearly identical to those obtained in uniaxial tensile tests (Figs. 92, 93, and 94). This evidence virtually acquitted the geometry factor as a primary cause of braze strength reduction and scatter at cryogenic temperatures.

A more probable cause was structural instability of the braze alloy matrices and/or braze-affected base metal which conceivably could produce undesirable beta

transformation products upon holding at cryogenic temperatures. It was felt that this could explain why strength reduction was usually most pronounced at -100 F, and why strength recovery was frequently noted at -320 F (e.g., through quench suppression of beta phase transformation). It was hoped that post-braze heat treatment, such as cyclic annealing and/or isothermal aging, would minimize or eliminate the problem by providing a stable structure.

3.5.4 Cyclic Annealing Studies

The objective of this study was to determine whether or not cyclic annealing can reduce or eliminate the following adverse effects noted in tensile testing of the as-brazed condition:

- Ductile-brittle transition behavior in the cryogenic temperature range
- More scatter in the foil stress to produce braze failure at cryogenic temperatures than at room temperature

In addition, the potential for cyclic annealing to increase the strength of brazements at various test temperatures was investigated.

Only the CS series braze alloys were evaluated in cyclic annealing studies. This was done for the following reasons:

- To this point, no satisfactory cyclic anneal had been obtained for RM8 and RM12 braze alloys. (The effect of an isothermal (1200 F) stress-relief anneal on tensile properties of RM series brazements was investigated in this phase, however.)
- Ductile-brittle behavior in the cryogenic temperature range was generally more pronounced for CS series braze alloys than for RM8 and RM12.

The Ti-5Al-2.5Sn, Ti-8Al-1Mo-1V, and Ti-6Al-4V foils (0.010-inch thick) were used in the cyclic annealing study. Cyclic anneal "F" (Table XXXIX) was employed. This empirically derived cyclic anneal "F" was found to benefit strength, reliability, and toughness properties for CS217C/Ti-5Al-2.5Sn lap-shear brazements in prior tests at room temperature.

Lap-joint shear specimens of Ti-6Al-4V, Ti-8Al-1Mo-1V, and Ti-5Al-2.5Sn foils, each about 0.010-inch thick and 0.5-inch wide were used. Typical overlap was 0.20 inch. Lap-shear testing of Ti-6Al-4V and Ti-5Al-2.5Sn brazements (cyclic annealed) was carried out at room temperature, -320 F in liquid nitrogen, -100 F in

TABLE XLIII

AVERAGE STRENGTH OF CS SERIES BRAZE ALLOYS/Ti-6Al-4V FOIL

Braze Alloy	Condition		Average Foil Stress (for failure in lap shear tests) in ksi at Various Test Temperatures											
	As-Brazed B	As Cyclic Annealed C	-320 F			-100 F			75 F			600 F		
			B or C	S	Degradation[1]	B or C	S	Degradation[1]	B or C	S	Degradation[1]	B or C	S	Degradation[1]
CS217	X		102.0	107.5	None	111.5	---	---	95.5	77.5	18.2	93.8	77.0	16.3
Percent Change[2]		X	107.1	112.0	None	108.0	116.4	None	106.4	94.9	11.4	98.5	85.3	2.3
			+5.0	+4.5	---	-3.9	---	---	+11.4	+21.3	---	+4.4	+10.8	---
CS217C	X		113.0	89.0	47.4	94.6	---	---	107.7	97.1	21.6	97.2	76.7	20.5
Percent Change[2]		X	120.1	62.4	25.0	107.1	114.9	None	101.2	93.0	8.0	87.5	87.5	None
			+3.7	+30.7	---	+12.9	---	---	-6.0	+6.9	---	-10.0	+14.1	---
CS217F	X		97.4	91.6	6.0	93.4	---	---	97.5	84.4	13.8	77.5	77.2	None
Percent Change[2]		X	100.5	91.0	9.0	93.5	97.1	None	93.2	92.1	None	74.0	77.2	None
			+3.2	Negative	---	-6.2	---	---	-4.7	+9.1	---	-4.9	Nil	---
CS217G	X		108.1	79.9	23.8	77.6	---	---	100.9	79.4	20.8	79.6	72.3	7.6
Percent Change[2]		X	94.5	+5.2	5.6	85.4	90.0	None	81.6	84.7	None	66.6	69.4	None
			-10.1	+6.6	---	+10.0	---	---	-19.2	+5.7	---	-17.6	-4.0	---

B As-Brazed

C As Cyclic Annealed: 1550 F minutes/1450 F - 10 minutes -- Repeat 1 hour

S After 100 hours exposure to salt spray at 95 F.

1. Percent degradation due to salt spray exposure.

2. Change due to cyclic annealing (+ denotes improvement and - denotes degradation).

methyl alcohol plus dry ice, and at 800 F in argon. Cyclic annealed Ti-8Al-1Mo-1V brazements were tested at -320 F, -100 F, room temperature, 300, 500, 800, and 900 F in argon. The Ti-8Al-1Mo-1V brazements in the as-brazed condition also were tested at room temperature to generate baseline strength data. Other Ti-8Al-1Mo-1V brazements made with RM8 and RM12 braze alloys were tested over the same -320 to 900 F temperature range to determine the possible benefits of an isothermal stress-relief anneal (1200 F, 0.5 hour, high-vacuum environment). Two to four data points were obtained at each test temperature.

Metallographic examination of all foil T-joints of every braze/foil combination was conducted in the following conditions:

- Condition 1 - As-brazed at the minimum flow temperature for 5 minutes
- Condition 2 - As-cyclic annealed (post-brazing)

Ti-6Al-4V and Ti-5Al-2.5Sn Foil Brazements

Actual and average foil stress values (Ti-6Al-4V and Ti-5Al-2.5Sn foils) for lap shear failure of the four CS series braze alloys (CS217, CS217C, CS217F, and CS217G) at the various test temperatures are plotted in Figures 95 and 96. (These curves may be compared directly with Figure 91 and 92 for the as-brazed condition.) The average foil stress values for failure of the four candidate braze alloys at various test temperatures are given also in Table XLIII and XLIV. These tables also include percent change in average foil stress values due to cyclic annealing at the various test temperatures.

TABLE XLV

AVERAGE STRENGTH OF CS SERIES BRAZE ALLOYS/Ti-5Al-2.5 Sn FOIL

Braze Alloy	Condition		Average Foil Stress (for failure in lap shear tests) in ksi at Various Test Temperatures											
			-320 F			-100 F			75 F			900 F		
	As Brazed B	As Cyclic Annealed C	B or C	S	Degradation[1]	B or C	S	Degradation[1]	B or C	S	Degradation[1]	B or C	S	Degradation[1]
CS217	X		46.4	46.5	51.8	85.7	---	---	108.8	102.8	6.4	78.8	52.8	27.3
Percent Change[2]		X	111.8 +19.0	129.6 +178.7	None ---	127.0 +32.6	138.9 ---	None ---	119.0 +9.6	150.7 +16.3	None ---	72.1 N/I	74.4 +41.0	None ---
CS217C	X		87.4	72.5	16.9	86.4	---	---	104.0	107.1	None	73.9	63.6	11.7
Percent Change[2]		X	94.5 +8.1	96.9 +33.6	None ---	113.6 +34.7	116.1 ---	None ---	116.6 +12.1	119.9 +12.0	None ---	77.6 +7.8	74.2 +16.7	4.4 ---
CS217F	X		63.3	67.3	4.1	61.4	---	---	99.5	92.1	7.4	66.7	68.6	None
Percent Change[2]		X	119.5 +36.1	122.8 +82.1	None ---	151.3 +49.3	136.9 ---	None ---	109.5 +10.0	104.5 +11.9	4.8 ---	75.8 +13.8	71.2 +3.8	6.5 ---
CS217G	X		98.9	99.3	9.7	96.2	---	---	110.5	101.3	8.3	67.5	67.5	None
Percent Change[2]		X	96.8 -2.1	93.2 +3.2	4.7 ---	97.9 +3.6	96.6 ---	None ---	84.1 -23.9	80.3 -20.9	4.8 ---	46.0 -31.8	61.6 -8.4	None ---

A As-Brazed

C As Cyclic Annealed: 1550 F - 10 minutes/1450 F - 10 minutes -- Repeat 1 time.

S After 100 hours exposure to salt spray at 95 C.

1. Percent degradation due to salt spray exposure.
2. Due to cyclic annealing (+ denotes improvement and - denotes degradation).

The average Ti-8Al-1Mo-1V foil stress values for failure of brazed lap joints in the cyclic annealed condition at various test temperatures (-320 to 900 F) are listed in Table XLV along with the room temperature test results for candidate alloy/Ti-8Al-1Mo-1V brazements in the as-brazed condition. Degradation in strength of RM8 and RM12 brazements was observed at room temperature due to 1200 F stress relief treatment. Therefore, study of post-braze treatment for RM series alloys was suspended, and the strength of RM8 and RM12 brazements was evaluated in the as-brazed condition over the entire temperature range of -320 to 900 F. These values are included in Table XLV. The foil stress values at brazement failure versus test temperature for the CS series brazements are shown in Figure 97; Figure 98 shows the RM series.

The single cyclic anneal evaluated definitely improved the cryogenic braze strength patterns for most CS series alloys. First, no trace of cryogenic ductile-brittle transition behavior (i.e., as evidenced by an anomalous drop in strength with decreasing test temperature) was observed for the following combinations: CS217G/Ti-6Al-4V, CS217C/Ti-6Al-4V, and CS217G/Ti-5Al-2.5Sn. Second, the same cyclic anneal lowered the observed ductile/brittle transition temperature range from between room temperature/-100 F (as-brazed condition) to -100/-320 F on the

TABLE XLV

LAP-SHEAR TEST RESULTS, Ti-8Al-1Mo-1V BRAZEMENTS

Braze Alloy	Foil Stress in ksi at Failure in Lap Shear Tests at Test Temperature (F)								
			75 F						
	-320 F	-100 F	As Brazed	As Cyclic Annealed	Percent Increase(1)	300 F	500 F	800 F	900 F
CS217	152.0	147.1	106.6	127.5	18.6	121.1	105.0	96.7	91.8
CS217C	116.0	99.3	108.3	112.2	3.6	107.9	106.1	96.9	88.7
CS217F	126.6	113.9	96.2	127.3	30.6	105.3	106.2	96.8	92.4
CS217G	116.3	106.6	93.9	111.6	18.8	97.0	91.5	89.8	81.1
RM8 (as brazed)	105.9	93.4	94.7	---	---	---	90.6	100.2	91.4
RM8 (as stress relieved)	85.2	81.0	75.8	---	---	82.1	75.5	76.1	79.5
Percent decrease(2)	19.5	13.3	20.0	---	---	---	32.3	24.0	13.3
RM12 (as brazed)	111.0	96.4	100.3	---	---	---	90.5	96.9	96.0
RM12 (as stress relieved)	95.0	94.5	82.8	---	---	78.3	87.4	82.8	86.1
Percent decrease(2)	14.4	2.0	17.5	---	---	---	3.4	16.3	10.3

1. Increase in average foil stress due to cyclic annealing.
2. Decrease due to stress relief.

CS217, 217C, 217F and 217G: As cyclic annealed
1550 F, 10 minutes
1450 F, 10 minutes
Repeat 1 hour

RM8 and RM12: As brazed and as stress relieved (1200 F, 30 minutes)

CS217/Ti-5Al-2.5Sn brazement. Data scatter at cryogenic temperatures was reduced by cyclic annealing for certain foil/braze combinations (notably CS217G/Ti-6Al-4V, CS217F/Ti-6Al-4V, CS217C/Ti-6Al-4V, and CS217G/Ti-5Al-2.5Sn), but the remaining four combinations still exhibited considerable scatter. In the category of braze strength improvement, cyclic annealing provided significant improvements in strength (typically 10 percent increases) in 12 cases out of a possible 32 (foil/braze/test temperature combinations), while causing a significant decrease in strength (>10 percent reduction) in only six cases. The braze alloys CS217, CS217C, and CS217F benefitted the most from cyclic annealing, especially on Ti-5Al-2.5Sn foils. The following tabulation illustrates the point:

Braze Alloy	Percent Strength Improvement Due to Cyclic Annealing			
	-320 F	-100 F	Room Temperature	800 F
CS217	16.0	32.8	9.6	Nil
CS217C	8.1	24.1	12.1	7.8
CS217F	26.1	49.3	10.0	13.8

As shown in Tables XLIII and XLIV, and Figures 95 and 96, a given cyclic annealing treatment definitely can induce different effects upon different braze/foil combinations. The inference again was strong that each foil/braze combination of interest has its very own optimum cyclic anneal which must be tailored to it through study and experimentation.

Ti-8Al-1Mo-1V Foil Brazements

The percent improvement in average foil stress values at room temperature for the CS series alloys/Ti-8Al-1Mo-1V brazements due to cyclic annealing is shown in Table XLV and is summarized as follows:

- CS217 = 18.6 percent improvement
- CS217C = 3.6 percent improvement
- CS217F = 30.6 percent improvement (maximum response)
- CS217G = 18.8 percent improvement

Thus, the CS217F alloy exhibited the maximum increase in room temperature strength due to cyclic annealing and as shown in Figure 99, the alloy also showed the maximum tendency for beryllide spheroidization due to cyclic annealing. It seemed reasonable to assume the two observations were related.

Stress relief treatment (1200 F for 30 minutes) of the RM8 and RM12 brazements resulted in varying degrees of degradation of strength over the temperature range -320 to 900 F (Fig. 98). The percent decrease in average foil stress for failure of the RM8 and RM12 alloys at various test temperatures due to stress relief is given in Table XLV. This decrease varied between 13 and 33 percent for RM8 and between 2 and 17.5 percent for RM12. The noted stress relief treatment was thus detrimental to both RM8 and RM12 brazement strengths.

In general, braze strength increased with decreasing test temperature (the expected pattern) for the cyclic annealed CS series brazements. Minor dips in braze strength for CS217C, CS217F, and CS217G between room temperature and -320 F were interpreted as evidence of a still active ductile/brittle transition phenomenon related to braze matrix instability in the cryogenic temperature range. It was felt that a better (experimentally determined) cyclic annealing and aging treatment could eliminate this problem and generally improve stability, strength, and toughness of

TABLE XLVI

SUMMARY OF CYCLIC ANNEALING EFFECTS ON CS SERIES BRAZE ALLOY/FOIL COMBINATIONS

Effect	BRAZE ALLOY/FOIL ALLOY COMBINATION											
	CS217			CS217C			CS217F			CS217G		
	6-4	8-1-1	5-2.5	6-4	8-1-1	5-2.5	6-4	8-1-1	5-2.5	6-4	8-1-1	5-2.5
Eliminated Ductile/Brittle Transition Behavior (Cryogenic Temperatures)	No	Yes	No	Yes	No	No	No	No	No	Yes	No	Yes
Reduced Ductile/Brittle Transition Temperature	No	Yes	Yes	Yes	No	No	No	No	Yes	Yes	No	Yes
Reduced Data Scatter (Cryogenic Temperatures)	No	No	No	Yes	No	No	Yes	No	No	Yes	No	Yes
Improved Brazement Strength (±10 percent)	Yes RT	Yes RT	Yes -320F -100F RT	Yes -100F O	No	Yes -100F RT	No	Yes RT	Yes -320F -100F RT 900F	Yes -100F O	Yes RT	O

Note: O denotes significant strength reduction at certain temperatures.

these brazements at cryogenic temperatures. Fortunately, the Ti-8Al-1Mo-1V brazements made with the CS217 alloy responded very well to the particular cyclic anneal used, yielding the highest average braze strengths recorded in the program for any lap-shear brazement over the temperature range of -320 to 900 F. No ductile/brittle behavior was observed with CS217 after cyclic annealing.

Both RM series alloys also yielded interesting strength levels in the as-brazed condition, but strength variations with test temperatures were quite anomalous (indicating some form of structural instability). Again, it is probable that proper post-braze heat treatment would be capable of eliminating the anomalies.

Summary of Cyclic Annealing Effects

A summary of the cyclic annealing effects on the CS series alloys/foil combination are shown in Table XLVI.

3.5.5. Environmental Stability Tests

The objective of the environmental stability tests was to determine relative sensitivities of the candidate alloy brazements to potentially reactive service environments such as salt-water spray (200 F), air oxidation (1000 F), and encrusted hot salt in excess-oxygen, turbine exhaust gases (1000 F). Many studies have been cited

in the literature on the hazardous nature of these environments (Ref. 94 through 101). The effects of each environment on braze stability are discussed individually in succeeding paragraphs.

Salt Spray Corrosion Tests

Lap-shear specimens of Ti-5Al-2.5Sn and Ti-6Al-4V foils (both 0.010-inch thick) in the as-brazed condition were exposed to salt spray at 200 F for 100 hours (NaCl = 5.0 wt %). After the salt spray exposure, the specimens were cleaned and tested at -320 F (in liquid nitrogen), room temperature, and at 800 F (in argon). Foil stress values for braze or foil failure in lap-shear tests after exposure to salt spray were compared with foil stress values obtained in the as-brazed condition. A second group of lap-shear specimens was cyclic annealed (cyclic anneal "F") in vacuum prior to salt spray exposure.

Foil stress values for failure at various test temperatures (-320, 75, and 800 F) in the as-brazed condition and after exposure to salt spray are plotted in Figure 100 (for specimens of Ti-5Al-2.5Sn foil) and in Figure 101 (for specimens of Ti-6Al-4V foil). The average foil stress values are included in Tables XLI and XLII. Comparable data for cyclic annealed specimens are plotted in Figures 95 and 96 and compiled in Tables XLIII and XLIV.

Results of As-Brazed Tests

With as-brazed specimens made of Ti-5Al-2.5Sn foils, all the candidate braze alloys except CS217 were found to be insensitive to salt spray corrosion in the temperature range of -320 to 800 F. The CS217 alloy experienced the following degradation in average foil stress values:

-320 F - about 52 percent
75 F - negligible
800 F - about 27 percent

It appeared unlikely that the observed degradation in the CS217 alloy strength resulted from corrosion effects inasmuch as no metallographic evidence of corrosion was found. It seemed more reasonable to assume an aggravation of the presumed structural instability of the as-brazed condition leading to ductile/brittle transition phenomena. The ductile/brittle transition behavior observed for CS217 and the other CS series braze alloys in the as-brazed condition was also observed after exposure to salt spray and the results shown in Figure 100.

The scatter in foil stress values at -320, 75, and 800 F after 100 hours salt spray exposure frequently was higher than in the as-brazed condition. This was true for all the candidate braze alloys except RM12. For the RM12 alloy, the scatter in foil stress values was appreciably lower, and about the same both before and after exposure to salt spray.

With as-brazed lap-shear specimens made of Ti-6Al-4V foil, the least degradation in average foil stress values following salt spray exposure was observed with the CS217, CS217F, and RM12 braze alloys. However, all braze alloys and especially the CS217C, CS217G, and RM8 braze alloys underwent considerable deterioration in strength (15 to 50 percent) following salt spray exposure (Fig. 101). The degradation in strength was, in general, maximum at -320 F, although the CS217 alloy was a notable exception. Again, greater scatter in foil stress values at failure was observed after exposure to salt spray than in the as-brazed condition. No metallographic evidence of corrosion was found in any specimen.

At this point, there were strong indications that structural instability of braze affected base metal foils precluded obtaining meaningful corrosion data in the as-brazed condition. The structural instability appeared to be aggravated by the thermal regime of salt spray conditioning, especially for Ti-6Al-4V brazements. The indicators were:

- Metallographic examination had not produced any evidence of salt corrosion for any Ti-Zr base braze alloy or foil brazement.
- Ductile-brittle transition phenomena had been observed in the as-brazed condition for all candidate braze alloys. Braze-affected foil frequently was the locus of failure.
- Presumed "corrosion effects" on braze strength were erratic and not in evidence for every test temperature or braze/foil combination, as would be expected.

Consequently, before significant stability tests could be made to gage true corrosion effects, it was felt that structural instability in foil brazements first must be eliminated. Therefore, cyclic annealed brazements were tested next.

Results of Cyclic Annealing Tests

The most important and apparently most applicable advantage of cyclic annealing CS series brazements was brought out in this test phase (Tables XLIII and XLIV). It was in the ability of cyclic annealing to virtually eliminate susceptibility

to braze strength degradation following 200 F salt spray exposure. Strength losses as high as 15 to 30 percent were not uncommon in many foil/braze combinations (as-brazed condition) following exposure to salt spray. The single cyclic anneal evaluated completely changed this picture, so that in only two instances (braze/foil/test temperature combinations) out of a possible 32 did the strength loss exceed 10 percent following salt spray exposure. (The greatest actual loss of these two was 25 percent after cyclic annealing, still an improvement over the experience of the as-brazed condition.) In fact, in 27 instances, no significant change in braze strength was recorded (strength loss, 5 percent or less). In all instances, braze strength of cyclic annealed specimens following 100 hours of salt spray exposure was measured at 80,000 psi or higher (-320 to 75 F test temperatures) and the RM series brazements, not responsive to the cyclic anneal employed, still exhibited strengths ≥70,000 psi following salt spray exposure in the as-brazed condition (-320 to 800 F). No metallographic evidence of general corrosion or crevice corrosion was observed on any of the brazements in this test phase.

Air Oxidation Tests

Lap-shear test specimens (0.010-inch foils; overlap 0.020-inch) and small foil T-joints (for metallography) were used for the air oxidation tests. The lap-shear specimens were prepared as follows:

- Six candidate braze alloys/Ti-5Al-2.5Sn brazements (as-brazed condition)
- Six candidate braze alloys/Ti-6Al-4V brazements (as-brazed condition)
- Three CS series alloys/Ti-5Al-2.5Sn cyclic annealed "F" brazements.
- Self-diffusion bonded Ti-5Al-2.5Sn specimens (as-bonded).
- Self-diffusion bonded Ti-6Al-4V specimens (as-bonded)

Self-diffusion bonding of both Ti-5Al-2.5Sn and Ti-6Al-4V lap-shear specimens was accomplished using the parameters: 1650 F, 1200 psi, 20 seconds (gettered argon atmosphere). Type 1010 plain carbon steel foil (0.002-inch thick) and tungsten foil (0.001-inch thick) were used as stopoffs to prevent electrode sticking (Fig. 102).

All lap-shear and T-joint specimens were subjected to static air oxidation at 1000 F for 100 hours in a Globar furnace. The oxidized lap-shear specimens were tested at -320 F (in liquid N_2), -100 F (in methyl alcohol and dry ice), room temperature and 800 F (argon). The foil stress values for failure of oxidized lap-shear

specimens were compared with baseline data previously obtained. This comparison revealed the degree of degradation in strength of brazements and of the base metal itself due to 1000 F air oxidation. The foil stress values at failure of oxidized specimens were also compared with data obtained after 100 hours aging at 1000 F in high vacuum. This comparison revealed the effect of air oxidation alone on aged brazement strength.

Small foil T-joints were examined metallographically to determine the effects of oxidation on braze and foil microstructure. Microhardness measurements were also made on these specimens. Chemical analyses for oxygen content of Ti-5Al-2.5Sn and Ti-6Al-4V foils (as-received and after 100 hours oxidation at 1000 F) were conducted to determine the extent of oxygen absorption.

Results of lap-shear tests on various specimens are tabulated in Tables XLVII and XLVIII. The strength data are plotted in Figures 34, 103, 104, and 105, which also describe the location of failure (joint or braze affected base metal foil). The average foil stress values for failure at different test temperatures (-320 F, -100 F, room temperature, and 800 F) are listed in Table XLVII for the following conditions:

- Six candidate braze alloys/Ti-5Al-2.5Sn brazements, in both as-brazed condition and after air oxidation (Fig. 103)
- Three CS series alloys/Ti-5Al-2.5Sn brazements, in both cyclic annealed condition and after air oxidation (Fig. 104)
- Self-diffusion bonded Ti-5Al-2.5Sn specimens, as bonded and after air oxidation (Fig. 94)

The average foil stress values at different test temperatures (-320 F, -100 F, room temperature, and 800 F) for the following test conditions are included in Table XLVIII:

- Six candidate braze alloys/Ti-6Al-4V brazements in both as-brazed condition and after air oxidation (Fig. 105).
- Six candidate braze alloys/Ti-6Al-4V brazements after thermal aging at 1000 F for 100 hours in high vacuum (Fig. 105).
- Self-diffusion bonded Ti-6Al-4V specimens, as-bonded and after air oxidation (Fig. 94).

The results of the microhardness determinations are included in Table XLIX.

TABLE XLVII

RESULTS OF LAP-SHEAR TESTS OF CANDIDATE ALLOY/Ti-5Al-2.5Sn SELF-DIFFUSION BONDED SPECIMENS

Candidate Braze Alloys	Condition		Average Foil Stress, ksi, for Failure of Lap-Shear Specimens at Various Test Temperatures											
	As-Brazed B	As Cyclic Annealed C	-320 F			-100 F			75 F			800 F		
			B or C	O	Degradation[1]	B or C	O	Degradation[1]	B or C	O	Degradation[1]	B or C	O	Degradation[1]
CS217	X	X	96.4	90.4	6.2	95.6	---	---	108.6	[illegible].0	24.5	72.6	69.1	4.8
Percent Change[2]			111.8	97.2	13.0	127.0	131.1	None	119.0	[illegible].6	7.9	72.1	70.3	2.4
			+16.0	+7.5	---	+32.8	---	---	+9.6	+33.6	---	Nil	Nil	---
CS217C	X	X	87.4	77.5	11.3	85.4	---	---	104.0	83.7	19.5	72.0	66.0	8.3
Percent Change[2]			94.5	92.6	2.0	112.6	103.9	7.7	118.6	103.8	10.9	77.6	67.2	13.4
			+8.1	+19.5	---	+24.1	---	---	+12.1	+24.0	---	+7.8	+1.8	---
CS217F	X	X	88.3	83.3	5.7	81.4	---	---	99.5	79.9	19.6	65.7	65.2	None
Percent Change[2]			119.5	89.8	24.8	121.3	92.8	23.5	109.5	89.2	18.5	75.5	63.3	16.2
			+26.1	+7.8	---	+49.3	---	---	+10.0	+10.6	---	+13	-2.9	---
CS217G	X		98.9	88.7	10.3	95.2	---	---	110.5	84.0	24.0	67.5	57.1	15.4
RM8	X		79.0	71.9	9.3	78.4	---	---	84.3	80.3	28.8	59.0	58.8	None
RM12	X		99.1	83.7	15.5	90.9	---	---	94.8	73.4	23.6	68.5	68.4	None
Sel. diffusion bonded Ti-5Al-2.5Sn specimens	---	---	181.7	183.1	10.2	154.0	127.4	17.3	128.4	126.4	1.6	69.0	69.2	None

B - As-Brazed

C - As Cyclic Annealed: 1550 F - 10 minutes/1450 F - 10 minutes -- Repeat 1 hour.

O - As oxidized 1000 F - 100 hours in air

1. Percent degradation in brazement strength due to 1000 F - 100 hours air oxidation

2. Change in brazement strength due to cyclic annealing

TABLE XLVIII

RESULTS OF LAP-SHEAR TESTS OF CANDIDATE ALLOY / Ti-6Al-4V SELF-DIFFUSION BONDED SPECIMENS

Candidate Braze Alloys	Average Foil Stress, ksi, for Failure of Lap Shear Specimens at Various Test Temperatures											
	-320 F				75 F				800 F			
	B	(a) or (v)	1000 F 100 Hours Exposure	Percent Change(2)	B	(a) or (v)	1000 F 100 Hours Exposure	Percent Change(2)	B	(a) or (v)	1000 F 100 Hours Exposure	Percent Change(2)
CS217	102.6	(a)	106.9	+ 4.8	96.5	(a)	94.8	- 0.7	92.6	(a)	90.1	- 2.2
Percent Change(1)		(v)	129.0 -17.4	+26.8		(v)	105.5 -10.1	+19.5		(v)	96.0 - 8.1	+ 5.8
CS217C	112.0	(a)	99.1	-11.5	107.7	(a)	79.6	-26.1	97.2	(a)	76.3	-21.5
Percent Change(1)		(v)	117.0 -15.3	+ 4.5		(v)	88.5 -10.0	-17.8		(v)	84.3 - 9.5	-13.3
CS217F	97.6	(a)	73.2	-24.8	97.8	(a)	76.1	-22.2	77.8	(a)	74.3	- 4.5
Percent Change(1)		(v)	117.9 -37.5	+21.0		(v)	88.0 -13.5	10.0		(v)	77.9 - 4.6	Nil
CS217G	105.1	(a)	102.9	- 2.1	100.9	(a)	87.3	-13.5	78.8	(a)	71.4	-10.3
Percent Change(1)		(v)	94.5 + 8.8	-10.1		(v)	101.6 -14.1	Nil		(v)	90.6 -20.7	-13.1
RM8	110.8	(a)	75.5	-31.9	85.1	(a)	67.1	-21.1	89.7	(a)	64.1	-20.6
Percent Change(1)		(v)	109.6 -23.2	Nil		(v)	62.9 + 6.7	-26.1		(v)	81.5 -21.3	Nil
RM12	106.6	(a)	93.3	-12.5	102.9	(a)	92.3	-10.7	87.7	(a)	67.3	-23.3
Percent Change(1)		(v)	101.3 7.9	- 5.0		(v)	79.9 +13.9	-21.0		(v)	70.6 - 4.7	-19.5
Self diffusion bonded Ti-6Al-4V	170.0	(v)	138.3	-18.6	123.0	(a)	148.0	+20.2	--	-	93.2	--

B - As-brazed
(a) - As air oxidized 1000 F - 100 hours
(v) - After 1000 F - 100 hours thermal exposure in high vacuum (10^{-5} torr)

1. Percent change due to air oxidation only at 1000 F (difference between brazement strength after 1000 F - 100 hours thermal exposure in vacuum and after 1000 F - 100 hours air oxidation). + denotes an increase and - denotes a decrease in brazement strength.

2. Percent change due to air oxidation at 1000 F - 100 hours.

Results of Air Oxidation Tests

As-Brazed Condition. The most obvious effect of the 1000 F air oxidation test was a typical 20 to 30 percent reduction in average room temperature brazement strength, the maximum strength loss most frequently occurring at room temperature for both CS and RM series brazements and both foil alloys. Strength losses at -320 and 800 F were generally much less than 20 percent, the most notable exceptions being:

Brazement	Test Temperature (F)	Strength Loss (%)
CS217C/Ti-6Al-4V	800	21.5
RM8/Ti-6Al-4V	800	23.5
	-320	31.9

The braze/foil combination CS217/Ti-6Al-4V was the only one which exhibited no significant changes in strength at any test temperature due to 1000 F oxidation.

TABLE XLIX

MICROHARDNESS DETERMINATION OF CANDIDATE ALLOY BRAZEMENTS

Candidate Braze Alloy	Foil		Hardness R_C											
			As Brazed			1000 F (100 hr in vacuum)			As Brazed and 1000 F (100 hr in air)			As Cycle Annealed and 1000 F (100 hr in air)		
	5Al-2.5Sn	6Al-4V	M	O	I	M	O	I	M	O	I	M	O	I
CS217	X		51.0	--	71.0	51.5 to 52.5	DZ to 36.0 to 39.0	68.0	58.5	58.5	63.0	60.0	DZ to 40.0	--
		X	--	--	--	51.5 to 52.5	--	--	51.0	45.0	57.5	--	--	--
CS217C	X		52.0 to 56.0	--	--	53.5 to 56.0	DZ to 46.5	--	58.5 to 60.0	DZ to 41.0	--	50.0 to 65.0	DZ to 45.0	--
		X	--	--	--	--	--	--	51.0 to 55.5	--	57.5	--	--	--
CS217F	X		46.9 to 50.5	--	67.5	54.0	DZ to 43.5	64.5	45.5	--	64.5	68.0	--	--
		X	--	--	--	--	--	--	59.5 to 65.0	--	--	--	--	--
CS217G	X		56.5 to 59.0	--	66.5	60.0 to 63.1	DZ to 36.5	--	45.0	--	64.0	--	--	--
		X	--	--	58.5		--	--	47.5 to 53.5	--	65.5	--	--	--
RM8	X		52.2	--	--	45.0 to 56.0	DZ to 38.5	59.5	46.5 to 51.0	--	64.5	--	--	--
		X	--	--	--	--	--	--	53.0 to 60.0	DZ to 40.0	--	--	--	--
RM12	X		60.0	--	--	44.5 to 60.0	DZ to 25.0	--	--	--	--	--	--	--
		X	--	--	--	--	--	--	54.0 to 61.0	DZ to 41.0	--	--	--	--

M - Matrix
O - Other phases
I - Intermetallics
DZ signifies braze/foil zone

As shown in Figures 106 through 110, very light external oxidation of most braze alloys was observed. However, in two cases, the entire braze alloy matrix appeared to be oxidized internally (CS217/Ti-6Al-4V and CS217F/Ti-5Al-2.5Sn). All T-joints brazed with CS217F were found distorted and prone to crack after 1000 F oxidation (Fig. 108); brazement cracks were also observed in lap-shear specimens brazed with CS217F. Brazements of CS217F had shown an unexplained tendency toward accelerated oxidation at 1000 F, producing voluminous oxide products (approximately 10 to 15 times that observed for the other candidate braze alloys). Curiously, the effect of 1000 F oxidation upon braze strength of CS217F was not appreciably different from the other candidate alloys.

Diffusion Bonded Specimens. Strength degradation of self-diffusion bonded Ti-5Al-2.5Sn and Ti-6Al-4V specimens due to air oxidation was most evident at cryogenic temperatures; however, the decrease in strength was much more pronounced for Ti-6Al-4V specimens than for Ti-5Al-2.5Sn specimens. As the result of air oxidation, self-diffusion bonded Ti-6Al-4V specimens showed evidence of ductile-brittle behavior in the cryogenic temperature range (-100 and -320 F). Even so, the diffusion bonded and oxidized specimens exhibited appreciably greater joint strength than as-brazed or brazed and oxidized specimens through the temperature range, -320 F to room

temperature. This indicated that structural instability of the braze materials, aggravated by 1000 F oxidation effects, were responsible for the lower strength of brazements in this temperature range.

Isolated Effect of Air Oxidation. The isolated effect of 1000 F air oxidation on brazement strength was determined from the difference in brazement strengths after aging at:

- 1000 F - 100 hours in high vacuum ($\sim 10^{-5}$ Torr)
- 1000 F - 100 hours in static air environment.

The percent strength change due to air oxidation for candidate alloys/Ti-6Al-4V brazements is included in Table XLVIII.

In general, the CS series alloy brazements were somewhat stronger in the vacuum-aged condition as opposed to the oxidized condition (i.e., after thermal exposure at 1000 F for 100 hours in vacuum). This condition was probably due to more uniform transformation of metastable (but uncontaminated) braze matrix structures to equilibrium structures during vacuum aging. Braze alloy RM8 followed the same trend as the CS series; however, RM12 reversed the trend, showing somewhat greater strength reduction due to 1000 F vacuum aging at most test temperatures. The reason for the varying effects of oxidation on candidate braze strength could not be discerned from the braze structures studied; however, the generally good retention of all candidate braze strengths following both types of aging conditions was gratifying.

Cyclic Annealing Effects. The CS series/Ti-5Al-2.5Sn brazements were cyclic annealed and oxidized at 1000 F for 100 hours, and the results shown in Figures 111, 112, and 113. Cyclic annealed brazements of CS217 and CS217C exhibited some slight degradation in strength due to air oxidation but, in most cases, significantly less than for the as-brazed and oxidized condition (typically between 0 and 13 percent). In addition, cyclic annealing increased initial braze strengths appreciably, so that even after 1000 F oxidation, all CS217 and CS217C brazements possessed strengths $\geq$90,000 psi over the temperature range -320 F to room temperature. At 800 F, cyclic annealed and oxidized braze strength levels were essentially equivalent to the original as-brazed strength levels.

Cyclic annealed CS217F/Ti-5Al-2.5Sn brazements exhibited maximum degradation of strength (between 16.5 to 24.8 percent at the various test temperatures).

T-joint specimens brazed with CS217F and cyclic annealed were found distorted and cracked after air oxidation, indicating no improvement in oxidation resistance over the as-brazed condition.

Metallography Studies. Typical microstructures of candidate alloy brazements following oxidation at 1000 F are shown in Figure 106 through 113. Brazed T-joints of CS217F alloy (as-brazed and as-cyclic annealed) were found distorted and braze cracked after air oxidation at 1000 F (Fig. 101 and 113).

Formation of a subsurface oxidation diffusion zone, about 0.75 mil thick, was observed beneath the exposed foil surfaces of most oxidized brazements. This diffusion zone was the result of prolonged exposure (100 hours) at 1000 F. Hardness of this diffusion zone was about 40 to 42 R_C contrasted with 34 to 38 R_C in the unoxidized portions of the foils.

The beryllides, in general, were not oxidized; rather they were preserved intact in the oxide films. However, cracking of some exposed beryllides because of oxidation forces were observed in brazements of CS217G/Ti-6Al-4V (Fig. 109).

Microhardness Studies. Microhardness values for the following conditions of the braze matrix and the braze/foil diffusion zone are shown in Table XLIX:

- As-brazed
- Brazed + 100 hours thermal aging in vacuum at 1000 F
- Brazed + oxidized at 1000 F for 100 hours in static air environment
- Cyclic annealed and then oxidized at 1000 F for 100 hours in static air environment

No significant changes in braze matrix hardness (from the as-brazed condition) were recorded due to 1000 F thermal treatment in air or in vacuum, or from cyclic annealing. Eutectic braze matrix hardness for all candidate braze alloys varied between R_C 45 to 59, depending upon local variations in the hard, intermetallic phase content.

Chemical Analysis of Foils. Chemical analyses of the Ti-5Al-2.5Sn and Ti-6Al-4V foils before and after 1000 F oxidation were determined as follows:

Foil (0.010-in.)	Oxygen Content As-Received Condition (wt %)	Oxygen Content After Air Oxidation At 1000 F for 100 Hours (wt %)
Ti-5Al-2.5Sn	0.076	0.112
Ti-6Al-4V	0.074	0.105

The analysis shows an approximate 40 percent increase in the oxygen content due to air oxidation at 1000 F. This increase in contaminant level was anticipated on the basis of both internal and external oxidation, which was observed metallographically, and corroborated by foil subsurface hardness increases. After oxidation, the Ti-5Al-2.5Sn foils displayed irridescent films (mainly blue), whereas the Ti-6Al-4V foil surfaces were dark gray.

Hot-Salt Corrosion Tests

To gage relative susceptibility of candidate alloy brazements to hot-salt stress corrosion cracking, both brazed and self-diffusion bonded lap-shear specimens (Fig. 114) were encrusted with salt (NaCl) and dead weight loaded (10,000 and 20,000 psi levels) in the stress rupture rig shown in Figures 115, 116, and 117. A special forced convection furnace using simulated jet-engine exhaust gases (oxidizing) was employed to directly heat the specimens (Fig. 116). Foil stress levels were chosen to yield minimum rupture times (salt-free air) of 5000 hours (10,000 psi) and 700 hours (20,000 psi). Only the Ti-5Al-2.5Sn foil brazements were tested and the results are shown in Table L.

The most obvious result was that all foil brazements and even the self-diffusion bonded (braze-free) foil specimens suffered premature foil rupture failures as the result of hot-salt corrosion. By virtue of having somewhat longer rupture times, the RM series brazements appeared to be the most corrosion resistant. Using the same reasoning, the silver-base brazements appeared least corrosion resistant to the hot salt. However, in consideration of the greatly reduced rupture lives of all specimens (0.25 to 10.4 hours) and a probable log-time relation, it was concluded that all candidate brazements (and the program foil alloy itself) are adversely affected by hot salt to approximately the same degree.

Metallographic examination of failed specimens (Fig. 118 and 119) after hot-salt testing revealed many transverse, intergranular, corrosion-induced cracks in each specimen foil. Some cracks initiated at braze surfaces and propagated into the adjacent foils, other cracks initiated in the foil materials. Neither diffusion bonded nor brazed lap-joint regions (joint interfaces) were affected by corrosion. As shown in Figure 120, the RM8 and RM12 braze materials were particularly resistant to hot-salt cracking although adjacent foil materials did crack and fail prematurely.

TABLE L

HOT-SALT CORROSION TEST DATA

Test Temperature:	1000 F
Test Environment:	Simulated jet-engine exhaust gasses (oxidizing)
Program Brazement:	Lap-shear specimen of 0.010 inch Ti-5Al-2.5Sn foils (0.020 inch overlap by 0.5 inch width)
Braze Condition: (Prior to Salt Encrustation)	CS Series alloys Cyclic annealed 1550 F, 10 minutes 1450 F, 10 minutes Cycled 3 times
RM series alloys:	As-brazed
Ag-base alloys:	As-brazed

Braze Alloy	Foil Stress (psi)	Time to Failure (min.)		Failure Location
		Actual Values	Average	
CS217	20,000	15 - 30	23	Braze-affected foil
CS217C	20,000	35	35	Braze-affected foil
CS217F	20,000	35 - 35	35	Braze-affected foil
CS217G	20,000	15	15	Braze-affected foil
RM8	20,000	62 - 62	62	Braze-affected foil
RM12	20,000	63 - 63	63	Braze-affected foil
Diffusion bonded lap joint (baseline) (1650 F, 1 minute, 1200 psi)	20,000	53 - 125	89	Foil
CS217	10,000	465 - 465	465	Braze-affected foil
CS217C	10,000	255	255	Braze-affected foil
CS217F	10,000	405 - 315	360	Braze-affected foil
RM8	10,000	465 - 555	510	Foil
RM12	10,000	595 - 645	615	Foil
Diffusion bonded lap joint	10,000	345 - 345	345	Foil
Ag-5Al-2Mn	10,000	195	195	Braze-affected foil

3.5.6 Stress-Rupture Tests of Brazements

To determine the effect of a constant, long-period service stress upon brazement reliability, brazed lap-shear specimens of the six candidate alloys as well as the self-diffusion bonded specimens were dead weight loaded to produce 30,000 psi foil stress at 1000 F. Duplicate tests were conducted on each joint variety. The hot-gas, stress-rupture rig shown in Figure 115 was used. The 30,000 psi stress level was chosen to yield a minimum 100-hour rupture life. All brazements were made with 0.010-inch thick Ti-5Al-2.5Sn foils, using a controlled overlap of 0.020-inch. The CS series braze specimens were cyclic annealed, the RM series brazements were tested in the as-brazed condition.

All diffusion bonded specimens remained intact to the 100-hour test point.

Three cyclic annealed braze alloys endured 100 hours of stress-rupture exposure without failing; they were:

- CS217
- CS217C
- CS217G

However, the following braze alloys recorded one or more rupture failures prior to attaining 100 hours test time:

- CS217F - One specimen failed at 11 hours and 20 minutes
- RM8 - One specimen failed at 25 hours and 30 minutes
- RM12 - Both specimens failed at 25 hours and 30 minutes

All rupture failures occurred through the braze joint by a shear mechanism. No excessive external oxidation or corrosion effects were noted, indicating the failures of the above brazements were induced primarily by stress rupture. Typical braze structures (post-rupture testing) are shown in Figures 121, 122, and 123.

The significantly improved stress-rupture performance of the candidate alloy brazements in a salt-free environment was very striking.

3.5.7 Fatigue Tests of Brazements

To gain information on the relative abilities of candidate alloy brazements to withstand cyclic loading, a series of tension-tension fatigue tests were conducted on lap-shear specimens (0.020-inch overlap) at room temperature. The electronically

TABLE LI

FATIGUE STRENGTH OF CANDIDATE ALLOYS AND SELF-DIFFUSION BONDED Ti-5Al-2.5Sn SPECIMENS

Candidate Braze Alloy	Fatigue Strength for Joint Failure[1] (ksi)	Fatigue Strength (ksi) Maximum Stress at N, Number of Cycles (fatigue life) 10^4 Cycles	10^5 Cycles	10^6 Cycles	10^7 Cycles	Brazement Tensile Strength at Room Temperature (ksi)	Ratio of Tensile Strength to Fatigue Strength, 10^4 Cycles
Self-diffusion bonded Ti-5Al-2.5Sn specimens	>64.3 <78.9	37.5	21.0	~18.0	≤18.0	128.4	3.42
CS217	>[illegible]	39.0	26.[illegible]	22.0	~20.0	127.0	3.26
CS217C	>37.7 <49.8	37.0	25.0	19.0	~17.0	116.1	3.14
CS217F	~52.8	31.5	23.5	20.0	~20.0	121.3	3.86
RM8	~30.5	28.2	20.0	17.0	~15.0	84.3	2.98
RM12	>49.8 <61.0	27.5	18.5	~15.0	≤15.0	94.7	3.45

1. N ≤ 100

CS Series Alloys - Cyclic Annealed
1550 F, 10 minutes
1450 F, 10 minutes
Repeat one hour

RM Series Alloys - As-Brazed

controlled, hydraulically actuated, MTS fatigue tester used is illustrated in Figures 124 and a fixed alternating stress/mean stress ratio = 1/1 (i.e., minimum stress = zero). All lap-shear specimens were made of 0.010-inch thick Ti-5Al-2.5Sn alloy foils. Self-diffusion bonded specimens were tested to provide baseline data, particularly necessary in view of the unknown (but largely reproducible) geometric stress concentration factor in each lap-shear specimen. Maximum fatigue test stress is plotted against fatigue cycles to failure in Figure 126 (self-diffusion bonded condition); Figure 127 (CS217 and CS217C brazements); and Figure 128 (RM8 and RM12 brazements). A plot of fatigue strength (10^4 cycles) versus average brazement tensile shear strength (lap-shear specimens) is shown in Figure 129. All fatigue strength data generated in this study is shown in Table LI.

The fatigue strength levels obtained were gratifying in light of the geometric stress concentration factor inherent in the specimen and the presumed marginal toughness of the candidate braze alloys. As shown in the following tabulation, the endurance limits (10^6 cycles) for the better braze alloys compared favorably with that for the diffusion bonded joints (baseline).

Braze Alloy	Endurance Limit (10^6 cycles) (ksi)
CS217	22.0
CS217F	20.0
CS217C	19.0
RM8	17.0
Diffusion bonded	18.0

A plot of fatigue strength (10^4 cycles) versus average brazement tensile strength (Fig. 129) indicates that all specimen types follow the 30 percent ratio line, (i.e., $\frac{\text{Fatigue strength}}{\text{Tensile strength}} = 0.30$). This relation is considered a good one for effectively notched specimens. (A 50 percent ratio is usually normal for smooth fatigue and tensile specimens.) Such a consideration is valid inasmuch as all fatigue failures in the 10^4 to 10^7 cycle range have occurred in the foil materials near the lap step.

3.5.8 Summary of Task V, Braze Systems Evaluation

The preceding Task IV evaluation demonstrated the suitability of eight Ti-Zr base braze alloys for titanium foil joining in terms of brazing characteristics, peel resistance, joint strength, strain accommodation ability, and insensitivity to corrosive media, principally through mechanical tests at room temperature. Task V expanded the evaluation to include a range of test temperature simulating service (-320 to 1000 F) and different test regimes. (Two candidate braze alloys, RM26 and RM40, were eliminated early in the task because of markedly lower strength levels than the remaining six: RM8, RM12, CS217, CS217C, CS217F, and CS217G.)

Lap-joint shear tests (and in some cases, T-joint tensile tests) were conducted after the following preconditioning treatments, each simulating some adverse aspect of service exposure:

- As-brazed condition (baseline)
- Aging at 1000 F for 100 hours in vacuum or air environment
- 100 hours salt-spray exposure (200 F)

Specimens of Ti-5Al-2.5Sn, Ti-6Al-4V, and Ti-8Al-1Mo-1V foils were prepared and tested. Some self-diffusion bonded specimens were included to assess the influence of braze/foil interaction.

The influence of cyclic annealing post-braze was assessed in these test programs. In addition, cyclic annealed (as well as as-brazed) lap-joint specimens were subjected to three special tests:

- Stress rupture tests in oxidizing environment at 1000 F (30,000 psi foil stress).
- Stress rupture tests in oxidizing environment at 1000 F (10,000 psi and 20,000 psi foil stress levels); specimens encrusted with salt (NaCl).
- Tension-tension fatigue tests at room temperature to determine 10^5 to 10^6 cycle endurance limits.

Reliability Studies

Statistical variance in room temperature braze strength (lap-shear specimens) was calculated, using 10 data points per braze/foil combination (Table LII). Standard deviations of nearly all braze strength populations were found to be within reasonable limits for the as-brazed condition (i.e., standard deviation expressed as a percent of the average strength, < 10 percent). In practical terms, reproducibility of braze strength levels was considered satisfactory for an industrial joining process. Promising improvements in both lap-joint and T-joint braze strength reproducibility were obtained through cyclic annealing post-braze, although time permitted only one braze/foil variety to be evaluated (CS217C/Ti-5Al-2.5Sn). The best combinations of average braze joint strength and strength reproducibility were afforded by cyclic anneal "F". On the basis of these results, cyclic anneal "F" was incorporated as the preferred post braze treatment in all subsequent tests.

Variation of Brazement Strength with Temperature

Over the descending temperature range (800 F to room temperature), all brazed lap-joint strengths normally increased systematically with decreasing temperature. Braze strengths generally increased from ~60 to 70 ksi (Ti-5Al-2.5Sn) or ~ 80 to 90 ksi (Ti-6Al-4V) at 800 F to ~ 95 to 100 ksi (both foil alloys) at room temperature. This pattern of increasing strength with decreasing temperature parallels reasonably

TABLE LII

RELIABILITY TESTS ON CANDIDATE BRAZE ALLOYS/TITANIUM FOILS

	As Brazed			
Braze Alloy	Foil (10 mil thick)	Average Foil Stress at Failure (ksi)	Standard Deviation	Standard Deviation (%)
CS217	Ti-6Al-4V	95.5	6.9	7.2
	Ti-5Al-2.5Sn	108.6	5.0	4.6
	Ti-8Al-1Mo-1V	106.6	6.3	5.9
CS217C	Ti-6Al-4V	107.7	10.3	9.6
	Ti-5Al-2.5Sn	104.0	8.3	8.0
	Ti-8Al-1Mo-1V	108.3	13.6	12.5
CS217F	Ti-6Al-4V	97.8	6.3	6.5
	Ti-5Al-2.5Sn	99.5	3.7	3.7
	Ti-8Al-1Mo-1V	98.2	4.4	4.5
CS217G	Ti-6Al-4V	100.9	3.2	3.2
	Ti-5Al-2.5Sn	110.5	5.5	5.2
	Ti-8Al-1Mo-1V	93.9	18.6	19.8
RM8	Ti-6Al-4V	85.1	3.8	4.5
	Ti-5Al-2.5Sn	84.3	6.6	7.9
	Ti-8Al-1Mo-1V	94.7	4.2	4.4
RM12	Ti-6Al-4V	100.0	6.6	6.6
	Ti-5Al-2.5Sn	94.8	4.6	4.9
	Ti-8Al-1Mo-1V	100.3	7.0	7.0

well that pattern displayed by all program alloy foils in uniaxial tensile tests and self-diffusion bonded lap-joint tests. Below room temperature, all braze/foil combinations underwent a form of ductile-brittle transition (usually between room temperature and -100 F) wherein strength decreased slightly or became stabilized with decreasing temperature. Strength losses never exceeded 20 ksi, but uniaxial foil tensile specimens and diffusion bonded lap joint specimens showed marked strength increases in the same cryogenic temperature range (RT to -320 F).

Structural instability of the braze aterials and/or braze-affected foils was believed responsible for the mediocre showing of lap-joint braze strength at cryogenic temperatures[1]. Therefore, cyclic annealed brazements were evaluated. The single cyclic anneal employed (cyclic anneal "F") definitely improved the cryogenic strength patterns for half the braze/foil combinations, either eliminating the ductile-brittle transition behavior altogether or lowering the transition temperature. A study of these data, however, produced a strong inference that each braze/foil combination of interest has its own optimum cyclic anneal, which must be tailored to it experimentally at the present stage of understanding.

The most interesting development was that provided by the cyclic annealed CS217/Ti-8Al-1Mo-1V combination which yielded the highest average braze strengths recorded for lap-shear specimens over the entire temperature range of -320 to 900 F. There was no ductile-brittle transition behavior.

Thermal and Environmental Stability Tests

In general, candidate brazements withstood vacuum aging at 1000 F (100 hours) with little or no impairment of as-brazed strength properties. Principal exceptions were RM8 and RM12 brazements which experienced ~25 and 20 percent strength reductions, respectively, at room temperature, and ~ 20 percent reduction (RM8) at 800 F (Ti-6Al-4V foils). There were no adverse changes in braze microstructures due to aging. For Ti-5Al-2.5Sn foil joints, the usual effect of 1000 F air oxidation (100 hours) was a 10 to 30 percent strength reduction at room temperature and normally somewhat smaller reductions at cryogenic and elevated temperatures. Oxidation effects upon Ti-6Al-4V foil specimens were more random and unpredictable. All candidate brazements suffered 10 to 30 percent strength losses at a minimum of two of the three test temperatures (-320 F, RT, 800 F). A notable exception was the braze/foil combination, CS217/Ti-6Al-4V, which exhibited no significant changes in strength due to 1000 F air exposure. However, cyclic annealing "F" post-braze (CS series) in many cases not only reduced the degree of strength degradation due to subsequent 1000 F oxidation, but because cyclic annealing improved initial braze strengths, all CS217 and CS217C lap-joint brazements after 1000 F oxidation possessed

1. An interesting analog was drawn with tensile test data for self-diffusion bonded lap-joint specimens oxidized at 1000 F for 100 hours. Ductile/brittle transition behavior was evidenced also for these braze-free specimens in the room temperature to -100 F range.

as high or higher strength levels than for the as-brazed condition (-320 to 800 F). Electron micrographs revealed the marked changes in eutectic structure (lamellar to spheroidized beryllides) effected by cyclic annealing.

The CS217F braze alloy exhibited accelerated oxidation with voluminous oxidation products at 1000 F (both as-brazed and cyclic annealed conditions). Hence, CS217F was rated not suitable for 1000 F service in air. Metallographic examination of T-joint structures of the other candidate alloys showed only minimal surface oxidation films after 1000-hours exposure.

Salt-Spray Corrosion Tests

Most as-brazed Ti-5Al-2.5Sn specimens showed little effect of salt-spray exposure on braze strength (-320 to 800 F). However, the combination CS217/Ti-5Al-2.5Sn and all candidate braze alloys with Ti-6Al-4V foils (as-brazed condition) suffered serious losses in braze strength due to the 100-hour, salt-spray conditioning. Greatest losses were recorded at -320 F. No visual or metallographic evidence of general corrosion or crevice corrosion was found in the lap-joint specimens. Therefore, it was assumed that the 100-hour, 200 F thermal cycle associated with the salt-spray conditioning served to aggravate the structural instability of the as-brazed specimens, previously inferred from tensile test data at cryogenic temperatures.

The most important benefits of cyclic annealing CS series brazements were brought to light in this test series. It was demonstrated that cyclic annealing post-braze virtually abolished susceptibility of CS series brazements to strength deteriorations following salt-spray. The single cyclic anneal that was evaluated (cyclic anneal "F") completely altered this picture, so that in only two braze/foil/test temperature combinations of a possible 32 did the strength loss exceed 10 percent following salt-spray exposure. Maximum strength loss due to salt-spray was 25 percent; still an improvement over the as-brazed condition. In 27 instances, no significant change in braze strength following salt-spray exposure was recorded. In all instances, braze strengths of cyclic annealed specimens following 100-hour salt-spray exposure were measured at 80 ksi or higher (-320 F to room temperature). Again, there was no visual or metallographic evidence of corrosion.

Hot-Salt Rupture Tests

To determine relative susceptibility of candidate alloy brazements to hot-salt stress corrosion cracking, both brazed and self-diffusion bonded lap-joint specimens (Ti-5Al-2.5Sn) were encrusted with salt (NaCl) and dead-weight loaded in an oxidizing environment at 1000 F. Foil stress levels were chosen to yield minimum rupture times (in salt-free air) of 5000 hours (10,000 psi) and 700 hours (20,000 psi).

All brazed and diffusion bonded (braze-free) specimens suffered premature failures, due primarily to pronounced intergranular corrosion and cracking of the titanium alloy foils. Braze fillets of CS series alloys occasionally were involved in the foil failure mechanism but, in general, the braze materials themselves (especially RM8 and RM12) and all joint interface regions appeared particularly resistant to hot-salt corrosion phenomena.

Stress Rupture Tests

Brazed as well as self-diffusion bonded lap-joint specimens (Ti-5Al-2.5Sn) were stress rupture tested in an oxidizing environment at 1000 F. A constant foil stress of 30,000 psi was applied to produce a minimum expected rupture life of 100 hours. The following cyclic annealed braze alloys endured 100 hours of test time (duplicate tests) without failing:

- CS217
- CS217C
- CS217G

The following braze alloys yielded one or more premature rupture failures through the braze, indicating somewhat inferior rupture strength levels at 1000 F:

- CS217F (11.5 hours)
- RM8 (22.5 hours)
- RM12 (25.5 hours)

The diffusion bonded specimens did not fail.

Fatigue Tests

Room temperature fatigue strength levels obtained for most of the candidate braze alloys were quite gratifying in view of the geometric stress concentration inherent in the lap-joint specimen and the (presumed) marginal t[illegible]ess of the

braze alloys. Endurance limits (10^5 to 10^6 cycles) for the better braze alloys compared favorably with that for the diffusion bonded (braze-free) lap-joints as baseline:

Braze Alloy	Endurance Limit (10^6 cycles) (ksi)
CS217	22.0
CS217F	20.0
CS217C	19.0
RM8	17.0
Diffusion bonded	18.0

A plot of fatigue strength (10^4 cycles) versus average brazement tensile strength illustrated that all brazed and diffusion bonded specimens follow the 30 percent ratio line, i.e., $\frac{\text{Fatigue Strength}}{\text{Brazement Tensile Strength}} = 0.30$. This relation was considered satisfactory for effectively notched specimens. A 50 to 60 percent ratio might be considered normal for smooth fatigue and tensile specimens.

3.5.9 Selection of Braze Alloys for Phase II

Rigorous tests of over 100 candidate braze alloys were conducted to determine suitability for titanium alloy foil brazing in Phase II. On the basis of foil brazing characteristics, corrosion and oxidation resistance, and brazement mechanical properties (tensile, rupture, and fatigue strengths; bend toughness; peel resistance; and strain accommodation ability), the four braze alloys listed below were selected as uniformly good and reliable:

Designation	Composition (wt %)	Density (gm/cc)
CS217	Ti-47.5Zr-5.0Be	4.83
CS217C	Ti-45.1Zr-4.8Be-5.0Al	4.67
RM8	Ti-43.0Zr-12.0Ni-2.0Be	5.46
RM12	Ti-45.0Zr-8.0Ni-2.0Be	5.33

These four alloys are Ti-Zr or Ti-Zr-Ni base and offer significant advantages in the areas of salt-corrosion resistance and strength over the silver-base braze alloys commonly used for brazing titanium. Post-braze thermal treatment was recommended for the two CS series alloys.

Ultimate selection of a single braze alloy for each foil structure type was made following subscale module braze tests (Phase II).

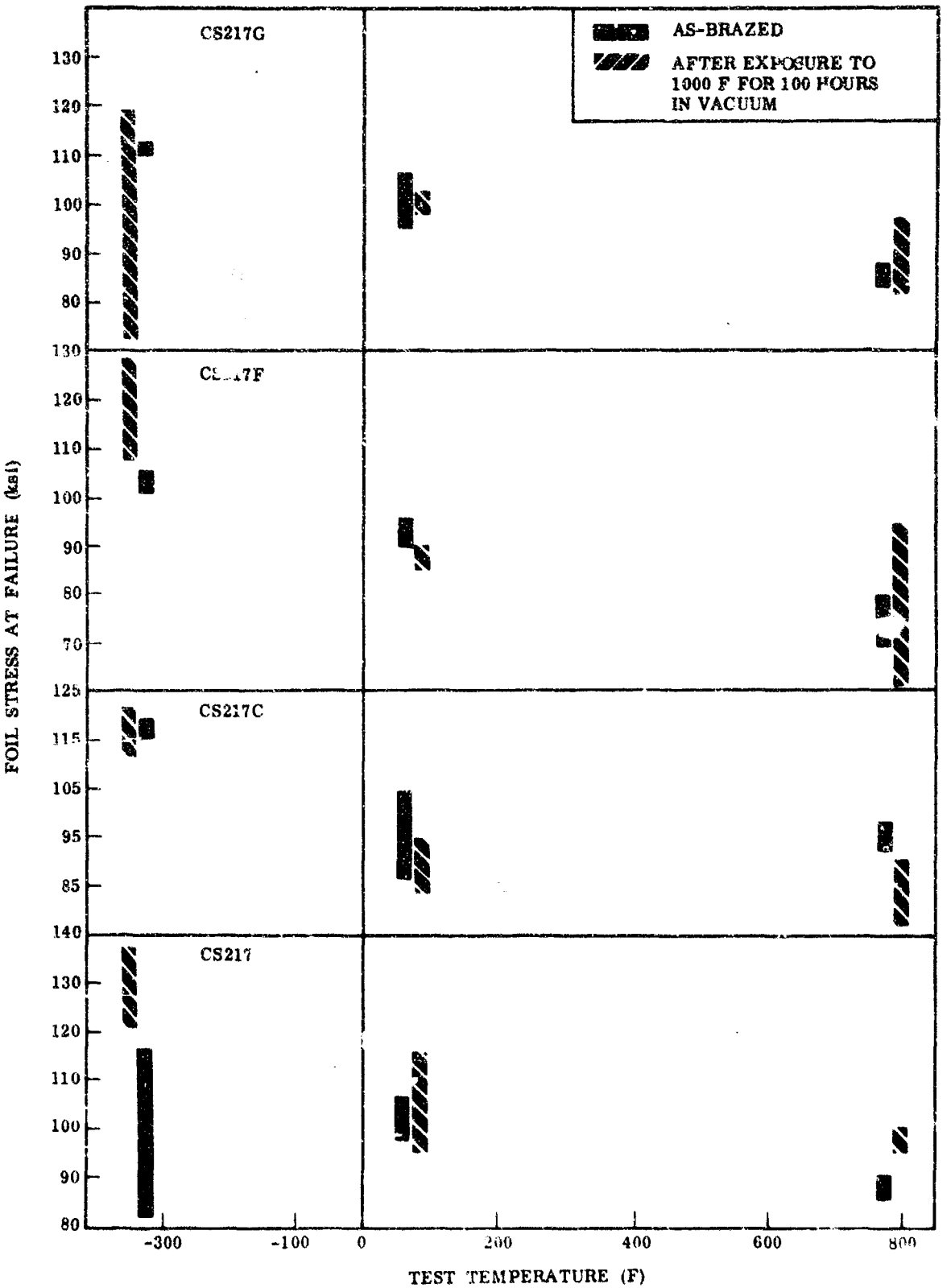


FIGURE 77. THERMAL STABILITY TESTS ON CS SERIES BRAZE ALLOYS; Lap-Shear Tests

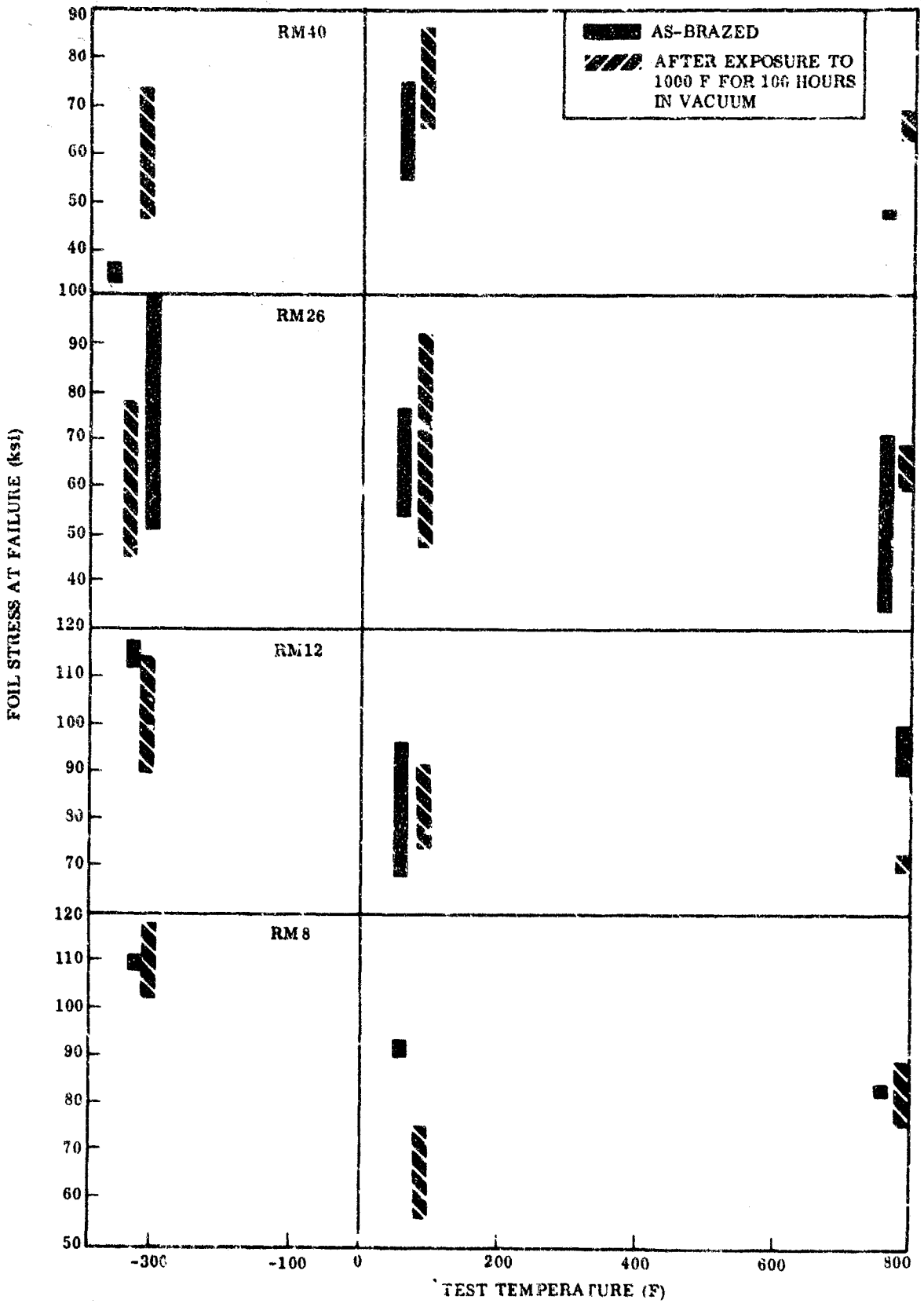
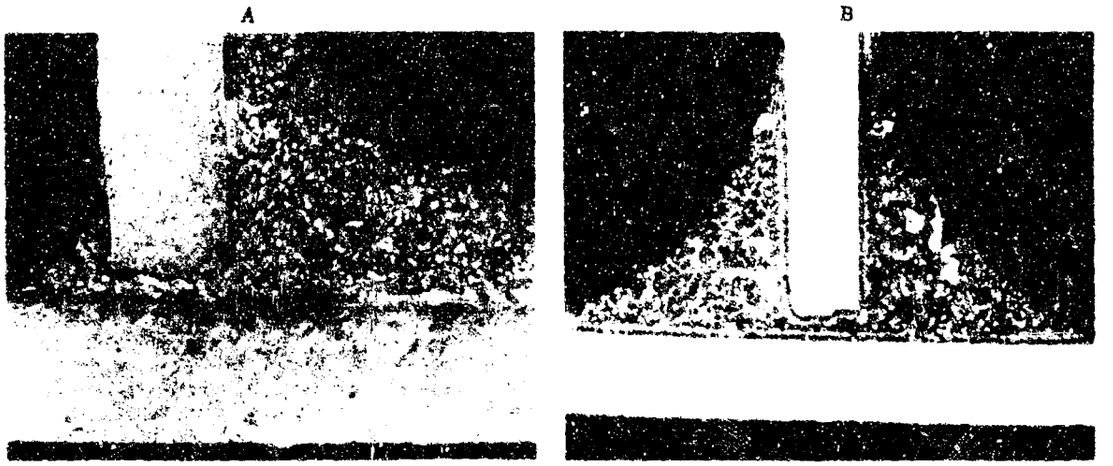


FIGURE 78. THERMAL STABILITY TESTS ON RM SERIES BRAZE ALLOYS; Lap-Shear Tests

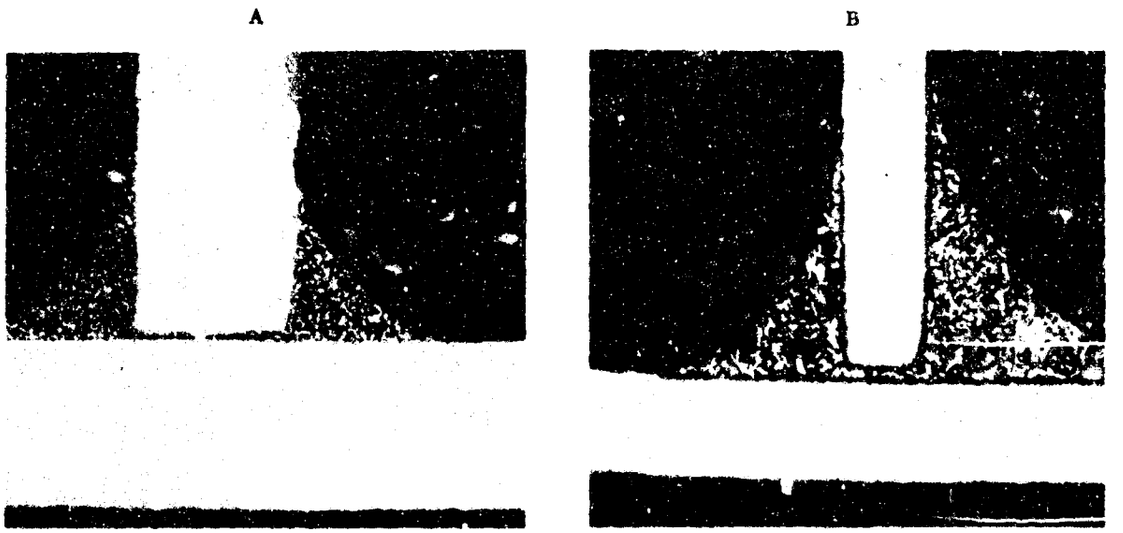


As-brazed for 5 minutes

Brazed and aged 1000 F for 100 hours in vacuum

Magnification: 100X

FIGURE 79. T-JOINTS BRAZED WITH CS217 ALLOY

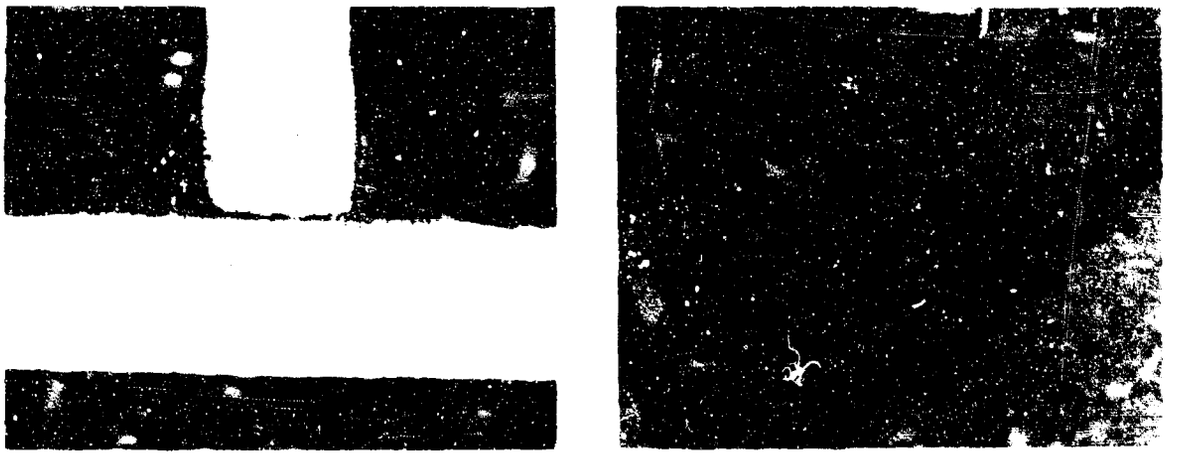


As-brazed for 5 minutes

Brazed and aged 1000 F for 100 hours in vacuum

Magnification: 100X

FIGURE 80. T-JOINTS BRAZED WITH CS217F ALLOY



As-brazed for 5 minutes Magnification: 100X As-brazed for 5 minutes Magnification: 1000X

FIGURE 81. T-JOINTS BRAZED WITH CS217C ALLOY

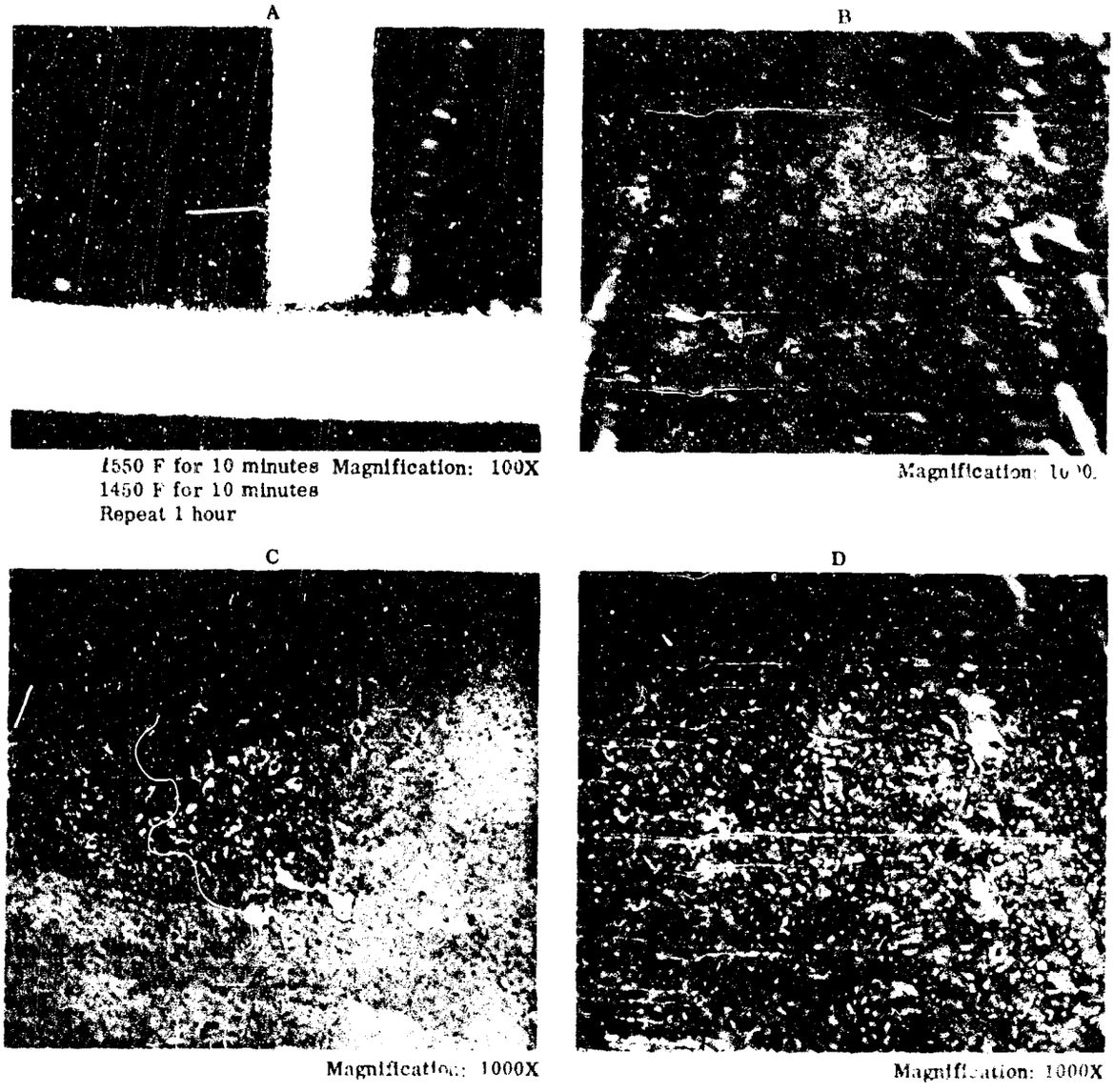


FIGURE 82. T-JOINTS BRAZED WITH CS217C ALLOY, CYCLIC ANNEALED CONDITION

Magnification 10,000X



FIGURE 83. SPHEROIDIZED EUTECTIC BERYLIDES IN CYCLIC ANNEALED CS-17C ALLOY BRAZEMENT

Magnification 10,000X



FIGURE 51. FINE LAMELLAR STRUCTURE OF [illegible] ELECTRO-
CSEB-6 ALLOY BRAZEMENT (Sheet 1 of 2)



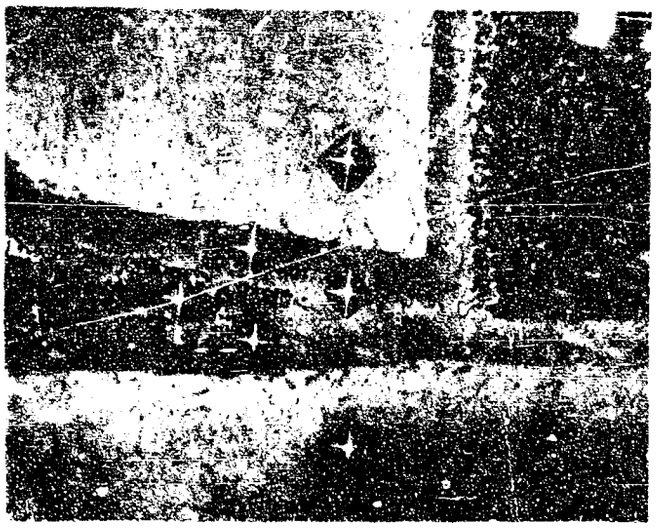


FIGURE 85. SPHEROIDIZED EUTECTIC BERYLLIDES IN CYCLIC ANNEALED CS13-5 ALLOY BRAZEMENT

Base alloy CS217C cyclic annealed

1550 F for 10 minutes
1450 F for 10 minutes
Repeat 1 hour

Braze joint of Ti-5Al-2.5Sn foil (6 mils thick)



R_C hardness
(50 gms load DPH)

		37.7
	40.0	
42.5		42.5
	42.5	
		36.1

R_C hardness of braze matrix

46.1, 45.0, 50.0,
4[illegible]9

Thickness of diffusion zone: 0.5 mil

FIGURE 86. HARDNESS SURVEY OF CYCLIC ANNEALED CS217C/Ti-5Al-2.5Sn BRAZEMENT

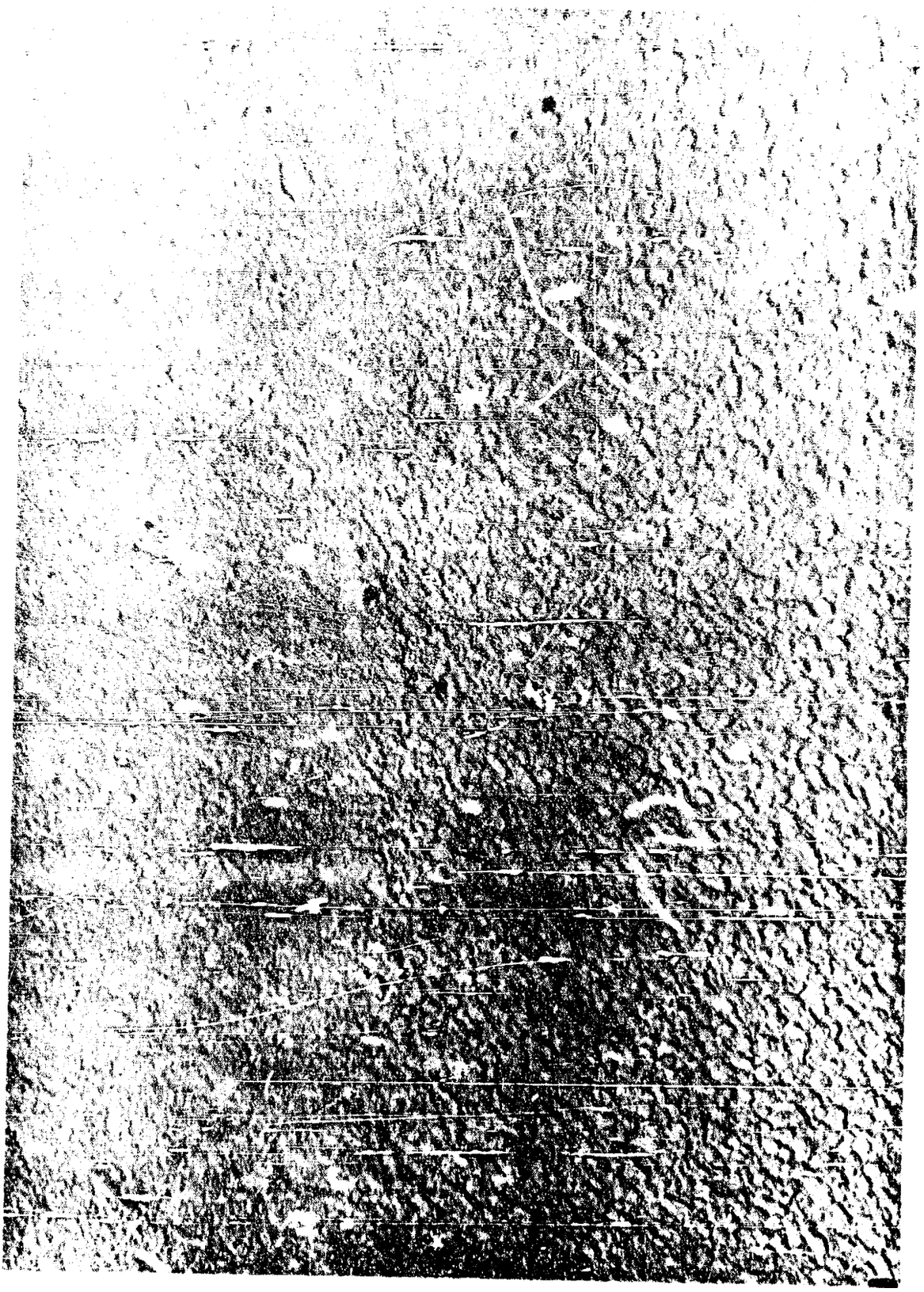


FIGURE 87. BASE METAL/DIFFUSION ZONE INTERFACE OF CYCLIC ANNEALED CS-17C, Ti-5Al-2.5Sn BRAZEMENT



FIGURE 88 DIFFUSION ZONE/BRAZE MATRIX INTERFACE OF CYCLIC ANNEALED CS217C/Ti-5Al-2.5Sn BRAZEMENT

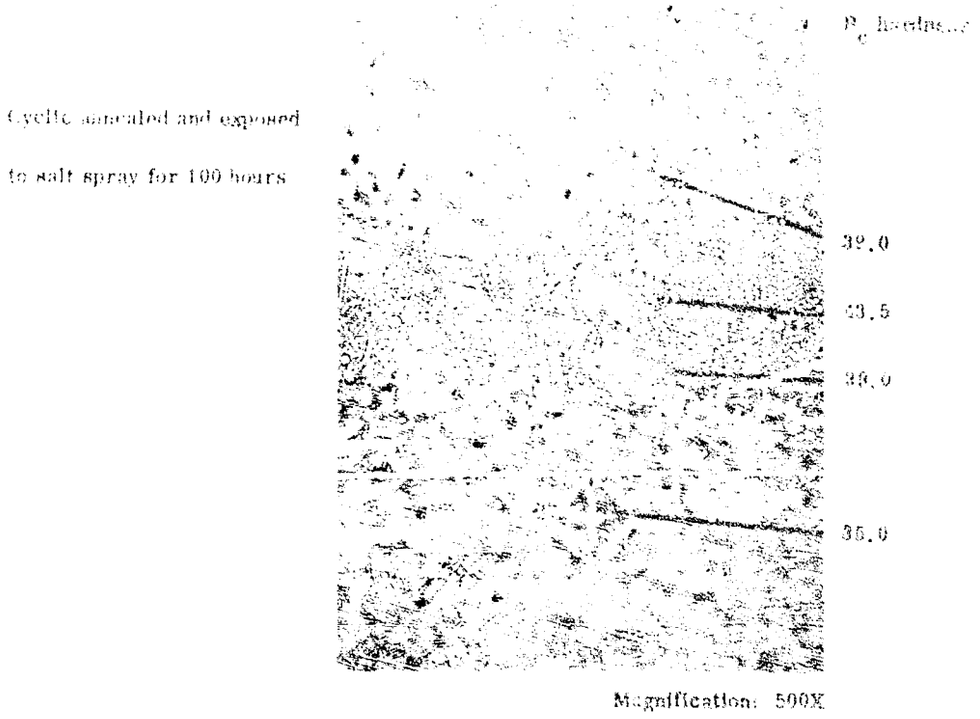


FIGURE 89. HARDNESS SURVEY OF CYCLIC ANNEALED CS217C/Ti-6Al-4V BRAZEMENT

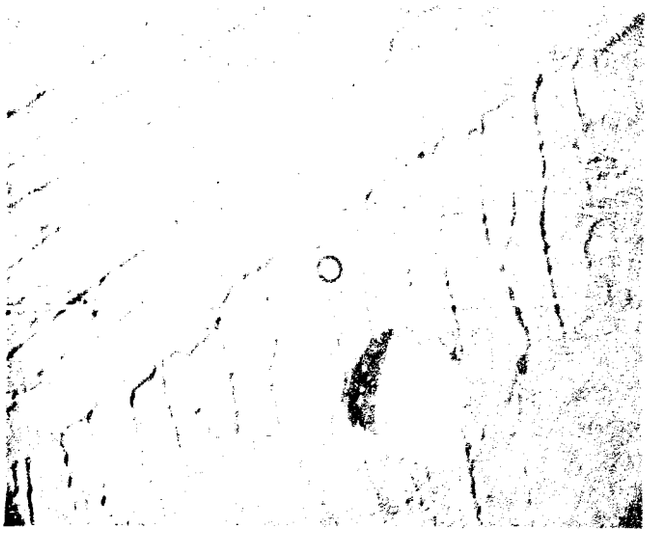


FIGURE 90. MARTENSITIC (Widmanstatten) STRUCTURE IN CYCLIC ANNEALED CS217C/Ti-6Al-4V BRAZEMENT

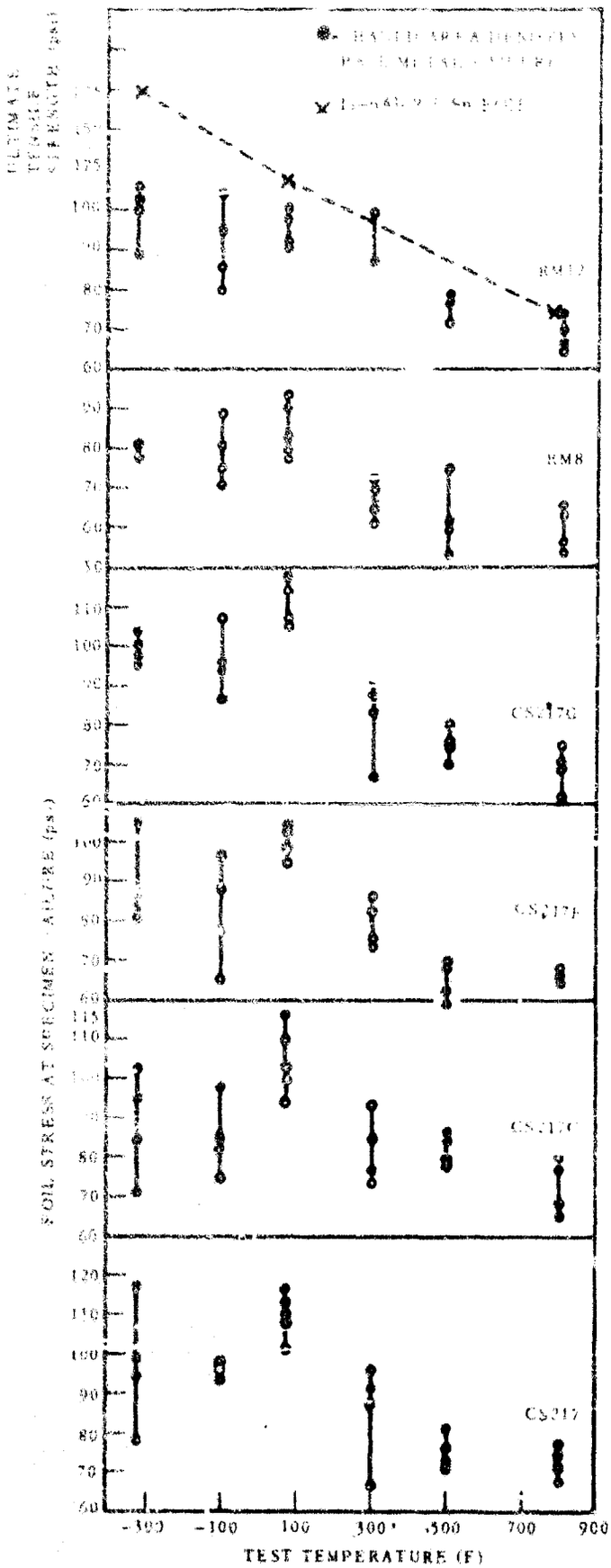


FIGURE 91. LAP-SHEAR TESTS ON BRAZE ALLOYS/Ti-5Al-2.5Sn, AS-BRAZED

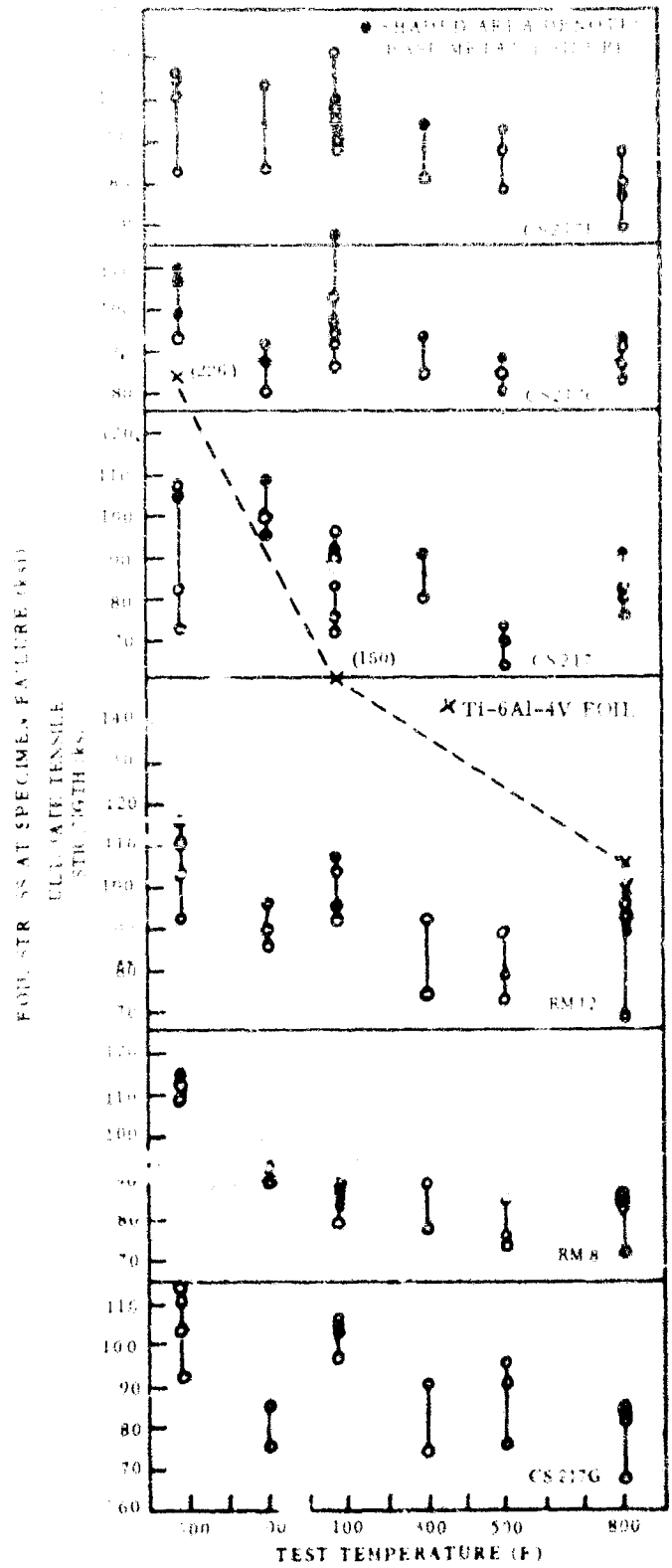


FIGURE 92. LAP-SHEAR TESTS ON BRAZE ALLOYS/Ti-6Al-4V, AS-BRAZED

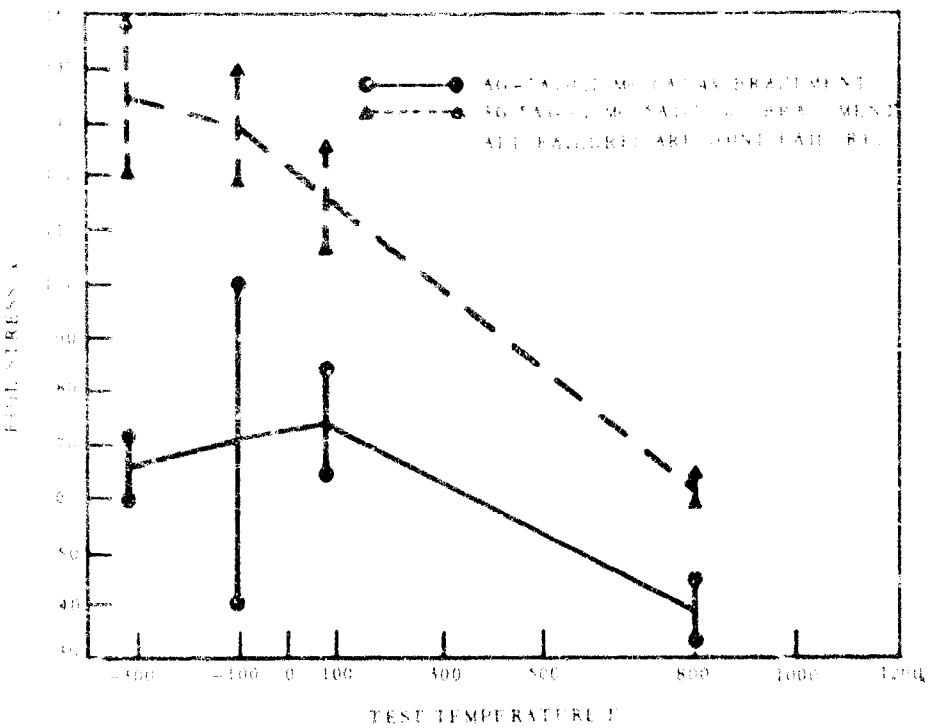


FIGURE , LAP-SHEAR TESTS ON Ag-5Al-0.2Mn BRAZE ALLOY, BASELINE

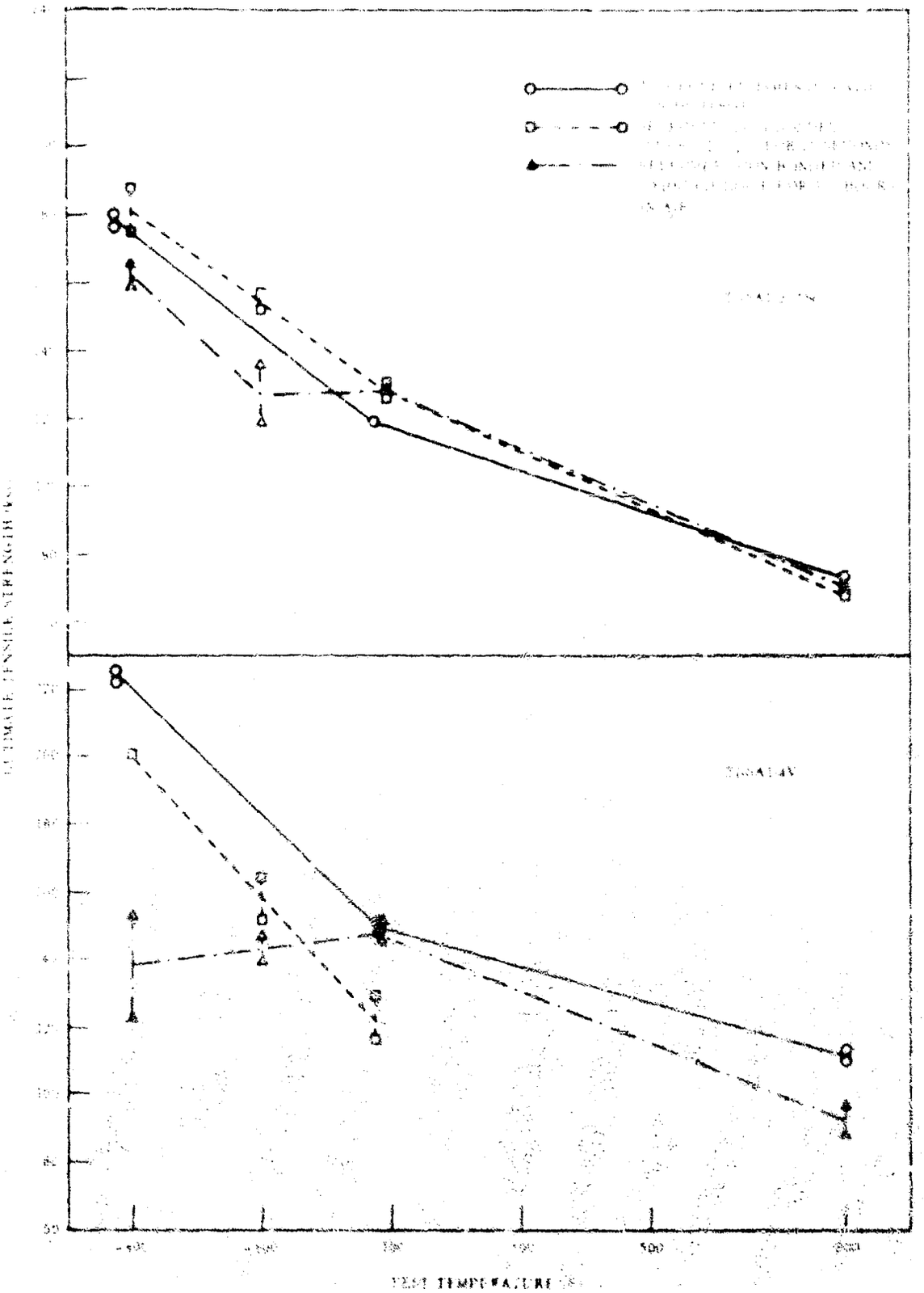


FIGURE 94. ULTIMATE TENSILE STRENGTH VERSUS TEMPERATURE OF Ti-5Al-2.5Sn AND Ti-6Al-4V FOILS

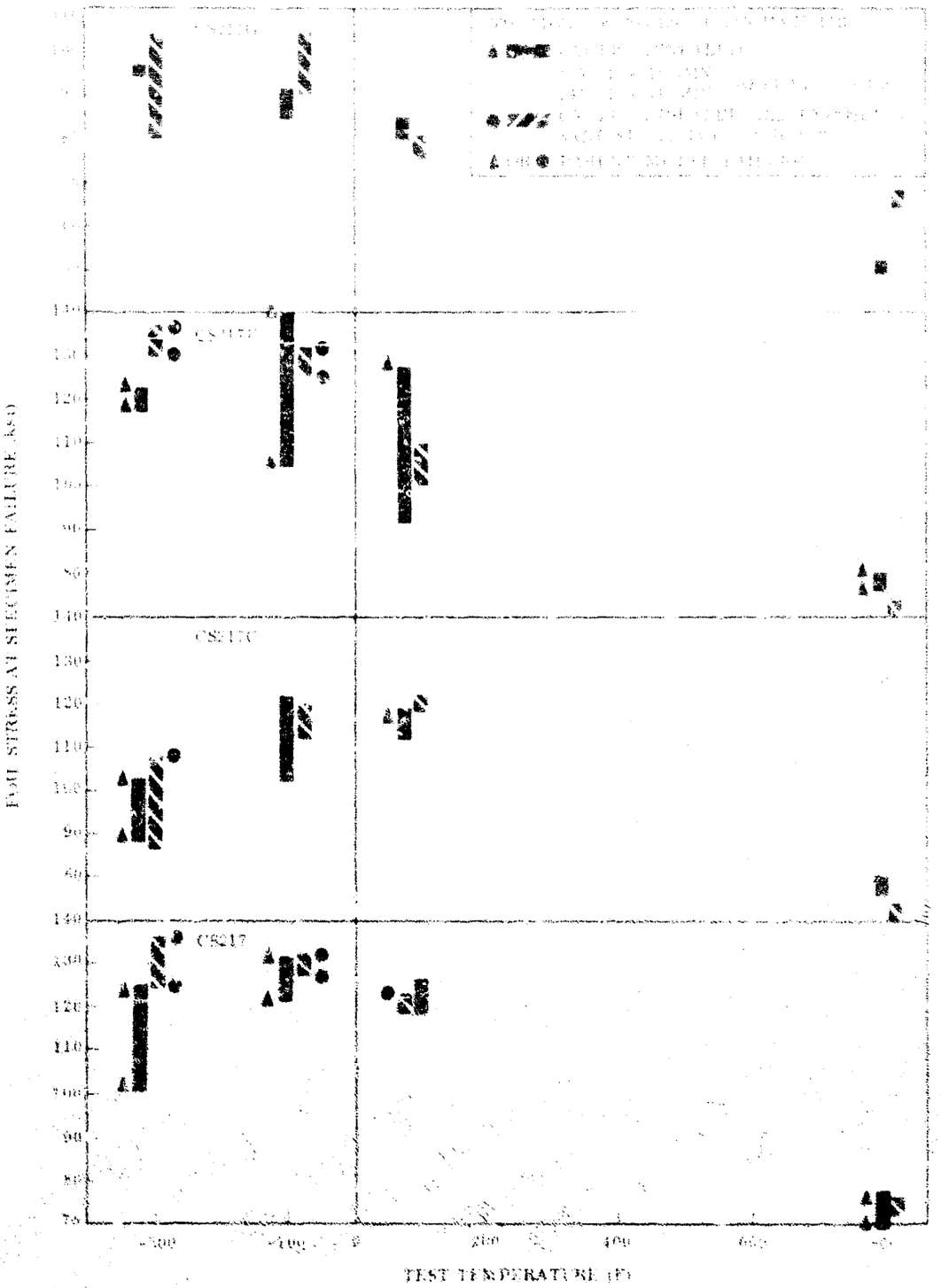


FIGURE 85. SALT SPRAY CORROSION TESTS ON CYCLIC ANNEALED CS SERIES ALLOYS/TI-6AL-4V FOIL BRAZEMENTS

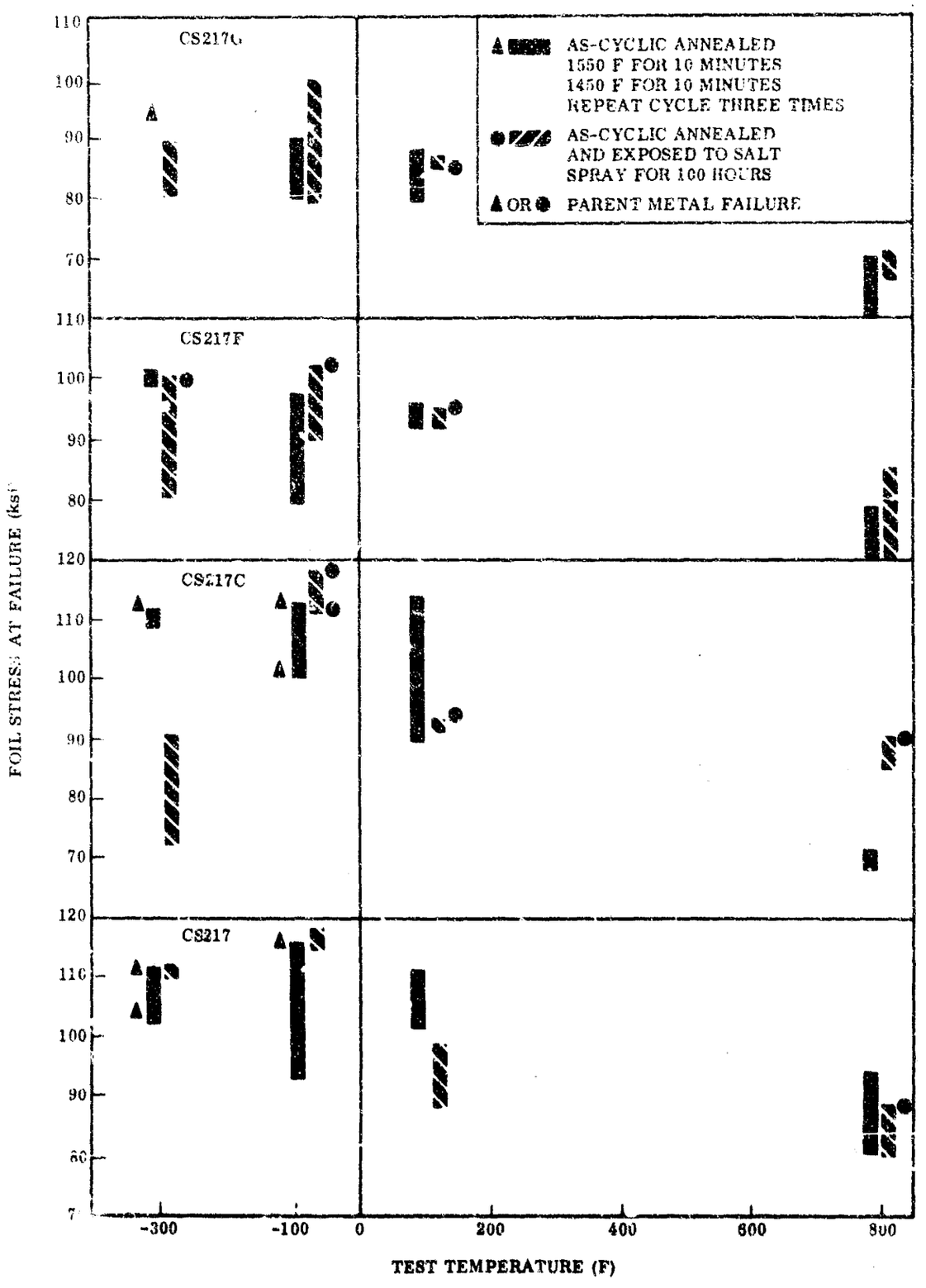


FIGURE 96. SALT SPRAY CORROSION TESTS ON CYCLIC ANNEALED CS SERIES ALLOYS/Ti-5Al-2.5Sn FOIL BRAZEMENTS

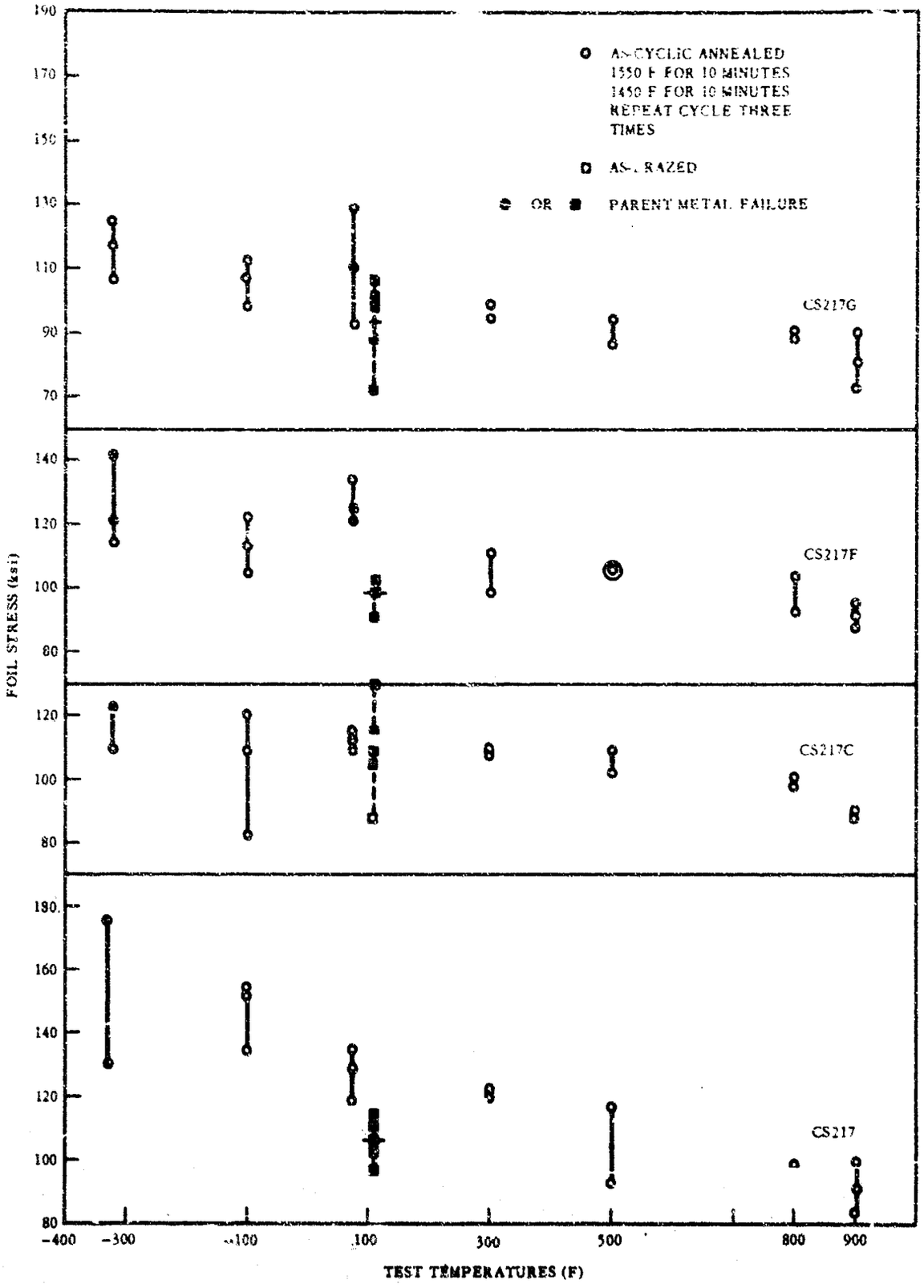


FIGURE 97. STRENGTH OF CYCLIC ANNEALED CS SERIES ALLOYS/Ti-8Al-1Mo-1V BRAZEMENTS

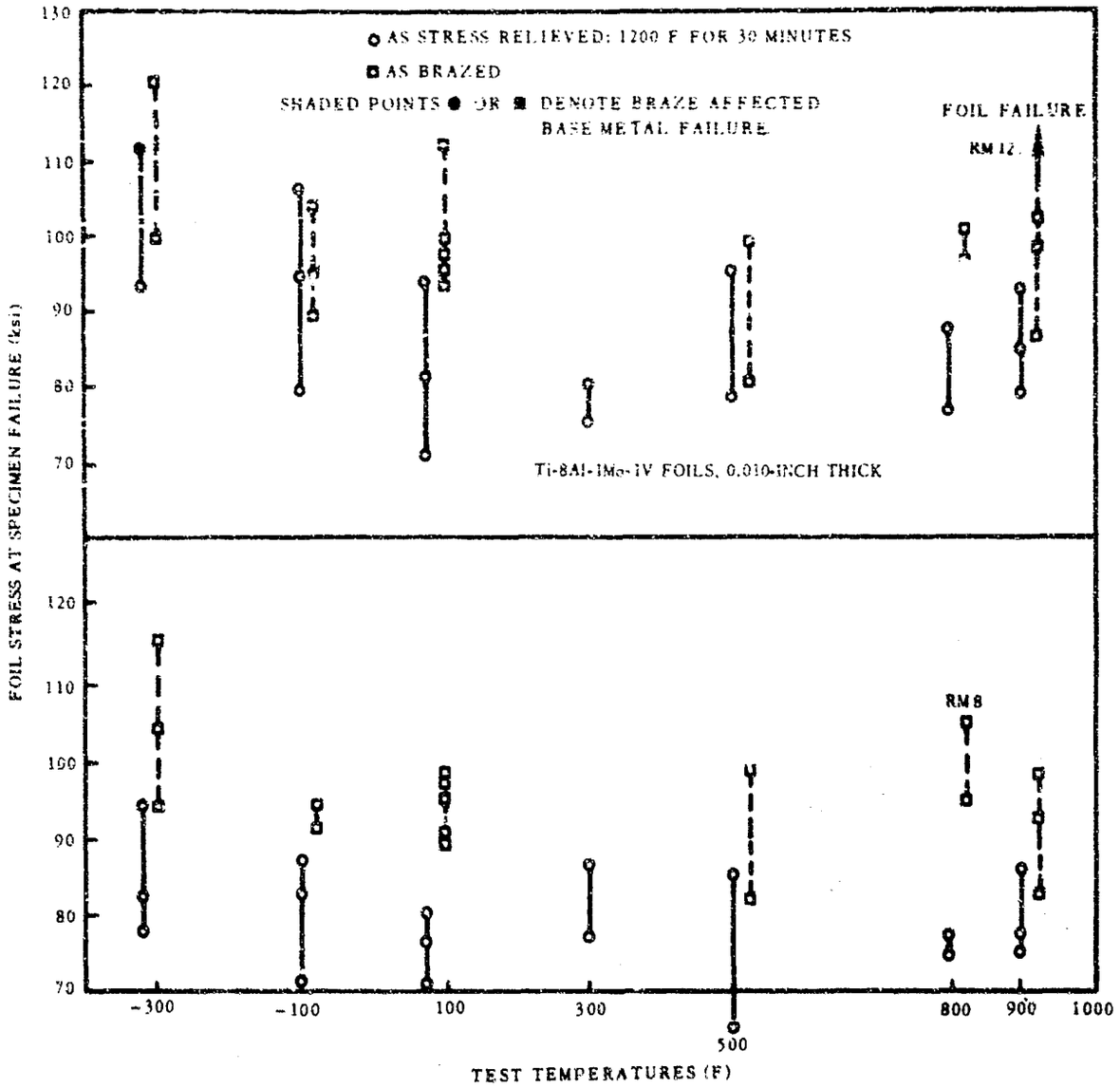
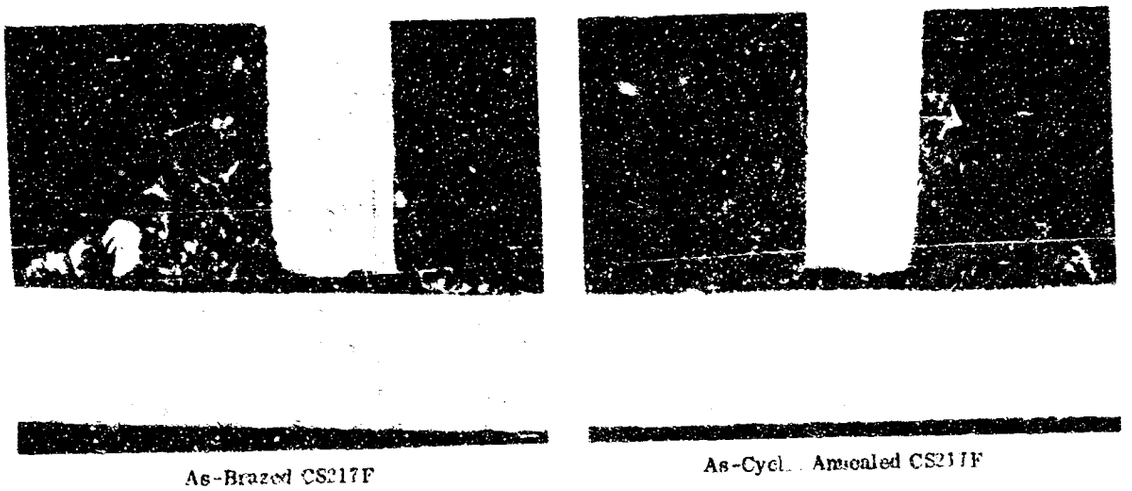


FIGURE 98. STRENGTH OF RM SERIES/Ti-8Al-1Mo-1V BRAZEMENTS



As-Brazed CS217F

As-Cycl.. Annealed CS217F

Magnification: 100X

FIGURE 99. CYCLIC ANNEALED CS217F/Ti-8Al-1Mo-1V BRAZEMENT

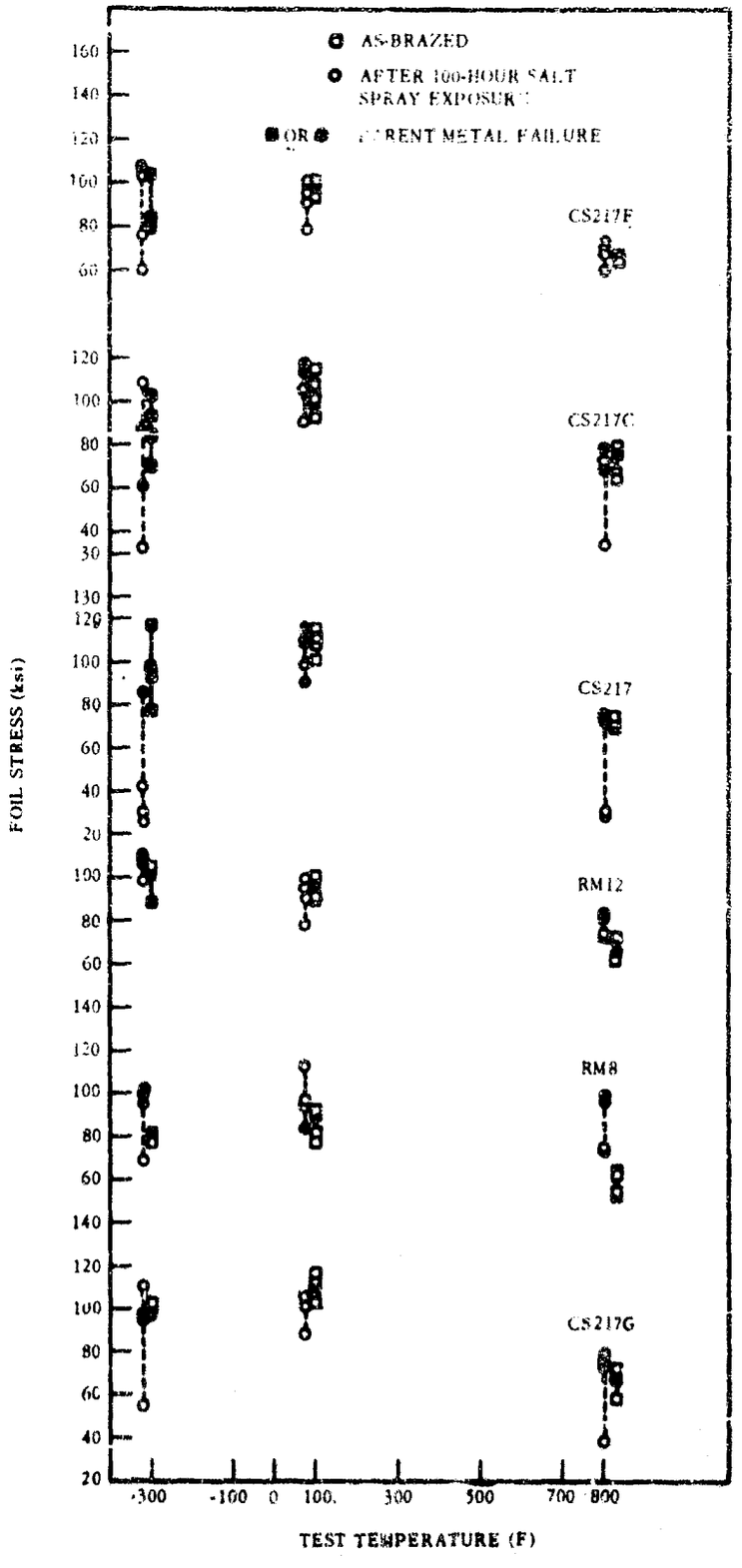


FIGURE 100. SALT SPRAY CORROSION TEST RESULTS, CANDIDATE ALLOYS/ Ti-5Al-2.5Sn BRAZEMENTS

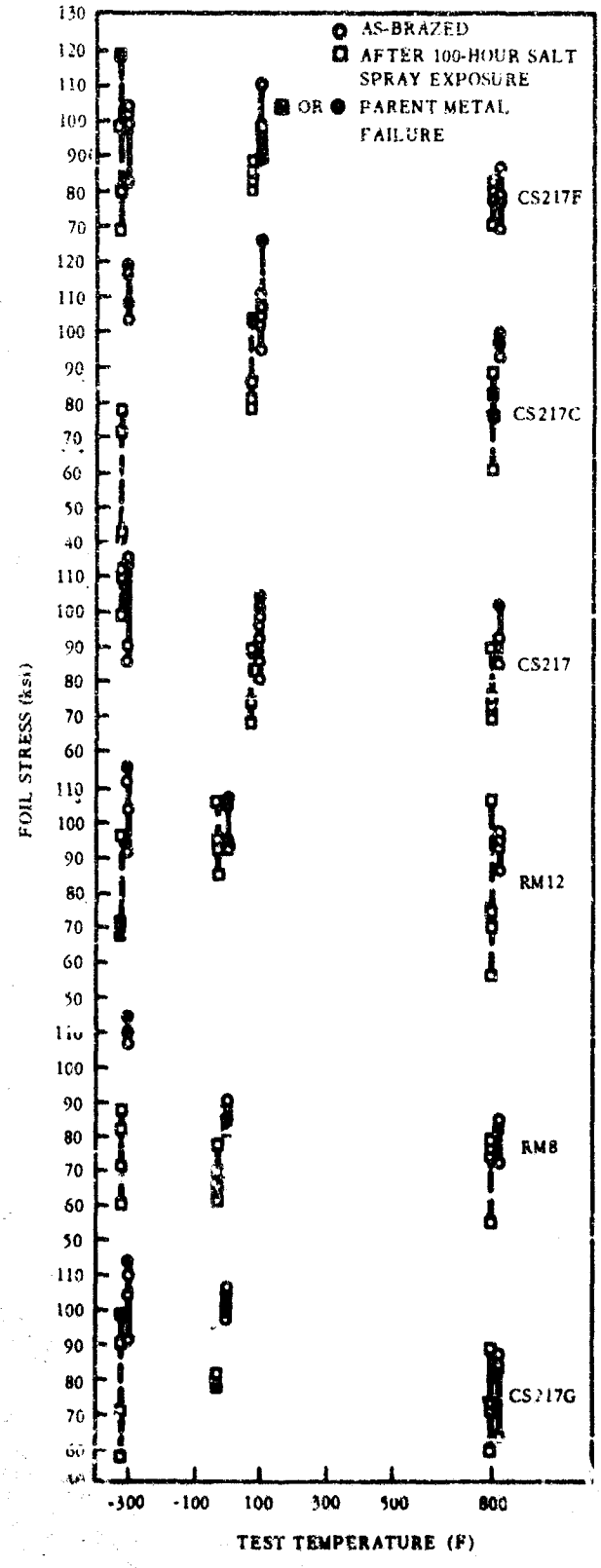


FIGURE 101. SALT SPRAY CORROSION TEST RESULTS, CANDIDATE ALLOYS/ Ti-6Al-4V BRAZEMENTS

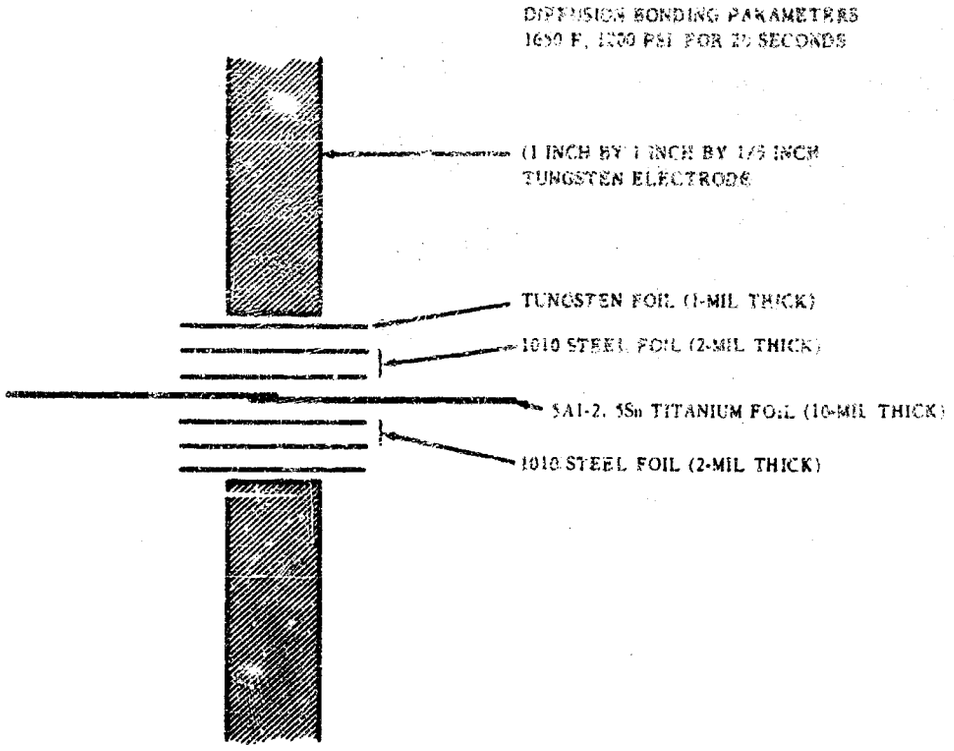


FIGURE 102. DIFFUSION BONDING OF TITANIUM ALLOY FOILS

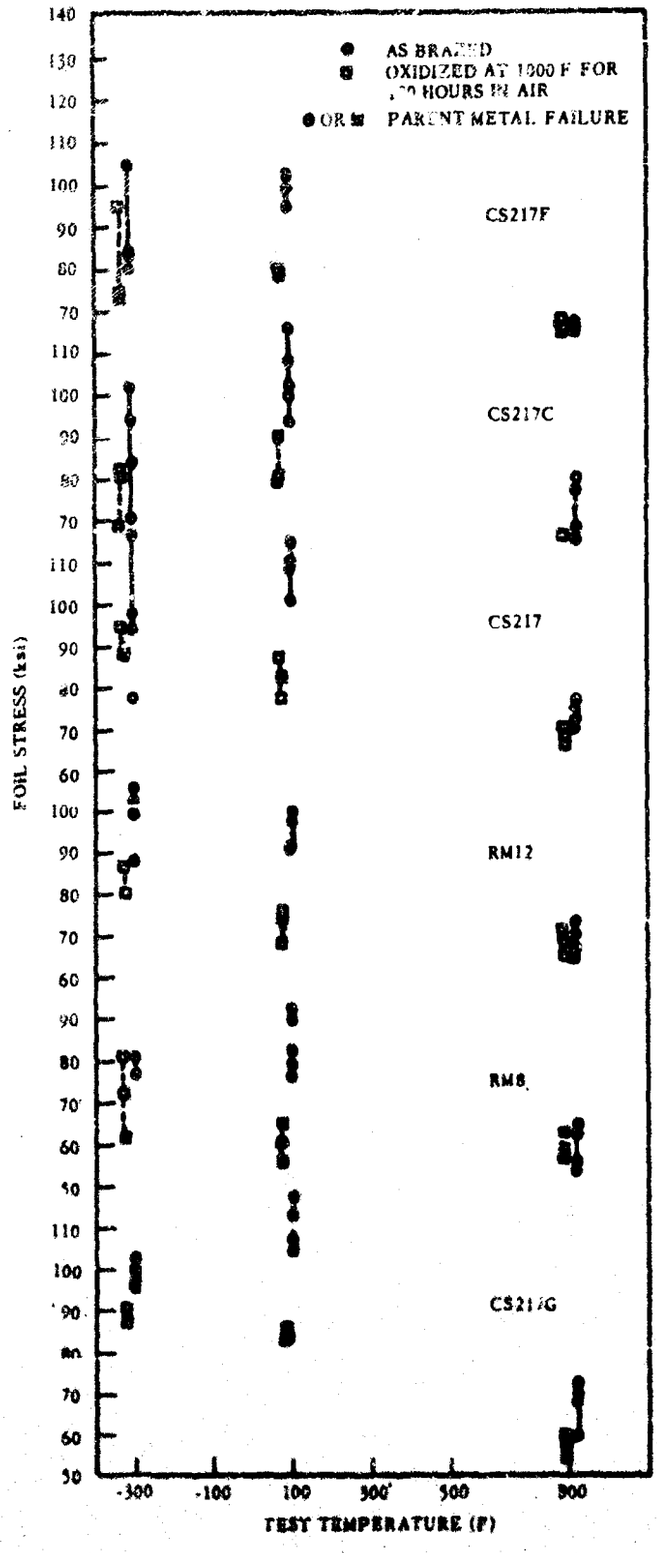


FIGURE 105. THERMAL STABILITY TEST RESULTS, CANDIDATE ALLOYS/ Ti-6Al-2.5Sn BRAZEMENTS

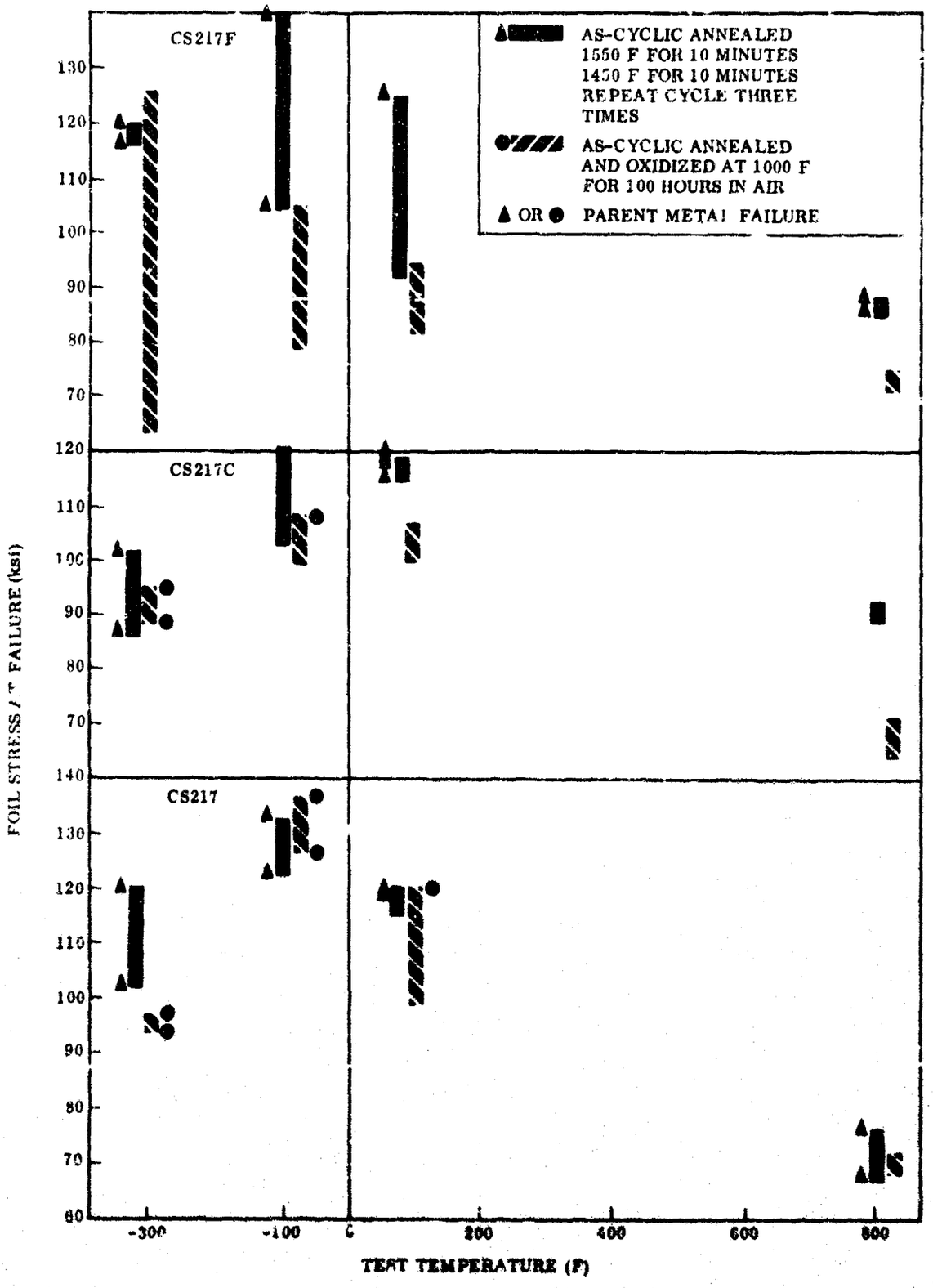


FIGURE 104. THERMAL STABILITY TEST RESULTS, CYCLIC ANNEALED CANDIDATE ALLOYS/Ti-5Al-2.5Sn BRAZEMENTS

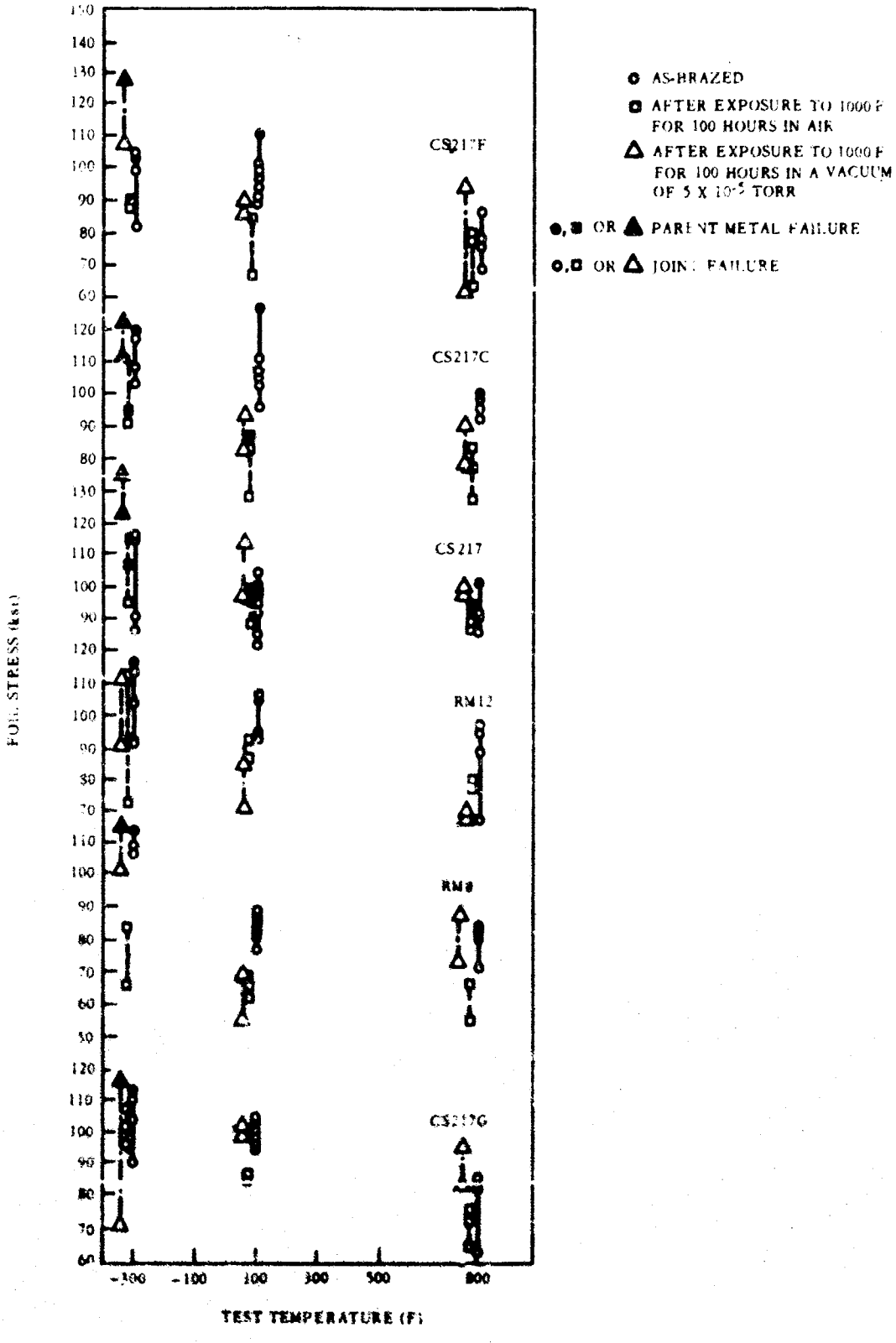
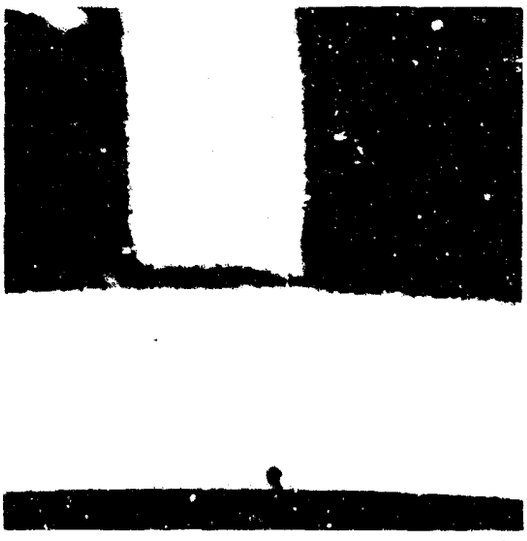


FIGURE 105. THERMAL STABILITY TEST RESULTS, CANDIDATE ALLOYS/ Ti-6Al-4V BRAZEMENTS



Magnification 100X

CS217-Ti-5Al-2.5Sn



Magnification 100X

CS-217-Ti-6Al-4V



Magnification 500X

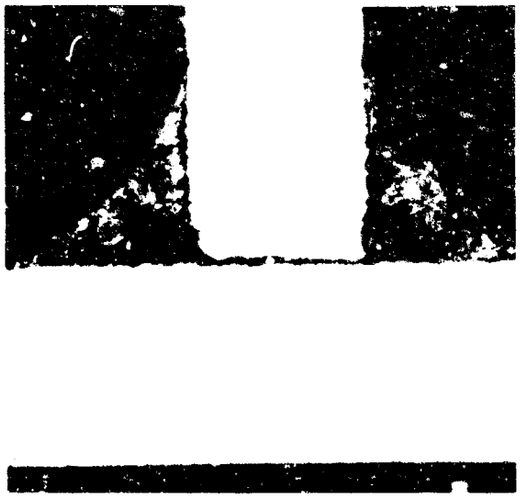
CS217-Ti-5Al-2.5Sn

FIGURE 106. BRAZEMENTS OF CS217 OXIDIZED AT 1000 F FOR 100 HOURS IN AIR



Magnification 100X

CS217C Ti-6Al-2.5Sn



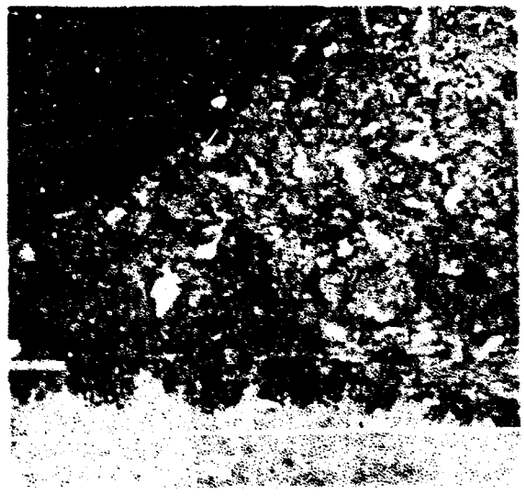
Magnification 100X

CS217C Ti-6Al-4V



Magnification 500X

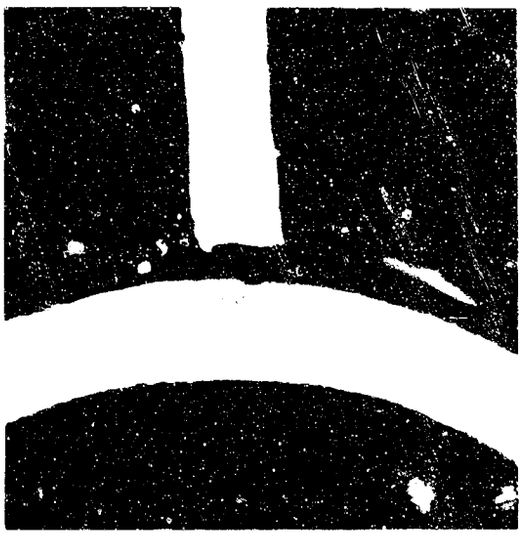
CS217C Ti-6Al-2.5Sn



Magnification 500X

CS217C Ti-6Al-4V

FIGURE 107. BRAZEMENTS OF CS217C OXIDIZED AT 1000 F FOR 100 HOURS IN AIR



Magnification 100X

CS-217F/Ti-5Al-2.5Sn



Magnification 250X

CS-217F/Ti-5Al-2.5Sn



Magnification 500X

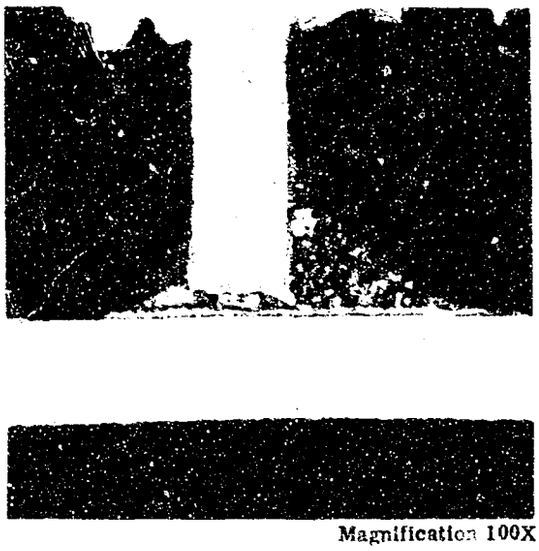
CS-217F/Ti-5Al-2.5Sn



Magnification 500X

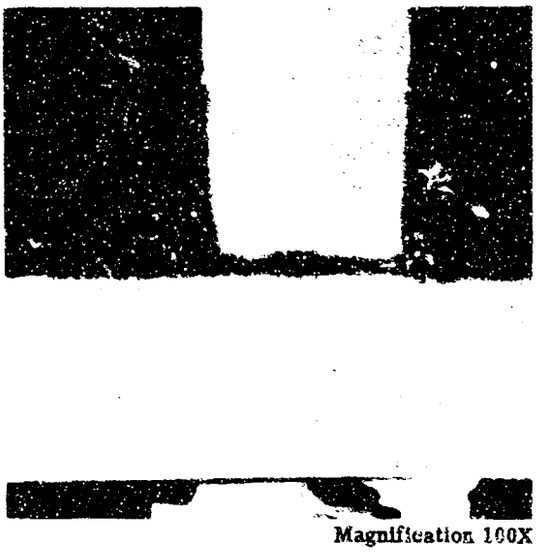
CS-217F/Ti-6Al-4V

FIGURE 108. BRAZEMENTS OF CS217F OXIDIZED AT 1000 F FOR 100 HOURS IN AIR



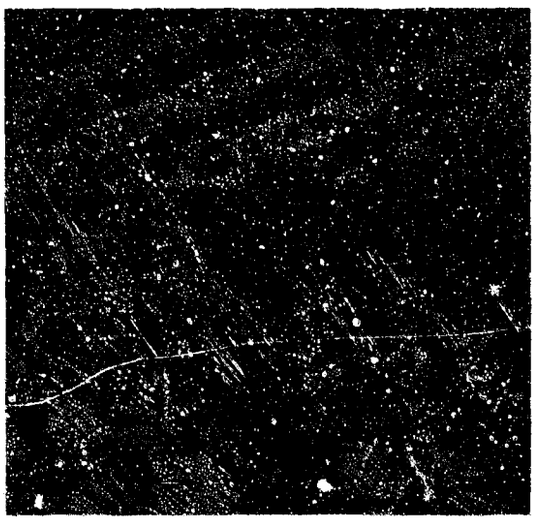
Magnification 100X

CS-217G/Ti-5Al-2.5Sn



Magnification 100X

CS-217G/Ti-6Al-4V



Magnification 500X

CS-217G/Ti-5Al-2.5Sn



Magnification 500X

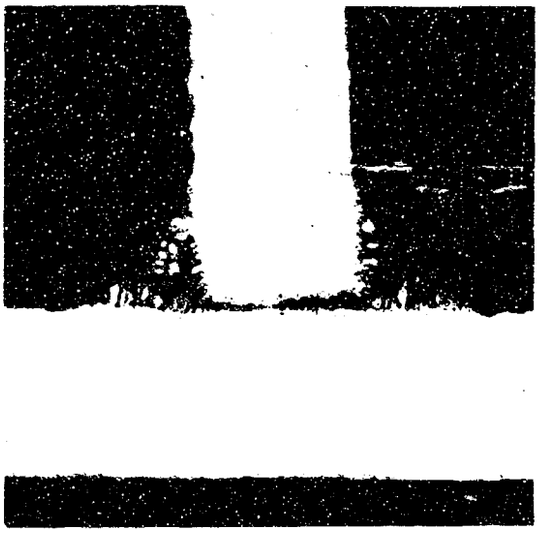
CS-217G/Ti-6Al-4V

FIGURE 109. BRAZEMENTS OF CS217G OXIDIZED AT 1000 F FOR 100 HOURS IN AIR



Magnification 100X

RM-8/Ti-5Al-2.5Sn



Magnification 100X

RM-8/Ti-6Al-4V



Magnification 500X

RM-8/Ti-5Al-2.5Sn

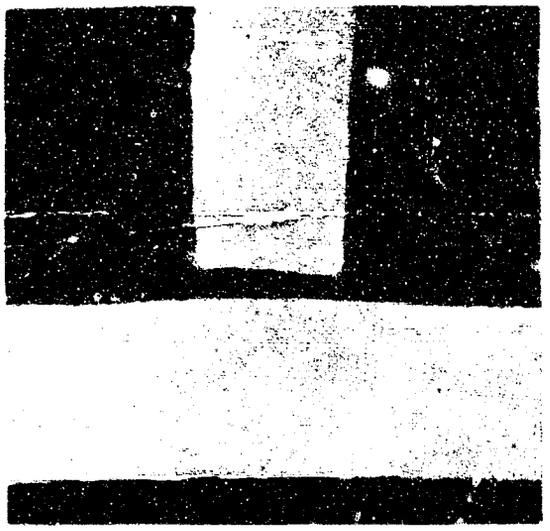


(M6987)

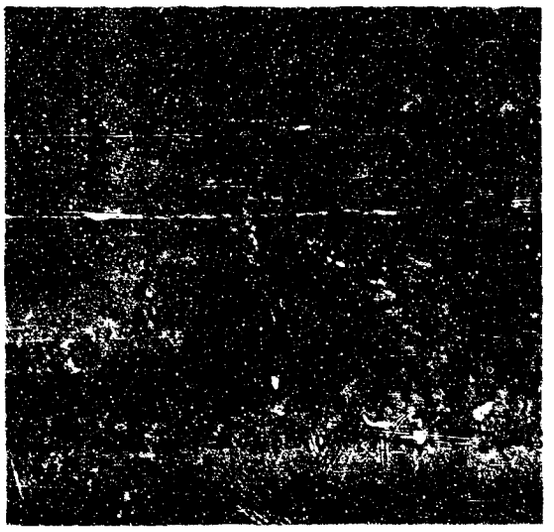
Magnification 500X

RM-8/Ti-6Al-4V

FIGURE 110. BRAZEMENTS OF RM8 OXIDIZED AT 1000 F FOR 100 HOURS IN AIR

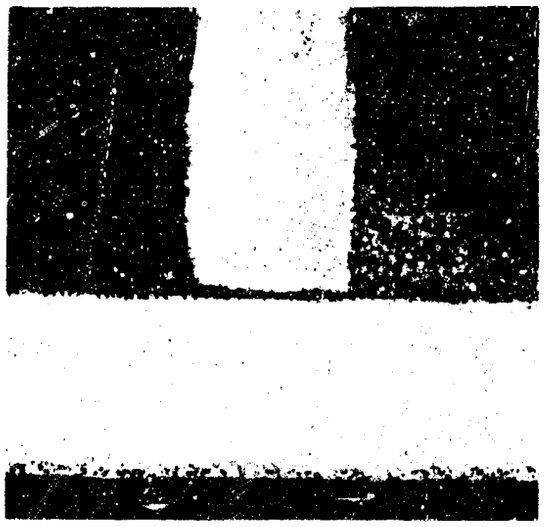


CS217/Ti-5Al-2.5Sn Magnification 100X



CS217/Ti-5Al-2.5Sn Magnification 500X

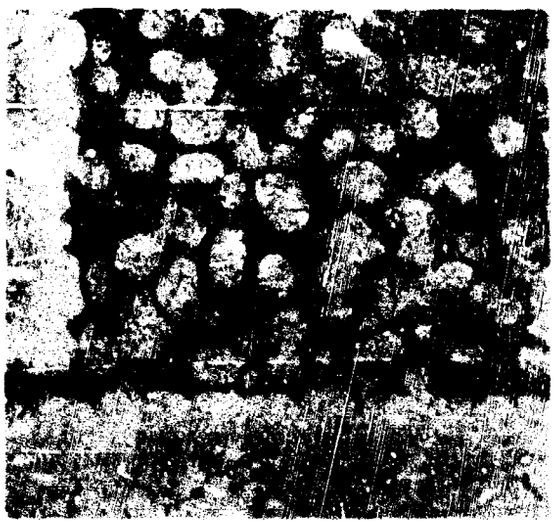
FIGURE 111. CYCLIC ANNEALED BRAZEMENTS OF CS217 OXIDIZED AT 1000 F FOR 100 HOURS IN AIR



CS217C/Ti-5Al-2.5Sn Magnification 100X

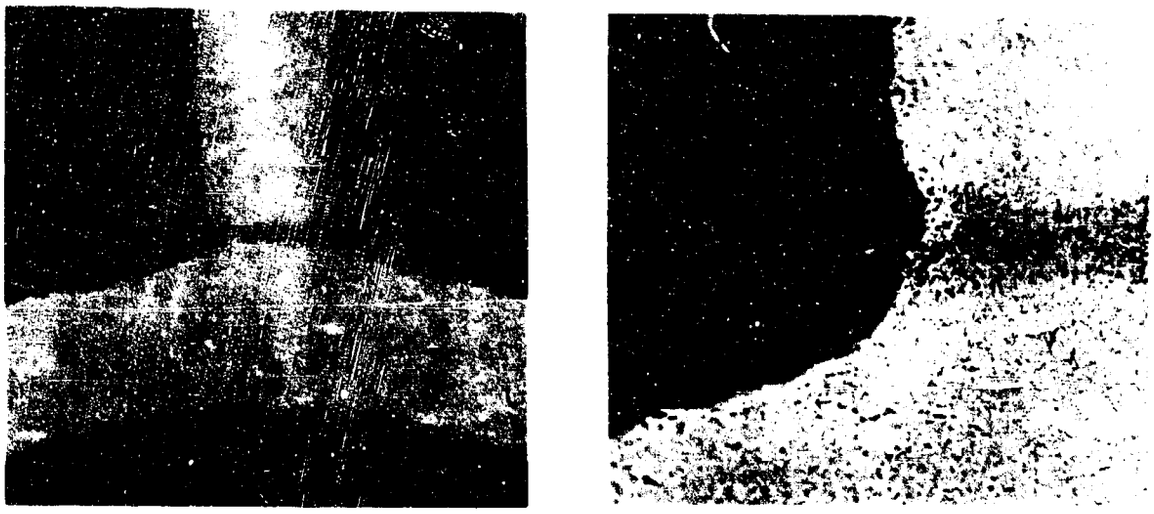


CS217C/Ti-5Al-2.5Sn Magnification 500X



CS217C/Ti-5Al-2.5Sn Magnification 500X

FIGURE 112. CYCLIC ANNEALED BRAZEMENTS OF CS217C OXIDIZED AT 1000 F FOR 100 HOURS IN AIR



CS217F/Ti-5Al-2.5Sn **Magnification 100X** CS217F/Ti-5Al-2.5Sn **Magnification 500X**

FIGURE 113. CYCLIC ANNEALED BRAZEMENTS OF CS217F OXIDIZED AT 1000 F FOR 100 HOURS IN AIR

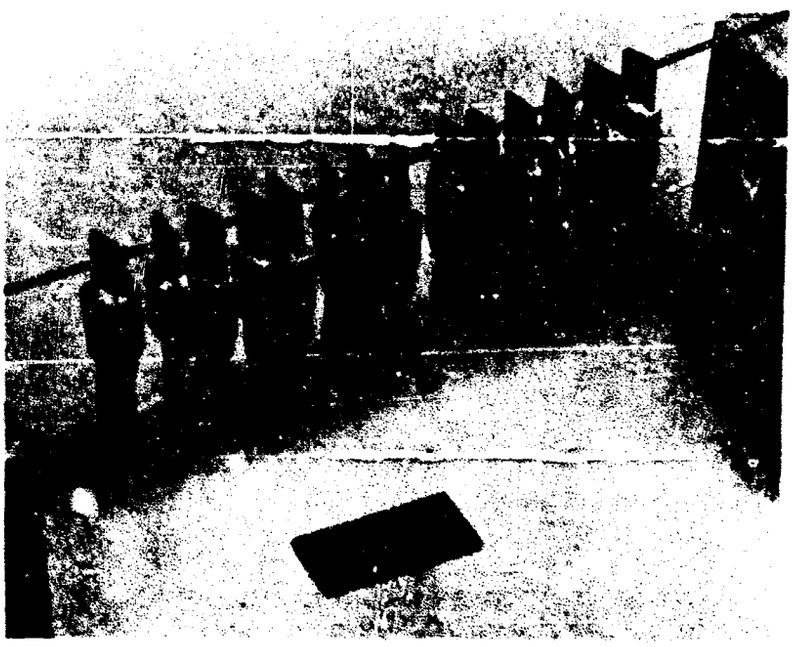


FIGURE 114. HOT-SALT STRESS RUPTURE TEST SPECIMENS

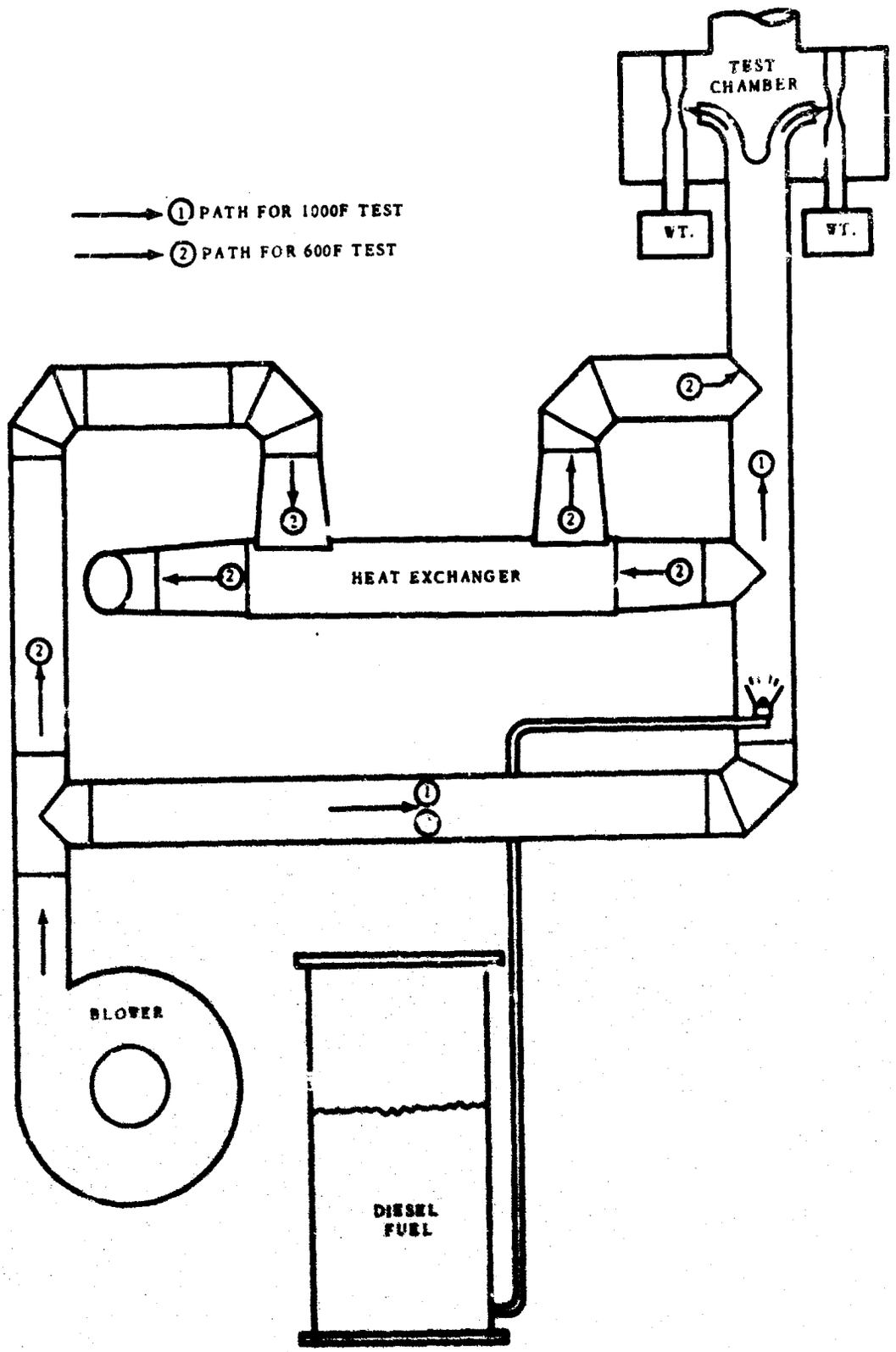


FIGURE 116. HOT-GAS STRESS RUPTURE TEST RIG

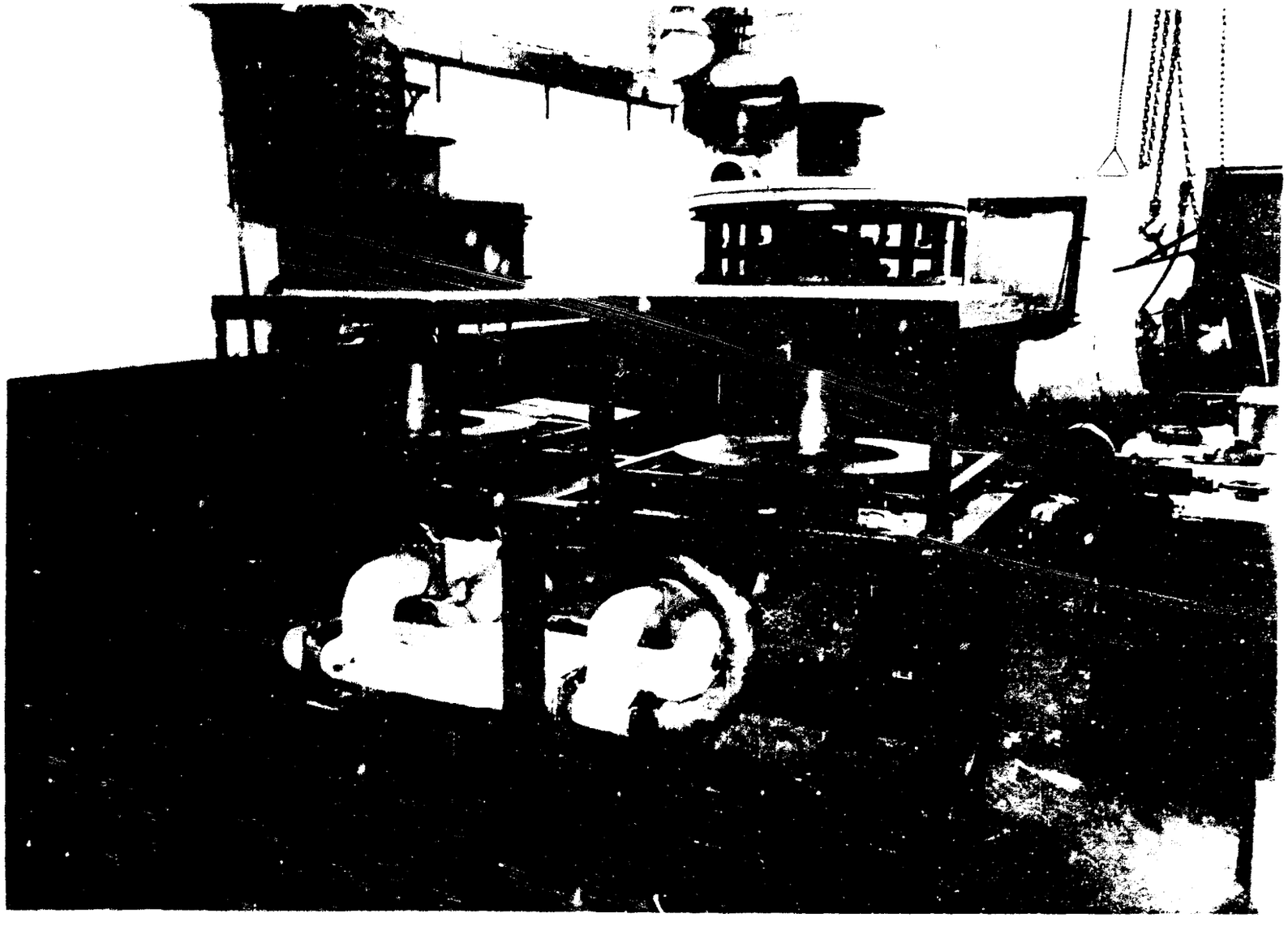


FIGURE 116. HOT-SALT CORROSION TEST RIG

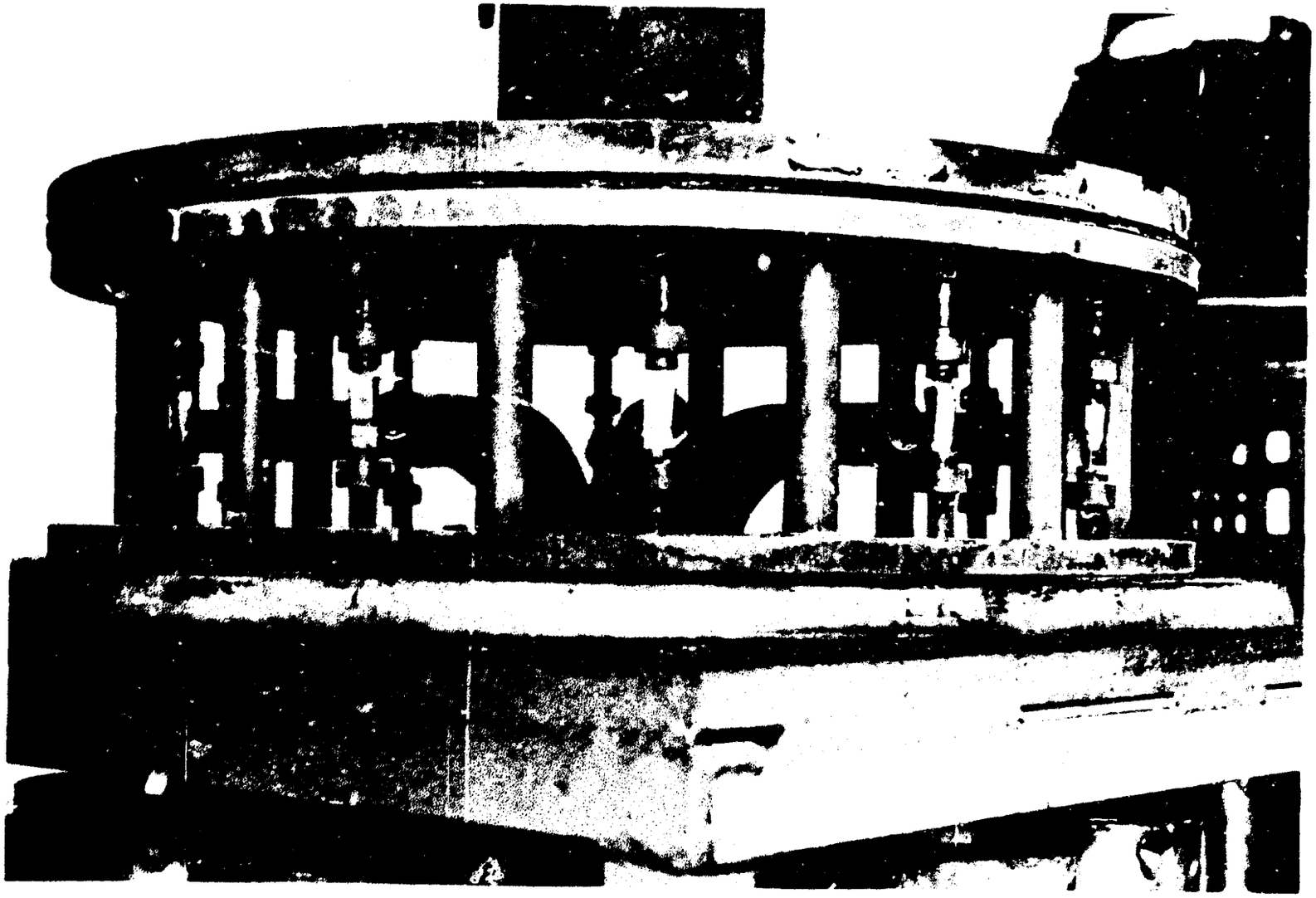
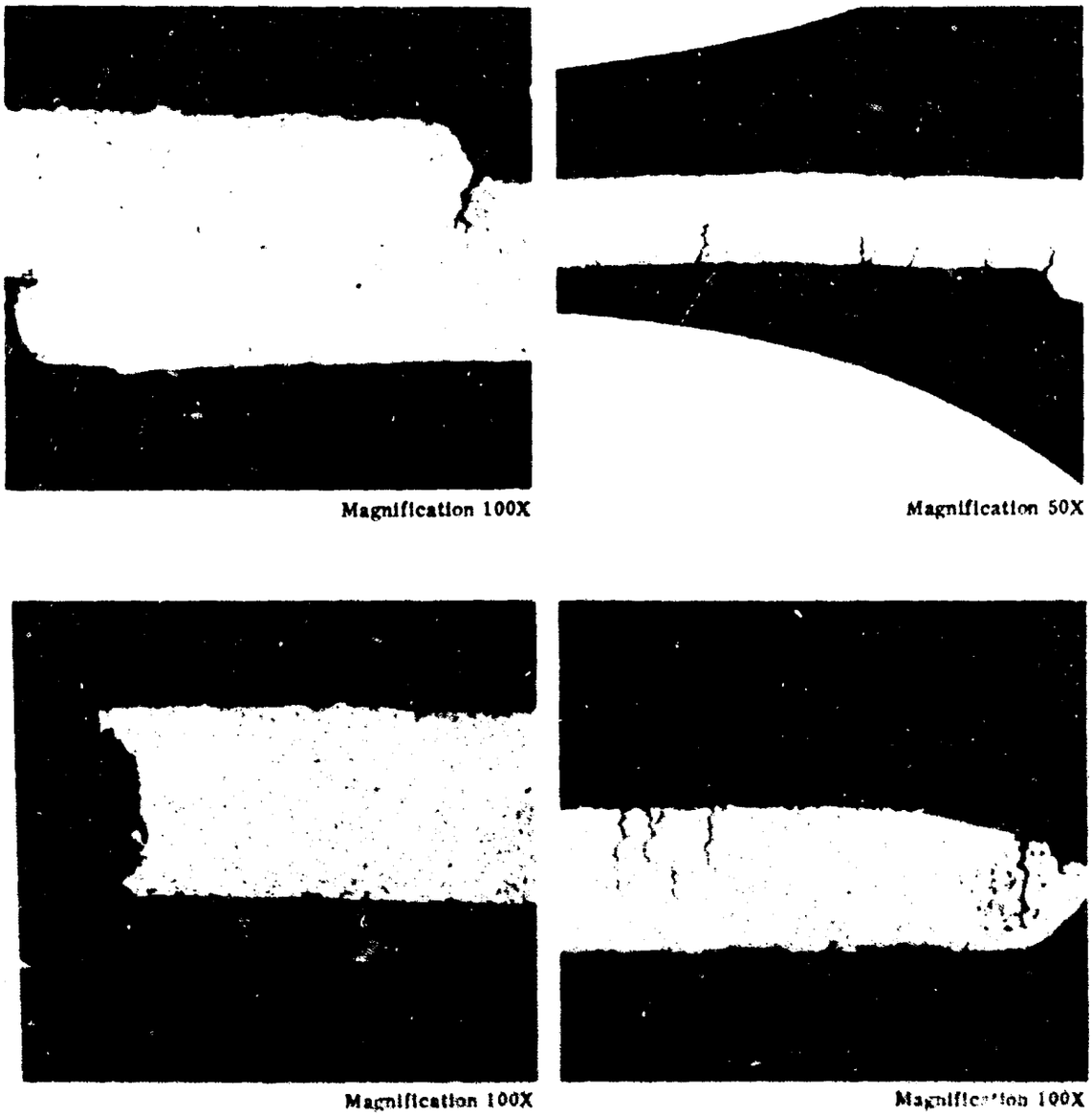


FIGURE 117. HOT-SALT STRESS RUPTURE TEST IN PROGRESS



Magnification 100X | Magnification 50X

Magnification 100X | Magnification 100X

Note the Cracks and Ductile Failure of 5Al-2.5Sn Foil

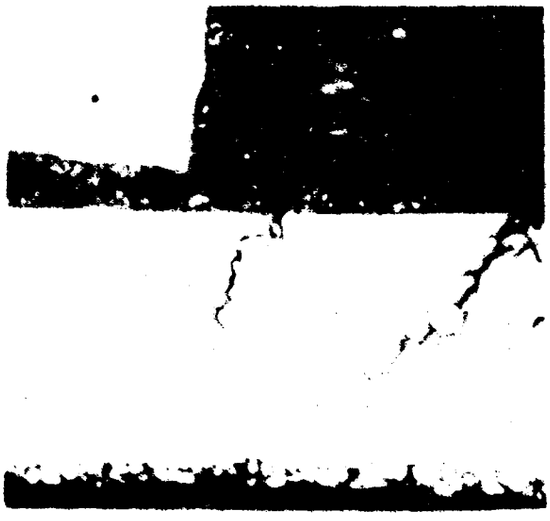
FIGURE 116. SELF-DIFFUSION BONDED Ti-5Al-2.5Sn SPECIMENS AFTER HOT-SALT CORROSION TESTING AT 1000 F



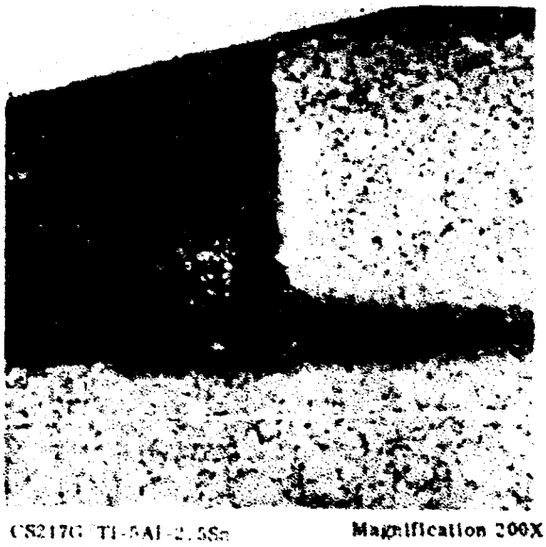
CS217/Ti-5Al-2.5Sn Brazement Magnification 50X
Cyclic Annealed



CS217/Ti-5Al-2.5Sn Brazement Magnification 200X
Cyclic Annealed



CS217F Ti-5Al-2.5Sn Magnification 200X
Cyclic Annealed

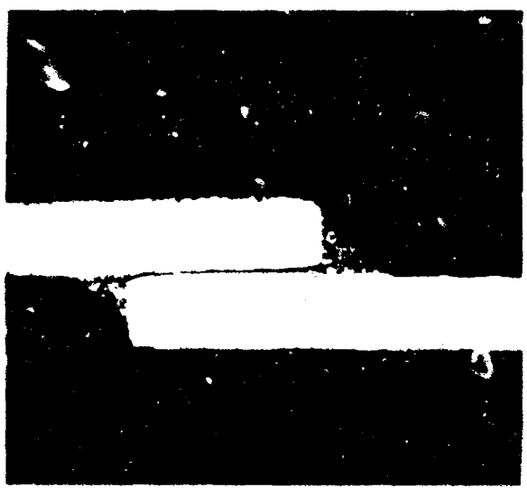


CS217G Ti-5Al-2.5Sn Magnification 200X
Cyclic Annealed

FIGURE 119. CS SERIES/Ti-5Al-2.5Sn BRAZEMENTS AFTER HOT-SALT CORROSION TESTING AT 1000 F



RMS/Ti-6Al-2.5Sn Magnification 50X

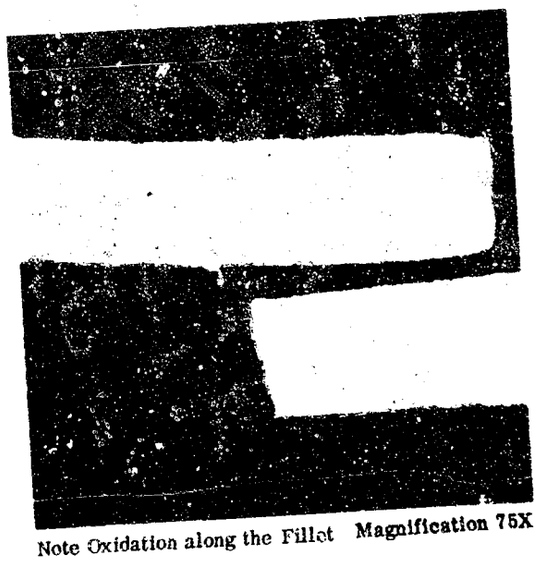


RM12/Ti-6Al-2.5Sn Magnification 50X



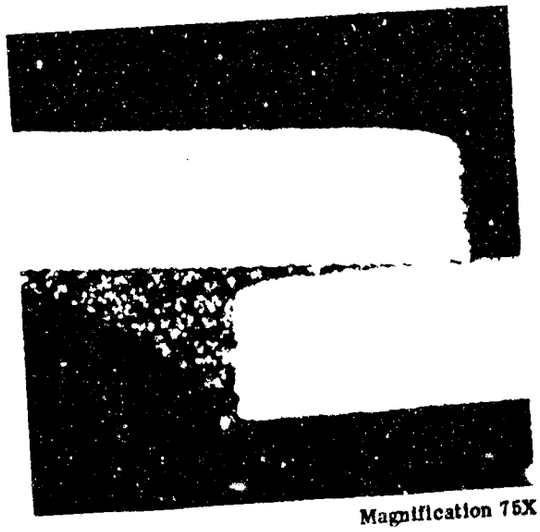
RM12/Ti-6Al-2.5Sn Magnification 200X

FIGURE 120. RM SERIES/ Ti-6Al-2.5Sn BRAZEMENTS AFTER HOT-SALT CORROSION TESTING AT 1000 F



Note Oxidation along the Fillet Magnification 75X

FIGURE 121. CYCLIC ANNEALED CS217/Ti-5Al-2.5Sn BRAZEMENT AFTER STRESS RUPTURE TEST AT 1000 F



Magnification 75X

FIGURE 122. CYCLIC ANNEALED CS217C/Ti-5Al-2.5Sn BRAZEMENT AFTER STRESS RUPTURE TEST AT 1000 F



Magnification 75X

Microphotograph Shows Excellent Braze Flow, No Oxidation And Absolutely No Cracking Of The Braze Matrix Or The Base Metal Foil.

FIGURE 123. CYCLIC ANNEALED RM8/Ti-5Al-2.5Sn BRAZEMENT AFTER STRESS RUPTURE TEST AT 1000 F

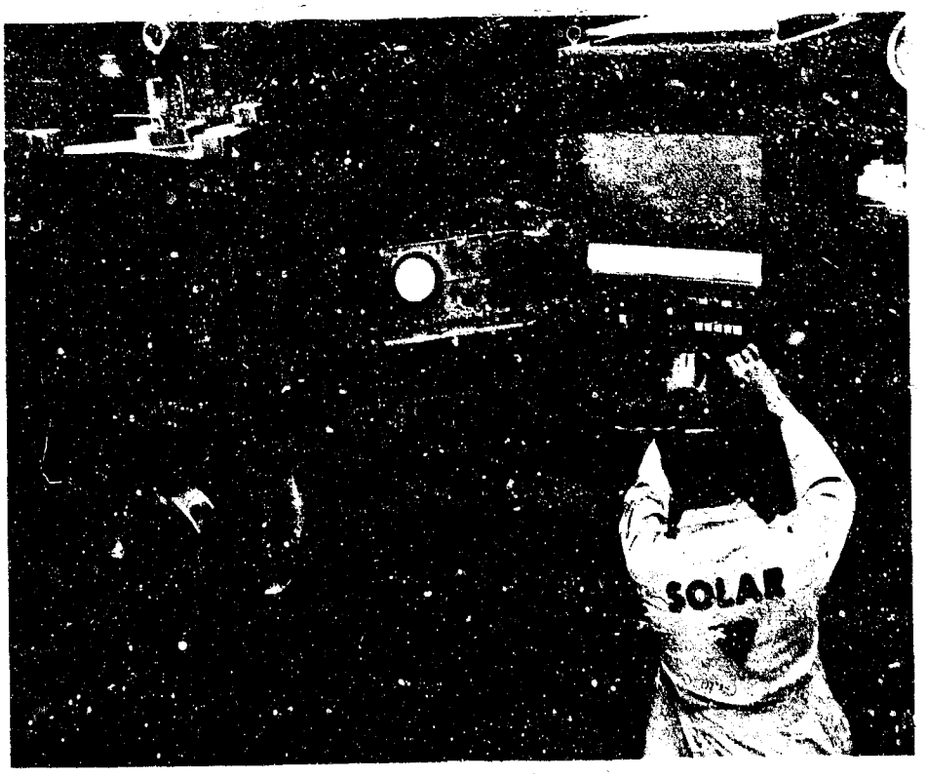


FIGURE 124. MTS FATIGUE TESTING MACHINE

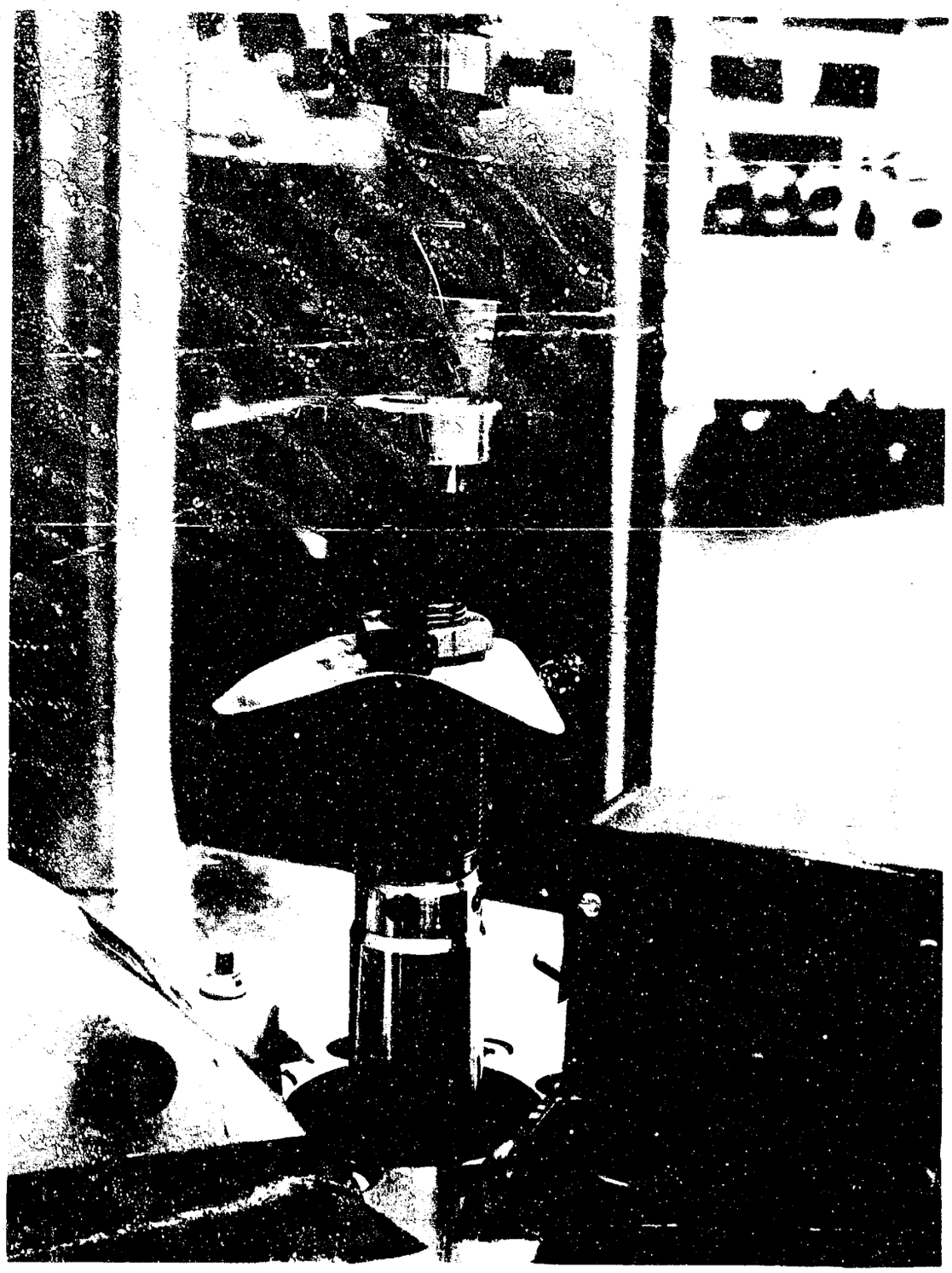


FIGURE 125. SPECIMEN HOLDING FIXTURE (Hole-and-Pin) IN MTS FATIGUE TESTING MACHINE

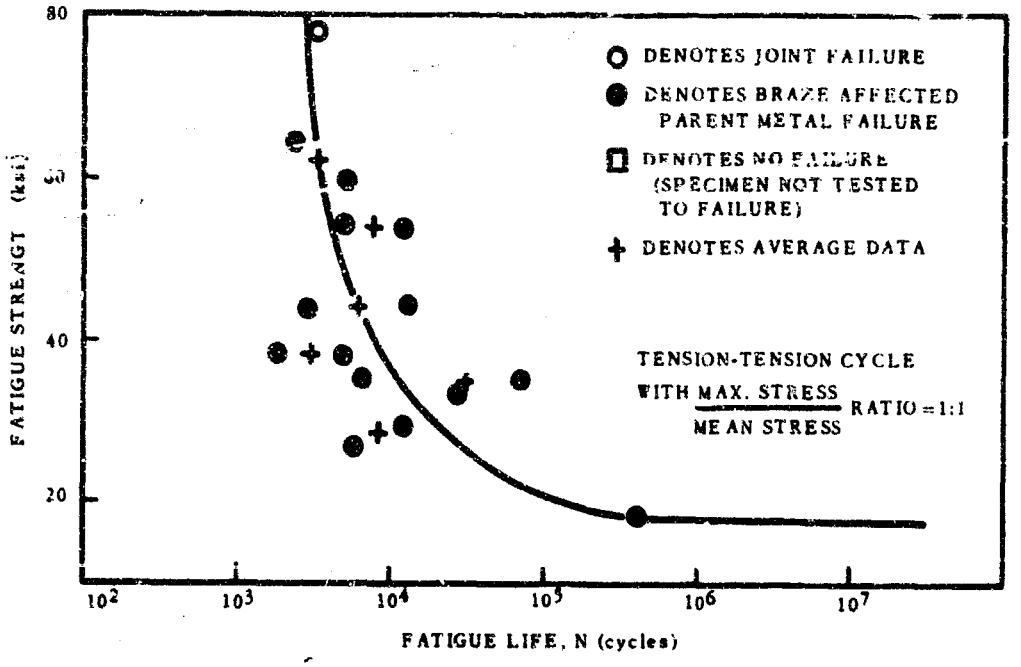


FIGURE 126. ROOM TEMPERATURE FATIGUE CURVE, SELF-DIFFUSION BONDED Ti-5Al-2.5Sn SPECIMENS

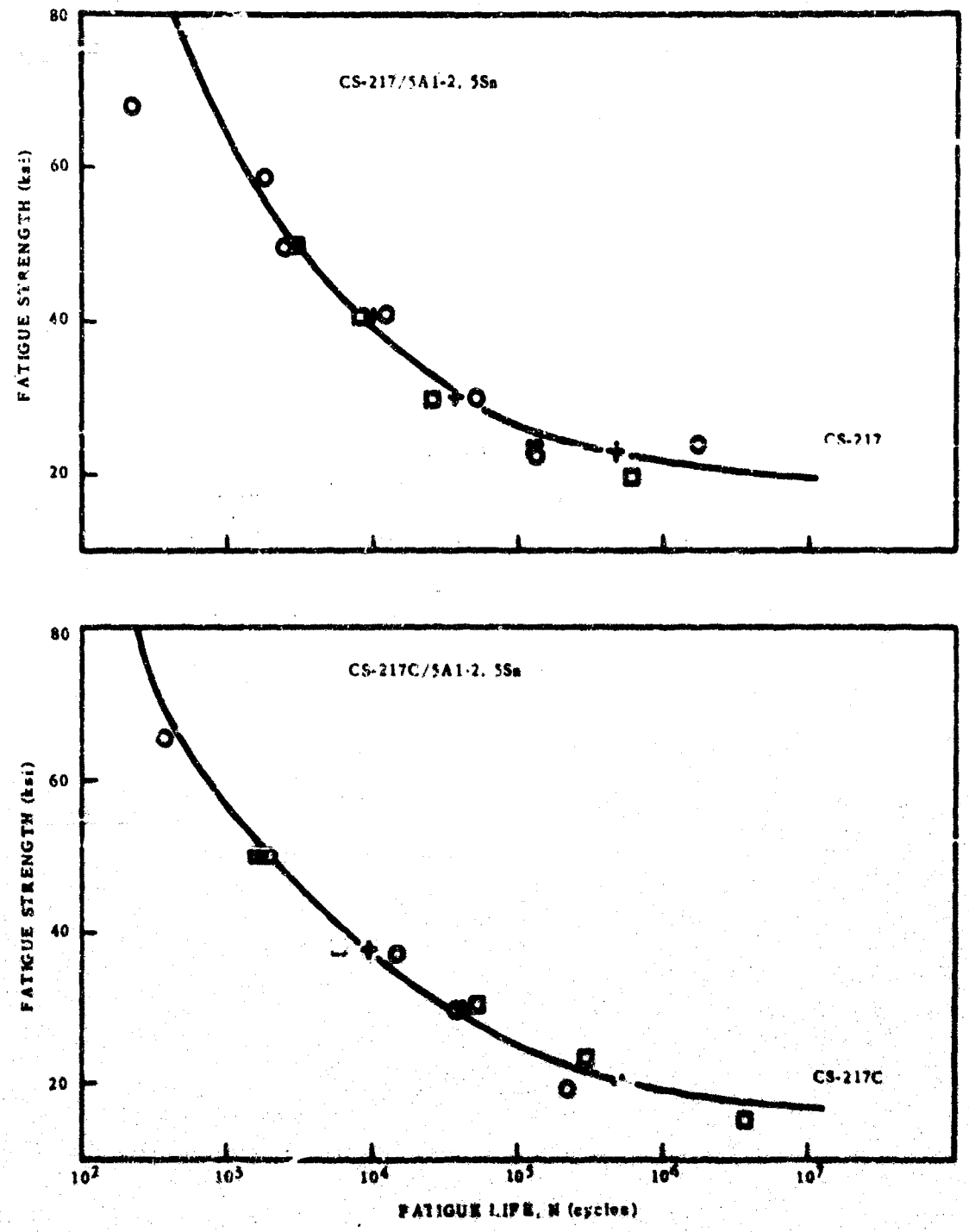


FIGURE 127. ROOM TEMPERATURE FATIGUE CURVE, CS SERIES/Ti-5Al-2.5Sn BRAZEMENTS

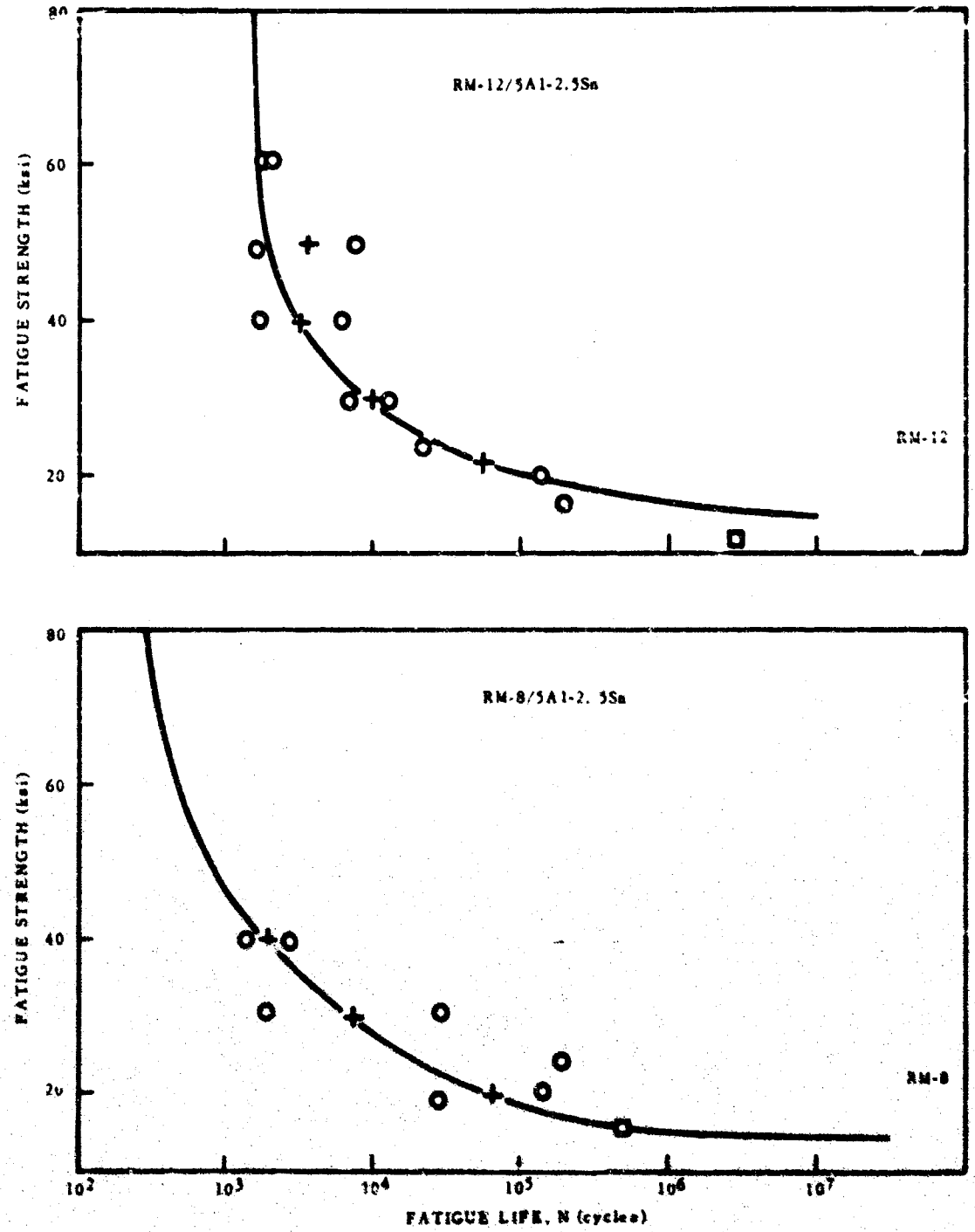


FIGURE 128. ROOM TEMPERATURE FATIGUE CURVE, RM SERIES/Ti-5Al-2.5Sn BRAZEMENTS

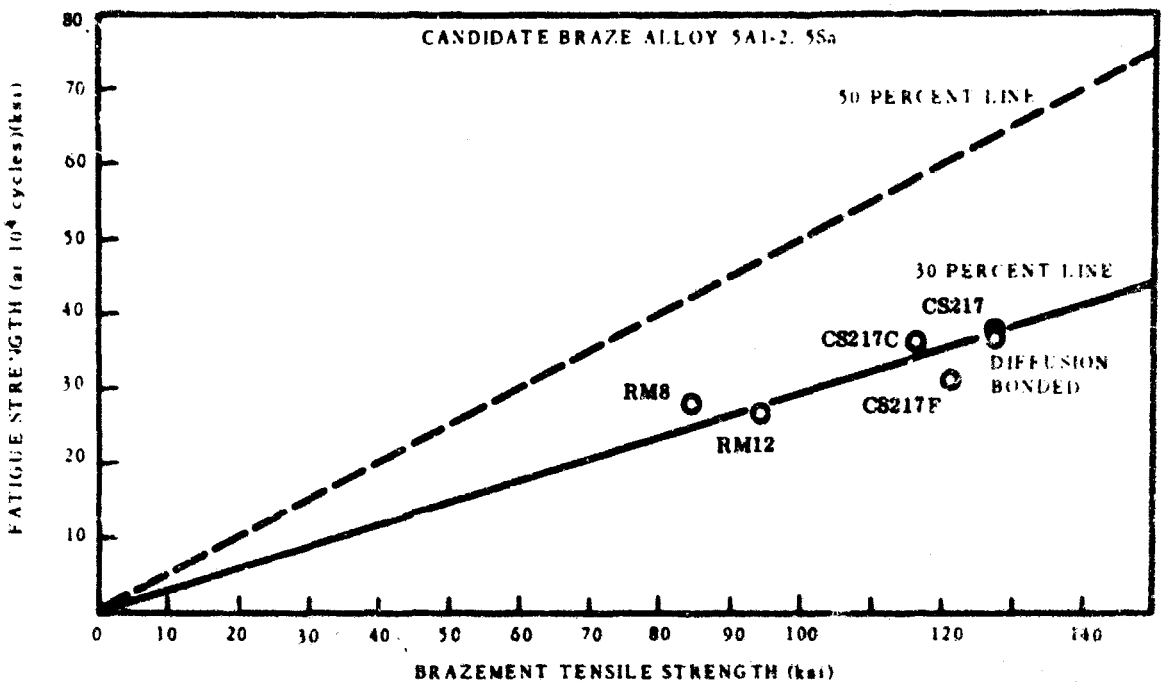


FIGURE 129. FATIGUE STRENGTH VERSUS BRAZEMENT STRENGTH, CANDIDATE ALLOYS AND SELF-DIFFUSION BONDED Ti-5Al-2.5Sn SPECIMENS

3.6 TASK VI - EXPLORATORY EFFORTS TO OPTIMIZE BRAZE MATERIALS AND TESTING METHODS

3.6.1 Effect of Melt Stock Purity (Ti, Zr, Be)

The principal concern with purity was the possibly deleterious effect to braze alloys resulting from uncontrolled quantities of interstitial element contaminants inadvertently added through commercial purity melt sock. It is well documented that small quantities of dissolved oxygen, nitrogen, or carbon in α-Ti (or β-Ti) cause significant increases in hardness level (Fig. 130 and 131), frequently resulting in undesirable β-transformation products and impairment of matrix toughness. Moreover, all three interstitial element contaminants (O, N, C) raise the solidus and liquidus temperatures rapidly with increasing concentration in the Ti-O, Ti-N, and Ti-C binaries (Ref. 102). The same situation exists for the corresponding zirconium-base binaries. The ultimate effect of excessive interstitial content in Ti-Be and Ti-Zr-Be alloys therefore is the degradation of brazing characteristics as evidenced by sluggish braze flow, incomplete melting, and heavy residual, as well as the impairment of engineering properties of brazements.

It was the purpose of this investigation to determine whether or not the interstitial contaminant levels derived from commercial purity melt stock are excessive (i.e., for the candidate braze alloy Ti-47.2Zr-5.6Be and the basic alloy, Ti-5.6Be) for comparison. The commercial purity melt stock of titanium typically contains 1500 ppm oxygen, the worst interstitial offender. Commercial purity zirconium has about the same average oxygen content. Commercial purity beryllium (AMV grade) is made by a powder metallurgy process and is high in BeO content (typically ~ 15,000 ppm oxygen). Fortunately, the beryllium addition to make braze alloys is small, otherwise the unintentional addition of oxygen would undoubtedly become excessive. However, even at the 5.6 percent beryllium level, the commercially pure beryllium addition raises the average oxygen concentration of Ti-5.6Be and Ti-47.2-5.6Be alloys to ~ 2200 ppm. This oxygen level need not necessarily be excessive, although it is sufficiently high to warrant attention. Very likely, the bulk of the BeO added during alloying remains as tiny, discrete, BeO particles rather than dissociating and dissolving in the titanium or Ti-Zr base alloys. This is due to the extremely great stability of BeO relative to Ti-O and Zr-O solutions (Fig. 132). Consequently, the true level of dissolved oxygen in the braze alloys might well be closer to the original 1500 ppm than to 2200 ppm.

The actual degree of importance in restricting interstitial element contaminants was assessed by melting Ti-5.6Be and Ti-47.2Zr-5.6Be alloys with both commercial purity and high purity melting stocks in different combinations; then comparing foil brazing characteristics, braze structures, and microhardness of microstructural components.

All of the compositions listed in Table XVIII were arc-melted and prepared for brazing. Brazing characteristics and minimum braze temperatures were determined in both argon atmosphere and high-vacuum environments on Ti-5Al-2.5Sn (0.002-inch) foil T-joints. The test braze cycle consisted of rapidly heating (~ 1000 F/minute) each candidate braze alloy to 1700 F (Ti-5.6Be alloys) or to 1500 F (Ti-47.2Zr-5.6Be alloys), holding for two minutes, then heating at a controlled rate (50 F/minute, 100 F/minute, or 300 F/minute) to the minimum temperature at which brazing could be accomplished. The relatively slow heating rate in the vicinity of the braze temperature was selected to simulate actual braze cycles.

Holding time at the brazing temperature was fixed at one minute. This was followed by a natural furnace cool (1000 F/minute, average) to room temperature.

The braze alloy heat of each nominal composition exhibiting the best brazing characteristics and lowest average braze temperature was then subjected to an even longer braze cycle. The holding time at 1500 and 1700 F was extended from two minutes to five minutes; followed by heating at the median rate of 100 F/minute (both argon and vacuum environments). Any deterioration of brazing characteristics or change in minimum flow temperature was then recorded. Finally, all test brazements were mounted for metallographic examination. Typical brazement microstructures are shown in Figures 133 through 136.

The results from the Ti-5.6Be modifications are shown in Table LIII. In both argon and vacuum and at all heating rates, the heats with the lower interstitial element contents (No. 1-23 and 1-24) yielded significantly lower braze temperatures (typically, 50 degrees F lower within a range of from 25 to 75 F). The heat with the highest interstitial content (No. 1-1) required braze temperatures ≥ 2000 F for all heating rates except one. All braze alloys were shown capable of being used at each heating rate; there being no strong trend relating heating rate and minimum braze temperature. However, heats No. 1-23 and 1-24 were capable of being brazed at just 1950 F at either 50 F/minute (vacuum) or at 50 F/minute and 100 F/minute (argon).

TABLE LIII

EFFECT OF BRAZE PURITY ON BRAZE TEMPERATURE AND BRAZING CHARACTERISTICS (Ti-5.6Be Alloy)

Heat Number	Variables in Braze Process		Minimum Braze Temperature (F)	Brazing Characteristics Upon Ti-6Al-2.5Sn Foils		
	Environment	Heating Rate deg (F/min)		Braze Fluidity	Fillet Formation	Unmelted Residue (size)
(1-1) (2200 ppm O_2)	Argon	50	2000	G	G	M
	Argon	100	1960	G	G	M-L
	Argon	300	2000	G	G	M
	Vacuum	50	2025	G	M-G	M
	Vacuum	100	2025	G	M-G	M-L
	Vacuum	300	2010	G	G	M
(1-23) (1430 ppm O_2)	Argon	50	1960	G	G	M
	Argon	100	1960	G	G	M
	Argon	300	2000	G	G	M
	Vacuum	50	1950	G	M-G	M
	Vacuum	100	2000	G	G	M
	Vacuum	300	1965	G	G	N-M
(1-24) (260 ppm O_2)	Argon	50	1950	G	G	N
	Argon	100	1950	G	G	N
	Argon	100[1]	1950	G	G	N
	Argon	300	1975	G	G	N
	Vacuum	50	1950	G	G	N
	Vacuum	100	2000	G	G	N
	Vacuum	100[1]	1950	G	G	N-M
	Vacuum	300	1970	G	G	N

1. Held at 1700 F (prior to controlled heating) for five minutes instead of the standard two minutes.

G - Good, S - Sluggish, P - Poor
G - Good, M - Mediocre, P - Poor
N - None, M - Moderate, L - Large

At faster heating rates of 100 F/minute and 300 F/minute (vacuum) or 300 F/minute (argon), higher braze temperatures in the range of 1970 to 2000 F were required. This rate-dependent behavior, although reversed from the expected trend, suggests a certain sensitivity to minor changes in braze surface composition (presumably Be concentration). The phenomenon appeared to be exaggerated by vacuum environment, inasmuch as the 5-minute hold at 1700 F resulted in aporeciable unmelted residue on subsequent brazing in vacuum, but not for the same heat (No. 1-24) when brazed in argon. Also, the heats brazed in vacuum exhibited higher minimum braze temperatures (averaging 12 to 37 degrees F higher) than the same heats brazed in argon. This may indicate that argon pressure serves to inhibit or slow down undesirable changes in braze surface chemistry (e.g., beryllium evaporation or surface diffusion).

The most important observations, however, are:

- The heat with the lowest interstitial content (No. 1-24) was observed to have the best brazing characteristics of all in terms of superb braze fluidity, smooth and continuous fillets, sound microstructure, and ease of brazing.

- The heat with the lowest interstitial content (No. 1-24) tended to melt and flow, leaving negligible unmelted residue (one minor exception in six attempts). This implied more efficient utilization of beryllium than the other heats, all of which displayed marked tendencies to leave unmelted residue.

- The minimum braze temperature of the high purity heat (No. 1-24) varied between 1950 and 2000 F, depending upon process heating rate and environment.

The results from the Ti-47.2Zr-5.6Be modifications showed similar trends with regard to the variables of interstitial element content and braze cycle (Table LIV). Braze temperatures were considerably lower due to the zirconium addition. With but one exception in six trials, the heat with lowest interstitial content (No. 13-4) exhibited the lowest braze temperatures of the three heats in each series (though the temperature progressions were not systematic in every case). Heat No. 13-5 could not be included in this general investigation because the high-purity Zr arrived too late. However, subsequent work with heat No. 13-5 showed it to be very similar in braze performance and structure to Heat No. 13-4. The minimum braze temperature was observed to vary throughout the survey between 1600 and 1700 F, with the lower minimum occurring in vacuum for Heat No. 13-4. (For the Ti-5.6Be heats, the lower minimums occurred in argon, suggesting a reversal in braze surface effects at the lower process temperatures.) The effect of heating rate on minimum braze temperature

TABLE LIV

EFFECT OF BRAZE PURITY ON BRAZE TEMPERATURE AND BRAZING CHARACTERISTICS (Ti-47.2 Zr-5.6Be Alloy)

Heat Number	Variables in Braze Process		Maximum Braze Temperature (F)	Brazing Characteristics Upon Ti-5Al-2.5Sn Foils		
	Environment	Heating Rate deg (F/min)		Braze Fluidity	Fillet Formation	Unmelted Residue (size)
(13-1) (2200 ppm O_2)	Argon	50	1700	S	G-M	M
	Argon	100	1660	S	G	M
	Argon	300	1700	G	G	N-M
	Vacuum	50	1650	S	G-M	M
	Vacuum	100	1700	G	G	M
	Vacuum	300	1700	G	G	M
(13-3) (1430 ppm O_2)	Argon	50	1650	S	G	N-M
	Argon	100	1650	S-G	G	N-M
	Argon	300	1700	G	G	N-M
	Vacuum	50	1700	G	G	M
	Vacuum	100	1680	G	G	N
	Vacuum	300	1700	G	G	N
(13-4) (850 ppm O_2)	Argon	50	1650	G	G	M
	Argon	100	1700	G	[illegible]	N
	Argon	200[1]	1670	[illegible]	G	N
	Argon	300	1670	G	G	N
	Vacuum	[illegible]	1650	S-G	M-G	M
	Vacuum	100	1700	G	G	N
	Vacuum	100[1]	1600	G	G	N
	Vacuum	300	1650	G	G	N

1. Held at 1500 F (prior to controlled heating) for five minutes instead of the standard two minutes.

G - Good, S - Sluggish, P - Poor
G - Good, M - Mediocre, P - Poor
N - None, M - Moderate, L - Large

again was vague, and certainly not consistent from heat to heat nor from argon to vacuum for a given heat. Good brazements were produced under all test conditions. Corroborative evidence that the influence of braze or foil surface phenomena is negligible at 1600 to 1700 F comes from the extended hold test at 1500 F (5 minutes) prior to brazing. In neither argon nor vacuum were the brazing characteristics altered by extended holding; in fact, the braze temperature was 30 degrees F lower than anticipated in argon.

Again, the most important observations were:

- The heat with the lowest interstitial content (No. 13-4) displayed the most outstanding braze characteristics of all in terms of braze fluidity, smooth and continuous filleting, sound brazement structures, and ease of brazing. In these respects, Heat No. 13-4 was superior to Heat No. 1-24.

- The heat with the lowest interstitial content (No. 13-4) tended to wholly melt and flow, leaving negligible unmelted residue. All other heats, with the exception of Heat No. 13-3 in vacuum, left appreciable unmelted residues. (This was invariably true at heating rates of 100 F/minute and 300 F/minute. At the slower rate of 50 F/minute, some moderate unmelted residue and braze sluggishness were noted, indicating the advisability of controlled heating rates in brazing with No. 13-4.)

3.6.2 Effects of Braze Holding Time and Cooling Rate

The relative effects and importance of braze purity, braze cycle heating rate, and braze process environment were previously studied and discussed. In this follow-up study on basic Ti-5.6Be and Ti-47.2Zr-5.6Be braze alloys, the effects of the following process variables were investigated:

- Holding time at the minimum braze temperature. (Periods of 1, 5, and 25 minutes were selected to represent a reasonable range of actual braze times encountered in practice. All prior braze screening studies were restricted to 1 minute holding time.)

- Cooling rate from the braze temperature to 1500 F (Ti-47.2Zr-5.6Be) or to 1700 F (Ti-5.6Be). Disparate rates of 1000 F/minute (natural furnace cool) and 25 F/minute (controlled furnace cool) were chosen for the aforementioned temperature ranges, characterized by the occurrence of brazement solidification.

The high purity heats (No. 1-24) and (No. 13-4) were used in this study. Six-mil foil T-joints of Ti-5Al-2.5Sn alloy were brazed in a high-vacuum environment. This was the same T-joint configuration used in previous tests. A constant heating rate of 100 F/minute was employed from the 1500 F or 1700 F equilization temperatures, as in previous work. Braze temperatures of 2000 F (No. 1-24) and 1700 F (No. 13-4) were used.

Holding time at the braze temperature was considered an important variable to be checked for two reasons. First, the potential for contamination of the liquid braze system and the titanium foils increases systematically with increased process time. Virtual leak sources of interstitial element contaminants abound even in high vacuum, and the liquid titanium- and Ti-Zr base braze alloys (and program alloy foils) provide an immense sink for them. Second, increased braze holding time permits the liquid braze/solid foil system greater opportunity to reach thermodynamic (compositional and structural) equilibrium. For the liquid braze alloy whose composition places it far from thermodynamic equilibrium with the solid foils it is to join, the ultimate result is often severe erosion and dissolution of the foils by the liquid braze. (However, this requires the allowance of sufficient time for the mechanism of braze erosion to be activated.) Naturally, the higher the braze temperature for a given degree of thermodynamic imbalance, the shorter the required time.

The results of the subject investigation are shown in Figures 137 and 138. In the case of the higher temperature braze alloy, Ti-5.6Be (No. 1-24), marked advances in the degree of foil erosion with process time were noted. Erosion at the 1-minute braze cycle was negligible (Fig. 137). After the 5-minute braze cycle, the foils immediately adjacent to the liquid braze appeared to be consumed (an estimated 15 to 20 percent, minimum). Some minor surface roughness was observed, but there was no undercutting of the foil or thinning of the fillet. After the 25-minute braze cycle, the vertical and horizontal foil members in the joint region were largely consumed by the braze, and few discernible vestiges of the foils remained in the braze joint. (The joint structure was essentially that of a casting, rather than a braze.) In spite of the condition described, no adverse washing, undercutting, or foil thinning effects were noted.

Metallographic examination of the Ti-47.2Zr-5.6Be (No. 13-4) brazements made at 1700 F revealed no serious alteration of the titanium foil microstructure, even after the 25 minute braze cycle (Fig. 136). In contrast, all of the titanium foils brazed with Ti-5.6Be at 2000 F showed a gross Widmanstatten pattern of coarse alpha phase, characteristic of titanium alloys heated inadvertently into the beta embrittlement range (above the beta transus). This foil structure was evident even after the 1-minute braze cycle at 2000 F.

The most important difference, however, was in the degree and nature of foil erosion. No significant erosion was noted for the 1-minute braze cycle at 1700 F. After the 5-minute braze cycle, the vertical foil members in contact with the liquid braze were observed to be uniformly thinner, some 8 to 17 percent. After the 25-minute braze cycle, the unaffected portion of each vertical foil member grew still thinner (an average 25 percent, to a thickness of about 4-1/2 mils). These amounts of foil dissolution were significantly less than those experienced with the Ti-5.6Be alloy. Of paramount importance, the braze fillet surface (No. 13-4) remained smooth where it initially met the foil surface, with no sign of foil undercutting, washing, or foil thinning. An interesting structural feature of the brazements made with Heat No. 13-4 was the uniform, primary beta solidification occurring on titanium foil surface contacting the liquid braze. The presence of pro-eutectic beta solidification indicated that the braze (originally a eutectic) was made progressively hypoeutectic with regard to beryllium by continuing foil dissolution. The volume of primary beta obviously increased with longer braze times. Primary beta was strongly promoted also by the slower solidification rate; the fast solidification rate clearly suppressed primary beta. As shown in Figure 138, solidification fronts (from vertical and horizontal foil members) actually met and fused together for combinations of long brazing time (25 minutes) and slow solidification rate (25 F/minute). These solid "bridges" of primary beta are structurally similar to the foils themselves and might tend to negate any detrimental effect of (partial) titanium foil dissolution. In fact, the "bridges" of the primary beta phase constitute a rudimentary form of solid-state bond, hence joint strength and reliability could well be enhanced by their presence.

3.6.3 Effect of Braze Process Over-Temperature

To ensure overall attainment of the minimum braze temperature in brazing large foil structures by radiant heating, it is often necessary to overheat portions of each structure as much as 100 to 200 degrees F beyond the minimum braze temperature, and to hold at this temperature for as long as 30 to 60 minutes. This situation is the result of some foil structures acting as large, natural heat shields (e.g., tube-and-fin heat exchangers). To determine the effects of such extended overtemperature cycles on braze structure, it was decided to braze and evaluate Ti-5Al-2.5Sn foil T-joints using selected CS and RM series alloys.

The following program was conducted:

Braze Alloy	Minimum Braze Temperature (F)
CS13-5	1620
RM1	1650
RM8	1470
RM12	1670

Actual Braze Cycles Studied

Temperature (F)	Braze Time (min)	
1825	60	All alloys
1700	30	All alloys
1600	30	RM8 only
1500	30	RM8 only

Severe erosion of the 0.006-inch foils was noted for all braze alloys following the 1825 F, 60-minute braze cycle (Fig. 139 through 141). Heavy, primary beta bridge formation was associated with the erosion, although actual bridging of the beta solidification fronts was imperfect in all cases. Because of the high braze temperature and the β stabilization afforded by zirconium, beryllium, and nickel infiltration from the braze alloys, the 1825 F braze cycle obviously placed the primary beta solids well above the beta transus temperatures. This resulted in a coarse Widmanstatten pattern of (α+β) in the bridge structures on cooling. Although the uneroded portions of foils remained all-alpha during the braze cycle, the severe foil erosion in the fillet regions coupled with the presence of beta-embrittlement type structure in the primary bridge material (also in the fillet region) could readily prove deleterious to brazement strength and toughness. No marked tendency toward foil undercutting was observed, but the fillet surfaces appeared moderately rough, which also was a bad structural aspect. The RM1 alloy appeared the worst offender in all the structural changes discussed (Fig. 141).

Brazements made at 1700 F for 30 minutes also underwent signficant foil erosion as well as similarly undesirable structural transformation in beta bridges, but to a lesser degree than at 1825 F. As shown in Figures 142 and 143, the structures appeared marginal and might be considered tolerable to ensure brazing throughout a foil structure. The fact that the lower melting alloy, RM8, produced erosion patterns and bridges of primary solid at 1700 and 1825 F very similar to the other braze alloys at 1700 and 1825 F, helped signify that the degree of erosion and bridging are primarily functions of the braze temperature for the family of titanium-zirconium base compositions studied. (Even at 1600 F, the titanium foils suffered easily recognized erosive attack by RM8 in 30 minutes (Fig. 144); however, as shown in Figure 145, a safe maximum braze temperature for RM8 appeared to be 1500 F.) In any event, it was shown that extended braze cycles involving over-temperature (as little as 30 to 50 degrees F above the minimum flow temperature) can result in appreciable foil erosion and undesirable braze structures. Consequently over-temperature situations must be carefully controlled to limit process time.

3.6.4 Study of Microstructural Components

To better understand the behavior and predict the applicability of the candidate braze alloys (Ti-5.6Be and Ti-47.2Zr-5.6Be), a study was conducted of their microstructural components as well as those of braze-affected foils (Ti-5Al-2.5Sn). All foil brazements made for the melt-stock purity study using Heats No. 1-1, 1-23, 1-24, 13-1, 13-3, and 13-4, as well as the arc-melted button ingots of these heats were examined metallographically. The work comprised classifying all the microstructural components and determining the relative hardnesses through microhardness surveys. Approximate hardness readings were taken using the Vickers microhardness tester indentor (DPH-100 gram indentor load).

The Ti-5.6Be braze ingot structure is composed predominantly of a very finely divided eutectic, the phases involved being the terminal titanium solid solution (~ 0.1 to 1.0 percent beryllium in solution) and the first titanium beryllide ($TiBe_2$) as shown in Figure 146. The hardness of the eutectic varies widely in the range R_C40 to 59[1], presumably the result of varying beryllide concentration in the eutectic, real or apparent. An apparent variation could arise from different beryllide particle

1. DPH readings were converted to the Rockwell "C" scale for more practical comparisons

sizes, orientation, and morphology within the same brazement. The most typical range of eutectic hardness is R_C45 to 50. No recognizable trend in eutectic hardness variation was seen for changes in braze purity level (ingot or brazement) or brazing environment. The sporadic occurrence of massive beryllide particles was noted in some brazements. The random distribution of the massive beryllide and its infrequent occurrence in brazements suggested that it was an unassimilated remnant of the coarse ingot structure, and not necessarily pre-eutectic by nature. The hardness of the beryllide is quite high, as anticipated (R_C63 to 71). Occasional islands of primary titanium solid solution (α or β-Ti) were seen in the braze joint structure, probably the result of local beryllium deficiency (effectively creating a hypoeutectic composition). These titanium islands are soft, about the same hardness as the titanium alloy foils before the brazing cycle (R_C33 to 34). The qualification, "before the brazing cycle" must be used because the 2000 F, 1-minute braze treatment can result in appreciable hardening of the exposed foil members in and adjacent to the braze. This hardening was due presumably to interstitital element contamination and beta embrittlement phenomena at this high temperature (both argon and high vacuum environments). Foil hardness post-brazing varied considerably, but readings as high as R_C47 were found. The most common hardness range was R_C37 to 44, although pockets of low original hardness could still be found (R_C30 to 35).

All of the preceding comments have been made in reference to Ti-5.6Be brazements produced by the standard one-minute, 2000 F braze cycle. The prolonged vacuum braze cycles (5 and 25 minutes) evaluated later added little new information because of the strong but variable foil dissolution effects observed which produced very confused braze structures (Fig. 137). In general, the quantity of eutectic structure was decreased by the longer braze cycles, being replaced by a titanium-rich conglomerate with variable structure and variable hardness (R_C35 to 45). The foil hardness continued variable with numerous high readings ($\geq R_C$40) for the five- and 25-minute cycles. After the 25-minute cycle, surface zones of highly contaminated, untransformed alpha phase also were observed upon the exposed foil surfaces. This surface phenomenon indicated that the increased concentration of alpha-stabilizing interstitials had served to boost the new beta transus $\geq$ 2000 F. The hardness of these alpha bands was found to be R_C40 to 45.

More meaningful and optimistic data resulted from the study of the Ti-47.2Zr-5.6Be alloy. Here again, the braze structure was composed predominantly of a very finely divided eutectic and a light etching region (Fig. 135 and 136). A dark etching, filigreed region (about one-fourth the area of the light region) frequently was observed in intimate association with the light etching eutectic. This dark region may have constituted a second eutectic involving a complex beryllide, which would be possible in the ternary Ti-Zr-Be system. However, because the hardnesses of the two regions were similar and their microstructures also similar, the two regions are discussed here as a unit (the eutectic structure).

A careful study of the eutectic structure in arc-cast button ingots (Heat No. 13-4) revealed two important features:

- The Ti-Zr solid-solution phase predominated volume-wise in the eutectic, and was the continuous matrix phase (Fig. 147). Therefore, it was reasoned that the eutectic structure possessed a good change of being a strong and tough engineering material, if the stress-raising potential of the beryllide could be minimized. Of course, a hypereutectic braze composition (with respect to beryllium) would be intolerable because brittle proeutectic beryllide, especially in connected-network form, would tend to cancel out the toughness advantage of the eutectic structure. Consequently, it was also felt that a slightly hypoeutectic braze might be more advisable than a straight eutectic, from the standpoint of promoting a safety margin for toughness.

- The semicontinuous, dendritic pattern of beryllide in the eutectic (ingot form) could coalesce in certain regions during brazing and, thus, being made massive, resist complete dissolution by the liquid braze. The massive beryllide particles seen in brazements might be formed in this way.

The systematic variation in eutectic hardness showed a definite influence derived from both braze purity and braze process environment. For example, the eutectic resulting from argon brazing using Heat No. 13-1, formulated from commercial purity stock, possessed the highest hardness (R_C54.3 average). As the braze purity was increased by using higher purity melt stock, the eutectic hardness was progressively reduced (R_C51.8 average for Heat No. 13-3 to R_C51.1 average for Heat No. 13-4). A similar progression was noted for vacuum brazing, except that the eutectic hardnesses generally were lower than for argon brazing (e.g., R_C52.1 average for Heat No. 13-1, R_C51.8 average for Heat No. 13-3, and R_C49.1 average for Heat No. 13-4). It was felt that the reduction in eutectic hardness by using high-purity melt stock reflects the corresponding reduction in hardness of the Ti-Zr solid

solution (component of the eutectic structure) due to reduced levels of interstitial contaminants in this phase. The same reasoning applied to the lower eutectic hardnesses acquired through vacuum brazing, since a high vacuum environment (10^{-4} to 10^{-5} Torr) is inherently a poorer source of interstitial contaminants than is the best gettered argon atmosphere.

A considerably more massive beryllide phase (R_C65 to 68) was observed in Ti-47.2Zr-5.6Be braze structures than with Ti-5.6Be. The observation suggested that the composition Ti-47.2Zr-5.6Be (or certain graded particle sizes of this alloy) might be slightly hypereutectic with respect to beryllium. This thought was strengthened by the absence of proeutectic titanium islands within the braze following the one-minute braze cycle. Of course, primary beta solidification was noted on foil surfaces following prolonged interaction with titanium foils.

All of the preceding comments have been in reference to Ti-47.2Zr-5.6Be brazements produced by the standard one-minute, vacuum or argon braze cycle. The prolonged vacuum braze cycles (5 and 25 minutes) evaluated developed some interesting additional structures and results (one being the primary beta solidification fronts just mentioned). For example, the rapidly cooled brazements[1] of Heat No. 13-4 showed a progressive increase in eutectic hardness with increased braze time (R_C49.1 average for one minute, R_C52 average for five minutes, and R_C56.7 for 25 minutes). This progression was expected due to atmospheric contamination; however, it was discovered that the eutectic hardness for all braze times investigated could be lowered to a near common level (considering probable differences in interstitial contaminants) by controlled slow cooling (25 F/minute to 1500 F) post-braze. Slow cooling results in hardness levels of R_C48.7 for one minute, R_C49.8 for five minutes, and R_C51.5 for 25 minutes. This study outlined the two possible advantages of controlled slow cooling post-braze; viz. reduced eutectic hardness and promoted formation of primary beta "bridges". It also suggested the possibility that even lower eutectic hardnesses might result from optimized annealing treatments, post-braze, to relieve "casting" stresses and to coalesce and spheroidize the beryllide particles in the eutectic, rendering them less effective as stress raisers. The

---

1. In all except special cases, test specimen brazements normally were rapidly cooled (natural furnace cool at the rate of ~1000 degrees F/minute.

combined effect of lower eutectic hardness and altered beryllide morphology could act to alleviate the problem of marginal braze toughness.

Finally, the relatively low braze temperature of 1700 F (and associated low interstitial absorption rates) permitted the retention of original foil hardness and structure, even for the long 25-minute braze cycles. (This result was in contrast to the high foil hardnesses and coarse Widmanstatten structures obtained with Ti-5.6Be at 2000 F.) Foil hardness varied considerably but never exceeded R_C36, the typical range being R_C25 to 35. The primary-beta structures of Heat No. 13-4 possessed hardnesses intermediate between those of the foils and the eutectic. The variation in primary-beta hardness showed the influence of braze cycle time and solidification rate (e.g., for the rapid cool - R_C35 for one minute, R_C38 for five minutes, and R_C40 for 25 minutes; and for the controlled slow cool - R_C33 for one minute, R_C39 for five minutes, R_C35 for 2. minutes).

3.6.5 Braze Particle Size Effects

It was recognized that in-situ brazing of titanium foil structures (Phase II) would require finely graded braze particles (≤100 mesh powders). To determine the suitability of Ti-47.2Zr-5.6Be braze alloy as a braze material in fine mesh sizes, 40-gram portions of facsimile heats (No. 13-4 and No. 13-5) were mechanically crushed and graded for brazing of Ti-foil T-joints (0.006-inch thick Ti-5Al-2.5Sn foils). The mesh sizes used were:

Mesh Size	Typical Yield (wt %)	Comment
+12	14.4	
- 12/+24	32.8	Size particles used in conventionally loaded braze screening tests.
- 24/+35	24.9	
- 35/+48	10.2	
- 48/+100	10.7	
-100/+200	3.7	Applicable to in-situ brazing techniques.
-200/+400	2.4	
-400 (fines)	0.9	
	100.0	

It was evident that the greatest yield by mechanical crushing occurs for the intermediate mesh size of -12/+35. Typical foil brazing tests were conducted in high vacuum at 1650 to 1700 F, using a standard heating rate of 100 degrees F/minute and a braze holding time of five minutes. Brazing was carried out using all graded particle sizes except -400 (fines). Various braze loading arrangements were tried (one lump on one side, one lump on each side, etc.), but the method settled on as best was uniform distribution of particles along both sides. This also provided the closest simulation of in-situ loading technique. Braze loads were maintained constant, the same level as for screening tests. The results were gratifying in that all particle sizes (except one) of both heats produced good brazements and exhibited uniformly excellent brazing characteristics (Fig. 148). Minimal foil dissolution was observed, about the same as that determined in previous tests. The one apparent exception was the particle size, -100/+200 mesh, of both heats. As shown in Figure 149, this fraction resulted in inordinate and complete foil dissolution, washing erosion, and foil undercutting.

The most logical explanation for this behavior called for the initial braze liquid to be rich in beryllium and improverished with respect to titanium (the fraction in question must be chemically segregated and strongly hypereutectic with respect to beryllium). Brazing at 1700 F with such a thermodynamically unbalanced composition would obviously tend to react with and erode the titanium foil as the solid/liquid system is activated toward chemical equilibrium. Chemical segregation of the type described can be brought about by the physical segregation of two dissimilar phases during crushing and screening of a multiphase structure (in this case, the eutectic structure of Ti-47.2Zr-5.6Be). Having the two phases dissimilar in resistance to mechanical disintegration would promote this segregation tendency. The softer, titanium-rich solid solution actually does tend to flatten out and resist breakdown and is concentrated in the heavier, larger particle sizes. At the opposite end, the beryllium-rich beryllide phase is hard and friable and does tend to concentrate in the finer particle sizes. As long as intermediate to large particles are employed in brazing, any segregation tendency is masked. This is true because the eutectic structure is fine (relative to the larger particle diameters) and the titanium matrix phase is continuous, effectively barring the loss of fine splintered beryllide particles except at exposed surfaces. (A typical button ingot structure is shown in Figure 150.) Note that the -12/+24 particle size (average diameter = 0.040 inch) is gross compared

with the fine detail of the eutectic. However, the average diameter of the -100/+200 particle size is only about 0.004 inch, roughly the same order of magnitude as the eutectic detail. Hence, splintered beryllide particles could readily escape composite particles of this finer size and concentrate by gravity separation within this fraction or in finer fractions. Segregation within the fraction probably explains the sporadic occurrence of severe erosion, inasmuch as only normal foil dissolution was noted for the same troublesome fraction (-100/+200) of Heats Nos. 13-5 and 13-4 during most repeat runs (Fig. 151).

To circumvent the mechanism which promotes beryllium segregation in fine particle sizes, Solar investigated the use of a hydriding process prior to comminution. It was hoped that hydrogen absorption would render the titanium solid solution phase brittle, therefore as friable and readily crushed to fine particle sizes as the beryllide phase. In practice, coarse particles of Heat No. 13-5 were exposed to flowing dry hydrogen in a Vycor tube furnace for a period of 0.5 hour at 1300 F. (It was found that the braze particles increased 1 to 2 percent in weight because of hydrogen absorption.) All of the hydrided braze material was crushed to ≤200 mesh and graded for brazing at -200/+400 mesh. High yields (>90 percent of original ingot weight) were obtained for this particle size. In fact, the material was so friable that the -100/+200 mesh fraction could not be obtained. Next, hydrogen was removed from the braze by heating in a high vacuum environment (1.0×10^{-4} Torr or better) at 1100 F. Braze holding times of 250 to 500 seconds produced the best results in subsequent brazing trials. It was found that this uniformly sized braze material performed exceptionally well in T-joint foil brazing at 1700 F. Only normal foil dissolution occurred in five brazing attempts (Fig. 152). It was concluded (tentatively) that hydriding is a suitable, high-yield procedure for procuring uniform and unsegregated fine particle sizes of Ti-47.3Zr-5.6Be alloy where required (as in-situ brazing). However, hydriding was not incorporated as a standard procedure for braze alloy production. Instead, homogenization heat treatment of button ingots (prior to crushing) was developed and established as a means to minimize beryllium segregation.

3.6.6 Homogenization of Braze Alloy Powders Through Heat Treatment of Button Ingots

Differences in flow and erosion characteristics with different particle sizes of arc-melted CS13-5 alloy were observed in preceding studies, and were found to be the result of increasing beryllium content with finer mesh sizes (Table LV). It was,

TABLE LV

CHEMICAL ANALYSES OF ARC-MELTED AND ARC-MELTED PLUS HOMOGENIZED CS13-5 AND RM8 BRAZE ALLOYS

Mesh Size	Weight Percent Beryllium in CS13-5		RM8 (homogenized)(2)	
	Arc Melted	Homogenized(1)	Weight Percent Nickel	Weight Percent Beryllium
+12	4.90	5.90	4.45	0.94
-12/+24	5.30	6.20	11.1	2.09
-24/+35	5.55	6.35	9.86	2.07
-35/+48	5.70	6.40	11.1	2.10
-48/+100	5.50	6.45	10.6	2.04
-100/+200	6.60	6.50	11.5	2.03
-200/+400	8.00	6.30	13.2	1.98
-400 (fines)	13.40	--	6.61	1.36

1. At 1450 F for 40 hours
2. At 1200 F for 65 hours

therefore, considered advisable to investigate thermal homogenization of braze alloys prior to ingot comminution. The CS13-5, CS217, CS217C, CS217G, RM1, RM23 RM32, RM40, RM42, and RM44 alloys were homogenized at 1450 F for 40 hours in high vacuum (1.0×10^{-5} Torr). In addition, the CS217E, CS217F, CS217I, RM8, RM12, RM26, RM28, and RM33 alloys were homogenized at 1200 F for 65 hours in high vacuum prior to comminution and brazing studies. As shown in Table LV, the chemical analyses of homogenized CS13-5 and RM8 resulted in very uniform compositions for the critical elements (beryllium and nickel) in various useful mesh sizes. The low nickel and beryllium levels observed in the coarsest mesh size (+12) of RM8 were probably due to incomplete solution of the alloy in acid during analysis, as coarse particles are quite difficult to dissolve. Microstructural examination of homogenized buttons (Fig. 153) showed considerably greater uniformity in the structure, whereas examination of arc-melted buttons (Fig. 154) revealed nonuniformity in many cases. The vacuum homogenizing treatment thus promoted a uniform alloy structure and composition, and was adopted as a necessary step for all braze alloy ingots prior to use.

3.3.7 Preliminary Studies of Cyclic Annealing

One feasible means found for inducing beryllide spheroidization and obtaining more uniform beryllide distribution in CS series brazements was a special heat treatment called "cyclic annealing". Cyclic annealing takes advantage of higher beryllium (and beryllide) solubility in the high temperature titanium (β phase) form than in the low temperature (α phase) form (Ref. 103). Cyclic heating between two temperatures, the higher of which progressively dissolves portions of both massive and eutectic beryllides in the beta-titanium matrix, while the lower temperature reprecipitates fine beryllides at different locations within the alpha matrix, was found to result in rounded (spheroidized) and more uniformly redistributed beryllides. (The analogy of cyclic annealing low alloy steels to promote spheroidized carbides is well known.)

Exploratory tests were conducted with 0.006-inch Ti-5Al-2.5Sn T-joints which were vacuum brazed with CS13-5 and CS217C braze alloys (five minutes at 1620 and 1700 F, respectively). Cyclic annealing over the temperature range of 1300 to 1550 F was conducted to the following parameters.

- Hold ten minutes at 1550 F, cool at rate of 12-1/2 degrees F/minute to 1300 F.
- 1300 F, hold ten minutes, then reheat to 1550 F at 12-1/2 degrees F/minute.
- Repeat the preceding steps through 12 cycles (4 hours total time), then furnace cool to room temperature.

As shown in Figures 155 and 156, the cyclic annealing resulted in a very marked definition of β-bridge structures, as well as an obviously spheroidized eutectic structure. Spheroidization later was confirmed by electron microscope. No decrease in eutectic hardness due to beryllide spheroidization was detected. However, cyclic annealing brazed T-joints of CS13-5 for a four-hour period permitted very good retention of joint strength throughout a 62-hour, 1000 F aging treatment in argon, while the as-brazed specimens suffered appreciable strength deterioration (Table LVI).

3.6.8 Effect of Salt Spray Environment Upon Braze Joint Strength

Although the braze alloy Ti-47.2Zr-5.6Be appeared promising from the viewpoints of adaptable braze processing and apparent resistance to salt spray corrosion, no measurement was available to gage braze joint strength (baseline) and retention of

TABLE LVI

CHANGE IN MECHANICAL PROPERTIES OF BRAZED T-JOINTS EFFECTED BY AGING

Alloy	Test	As-Brazed	After Aging (1)	After Cyclic Annealing	After Cyclic Annealing and Aging
CS13-5	T-joint tensile (ksi)	107.5, 107.5	63.0, 43.0	150.3	168.0(PM), 139.0
CS13-5	Lap-joint peel (lb./in.)	744 lb/in.	920, 627 lb/in.	950 lb/in.	670 lb/in.

1. 1000 F for 62 hours in Argon.

braze strength following exposure to salt spray. To measure these properties, large-base T-joints were made of 0.010-inch Ti-6Al-4V foils which were adaptable to tensile testing. Brazements were made in high vacuum at 1700 F, using Heat No. 13-4 (-12/+24 mesh particle size) and a five-minute braze cycle (rapid cooling rate).

Comparable large base T-joints were vacuum brazed with Ag-10Sn alloy, using the same braze cycle at 1700 F. These silver-base joints were considered standards for comparison of strength and corrosion-influenced properties. Standard foil tensile specimens of 0.010-inch Ti-6Al-4V alloy also were included to determine the effects of salt spray in the absence of braze. Tensile tests were conducted at room temperature; T-joint tensile tests were conducted both in the as-brazed condition and after exposure to salt spray for various times up to 238.5 hours. Results are listed in Table LVII.

As expected for the Ti-6Al-4V foil specimens (P series), the salt spray exposure up to 238.5 hours had no effect upon fully heat treated strength or ductility properties (e.g., ~150,000 psi, ultimate tensile strength; ~ 10 percent elongation).

The T-joints brazed with Ti-47.2Zr-5.6Be alloy (C series) fared quite well in salt spray, based upon metallographic examination both before and after tensile testing; and as shown in Figure 157, no signs of structural deterioration were found due to the salt spray exposure. The as-brazed tensile strength of ~132,000 psi was a good indication of the high inherent strength of the eutectic braze structure. However, the erratic and unsystematic variation of T-joint strength following different exposures to salt spray served to point out problems of structural instability, marginal

TABLE LVII

ROOM TEMPERATURE TENSILE STRENGTH OF Ti-6Al-4V T-JOINTS BEFORE AND AFTER SALT SPRAY EXPOSURE

Specimen Number	Salt Spray Exposure (hr)	Braze Alloy	Ultimate Tensile Strength[2] (psi)	0.2 Percent Yield Strength (psi)	Elongation (%)	Fracture Location
P4	0.0	(1)	150,900	144,200	11.	Foil
C9	0.0	Ti-47.2Zr-5.6Be	132,400	—	—	Braze
C10	0.0	(Heat 13-4)	152,800	—	—	Braze
D9	0.0	Ag-10Sn	35,800	—	—	Braze
P7	70.0	(1)	149,500	142,900	10.	Foil
C3	70.0	Ti-74.2Zr-5.6Be	41,200	—	—	Braze
C7	70.0	Ti-47.2Zr-5.6Be	75,300	—	—	Braze
D5	70.0	Ag-10Sn	—	(Braze ment fell apart on removal from salt spray.)		
P8-3	88.5	(1)	155,700	146,700	10.	Foil
C5	88.5	Ti-47.2Zr-5.6Be	80,900	—	—	Braze
C12	88.5	Ti-47.2Zr-5.6Be	106,300	—	—	Braze
D11	88.5	Ag-10Sn	—	(Braze ment fell apart on removal from salt spray.)		
P8	112.5	(1)	151,100	142,000	12.	Foil
C8	112.5	Ti-47.2Zr-5.6Be	125,100	—	—	Braze
C11	112.5	Ti-47.2Zr-5.6Be	126,100	—	—	Braze
P6	136.5	(1)	149,300	141,800	13.	Foil
C4	136.5	Ti-47.2Zr-5.6Be	33,300	—	—	Braze
C13	136.5	Ti-47.2Zr-5.6Be	62,900	—	—	Braze
D7	136.5	Ag-10Sn	—	(Braze ment fell apart on removal from salt spray.)		
P5	160.5	(1)	149,300	143,100	10.	Foil
C2	160.5	Ti-47.2Zr-5.6Be	75,200	—	—	Braze
C14	160.5	Ti-47.2Zr-5.6Be	559,900	—	—	Braze
P2	238.5	(1)	150,300	148,300	11.	Foil
C6	238.5	Ti-47.2Zr-5.6Be	44,200	—	—	Braze

1. Foil tensile specimen (not brazed).
2. Stress in foil member at specimen failure.

braze toughness, and notch sensitivity (Table LVII). T-joint testing imposed a stringent requirement upon braze toughness because of the natural stress concentration introduced by the T-joint geometry itself, and the easy possibility of loading the joint eccentrically through slight grip misalignment and/or braze line being off-center. This was supported by the fact that all T-joint specimens invariably failed in the joint region rather than in the foil over a wide range of failure stress (33,000 to 132,000 psi). That the braze toughness is only marginal and capable of improvement was borne out by two observations:

- Following 112.5 hours exposure, duplicate tensile strength determinations averaging ~125,000 psi showed that good strength retention is possible if load alignment and other test conditions are just right. Other strength readings at different exposure times varied erratically between 33,000 and 106,000 psi; the lowest strength after salt spray still being higher than the highest strength of as-brazed silver joints.

- In spite of the high stress levels frequently imposed upon the braze itself, in only one specimen (No. C10) were cleavage cracks noted in the massive beryllide particles (Fig. 158). The important observation was, however, that not one of these cleavage cracks extended into the surrounding eutectic structure, although many cracked beryllides were seen and a nominal failure stress of 132,800 psi was recorded. Therefore, the eutectic braze structure itself possesses a fair degree of toughness and notch insensitivity, with the possibility of improvement through heat treatment.

Whatever the interpretation of test data, one conclusion was evident; the Ti-Zr-Be alloy brazements exhibited vastly superior resistance to salt spray corrosion relative to the Ag-10Sn brazements. All silver-brazed specimens exposed ≥70 hours suffered severe crevice corrosion, predominantly along the TiAg/Ag interface, rendering them incapable of being tested. Simply touching them for visual examination resulted in their falling apart at the braze joint lines.

3.6.9 Preliminary Assessment of Elevated Temperature Brazement Strength

To gage the applicability of Ti-47.2Zr-5.6Be brazements at elevated temperatures, duplicate T-joint tensile tests were conducted at both room temperature and 800 F (as-brazed condition). The T-joint specimens consisted of 0.004-inch Ti-5Al-2.5Sn foil alloy brazed to a 0.0125-inch base of the same alloy; the results are shown in Table LVIII.

Obviously, the Ti-47.2Zr-5.6Be alloy provided sufficient brazement strength at the elevated temperature of 800 F to warrant its further evaluation in Phase I studies.

TABLE LVIII

ELEVATED TEMPERATURE STRENGTH OF Ti-47.2Zr-5.6Be BRAZEMENTS

Braze Alloy	Test Temperature (F)	Stress Level in Foil at Specimen Failure (psi)	Failure Location
Ti-47.2Z4-5.6Be (Heat No. 13-4)	Room	111,100	Braze material
	Room temperature	74,600	Braze material
	800 (1)	77,300	Braze material
	800 (1)	90,700	Braze material
Baseline Foil Properties (typical values)	Room temperature	115,000 to 120,000	--
	800	70,000 to 75,000	--

1. Held 0.5 hour at temperature (in air) prior to test.

3.6.10 Strain Accommodation Ability of Braze Alloys

Under ordinary circumstances, greater interest is expressed in the shear strength or toughness of a braze joint than in the ability of the braze alloy to withstand large strains imposed by loads. Braze alloys for foil structures must operate in the same strain field as the foil without failure. It, therefore, becomes necessary to devise some method of determining the maximum strain the braze alloy can withstand before fracture. To make this determination, a tapered tensile specimen was prepared with a groove to hold a thin film of the braze alloy, as illustrated in Figure 159. The Ti-47.2Zr-5.6Be and Ag-10Sn braze alloys were applied to the specimens by the developed vacuum brazing processes. As each specimen was loaded in tension, a linear stress and strain gradient existed along the tapered section in accordance with the change in cross-sectional area. The specimens with the Ti-47.2Zr-5.6Be alloy were then tensile loaded until plastic deformation occurred at the minimum cross-section. Examination of the specimen using the dye penetrant system revealed the crack pattern in the braze alloy shown in Figure 160. The first crack at the largest cross section (threshold strain) occurred at a parent metal stress of 107,000 psi, corresponding to a strain of 6700 micro in./in. A test on a second specimen gave

identical results. Shown in Figures 161 and 162 are microsections through the cracks of Figure 160. The crack which was just started at the 107,000 psi point (Fig. 161) stopped at the interface layer of the braze alloy; however, the larger crack (Fig. 162) extended approximately 0.003 inch into the parent material. This larger crack was in the region of plastic deformation for the parent material, which was subjected to a stress of approximately 120,000 psi.

A specimen tested with the 90Ag-10Sn silver braze alloy showed no braze cracking at all after testing to specimen failure.

The hardness of the parent material on the specimen with the Ti-47.2Zr-5.6Be braze alloy was R_C40, compared to R_C41 on the as-received material. The closeness of the two hardness values suggested little or no oxygen pickup during brazing.

The tapered tensile test is a measure of the strain sensitivity, rather than the strength of the braze alloy. Although during the test the braze alloy is required to conform to the strains in the parent material, the stresses in the braze alloy can be far different from those in the parent material. For example, the relatively weak 90Ag-10Sn alloy has high ductility, low yield strength, and low modulus, which allows the alloy to conform without cracking to the strains of the parent material up to the point of parent material failure. In contrast, the stronger Ti-47.2Zr-5.6Be alloy (with a higher modulus due to the beryllide content) tends to crack instead of yielding at strains somewhat below the yield point of the parent material.

The tests indicated that the Ti-47.2Zr-5.6Be braze alloy is capable of accommodating substrate strain almost to the point of plastic yield of the parent material. However, the braze was not as crack-resistant as the 90Ag-10Sn alloy. The tests showed also that cracks in the braze alloy can propagate into the parent material when plastic deformation occurs. The tapered tensile test specimen appeared to be a good tool for evaluating the relative strain accommodation of the braze alloys when subjected to strains from the parent material.

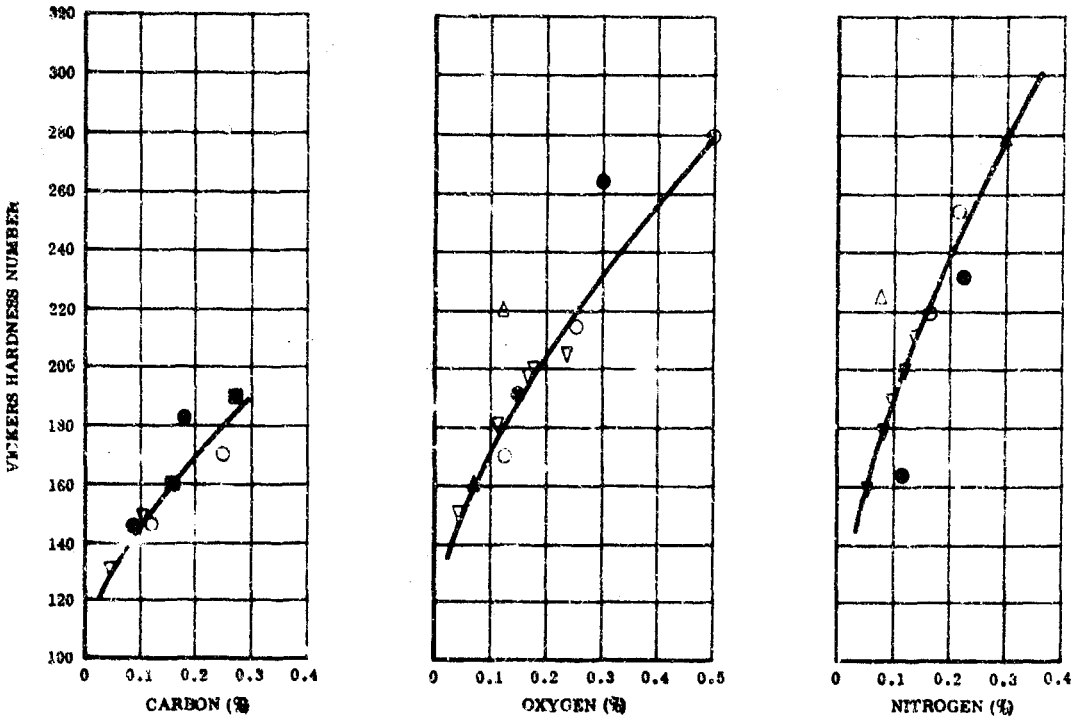


FIGURE 130. EFFECT OF CARBON, OXYGEN, AND NITROGEN ON THE VICKERS HARDNESS OF TITANIUM

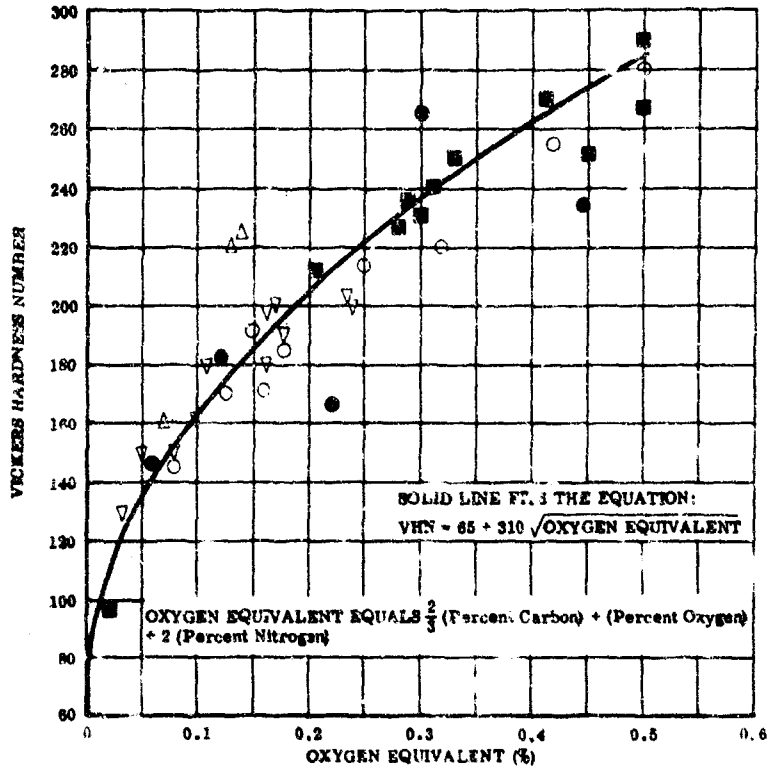


FIGURE 131. EFFECT OF TOTAL INTERSTITIAL CONTENT ON THE VICKERS HARDNESS OF TITANIUM

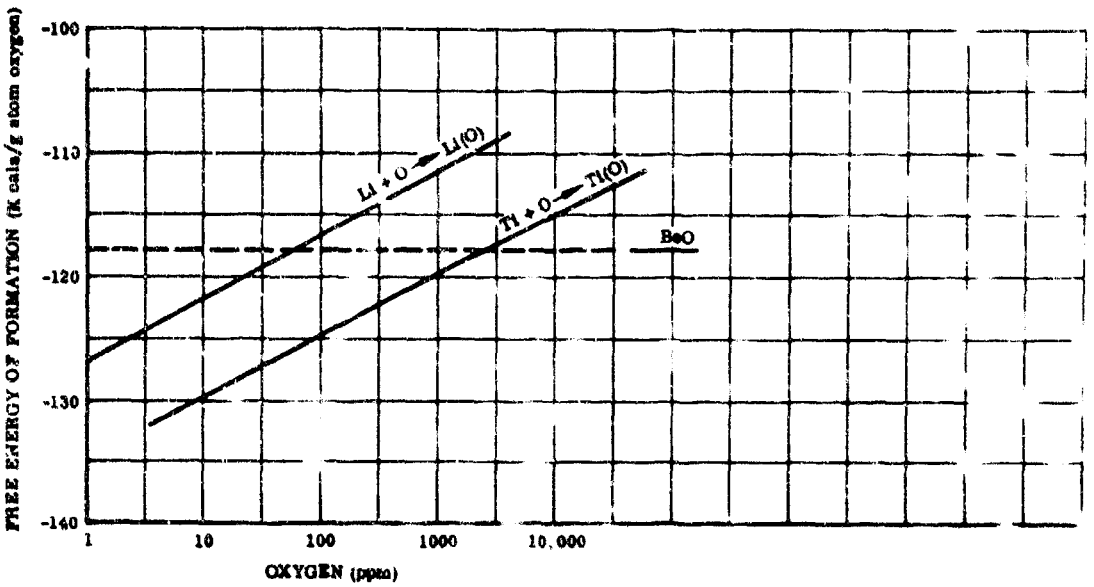
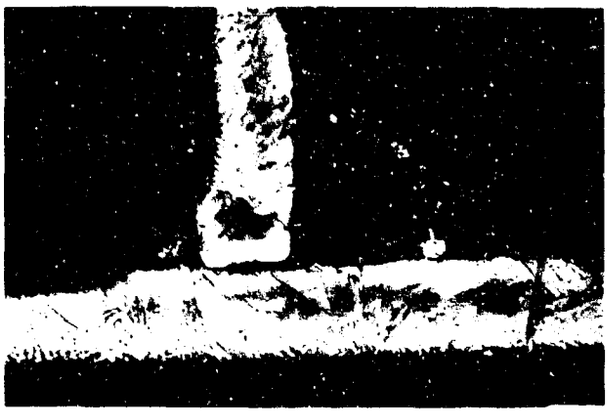
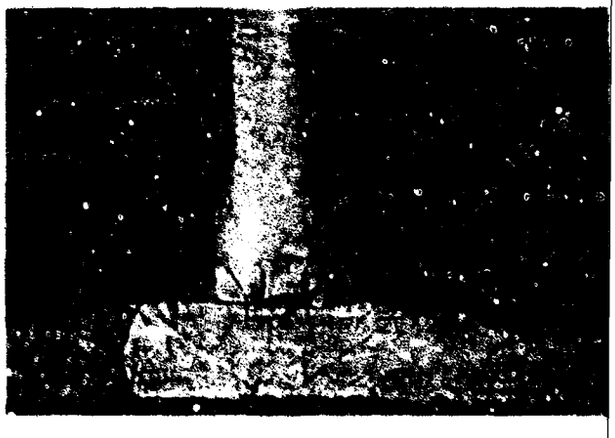


FIGURE 132. FREE ENERGY OF FORMATION OF PHASES AT 1500 K

Process Heating Rate From 1700 F	Heat No. 1-1 (2 minutes at 1700 F)	Heat No. 1-23 (2 minutes at 1700 F)
50 deg F/min		
	2000 F - R	1950 F - R
100 deg F/min		
	1950 F - R	1950 F - R
300 deg F/min		
	2000 F - R	2000 F - R

) F)

Heat No. 1-24
(2 minutes at 1700 F)





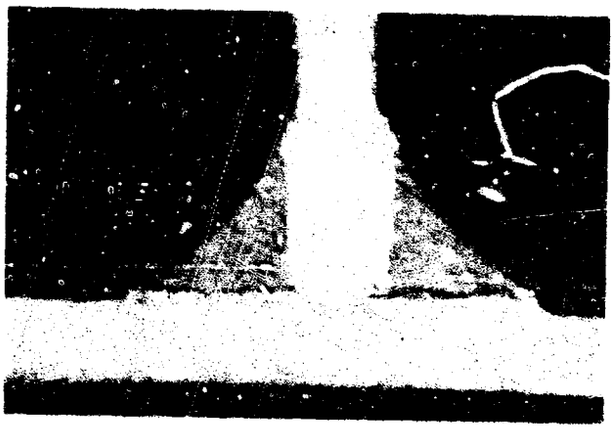
1950 F - E

Minimum braze temperature shown under each figure - dwell time at braze temperature - 1 minute

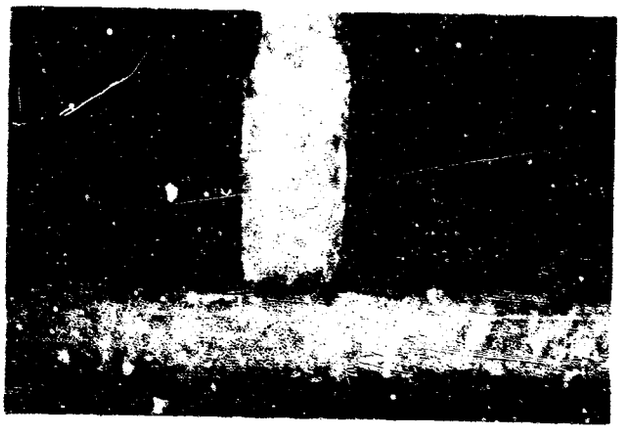
R = Unmelted residue
E = Negligible residue, excellent braze

Heat No. 1-24
(5 minutes at 1700 F)





1950 F - R



1950 F - E



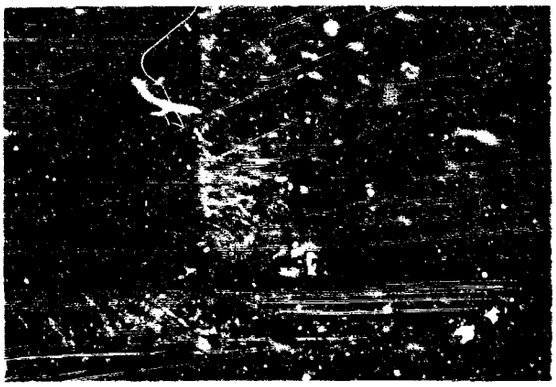
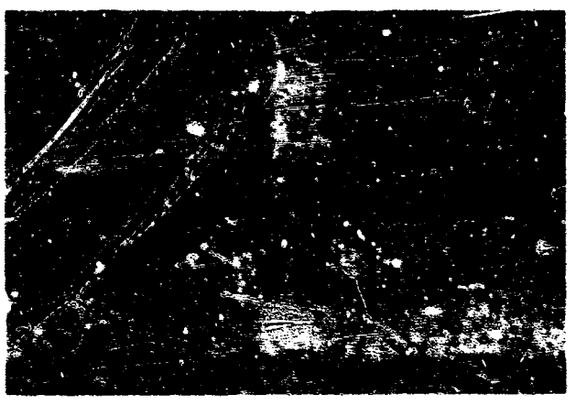
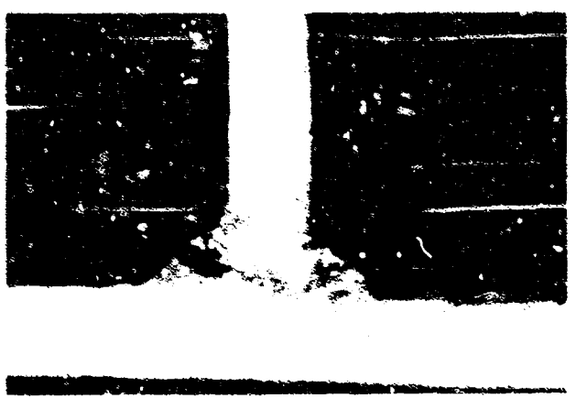


1975 F - E

FIGURE 38. TYPICAL MICROSTRUCTURES OF Ti-5Al-2.5Sn FOIL T-JOINTS BRAZED IN ARGON WITH Ti-6.0 Be BRAZE ALLOY

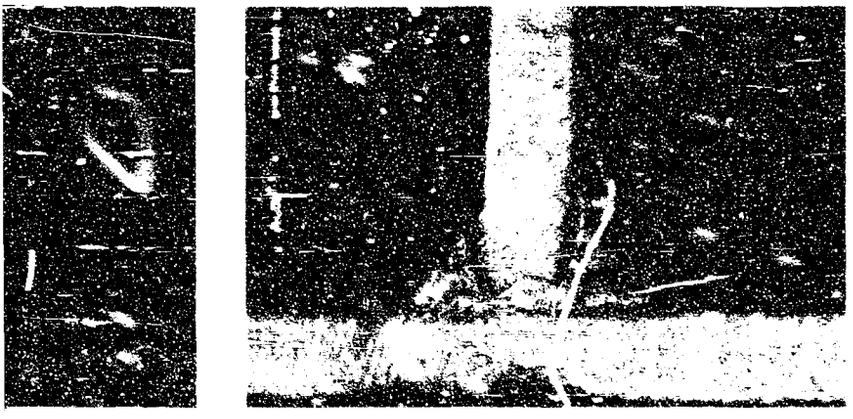
Magnification: 100X

2

Process Heating Rate From 1700 F	Heat No. 1-1 (2 minutes at 1700 F)	Heat No. 1-23 (2 minutes at 1700 F)
50 deg F/min		
	2025 F - R	1950 F - R
100 deg F/min		
	2025 F - R	2000 F - R
300 deg F/min		
	2050 F - R	1950 F - R

F)

Heat No. 1-24
(2 minutes at 1700 F)



1950 F - E

Minimum braze temperature shown under each figure - dwell time at braze temperature - 1 minute

- Unmelted residue
E = Negligible residue, excellent braze

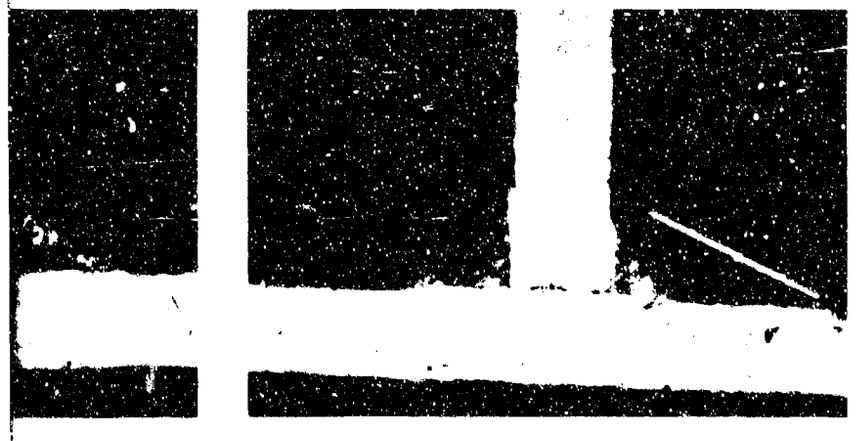
Heat No. 1-24
(5 minutes at 1700 F)



2000 F - E



1990 F - R

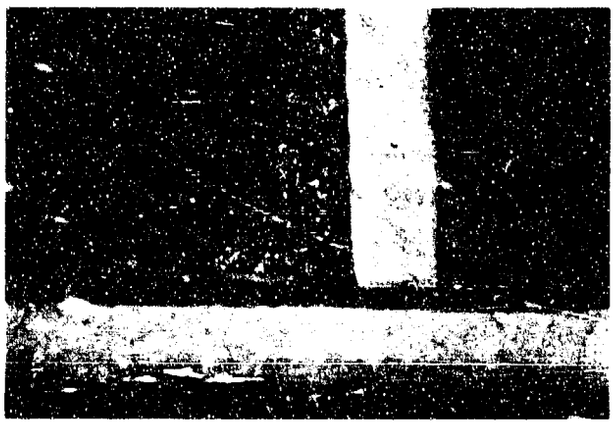
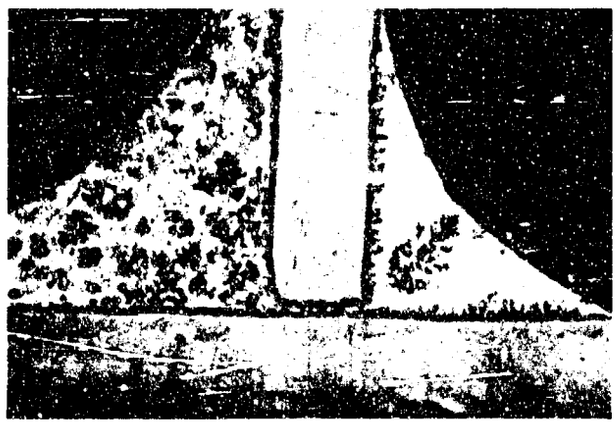


1970 F - E

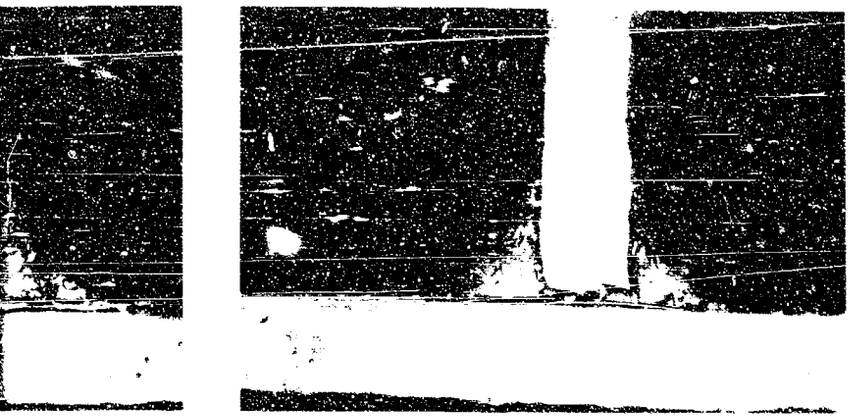
FIGURE 39. TYPICAL MICROSTRUCTURES OF Ti-5Al-2.5Sn FOIL T-JOINTS BRAZED IN VACUUM WITH Ti-5.6Be BRAZE ALLOY

Magnification: 100 X

2

Process Heating Rate From 1500 F	Heat No. 13-1 (2 minutes at 1500 F)	Heat No. 13-2 (2 minutes at 1500 F)
50 deg F/min		
	1700 F - R	1650 F - R
100 deg F/min		
	1660 F - R	1650 F - R
300 deg F/min		
	1700 F - R	1700 F - R

Heat No. 13-1
(2 minutes at 1500 F)

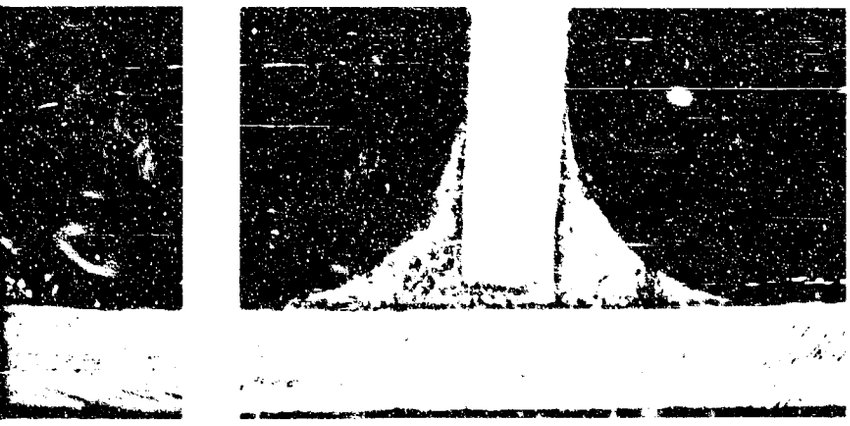


1650 F - R

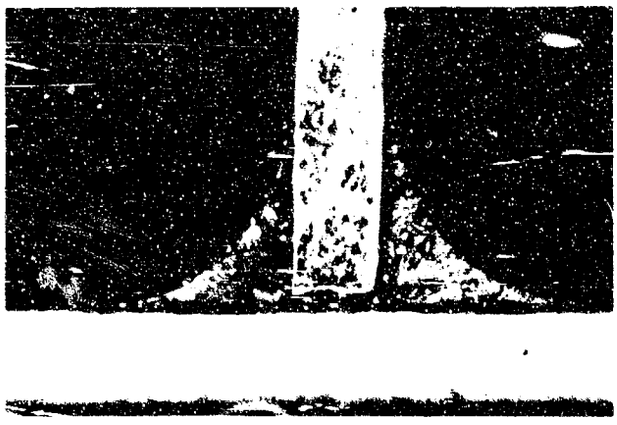
Minimum braze temperature shown under each figure - dwell time at braze temperature - 1 minute

R = Unmelted residue
E = Negligible residue, excellent braze

Heat No. 13-1
(5 minutes at 1500 F)



1700 F - E



1670 F - E



1670 F - E

FIGURE 40. TYPICAL MICROSTRUCTURES OF Ti-5Al-2.5Sn FOIL T-JOINTS BRAZED IN ARGON WITH Ti-47.2Zr-5.6Be BRAZE ALLOY

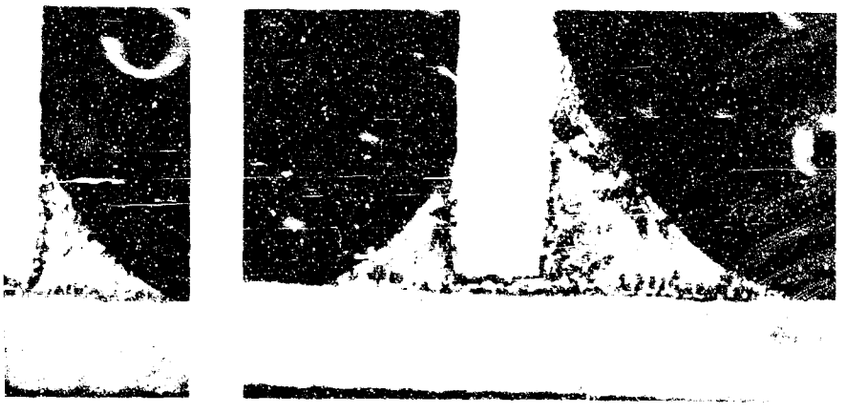
Magnification: 100 X

2

Process Heating Rate From 1500 F	Heat No. 13-7 (2 minutes at 1500 F)	Heat No. 13-8 (2 minutes at 1500 F)
50 deg F/min	 1650 F - R	 1700 F - R
100 deg F/min	 1700 F - R	 1680 F - E
300 deg F/min	 1700 F - R	 1700 F - E

F)

Heat No. 13-4
(2 minutes at 1500 F)

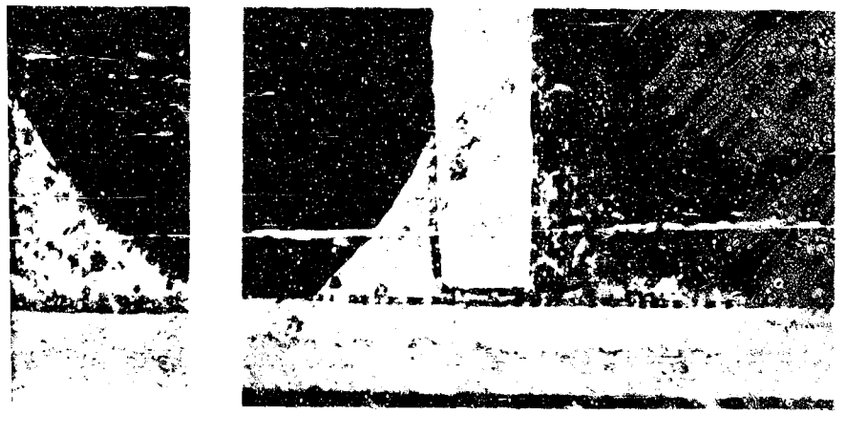


Minimum braze temperature shown under each figure - dwell time at braze temperature - 2 minute

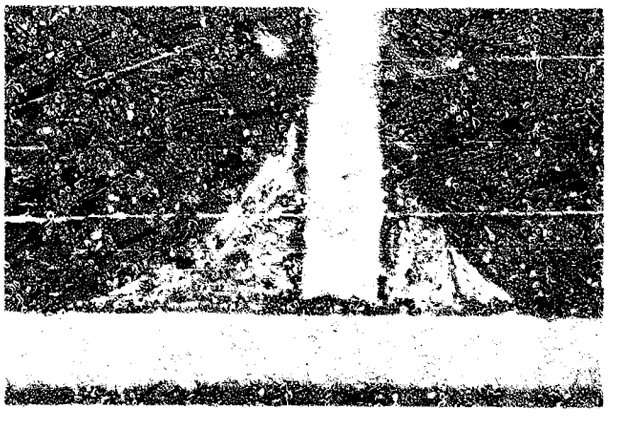
R = Unmelted residue
E = Negligible residue, excellent braze

1650 F - R

Heat No. 13-4
(2 minutes at 1500 F)



1600 F - E



1600 F - E



1620 F - E

FIGURE 41. TYPICAL MICROSTRUCTURES OF Ti-5Al-2.5Sn FOIL T-JOINTS EXCEPT BRAZED IN VACUUM WITH Ti-47.2Zr-5.3Be BRAZE ALLOY

Magnification: 100 X

2

Controlled
Cooling Rate

1000 deg
F/min

Heat No. 1-24

Braze Time - 1 minute

Braze Time

25 deg
F/min



ime - 5 minutes

Braze Time - 25 minutes

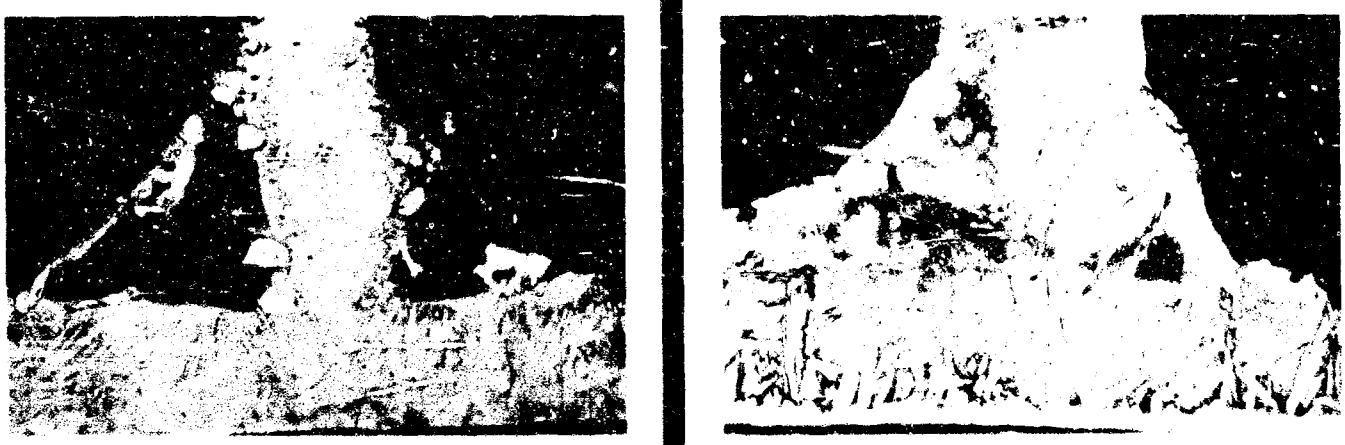


FIGURE 42. TYPICAL MICROSTRUCTURES OF Ti-5Al-2.5Sn T-JOINTS VACUUM BRAZED WITH Ti-5.6Be ALLOY AT 2000 F; Heated From 1700 F at 100 degrees F/minute

Magnification: 100 X

2

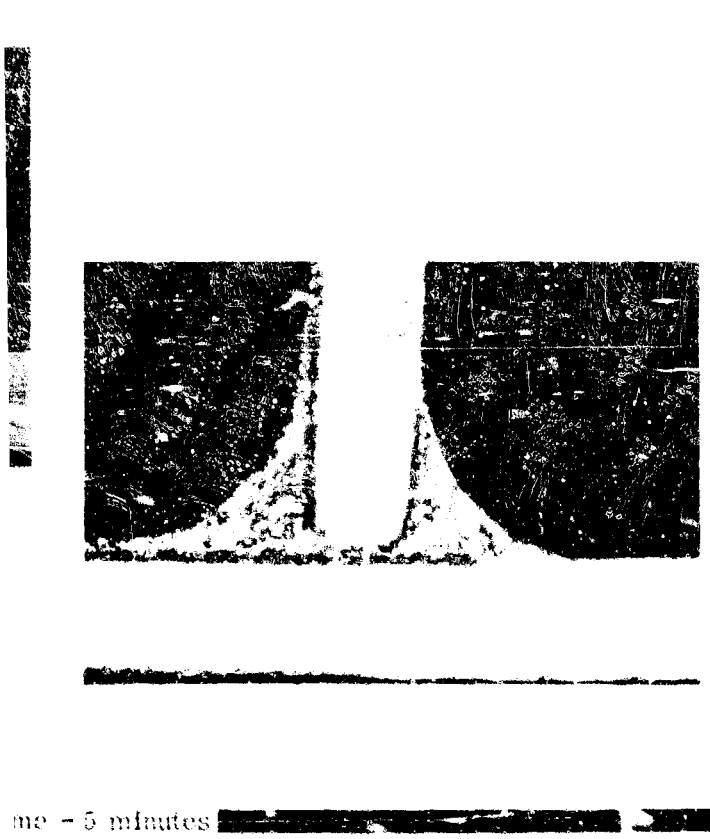
Controlled
Cooling Rate

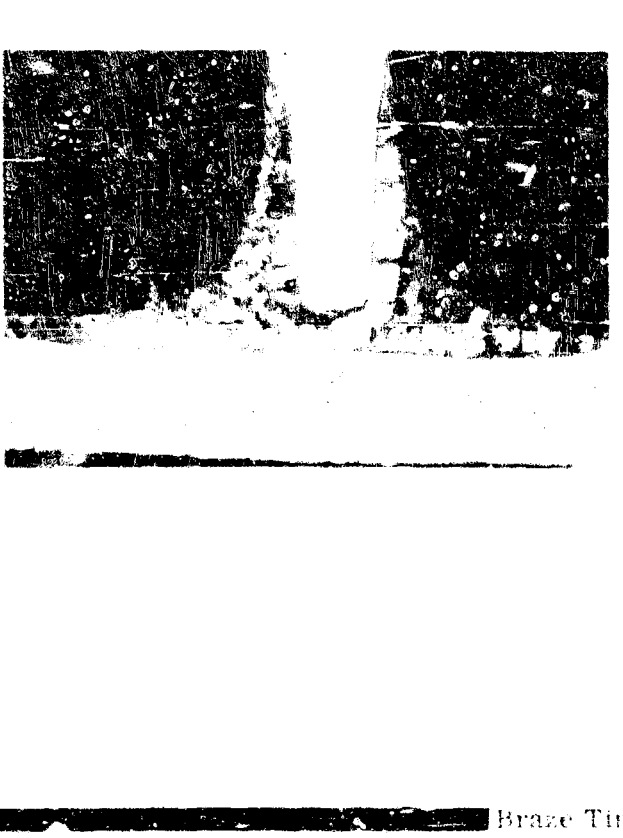
100° C g
F/min

Heat No. 15-4

Braze Time - 1 minute

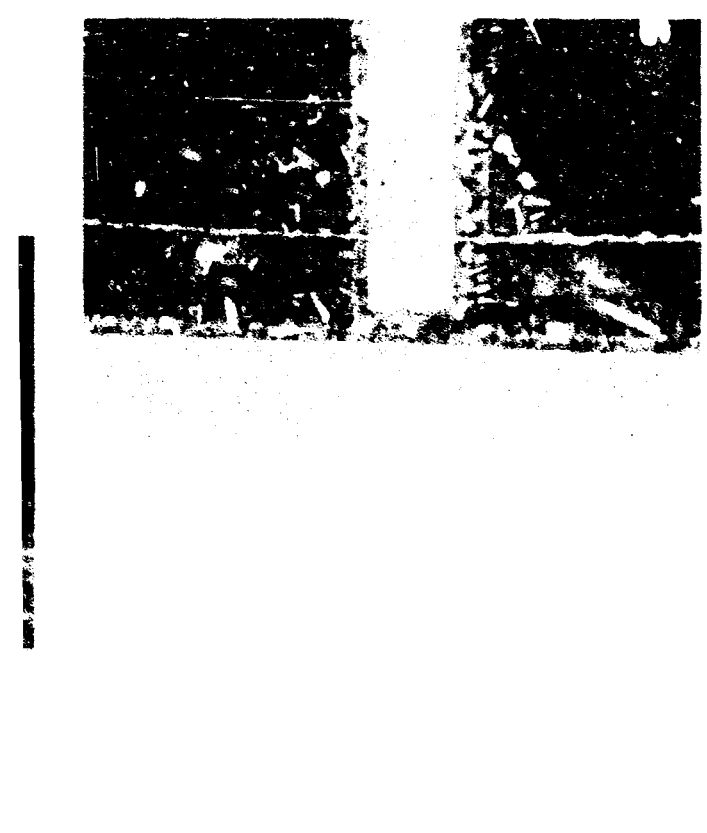
25 deg
F/min

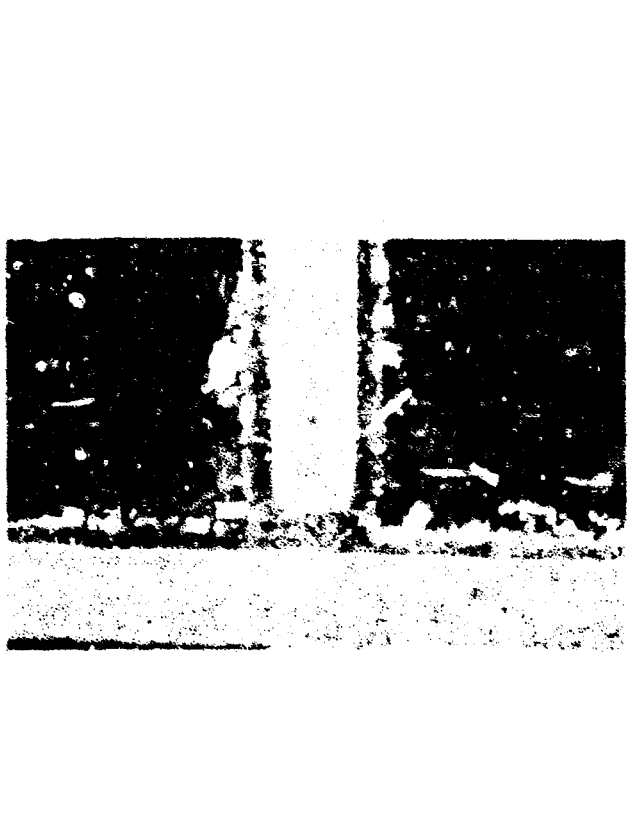


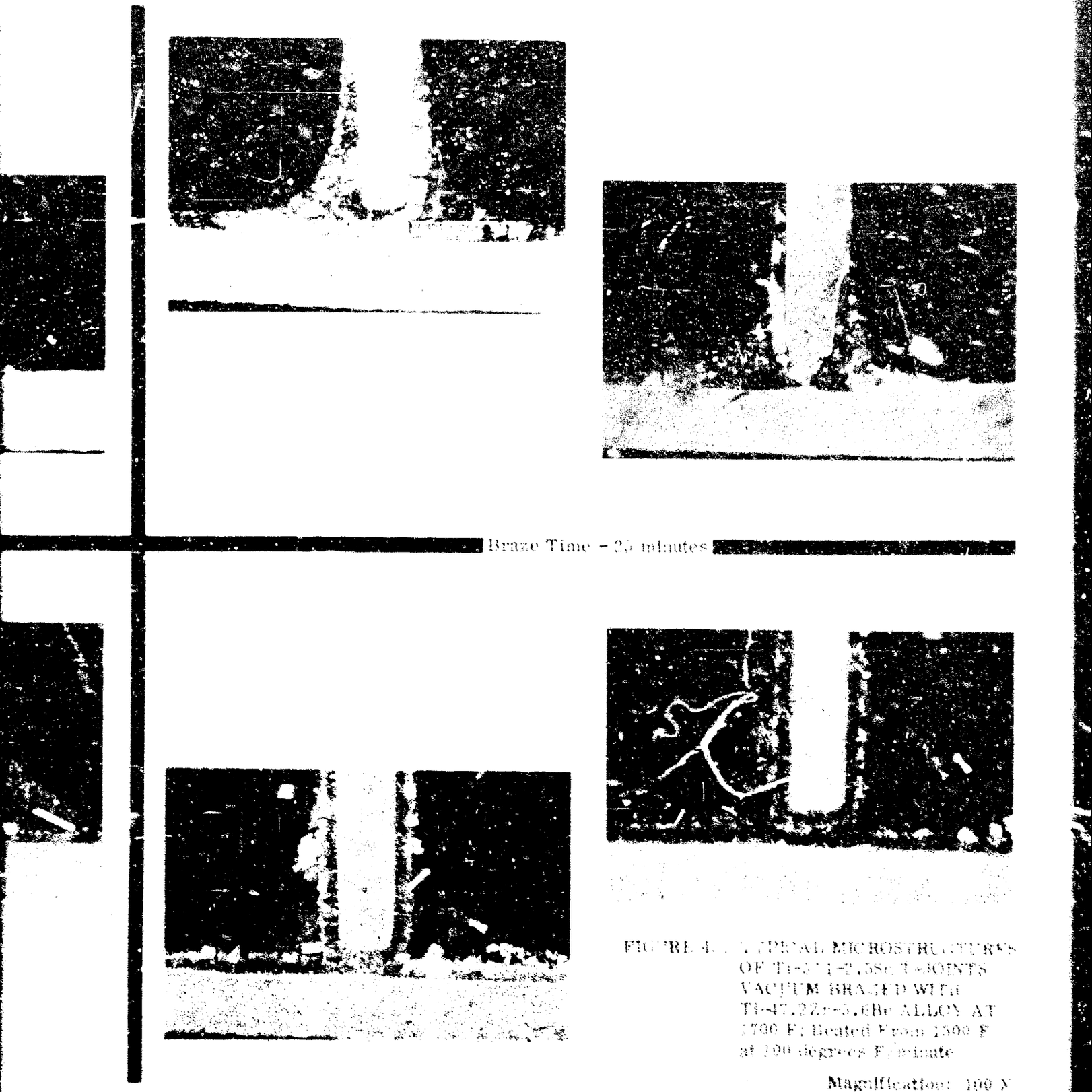


me - 5 minutes

Braze Tin - 2o







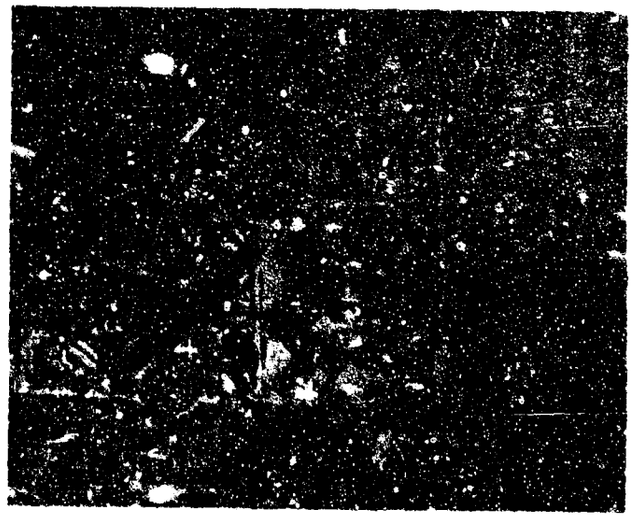
Braze Time = 25 minutes

FIGURE 4. TYPICAL MICROSTRUCTURES OF Ti-6Al-2.5Sn T-JOINTS VACUUM BRAZED WITH Ti-47.2Zr-5.0Be ALLOY AT 1700 F, Heated From 1500 F at 100 degrees F/minute

Magnification: 100 X

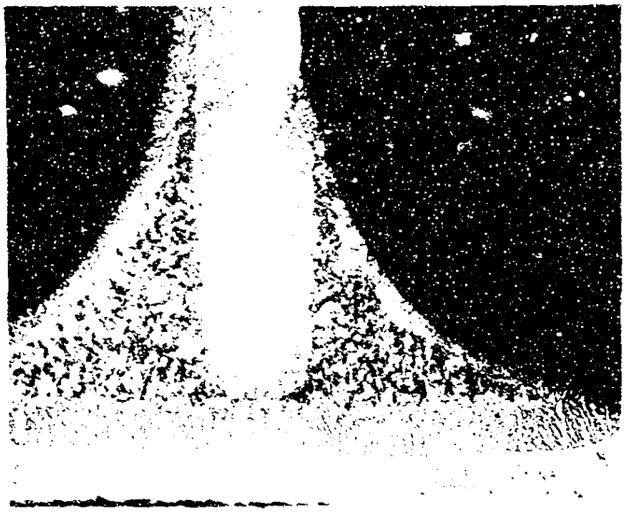


Magnification: 100X



Magnification: 250X

FIGURE 139. CS13-5 BRAZE JOINT; 1825 F for 60 Minutes



Magnification: 100X

FIGURE 140.

PMS BRAZE JOINT; 1825 F
for 60 Minutes

Magnification: 100X

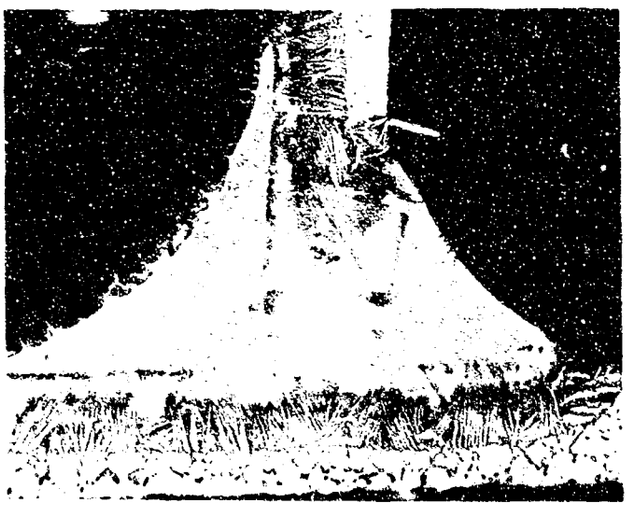
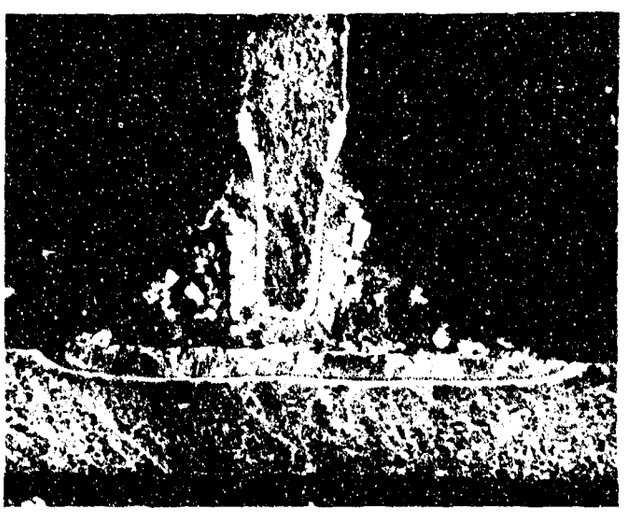


FIGURE 141.

RM1 BRAZE JOINT; 1825 F
for 60 Minutes



Magnification: 100X

FIGURE 142.

CS13-5 BRAZE JOINT; 1700 F
for 30 Minutes



Magnification: 100X

FIGURE 143.

RM8 BRAZE JOINT: 1700 F
for 30 Minutes



Magnification: 100X

FIGURE 144.

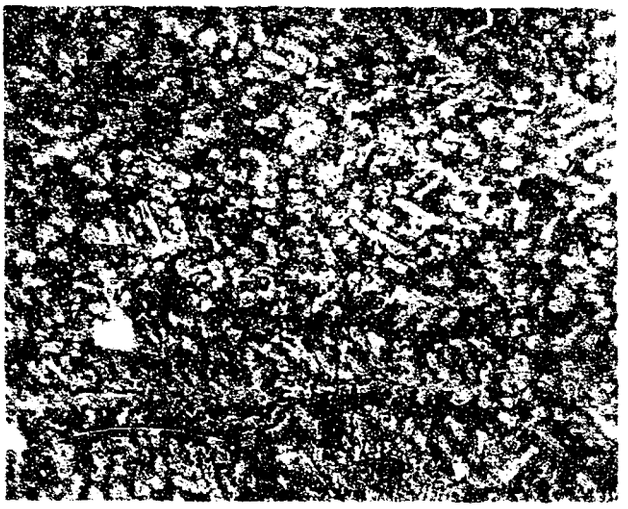
RM8 BRAZE JOINT; 1600 F
for 30 Minutes



Magnification: 100X

FIGURE 145.

RM8 BRAZE JOINT; 1500 F
for 30 Minutes



Heat No. 1-1
Etchant: Kroll's
Magnification: 100X

Grey matrix phase is the titanium solid solution; light-etching phase is the first titanium beryllide

Heat No. 1-23
Etchant: Kroll's
Magnification: 100X

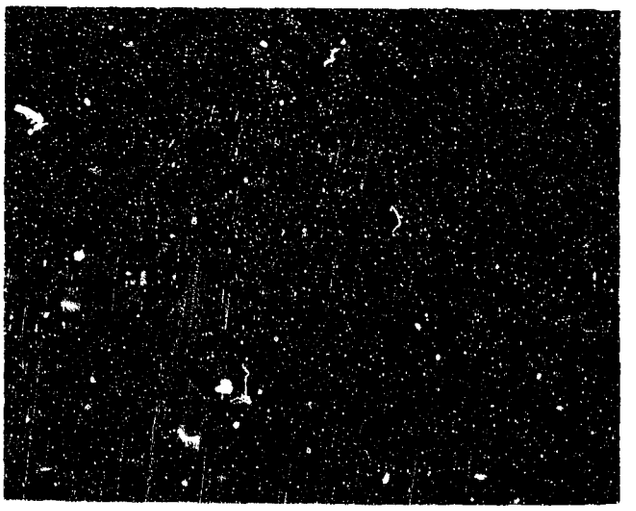
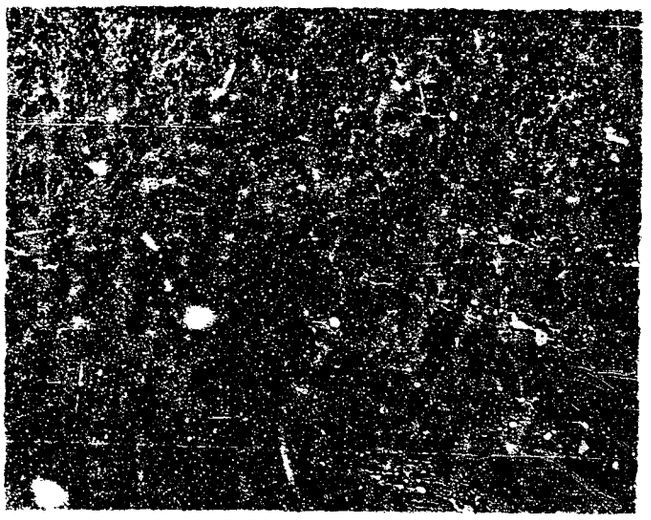


FIGURE 146. TYPICAL EUTECTIC STRUCTURES IN ARGON ARC-CAST INGOTS OF Ti-5.6Be ALLOY



Heat No. 13-5
Etchant: Kroll's
Magnification: 250X

Continuous matrix phase is the terminal Ti-Zr solid Solution; the light etching dendritic structure represents the first beryllide phase

Heat No. 13-1
Etchant: Kroll's
Magnification: 100X

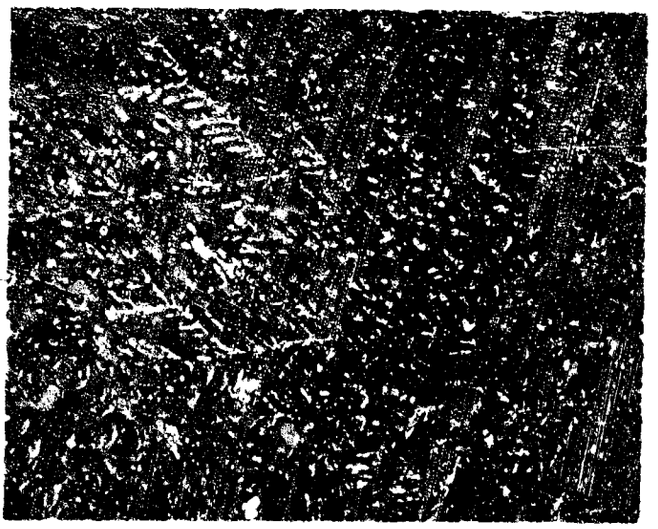
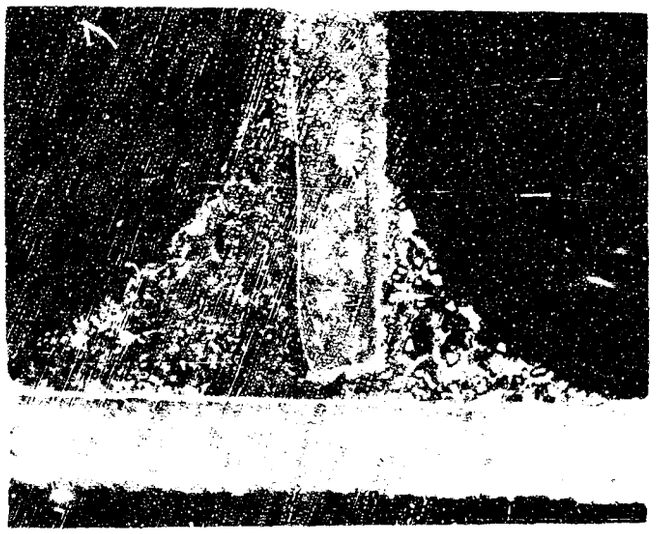


FIGURE 147. TYPICAL EUTECTIC STRUCTURES IN ARGON ARC-CAST INGOTS OF Ti-47.2Zr-5.6Be ALLOY



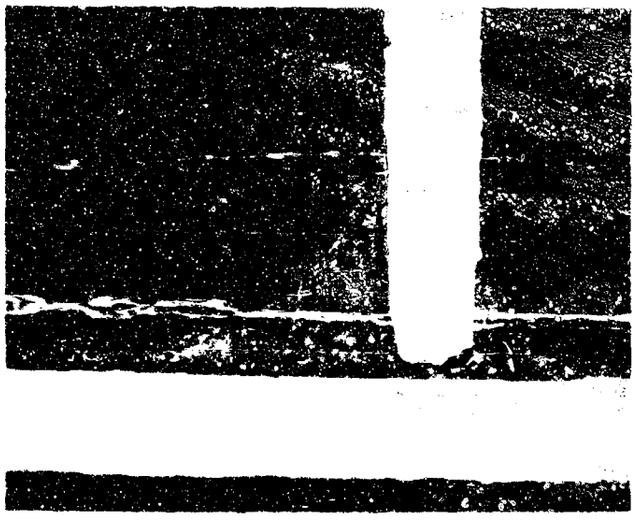
A.
Heat No. 13-4
(-48/+100 mesh)
Etchant: Kroll's
Magnification: 100X

FOILS: Ti-5Al-2.5Sn
(0.006 inch)



B.
Heat No. 13-4
(-12/+25 mesh)
Etchant: Kroll's
Magnification: 100X

FIGURE 146. FOIL T-JOINTS MADE WITH VARIOUS PARTICLE SIZE OF HEAT 13-4; Vacuum Brazed, 1700 F - 5 Minutes (Sheet 1 of 2)



C.
Heat No. 13-4
(-200/+4[illegible] mesh)
Etchant: Kroll's
Magnification: 100X

FOILS: Ti-5Al-2.5Sn
(0.606 inch)



D.
Heat No. 13-4
(-100 mesh)
Etchant: Kroll's
Magnification: 100X

FIGURE 148. FOIL T-JOINTS MADE WITH VARIOUS PARTICLE SIZE OF HEAT 13-4; Vacuum Brazed, 1700 F - 5 Minutes (Sheet 2 of 2)



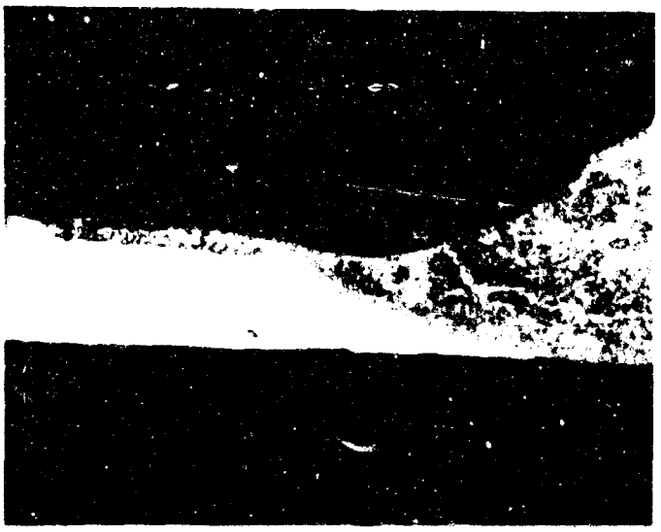
Heat No. 13-5
1650 F
(-100/+200 mesh)

Etchant: Kroll's

Magnification: 100X

Cycle: 1650 to 1700 F, 5 minutes (vacuum)

Foils: Ti-5Al-2.5Sn (0.006 inch)



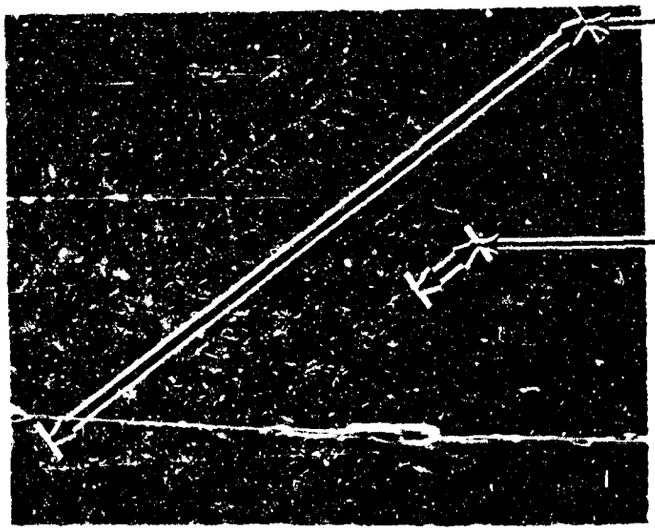
Heat No. 13-4
1700 F
(-140/+200 mesh)

Note portion of horizontal component of the T-joint

Etchant: Kroll's

Magnification: 100X

FIGURE 149. FOIL DISSOLUTION AND EROSION OBTAINED WITH PARTICLE SIZE -100/+200 MESH Ti-47.2Zr-5.6Be ALLOY



Etchant: Kroll's

Magnification: 100X

FIGURE 150.

RELATIVE MESH PARTICLE SIZES IN A CAST STRUCTURE; Heat No. 13-5



Heat No. 13-5
1650 F
(-100/+200 mesh)
Etchant: Kroll's
Magnification: 100X

Material from the same batches produced severe erosion in previous tests (Fig. 119)

Heat No 13-4
1700 F
(-100/+200 mesh)
Etchant. Kroll's
Magnification: 100X

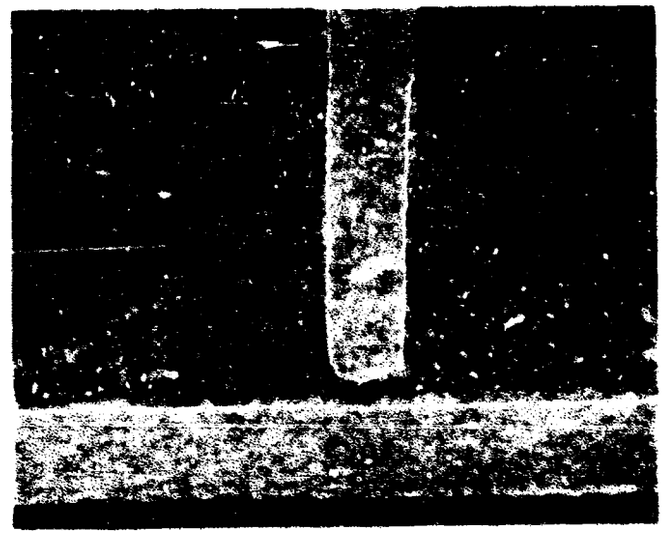
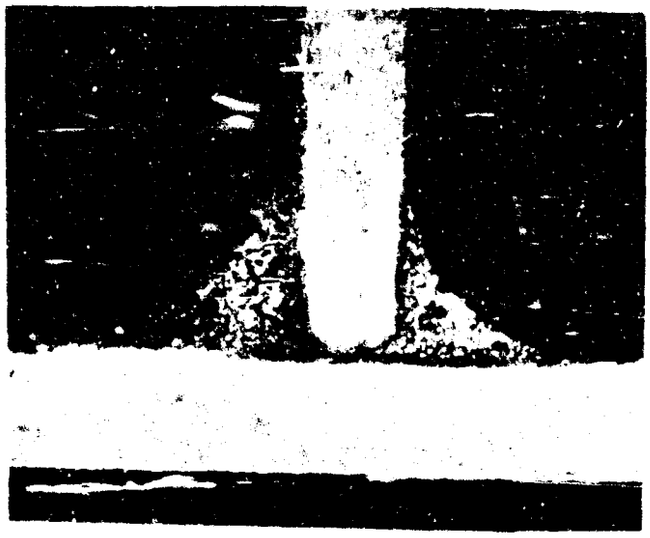


FIGURE 151. FOIL T-JOINT STRUCTURES OBTAINED WITH -100/+200 MESH PARTICLES

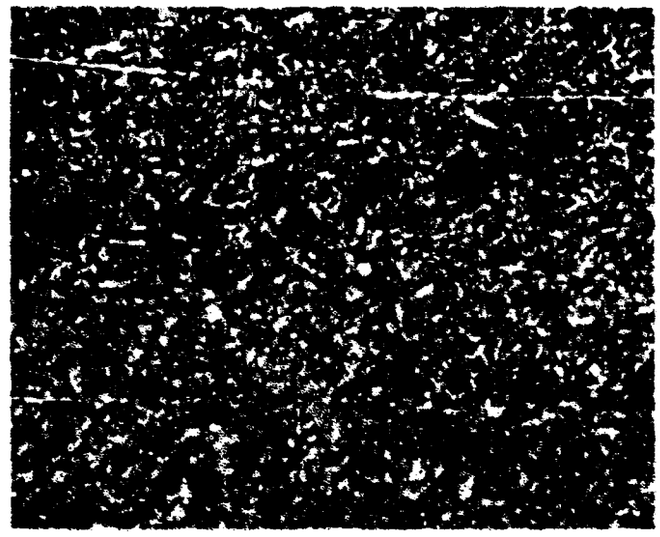


Etchant: Kroll's

Magnification: 100X

FIGURE 152.

TYPICAL FOIL BRAZE STRUCTURE OBTAINED WITH -200/+400 MESH PARTICLES



Homogenized 1450 F for 40 Hours

Magnification: 250X

FIGURE 153.

HOMOGENIZED RM40 ALLOY BUTTON INGOT



Arc Melted

Magnification - 250X

FIGURE 154.

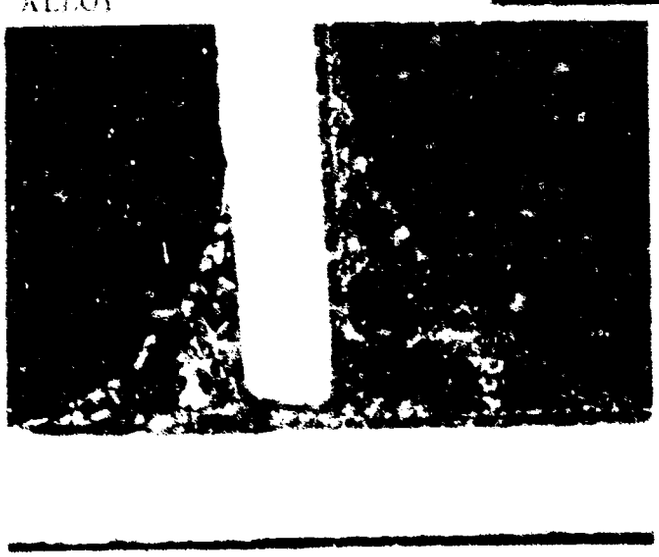
ARC-MELTED RM40 ALLOY BUTTON INGOT



Magnification - 100X

FIGURE 155.

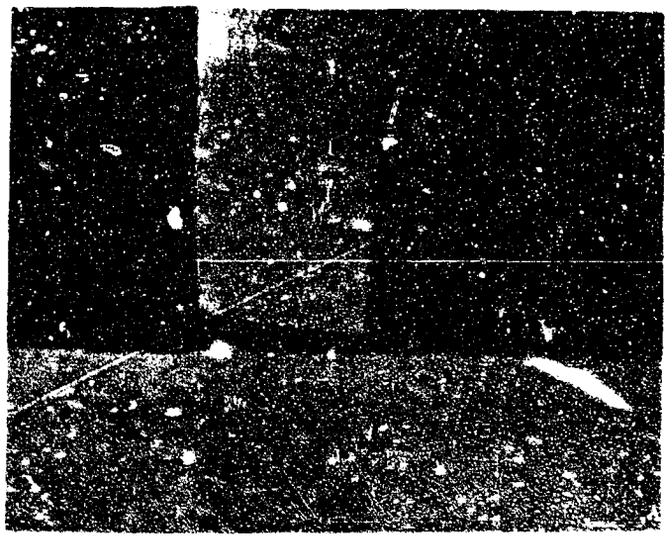
TYPICAL AS-BRAZED STRUCTURE, CSI3-5 HOMOGENIZED ALLOY



Magnification - 100X

FIGURE 156.

BRAZE STRUCTURE AFTER CYCLIC ANNEAL, CSI3-5 HOMOGENIZED ALLOY



Braze Alloy: Ti-47.2Zr-5.6Be
(Heat No. 13-4)

Foil Thickness: 0.010 inch

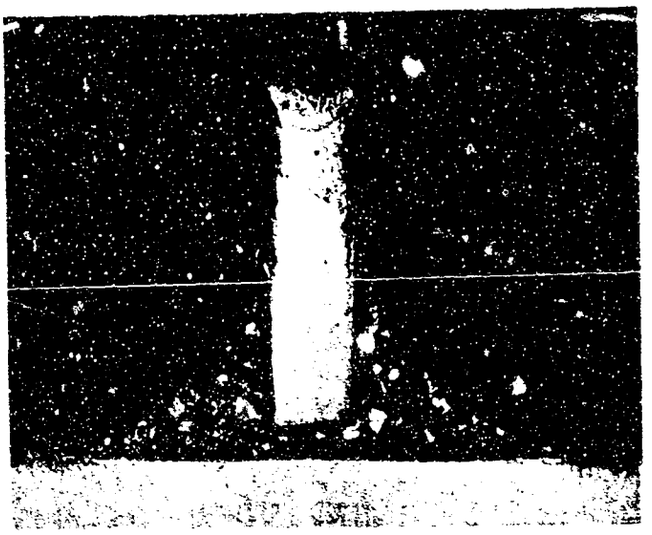
Etchant: Kroll's

Magnification: 50X

No Evidence of Corrosion

FIGURE 157.

STRUCTURE OF Ti-6Al-4V T-JOINT AFTER 112.5 HOURS SALT SPRAY EXPOSURE



Heat No. 13-4
Etchant: Kroll's
Magnification: 50X

Stress in Titanium Foil at Failure:
132,800 psi Specimen No. C10

Heat No. 13-4
Etchant: Kroll's
Magnification: 250X



FIGURE 158. CLEAVAGE CRACKS IN MASSIVE BERYLLIDE PARTICLES WITHIN THE BRAZE

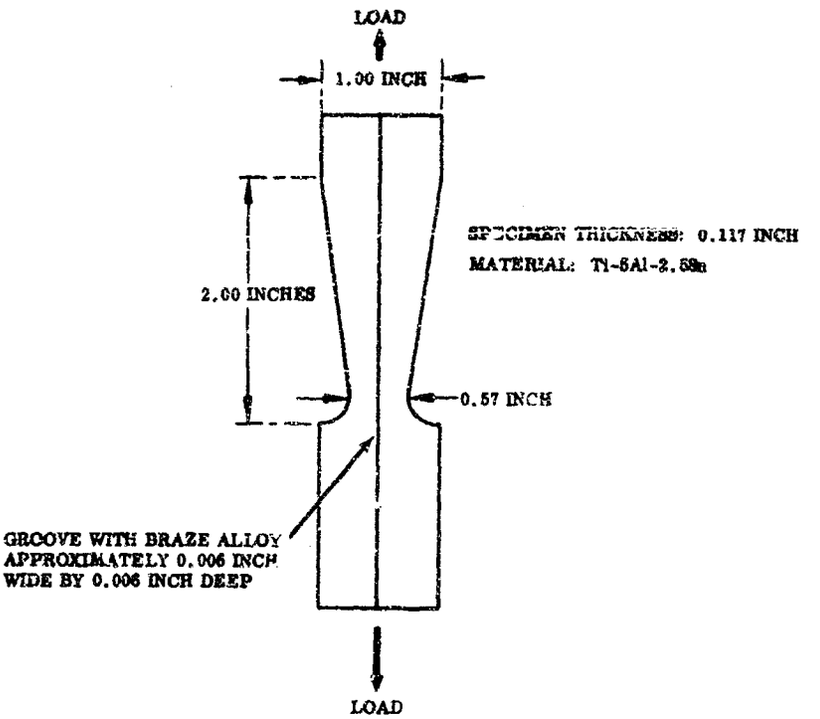
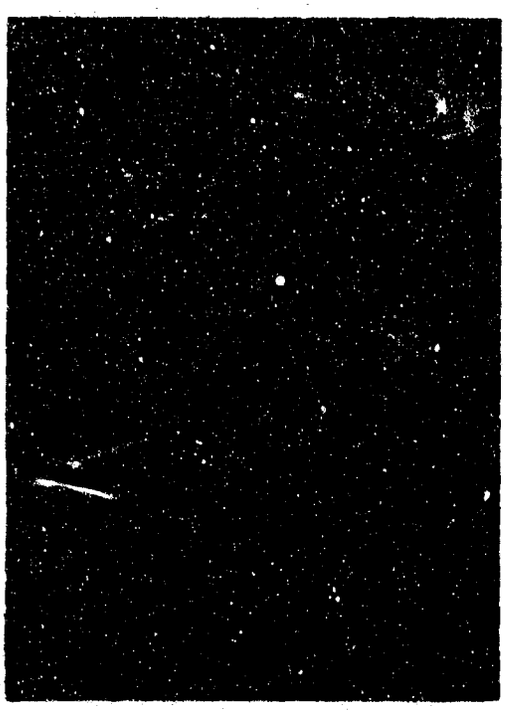


FIGURE 159. TAPERED TENSILE SPECIMEN WITH GROOVE



Magnification: 2X

FIGURE 160.

CRACK PATTERN IN Ti-47.2 Zr-5.6 BRAZE ALLOY AFTER TENSILE LOADING



Magnification: 250X

FIGURE 161.

CROSS SECTION OF CRACK IN BR E ALLOY; Strain Approximately 6700 Microinches/ Inch

Magnification: 250X



FIGURE 162.

CROSS SECTION OF CRACK IN BRAZE ALLOY AND PARENT METAL; Stress of 120,000 psi

3.7 TASK VII - DIFFUSION BONDING DEVELOPMENT

The principal objective of the diffusion bonding study was to determine the feasibility of making reliable, leak-tight, tube-to-header joints using a self-diffusion bonding process. The bonding processes were chosen to incorporate:

- A means of pressurizing the tube-to-header joint interface by expansion of the tube.
- A means to heat the interface to the proper process temperature and for the necessary time to permit bonding.
- An environment to prevent surface contamination which would inhibit bonding.

The complexity of the joints precludes diffusion bonding by conventional mechanical devices (anvil bonders); and the small diameter and tight spacing of the tubes impose severe limitations on the type of mechanical device which can be used internally. Differential thermal expansion and pneumatic pressurization of internal cylinders were the two methods selected as best filling the requirements of the bonding process.

Establishing an effective diffusion bonding process is principally a matter of satisfying the pressure-temperature-time requirements which control the bonding mechanisms (which, in turn, are functions of the interdiffusion rate, flow stress, and cleanliness of the faying surfaces). The upper temperature limit is imposed by the beta transus of the titanium, or by the tendency toward sticking or forming a low-melting eutectic with the bonding tool. The lower limit is imposed by the relationship of temperature and pressure which expresses the necessary minimum conditions for bonding. Similarly, pressure and time must be adjusted to remove the oxide film on the joint surfaces either by self-disolution or film rupturing (fragmentation). Further controls are imposed by the need for active interdiffusion of surface species without dissipation of pressure by creep and/or distortion. It should be noted that all of these relationships are functions of atomic diffusion rates and are exponential with respect to time.

3.7.1 Diffusion Bonding Parameters

An investigation was initiated to develop the solid-state diffusion bonding parameters needed to join Ti-3Al-2.5V tubes to Ti-6Al-4V headers. Other titanium alloy combinations included for study are listed in Table LIX. Establishment of minimum parameter levels of bond pressure, time, and temperature was undertaken

TABLE LIX

COMPLETE LIST OF DIFFUSION BONDED JOINTS

Log No.	Joint Foil Materials	Bonding Parameters		Electrode Surfaces and Stop Offs Used	Electrode Sticking	Tapered Lap Joint Pull Test		Micro-Structure
		Temperature (F)	Pressure (psi)			Failure Location	Load (T)	
1202	Ti-5Al-2.5Sn to Ti-5Al-2.5Sn	1825	1200	Iodine, 0.004-inch 1010 steel and 0.002-tungsten backup.	No	PM	0.04	--
1203		1650	2500	Two 0.004-inch 1010 steel and one 0.002-inch tungsten backup.	No	BJ	0.10	--
1204		1650	5000	Two 0.004-inch 1010 steel and one 0.002-inch tungsten backup.	No	PM	0.13	--
1205		1650	7500	Two 0.004-inch 1010 steel and one 0.002-inch tungsten backup.	No	PM	0.14	--
1206		1600	5000	Two 0.004-inch 1010 steel and one 0.002-inch tungsten backup.	No	PM	0.11	--
1207		1600	7500	Iodine, 0.004-inch 1010 steel and 0.002-inch tungsten backup.	No	--	--	--
1125		1650	1200	0.002-inch 1010 steel and tungsten backup.	Yes	--	--	--
1126		1650	2400	0.002-inch 1010 steel and tungsten backup.	Yes	--	--	--
1127	Ti-5Al-2.5Sn to Ti-5Al-2.5Sn	1650	5000	0.002-inch 1010 steel and tungsten backup.	Yes	--	--	--
1120	Ti-6Al-4V to Ti-6Al-4V	1550	1200	0.002-inch 1010 steel and 0.002 tungsten backup.	Yes	--	--	Good bond
1121		1550	1800	0.002-inch 1010 steel and 0.002 tungsten backup.	Yes	--	--	--
1122		1550	2400	0.002-inch 1010 steel and 0.002 tungsten backup.	Yes	--	--	--
1123		1550	3000	0.002-inch 1010 steel and 0.002 tungsten backup.	Yes	--	--	--
1124		1550	5000	0.002-inch 1010 steel and 0.002 tungsten backup.	Yes	--	--	--
1208		1725	1200	Iodine, 0.004-inch 1010 steel and 0.002-inch tungsten backup.	No	PM	0.255	--
1209		1775	2500	0.0625-inch thick 1010 steel and tungsten backup.	No	PM	0.295	--
1210		1550	5000	Two 0.004-inch 1010 steel and tungsten backup.	No	PM	0.290	--
1211		1550	7500	Two 0.004-inch 1010 steel and tungsten backup.	No	PM	0.265	--
1212		1600	800	Two 0.004-inch 1010 steel and tungsten backup.	No	PM	0.250	Good bond
1213		1600	7500	Two 0.004-inch 1010 steel and tungsten backup.	No	PM	0.250	--
1235		1600	800	Two 0.004-inch 1010 steel and tungsten backup	No	--	--	Good bond
1236	Ti-6Al-4V to Ti-6Al-4V	1725	800	Two 0.004-inch 1010 steel and tungsten backup.	No	--	--	--

TABLE LIX (Cont)

COMPLETE LIST OF DIFFUSION BONDED JOINTS

Log No.	Joint Foil Materials	Bonding Parameters		Electrode Surfaces and Stop Offs Used	Electrode Sticking	Tapered Lap Joint Pull Test		Micro-Structure
		Temperature (F)	Pressure (psi)			Failure Location	Load (T)	
1486	Ti-6. -4V to Ti-6Al-4V	1650	600	H_2 reduced 0.004-inch thick 1010 steel and tungsten backup.	No	--	--	--
1487	↕	1725	600	H_2 reduced 0.004-inch thick 1010 steel and tungsten backup.	No	--	--	--
1488	Ti-6Al-4V to Ti-6Al-4V	1650	600	Oxidized 0.004-inch 1010 steel and tungsten backup.	No	Forms a hole in bonded area.		
1115	Ti-5Al-2.5Sn to Ti-6Al-4V	1550	600	0.002-inch 1010 steel and tungsten backup.	Yes	PM	0.12	Good bond
1116	↕	1550	1200	0.002-inch 1010 steel and tungsten backup.	Yes	PM	0.14	Good bond
1117	↕	1600	600	0.002-inch 1010 steel and tungsten backup.	Yes	PM	0.11	Good bond
1118	↕	1600	1200	0.002-inch 1010 steel and tungsten backup.	Yes	PM	0.12	Good bond
1119	↕	1650	600	0.002-inch 1010 steel and tungsten backup.	Yes	PM	0.12	Good bond
1196	↕	1600	300	Two 0.004-inch steel and tungsten backup.	No	PM	0.135	--
1197	↕	1550	2500	Two 0.004-inch steel and tungsten backup with graphite.	No	BJ	0.140	--
1198	↕	1650	300	0.0025-inch steel and tungsten backup.	No	BJ	0.150	Good bond
1199	↕	1550	300	Two 0.004-inch steel and tungsten backup.	No	PM	0.145	Good bond
1200	↕	1600	2500	Two 0.004-inch steel and tungsten backup with graphite.	No	PM	0.140	--
1201	Ti-6Al-2.5Sn to Ti-6Al-4V	1600	5000	Two 0.004-inch steel and tungsten backup.	No	PM	0.155	--
1128	Ti-6Al-1Mo-1V to Ti-6Al-1Mo-1V	1650	300	0.002-inch steel and tungsten backup.	Yes	--	0.10	--
1129	↕	1650	1200	0.002-inch steel and tungsten backup.	Yes	--	0.20	Excellent bond
1130	↕	1750	300	0.002-inch steel and tungsten backup.	Yes	--	0.[illegible]	Excellent bond
1131	↕	1650	1200	0.002-inch steel and tungsten backup.	Yes	--	--	Excellent bond
1214	↕	1650	600	Inconel, 0.004-inch steel and tungsten backup.	No	--	--	--
1215	↕	1650	300	Two 0.004-inch steel and tungsten backup.	No	PM	0.21	Good bond
1216	↕	1600	1200	Two 0.004-inch steel and tungsten backup.	No	PM	0.23	Excellent bond
1217	↕	1600	600	Two 0.004-inch steel and tungsten backup.	No	PM	0.19	Good bond
1218	↕	1600	300	Two 0.004-inch steel and tungsten backup.	No	BJ	0.15	--
1219	Ti-6Al-1Mo-1V to Ti-6Al-1Mo-1V	1600	1200	Two 0.004-inch steel and tungsten backup.	No	BJ	0.155	--

TABLE LIX (Cont)

COMPLETE LIST OF DIFFUSION BONDED JOINTS

Log No.	Joint Foil Materials	Bonding Parameters: Temperature (F)	Bonding Parameters: Pressure (psi)	Electrode Surfaces and Stop Offs Used	Electrode Sticking	Tapered Lap Joint Pull Test: Failure Location	Tapered Lap Joint Pull Test: Load (T)	Micro-Structure
1483	Ti-8Al-1Mo-1V to Ti-8Al-1Mo-1V	1650	600	Steel (H_2 reduced) and tungsten backup.	No	--	--	--
1484	↕	1725	600	Steel (H_2 reduced) and tungsten backup.	No	--	--	--
1485	Ti-8Al-1Mo-1V to Ti-8Al-1Mo-1V	1650	600	Oxidized steel foil	--	--	Hole formed	--
1279	Ti-8Al-1Mo-1V to Ti-6Al-4V	165	600	Oxidized steel foil	No	PM	0.26	Good bond
1280	↕	1650	300	Oxidized steel foil	No	BJ	0.125	--
1281		1600	600	Oxidized steel foil	No	BJ	0.165	--
1282		1600	300	Oxidized steel foil	No	BJ	0.08	Good bond
1283		1550	1200	Oxidized steel foil	No	BJ	0.17	--
1284		1600	7500	Oxidized steel foil	No	--	--	--
1556	Ti-8Al-1Mo-1V to Ti-6Al-4V	1725	300	Oxidized steel foil	No	--	--	--
1285	Ti-6Al-4V Ti-3Al-2.5V	1600	600	Oxidized steel foil	No	--	--	--
1286	↕	1600	300	Oxidized steel foil	No	--	--	Poor bond
1287		1650	600	Oxidized steel foil	No	--	--	Excellent bond
1288		1650	300	Oxidized steel foil	No	--	--	--
1289		1550	600	Oxidized steel foil	No	--	--	Poor bond
1290		1550	1200	Oxidized steel foil	No	--	--	--
1558	Ti-6Al-4V Ti-3Al-2.5V	1600	7500	Oxidized steel foil	No	--	--	--

Note: PM stands for parent metal foil
BJ stands for diffusion bonded joint

using Ti-5Al-2.5Sn, Ti-8Al-1Mo-1V, and Ti-6Al-4V alloy foils. Self-bonded joints were accomplished in gettered argon atmosphere using simple lap-joint specimens and the diffusion bonder shown in Figure 163. An additional part of the evaluation was to search for an electrode material which would not stick to or embrittle the foil during the bonding sequence. Temperature in increments between 1500 and 1625 F, pressures between 300 and 5000 psi, and times between 10 and 60 seconds were evaluated with the alloy foil combinations. Electrodes of various materials (columbium, tantalum, tungsten with and without pyrolytic graphite surfaces, and Type 1010 steel) were tried and only the tungsten-graphite combination and Type 1010 steel did not stick to program alloy foils at temperatures up to 1700 F.

TABLE LX

MINIMUM DIFFUSION BONDING PROCESS PARAMETERS

Joint Materials	Temperature (F)	Pressure (psi)	Time (sec)
Ti-5Al-2.5Sn to Ti-5Al-2.5Sn	1600	300 to 5000 (variable)	20
Ti-6Al-4V to Ti-6Al-4V	1550	300 to 2500 (variable)	20
Ti-5Al-2.5Sn to Ti-6Al-4V	1550	300	20
Ti-8Al-1Mo-1V to Ti-8Al-1Mo-1V	1600	600	20
Ti-8Al-1Mo-1V to Ti-6Al-4V	1600	300	20
Ti-6Al-4V to Ti-3Al-2.5V	1650	600	20
Ti-3Al-2.5V to Ti-3Al-2.5V	1650	600	20

Varying degrees of interface bonding were obtained with the preceding parameters, with the initial conclusion being that the approximate parameter levels of 300 psi, 20 seconds, and 1650 F are required to yield acceptable bonds for the alloy foils (Fig. 164 and 165). Bonds can be obtained at higher temperatures; however, electrode sticking becomes a problem. At lower temperatures, considerably higher process pressures and longer times are required. The investigation has been restricted to short-time (≤ 60 seconds) bonding runs of the type usually referred to as "yield-strength controlled" (Ref. 104). Short process times are necessary to obviate progressive contamination and embrittlement of diffusion bond joints which because of their minimal mass and sharp angled geometry, cannot withstand a large amount of contamination. Therefore, minimum diffusion bonding parameters were established for single lap-joints (Table LX).

It is safe to assume that diffusion bonding parameters of 1650 F (maximum), 600 psi, and a process time of 20 seconds (maximum) would result in good joints of any combination of program alloy foils, without any associated problems of grain growth or matrix transformation effects (Fig. 166 through 171).

TABLE LXI

RESULTS OF DIFFUSION BONDING USING 0.3-Mil TITANIUM FOIL INTERLEAF

Log No.	Joint Foil Materials	Bonding Parameters		Electrode Surfaces and Stop Offs Used	Electrode Sticking	Tapered Lap Joint Pull Test		Micro-Structure
		Temperature (F)	Pressure (psi)			Failure Location	Load (T)	
1360	Ti-5Al-2.5Sn to Ti-5Al-2.5Sn	1500	300	Two 0.004-inch 1010 steel and tungsten backup.	No	BJ	0.145	--
1361		1500	600	Two 0.004-inch 1010 steel and tungsten backup.	No	BJ	0.115	--
1362		1600	300	Two 0.004-inch 1010 steel and tungsten backup.	No	BJ	0.145	--
1363	Ti-5Al-2.5Sn to Ti-5Al-2.5Sn	1550	300	Two 0.004-inch 1010 steel and tungsten backup.	No	BJ	0.150	--
1364	Ti-6Al-4V to Ti-6Al-4V	1550	300	Two 0.004-inch 1010 steel and tungsten backup.	No	BJ	0.145	--
1365		1550	300	Two 0.004-inch 1010 steel and tungsten backup.	No	PM	0.275	--
1366	Ti-6Al-4V to Ti-6Al-4V	1600	300	Two 0.004-inch 1010 steel and tungsten backup.	No	PM	0.270	Good bond
1370	Ti-6Al-4V to Ti-5Al-2.5V	1500	300	Two 0.004-inch 1010 steel and tungsten backup.	No	--	-	--
1367	Ti-6Al-1Mo-1V to Ti-6Al-4V	1500	300	Two 0.004-inch 1010 steel and tungsten backup.	No	PM Ti-6Al-1Mo-1V	0.170	Good bond
1369		1600	300	Two 0.004-inch 1010 steel and tungsten backup.	No	PM Ti-6Al-1Mo-1V	0.175	--
1368	Ti-6Al-1Mo-1V to Ti-6Al-4V	1600	300	Two 0.004-inch 1010 steel and tungsten backup.	No	PM Ti-6Al-1Mo-1V	0.24	--

Note: 1. PM stands for parent metal foil
BJ stands for diffusion bonded joint

2. Failure load is given in long tons (1 ton = 2240 lb)

3. Thickness of Ti-5Al-2.5Sn foil = 6 mils
Ti-6Al-1Mo-1V and Ti-6Al-4V = 10 mils
Ti-5Al-2.5Sn tube (0.125-in. dia) = 1.5 mils

Evaluation of diffusion bond quality was by metallography and by tensile testing of tapered foil lap joint (Fig. 172) to determine if failure occurred in parent metal or in the diffusion bonded area (overlap area >10t). Results of the evaluation revealed that most failures occurred in tapered parent metal foil just at the start of the joint; few occurred in diffusion bonded joints (Tables LIX and LXI).

3.7.2 Electrode Sticking Problem

Two approaches to eliminate the electrode sticking problem were investigated, which included:

- The use of interleaf of pure titanium
- The use of various electrode materials

Interleaf Approach

The use of an interleaf material was investigated to enable diffusion bonding at lower temperatures and pressures to minimize electrode sticking. As shown in Figure 173, good diffusion bonded joints of Ti-8Al-1Mo-1V to Ti-6Al-4V were obtained at process parameters of 1500 F, 300 psi, at 20 seconds. No significant advantage was observed by the use of 0.3 mil thick pure titanium foil as interleaf on joints of Ti-5Al-2.5Sn to Ti-5Al-2.5Sn or Ti-6Al-4V to Ti-6Al-4V, however. In view of this and the fact that use of an interleaf introduces an additional joint area, the interleaf approach was not considered sufficiently promising to warrant further study.

Electrode Material

The use of 0.002-inch, Type 1010 steel on the electrode surface and 0.002-inch tungsten as the backup material (to prevent sticking of the steel foil to the tungsten anvil) resulted in excessive electrode sticking in that the steel foil could not be removed from the titanium program alloy. However, this problem was eliminated by the use of two pieces of thicker (0.004-inch) Type 1010 steel (back-to-back) as the electrode surface and one piece of 0.002-inch tungsten as the backup. The thicker steel (0.004-inch) foils could be removed from the titanium alloys with ease. Iron contamination of the titanium foil surface, due to formation of a thin TiFe intermetallic compound layer, was observed (Fig. 171) and confirmed by X-ray fluorescence analysis.

Dissolved oxygen in the steel foil was not the factor which prevented sticking, as evidenced by tests of specially prepared 0.004-inch, Type 1010 steel foils (reduced in hydrogen at 1500 F for 0.5 hour). This material exhibited no greater tendency to stick than the as-received material.

Therefore, the mechanism actually responsible for eliminating the sticking problem was the formation of a very thin (~ 0.0002-inch), very brittle TiFe compound (interface layer) which acts as a barrier for further interdiffusion of iron and titanium.

Since the TiFe compound is so brittle, it was easily disrupted after the bonding process.

TABLE LXII

TENSILE DATA OF Ti-6Al-4V FOIL

Test Temperature	Vacuum (Torr)	Nominal Specimen Thickness (in.)	Strain Rate (in./in./min)	Ultimate Tensile Strength (ksi)	0.2% Yield Strength (ksi)	Reduction of Area (%)	Apparent Modulus (psi x 10^6)
70	760 (air)	0.010	0.12	--	--	--	18.6
800	5×10^{-6}	0.010	0.12	--	--	--	14.8
1000	3×10^{-6}	0.010	0.12	--	--	--	12.2
1400	3×10^{-6}	0.010	0.12	--	--	--	10.0
1500	760 (air)	0.125	0.006	13.5	12.4	100	1.8
1500	760 (air)	0.125	0.012	16.6	11.3	100	3.1
1650	4×10^{-6}	0.010	0.25	--	7.4	--	1.0
1650	4×10^{-6}	0.010	0.25	--	7.0	--	1.6
1650	4×10^{-6}	0.010	0.25	--	3.0	--	0.7

3.7.3 Generation of Baseline Data

An analytical solution of the tube stress-joint pressure relationship was derived for the tube-header joint (Appendix A). Although computed for elastic deformation only, it demonstrated that the limiting factor of this typical configuration is the hoop stress which can be developed in the thin wall tube.

Mechanical property tests were conducted on Ti-6Al-4V foil and sheet (an alloy structurally similar to the tube alloy) to determine its properties during heating to and at the diffusion bonding temperature. These tests consisted of:

- Tensile data
- Stress decay versus time

The tensile data (reported in Table LXII), indicate rapid loss of strength with increasing temperature and, more significantly, the variation in elastic modulus with strain.

Stress decay versus time curves were determined for 0.010-inch Ti-6Al-4V foil at test temperature from 1300 to 1700 F. The specimens were stressed in a Solar-designed, high-temperature foil tester (Fig. 174) at a rapid rate (0.6 ksi/sec)

TABLE LXIII

CREEP RELAXATION DATA FOR Ti-6Al-4V FOIL

Temperature (F)	Initial Stress (ksi)	Decay Time to Lower Stress (sec)						
		0.5 ksi	1.0 ksi	2.0 ksi	3.0 ksi	4.0 ksi	6.0 ksi	10.0 ksi
1300	11.0						100	8
1400	6.0			100	30	10		
1500	5.0		100	35	7	1		
1500	3.5		100	12	4			
1500	2.1		100	1				
1600	2.2	20	10	2				
1700	1	2						

to near the apparent proportional limit and then the machine cross head locked to fix strain. The drop in stress was plotted against time. It was found that relaxation increases with temperature, is very rapid, and appears to progress by a three-stage mechanism related to creep:

- First 30 percent drop - rapid decay rate, independent of initial stress magnitude.
- Transition - rate of stress decay, an inverse function of initial stress.
- Last 20 percent drop - asymptotic decay, independent of initial stress magnitude.

Typical stress relaxation values are given in Table LXIII, and an approximate plot for two test temperatures is presented in Figure 175.

It was apparent from these data that creep was very rapid above 1400 F and, in fact, influences the apparent modulus of the material to the point that slow strain rates (provided by differential thermal expansion devices) are unable to develop or maintain much pressure at the header joint. Reduction of temperature will increase the time for which the titanium will maintain a stress, but the time necessary for diffusion is similarly increased. Both creep rate and diffusion rate increase exponentially, and any benefits derived from temperature change will be second order effects.

3.7.4 Selection of Joint Pressurization Technique

Two different experimental techniques were selected for application of pressure to the tube-header joint:

- Differential thermal expansion of internal plugs
- Pneumatic pressurization of internal capsules

Their calculated efficiencies and design are explained in succeeding paragraphs.

Differential Thermal Expansion of Internal Plugs

Three differential thermal expansion plug designs were evaluated, which included:

- Solid plugs
- Hollow plugs
- Encapsulated liquid metal plugs

Solid Plugs. The differential thermal expansion of titanium ($\sim 5.5 \times 10^{-6}$ in./in./deg F) and high expansion nickel alloys ($\sim 9.0 \times 10^{-6}$ in./in./deg F) results in a diametral strain of about 5×10^{-3} in./in. between room temperature and 1600 F. The alloy selection and design of this type plug is shown in Figure 176. The raised step of this design is intended to circumvent some of the plug-to-tube sticking problems and also to concentrate heat transfer and pressure at the tube-header joint.

Hollow Plugs. This basic design (Fig. 177) and the pressurization obtainable are essentially the same as for solid plugs. Selective reduction of the conductive area by hollowing the plug was intended to amplify the presumed benefits of electrical resistance heating.

Encapsulated Liquid Metal Plugs. Assembly of multiple tubes in a heat exchanger configuration introduces severe limitations on the tightness of fit which can be used on the joints. Interface gaps of only 0.0001-inch constitute a third of the potential diametral expansion which one can expect from conventional high expansion alloys.

Expansions higher than those obtainable from solid plugs are therefore desirable and, with this intent, a steel encapsulated, lead plug was designed (Fig. 178 and 179). Internal pressure provided by the melted lead was computed as follows:

$$\Delta V_{\text{Lead}} = \Delta V_{\text{Fusion}} + \Delta T\alpha \text{ (room temperature to melting point)} + \Delta T\alpha \text{ (melting point to 871C)}$$

$$\Delta V_{\text{Lead}} = 3000 \times 10^{-6} + (327 - 20)\ 87 \times 10^{-6} + (871 - 327)\ 120 \times 10^{-6}$$

$$\Delta V_{\text{Lead}} = 95000 \times 10^{-6} = 9.5 \text{ percent}$$

$$\Delta V_{\text{Fe}} = \Delta T\alpha = (871 - 20)\ 36 \times 10^{-6} = 30600 \times 10^{-6} = 3.06 \text{ percent}$$

$$\text{Bulk Modulus} = X_T = \frac{\Delta V}{\Delta P \text{ (atm)}} = 3.8 \times 10^{-6}$$

$$3.8 \times 10^{-6} = \frac{(95000 - 30600) \times 10^{-6}}{\Delta P}$$

$$\Delta P = 1700 \text{ atm} \times 15 \frac{\text{psi}}{\text{atm}} = 250,000 \text{ psi}$$

Although the assumption of a value for the bulk modulus is only approximate[1] it is apparent that the high internal pressure developed by the melting lead will be of sufficient magnitude to expand the steel wall of the cylinder to accommodate most of the volumetric expansion, about 9.5 percent. Diametral expansion is probably slightly more than a third, 3.2 percent or $\sim 4 \times 10^{-3}$ inches. This amount is roughly seven times the expansion derived by differential thermal expansion of the best solid alloy plugs, and should compensate for relatively large gaps in the fitup.

Lead was chosen as the expansion liquid because of its high expansivity in the molten state, its reasonably high melting temperature (which permits it to withstand a certain amount of heat during welding closure of the steel capsule), and because it is mutually immiscible with iron (AISI Type 1010 steel).

Considerable care was required in sealing the ends of the plug to avoid melting the lead. The weld was made about 0.75 inch from the lead which is constrained by the AISI Type 321 stainless steel pin. The Type 321 stainless material has a lower heat

1. The compressibility of liquid mercury at 160 F, 3.76×10^{-6}, is taken to be roughly equivalent to that of liquid lead at 1600 F. This approach is justified since the densities, atomic diameters, and periodicity of the two are approximately equal and both are at a temperature about midway between their melting and boiling points.

conductivity and a much higher coefficient of thermal expansion than the Type 1010 steel, and is, therefore, effective in closing the gap between the pin-end and the steel case, both during welding and during the diffusion bonding cycle. The entire assembly was held in a copper chill block previously cooled with liquid nitrogen during welding (Fig. 180).

Swaging was found to be effective in minimizing internal voids which detract from the expected thermal expansion. The lead-filled plugs were held in a Jacobs chuck on a small horizontal mill and turned at about 200 rpm inside a four-step steel die, which was struck and closed repeatedly with a pneumatic hammer (Fig. 181 and 182). As closely as could be determined by radiographic and metallographic studies, the lead-filled cavities were free of post-swaging voids.

Pneumatic Pressurization of Internal Capsules

Pneumatic pressurization theoretically provides a method of increasing the plug diameter to match the creep in the titanium thereby maintaining relatively constant pressure on the joint for extended time. The heated, unsupported, tube wall will support only minimal internal gas pressurization, and it is necessary to provide an internal expansion cylinder to concentrate the stress at the header joint. In order to reuse the device, expansion ideally should be conducted in the elastic range, and the cylinder material therefore must have a low elastic modulus and high elastic limit (at diffusion bonding temperature). Type B66 columbium alloy comes closest to approximating the ideal conditions, having a modulus and yield strength at 1600 F of about 14×10^6 psi and 56×10^3 psi, respectively. Maximum strain within the elastic range is therefore about 0.004 in./in. or 0.0005 inch over the diameter of the plug. While slightly less than that developed by differential thermal expansion of solid plugs, this pneumatically induced strain can be made more rapid and will result in higher continuous stress and pressure on the tube-header interface during the 20- to 30-second bonding cycle desired.

Due to the immediate unavailability of the B66 alloy in a form suitable for manufacture of the expansion plugs, it was necessary to substitute Inconel 600 alloy in which permanent plastic deformation should occur in obtaining the necessary expansion. It was felt, nonetheless, that the Inconel tubes would provide experimental verification of the general theory. Their design is shown in Figures 183 and 184.

Wall thickness is such that 2000 psig produces 9000 to 15,000 psi hoop stress, corresponding to the yield and ultimate strengths of Inconel 600 at 1600 F. Under these conditions, the maximum diametral strain produced by the plug is limited only by the fracture elongation of the Inconel (or titanium) and is at least an order of magnitude greater than that provided by any of the other methods.

Another advantage of the pneumatic pressurization system is that the tubes need not be pressurized to any great degree until the 1400 to 1650 F bonding range is reached. It is therefore possible to delay the heating cycle at 1200 F long enough to promote self-dissolution of the oxides without distorting the joint in creep.

3.7.5 Experimental Heating Methods

In addition to conventional furnace heating of the entire tube-header-plug assembly, it was decided to evaluate electrical resistance heating of the internal expansion plugs (alone). This latter technique has a number of characteristics which might be advantageous in establishing the proper relationships of temperature and stress:

- Faster heating rates, and therefore faster (thermal expansion induced) strain rates, will develop higher joint pressures in the tube-header structure than is possible with furnace heating. As a corollary advantage, dwell time at intermediate temperatures, and consequent intermediate creep, is minimized.
- Resistance electrodes concentrate the heat in the tube and thereby improve the rigidity of the cooler header as well as the differential temperature between the tube and header. These factors all favor maximum differential strain and interface pressure.

3.7.6 Joint Design and Surface Cleanliness

The experimental work on basic bonding parameters was conducted with short (approximately 1 inch), 0.125 inch OD tubes and single-hole headers similar to that shown in Figure 185. Only 0.006-inch wall thickness tubing was evaluated.

Because the time requirements of diffusion bonding are largely a function of surface oxide elimination, the joint design was modified in some of the tests to include beveled edges of the header holes (Fig. 186). This modification was to increase the pressure at the joint interface, promoting a tendency for shearing of surface oxides which exposes the unoxidized substrate metal.

Tubes were abrasive-saw cut to 1-inch lengths and the ends were deburred. Header plates (0.015-inch thick) were sheared to blanks approximately 1-inch square. A central hole (to accommodate the tube) of 0.121-inch diameter was drilled and subsequently reamed to 0.125-inch diameter. Drilling and reaming operations were conducted on tightly clamped stacks of 50 header plates from which the top and bottom pieces were discarded. In some instances, the edges of the hole on both sides of the piece were beveled with a 45-degree tapered reamer to 40 percent the thickness of the material, leaving only the center 20 percent (0.003 inch) as the normal bearing surface for the tube.

The hole diameter was verified on an optical comparator as 0.1255 ± 0.0003 inch, approximately 0.001 inch less than the actual outside diameter of the tubes. Roundness of tubes and header holes were also checked with an optical comparator.

Three types of expansion plugs, solid, hollow, and lead-filled, were prepared as previously described, with a step diameter of 0.114 inch, providing a 0.001-interference fit with the tube inner diameters.

Tubes and headers were cleaned and stored in dessicator jars until immediately before use. The cleaning procedure consisted of:

- Hand wipe with acetone to degrease
- Oxide conditioned in Kolene Alko salt for 60 seconds at 400 F (proprietary product of Kolene Corporation, Detroit, Michigan)
- Quench in cold water
- Pickle, 10 seconds in 5% HNO_3-20%HF; rinse in distilled water, neutralize, rinse, and dry in air blast.

Metal removal due to cleaning was less than 0.0001 inch/surface.

The tubes were stiffened by a slip-fit, internal steel rod and then pressed into the headers, supported on a steel block drilled to accept the tube. The small, precision drill press shown in Figure 167 was used as an arbor press. Expansion plugs were similarly pressed into the tube, aligning the raised diameter under the header joint. Both tubes and headers were carefully handled to avoid contamination of the metal surfaces at the joint.

3.7.7 Bonding Tests and Results

Tests were conducted on both the differential thermal expansions method and the pneumatic pressurization method of applying pressure to the tube-header joint. Bonding procedures included electrical resistance heating and furnace heating. The procedures and results of these tests are discussed in the following paragraphs.

Differential Thermal Expansion Methods

Electrical Resistance Heating. The expansion plugs (solid, hollow, and lead filled) were heated by electrical resistance in an NRC vacuum furnace at 10^{-5} to 10^{-6} Torr (Fig. 188). An Ircon, Model 300, indicating optical pyrometer was used for temperature measurement. The pyrometer was calibrated against a 0.005-inch diameter chromel-alumel thermocouple tack-welded to a sample tube. Reproducibility of ± 10 degrees F was obtained in the range of 1550 to 1650 F. The heating rate was controlled with the manually variable rheostat of the vacuum furnace by reference to the Ircon pyrometer.

Subsequent to heating and bonding periods, vacuum was maintained until the assembly cooled to less than 500 F (about two minutes time).

The tube-header joints were microscopically examined at a magnification of 30X and manually flexed for evidence of diffusion bonding.

Results of this procedure are summarized in Table LXIV. Efficient radiation from the 1-inch square header lowered the tube surface temperature at the header joint so well below that of other sections of the tube. Concentration of conducted heat by the raised diameter on the plugs and by greater resistance in the hollow or lead-filled plugs was effectively demonstrated on tubes without headers; but the concentration was insufficient to overcome the extreme temperature gradient created by radiation from the header.

When the electrical power was increased to raise the joint temperature to about 1500 F, melting occurred at other areas of the tube by formation of Ti-Fe-Ni or Ti-Fe eutectics in the Inconel 750 and Type 1010 steel plugs, respectively (Fig. 189). Faster heating rates, while presumably more desirable from the standpoint of header rigidity, allow less time for equalizing temperature gradients in the tube and, therefore, accentuate the tendency for overheating and melting.

TABLE LXIV

TEST RESULTS OF ELECTRICAL RESISTANCE HEATING OF PLUGS FOR DIFFERENTIAL THERMAL EXPANSION

Specimen Number	Type Plug	Header (In. sq)	Time to Temperature (sec)	Time at Temperature (sec)	Approximate Temperature Distribution (F) (1)					Result
1	Solid	1.00	10	10	1850	1800	1500	1400	1200	Tube melted, no bond
2	Solid	1.00	30	30	1875	1750	1500	1425	1250	Tube melted, no bond
3	Solid	1.00	60	45	1875	1750	1500	1425	1250	Tube melted, no bond
4	Solid	1.00	120	60	1875	1750	1500	1425	1250	Tube melted, no bond
5	Solid	1.00	300	50	1875	1750	1500	1425	1250	Tube melted, no bond
6	Solid	1.00	60	30	1875	1750	1500	1425	1250	Tube melted, no bond
7	Solid	1.00	90	120	1875	1750	1500	1425	1250	Tube melted, no bond
8	Hollow	1.00	30	60	1850	1750	1525	1425	1225	Tube melted, no bond
9	Hollow	1.00	60	30	1850	1750	1525	1425	1225	Tube melted, no bond
10	Hollow	1.00	120	60	1850	1750	1525	1425	1225	Tube melted, no bond
11	Hollow	1.00	300	30	1850	1750	1525	1425	1225	Tube melted, no bond
12	Pb filled	1.00	30	--	--	--	1500	--	--	Pb leaked
13	Pb filled	1.00	30	60	1850	1750	1525	1425	1225	Tube melted, no bond
14	Pb filled	1.00	120	120	1850	1750	1525	1425	1225	Tube melted, no bond
15	Pb filled	1.00	300	120	1850	1750	1525	1425	1225	Tube melted, no bond
16	Solid	0.25	10	30	1750	1700	1610	1500	1575	Superficial bonding at joint
17	Solid	0.25	10	300	1750	1700	1610	1500	1575	Superficial bonding at joint
18	Hollow	0.25	10	30	1750	1700	1610	1500	1575	Superficial bonding at joint
19	Hollow	0.25	10	300	1750	1700	1610	1500	1575	Superficial bonding at joint
20	Pb filled	0.25	10	--	--	--	1500	--	--	Pb leaked
21	Pb filled	0.25	10	30	1750	1700	1610	1610	1575	Superficial bonding at joint
22	Pb filled	0.25	10	300	1750	1700	1610	1610	1575	Superficial bonding at joint

1. Control point; most other values approximate.

Reduction in the size of the header to a 0.25-inch square was partially effective in reducing the thermal gradient in the tube; the out-lying areas could be kept below melting temperature and, probably by further design modification, below the beta transus of the titanium tube alloy. At the same time, however, the entire header stabilized at almost the temperature of the joint, negating the rigidizing effects of a colder header, presumed to be one of the primary benefits of heating by electrical resistance.

No diffusion bonding was experienced in either the 1.0 or 0.25-inch square headers, although the latter developed a slight sticking at the joint (using solid and Pb-filled plugs). Negligible metal deformation was observed in microscopic examination of the header holes with beveled edges, indicative of insufficient pressure and/or temperature at the joint.

TABLE LXV

TEST RESULTS FOR FURNACE HEATING OF SOLID PLUGS FOR DIFFERENTIAL THERMAL EXPANSION

Specimen Number	Atmosphere (Torr)	Temperature (F)	Time (min)	Type Header	Permanent Diametral Expansion (in.)	Comments
S1	5×10^{-5}	1650	5	Beveled	Nil	No bond
S2	5×10^{-5}	1650	40	Beveled	Nil	Semibond one side
S3	5×10^{-5}	1650	35	Beveled	Nil	Semibond one side
S4	5×10^{-5}	1650	35	Square	Nil	No bond

While it may be possible to effect a satisfactory compromise of thermal gradients by adjusting the size or radiation efficiency of the header or by further regulation of heating rates and temperature, this approach is valid only for single test specimens. The complexity of thermal and electrical patterns in multiple tube-to-header assemblies precludes developing a reliable technique for resistance heating the internal expansion plugs. Further, the evidence indicates that in a workable resistance heating cycle the temperature of the header would be so nearly that of the joint and the heating rate so slow that resistance heating would offer little advantage over furnace heating.

Similarly, eutectic melting might be avoided by suitable coatings on the plugs, but it is unlikely that temperature could be held below the beta transus in all areas of the tube.

Furnace Heating. Bonding by differential thermal expansion was conducted in a cold-wall vacuum furnace (Fig. 190) using both solid and lead-filled plugs. Temperature was measured by micro optical pyrometer and adjusted with a manual rheostat.

Results of the furnace heating method indicated that:

- None of the solid plugs (Table LXV) resulted in permanent diametral expansion or in satisfactory bonding. Specimens S3 and S4 which had beveled and square header-hole edges, respectively, were run simultaneously. Only S2 evidenced sticking or preliminary superficial bonding, tending to confirm the benefits expected from higher interface pressures and shear stress at the joint.

TABLE LXVI

TEST RESULTS OF FURNACE HEATING LEAD-FILLED PLUGS FOR DIFFERENTIAL THERMAL EXPANSION

Specimen Number	Atmosphere Vacuum (Torr)	Temperature (F)	Time (min)	Type Header	Permanent Diametral Expansion (in.)	Results
L1	1×10^{-4}	1635	42	Beveled	0.002	No bond
L2	2×10^{-5}	1670	60	Beveled	0.002	Bond (not full circle)
L3	2×10^{-5}	1650	60	Square	0.001 to 0.003	Bond (not full circle)
L4	6×10^{-5}	1650	240	Beveled	0.001 to 0.002	Good bond (full circle)
L5	4×10^{-5}	1650	15	Beveled	Nil	Pb burst case
L6	5×10^{-5}	1650	5	Beveled	0.0005 to 0.001	No bond
L7	7×10^{-5}	1650	90	Square	0.0015 to 0.002	Intermittent bonding and cracking around circumference. Figure 193.
L8	5×10^{-5}	1900[1]	10	Square	0.002	Bond complete around circumference and through entire thickness of header. Excessive grain growth and cracking in Ti-3Al-2.5V tube. Figure 196.
L9	7×10^{-5}	1700	30	Square	0.002	Good bond around 360 degrees. Extensive diffusion from 1010 steel plug. Figure 195.
L10	6×10^{-5}	1675	50	Square	0.003	Partial bond. Figure 194.
L11	7×10^{-5}	1650	30	Square	0.0025	No bond. Figure 192.

1. Controller Malfunction

- Lead-filled plugs (Table LXVI) produced from 0.001- to 0.003-inch permanent diametral expansion and usually resulted in a bond of reasonably good quality (but seldom full circle) with process times less than 30 minutes. Specimen L-4 which had a 4-hour temperature cycle, developed a good quality bond around all of the tube circumference (Fig. 191).

Lead-filled plug expansion cycles indicate that this process is definitely creep-strength controlled and, therefore, requires temperatures precariously close to the beta transus point of the Ti-3Al-2.5V tubing (approximately 1700 F) or unreasonably long bonding times (at lower temperatures) in excess of one hour. As shown in Figures 192 through 196, an undesirable combination of beta embrittlement, grain growth, and cracking of the tube alloy is evidenced with increasing temperature.

TABLE LXVII

TEST RESULTS OF PNEUMATIC PRESSURIZATION PLUGS

Specimen[4] Number	Pneumatic Capsule Wall Thickness (in.)	Bonding Temperature (F)	Bonding Time (min)	Bonding Pressure (psig)	Atmosphere Vacuum (Torr)	Type Header	Permanent Diametral Expansion (in.)	Results
P1	0.010	1620	5-1/2	2000[1]	25 cfh A	Beveled	Nil	Over-cooled by argon
P2	0.010	1690	13	2400[1]	2 cfh A	Beveled	0.007	O_2 contaminated
P3	0.010	1700	13	2000[2]	1×10^{-4}	Beveled	0.003	O_2 contaminated
P4	0.010	1700	60	2000[3]	1×10^{-4}	Beveled	0.006	Burst, no bond
P5	0.010	1700	1	2000[3]	5×10^{-4}	Beveled	0.003	Burst, no bond
P6	0.010	1700	5	2000[3]	5×10^{-5}	Beveled	0.004	Burst, bond
P7	0.010	1675	5	2000[1]	7×10^{-4}	Square	0.010	Partial bonding. Figure 202.
P8	0.010	1675	5	2000[1]	6×10^{-4}	Square	---	Burst at pressure partial bond. Figure 203
P9	0.010	1675	5	1500[1]	Pump Malfunction	Square	0.003	O_2 contaminated, no bond
P10	0.010	1675	5	1500[1]	7×10^{-4}	Square	0.002	Partial bonding. Figure 204
PiFe-12	0.045	1675	5	1500[1]	9×10^{-4}	Square	0.0005	Sample clean, no bonding
PiFe-13	0.045	1675	5	2000[1]	4×10^{-4}	Square	0.001	Sample clean, no bonding
PiFe-14	0.045	1675	5	2475[1]	9×10^{-3}	Square	0.001	Sample contaminated, no bonding
PiFe-15	0.038	1675	5	1500[1]	1×10^{-3}	Square	0.001	Sample contaminated, no bonding
PiFe-16	0.038	1675	5	2000[1]	9×10^{-4}	Square	0.001	Sample contaminated, no bonding
PiFe-17	0.038	1675	5	2500[1]	4×10^{-4}	Square	0.0015	Sample contaminated, superficial bonding
PiFe-18	0.023	1675	5	1500[1]	6×10^{-4}	Square	0.001	Sample contaminated superficial bonding

1. Pressure applied and released at temperature
2. Cooled under pressure
3. Raised under pressure
4. Fe indicates AISI type 1010 steel pneumatic expansion capsule

Pneumatic Pressurization

A clam shell-type electrical resistance furnace was used to heat a Vycor glass or metal chamber (for inert gas or vacuum) containing the pneumatic pressurization tube and tube-header sample (Fig. 197). Process temperature was measured by a chromel-alumel thermocouple (within the furnace but external to the work chamber) and was maintained by an on-off controller. Compensation was allowed for a 50-degree F thermal gradient between the outside of the chamber and the test sample. Three programmed variations of temperature and pressure were evaluated as indicated in Table LXVII, and typically illustrated in Figures 198, 199, and 200. Internal pressurization was supplied by argon, controlled by a high-pressure regulator after evacuating and back-filling the pressure tube.

The results (listed in Table LXVII) indicate that pneumatic pressurization plugs provide a controllable tube expansion process. Slight surface contamination prevented bonding in the initial attempts on specimens P1, P2, and P3. This difficulty was rectified in subsequent attempts on specimens P4 and P5. Lack of bonding in these latter specimens is believed due to the restriction of expansion by the greater rigidity of the 0.003-inch land on the expansion plug, over which the header was positioned. The header of specimen P6 therefore was positioned over the small diameter at the end of the expansion plug. Considerable distortion resulted from the uneven resistance to plug expansion, but there was evidence of bonding the tube and header by this approach (Fig. 201). The raised land was eliminated from subsequent plugs.

Temperature and especially time requirements are considerably reduced by this process which incorporates rapid expansion and is yield-strength controlled. Partial bonding of three samples are shown in Figures 202 through 204. The degree of expansion accompanying the pressurization cycle suggests that the quality of the bonds should be better than that observed in the photomicrographs. The explanation most likely for this behavior is in the relatively poor vacuum environment in which these specimens were pressurized. One degree of magnitude separates the vacuum pressure at which the pneumatic plug and lead-filled plug specimens were diffusion bonded.

In all cases, it was noted that the diffusion from the Inconel pressure plugs into the titanium tube was many times greater than for the Type 1010 steel lead-filled plugs, although the Type 1010 plugs were subjected to longer times at higher temperatures. The Inconel alloy forms no intermetallic diffusion barrier as does the iron.

Pneumatic bonding tests P12 through P18 incorporated expansion plugs of Type 1010 steel rather than Inconel. None of these cycles resulted in more than superficial bonding. It was felt that the relatively poor vacuum environment of this particular furnace again was responsible for lack of bonding rather than the pneumatic pressurization which, in many of the specimens, produced adequate (0.0015- to 0.002-inch) expansion for bonding.

While the use of Type 1010 steel expansion capsules eliminated the interdiffusion and embrittlement problem, the difficulty of separating the tubes from the expansion capsule was relieved only in small measure and none of the pneumatic capsules could be reused.

3.7.8 Summary

- The technique of resistance heating internal expansion plugs does not provide a reliable diffusion bonding process. The header plate acts as a thermal radiator, overcooling the joint and inducing high thermal gradients in the tube.

- No diffusion bonding resulted from solid, high-expansion, nickel-base alloy plugs. The evidence indicates that the thermal expansion strain is either sufficiently rapid nor sufficiently great to compensate for dissipation of pressure by creep relaxation at the joint.

- Encapsulated liquid metal plugs (lead-filled) are capable of developing up to 0.003-inch permanent diametral strain. Diffusion bonded joints were produced by this technique, joining tubes to headers by a process which is creep-strength controlled, requiring extended time at temperature.

- Pneumatic pressurization is effective in expanding internal plugs and appears capable of being developed into a reliable diffusion bonding process. A problem is presented in removing the plugs after the bonding cycle due to permanent diametral expansion of the pressurization plug, but the technique appears basically sound.

- Sticking of the pressure transfer surface to the titanium foil workpiece remained a serious problem throughout this study. No perfect stop-off material was found to operate at the process temperatures and pressures used. However, Type 1010 steel shim stock provided a workable solution, in that the very thin film of iron-titanium intermetallics formed at the shim/workpiece interface could be disrupted readily

- In view of the excellent preliminary results and reliability of the brazed heat exchanger manufacturing process, further development of the diffusion bonding process within the limited time available on this program is not warranted, especially in consideration of the expansion plug-to-tube sticking and other related problems.

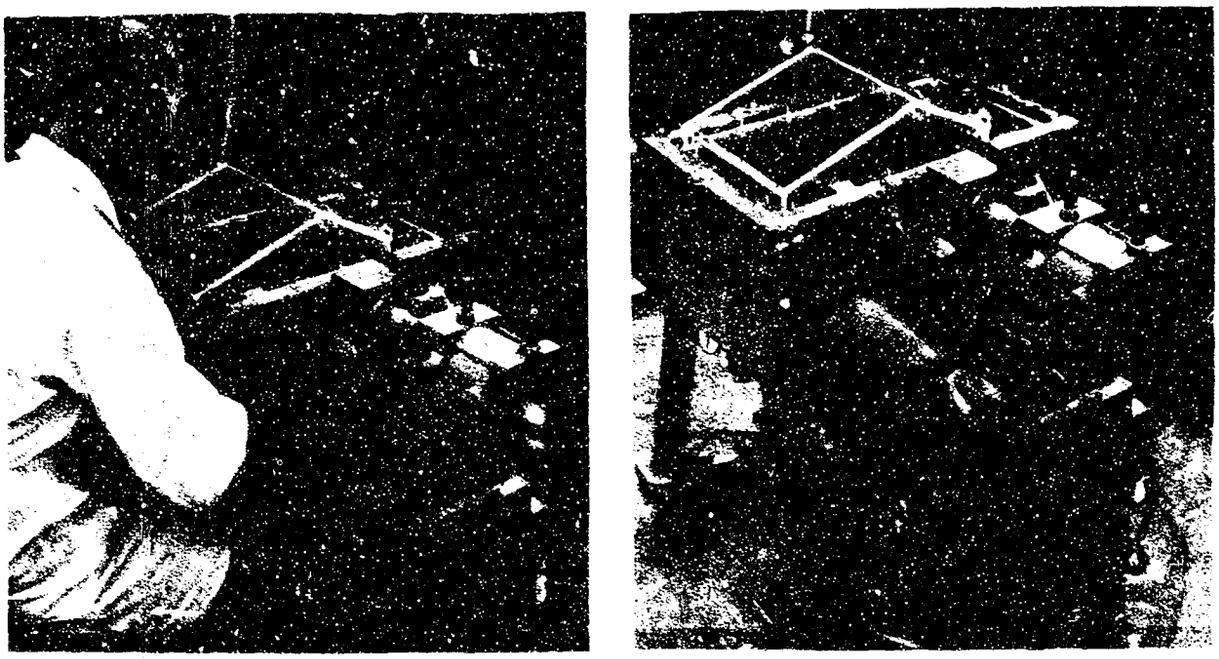
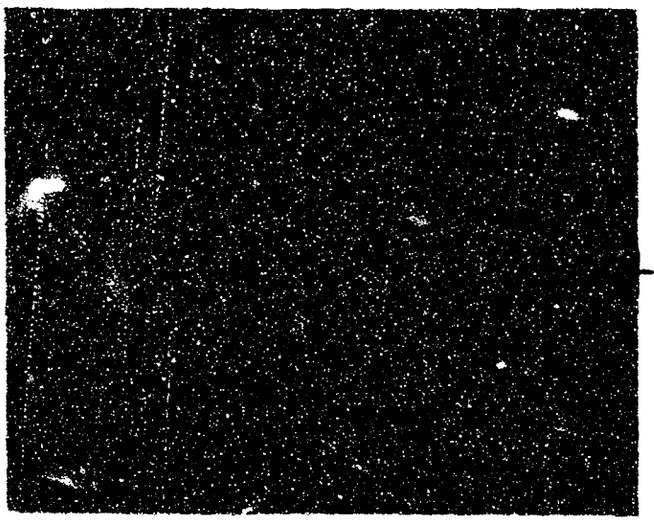


FIGURE 163. DIFFUSION BONDER



Bond Pressure: 300 psi

Temperature: 1650 F

Time: 20 sec

Magnification: 250X

Bond excellent - no electrode sticking (iron).

Bond Line

FIGURE 164.

SOLID-STATE DIFFUSION BONDED JOINT, Ti-5Al-2.5Sn/Ti-5Al-2.5Sn

Bond Pressure: 300 psi

Temperature: 1650 F

Time: 20 sec

Magnification: 250X

Bond excellent - no electrode sticking (iron).

Bond Line

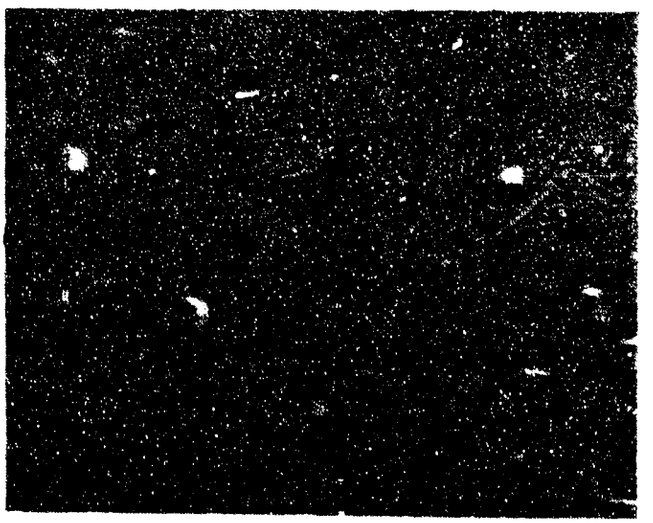


FIGURE 165.

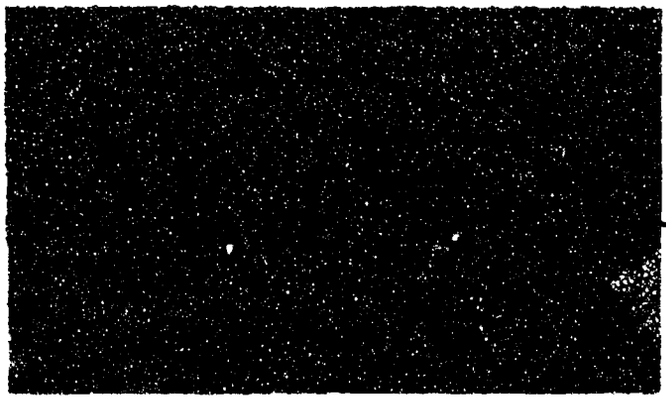
SOLID-STATE DIFFUSION BONDED JOINT, Ti-6Al-4V/Ti-6Al-4V



Bond Pressure: 1200 psi
Temperature: 1550 F
Time: 20 sec
Magnification: 250X

Bond Line

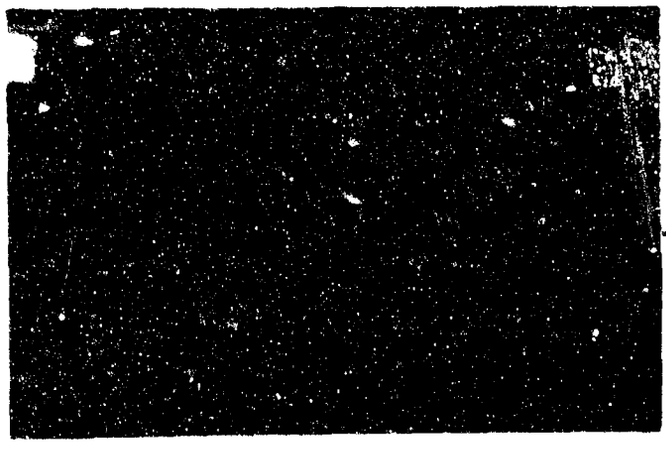
FIGURE 166.
DIFFUSION BONDED JOINT,
Ti-8Al-1Mo-1V/Ti-8Al-1Mo-1V



Bond Pressure: 300 psi
Temperature: 1600 F
Time: 20 sec
Magnification: 250X

Bond Line

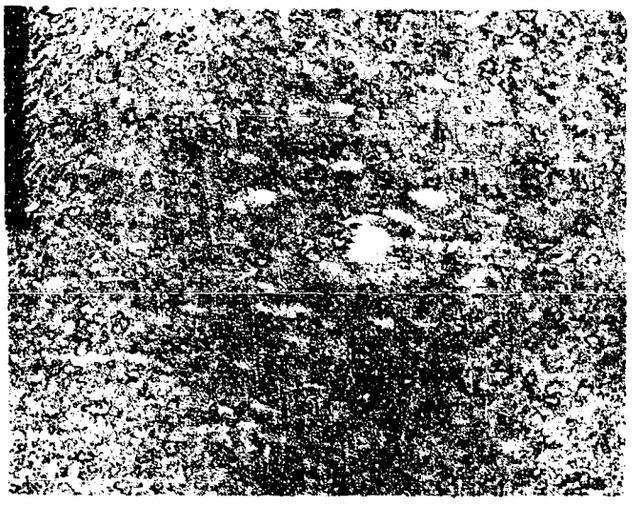
FIGURE 167.
DIFFUSION BONDED JOINT,
Ti-8Al-1Mo-1V/Ti-6Al-4V



Bond Pressure: 600 psi
Temperature: 1600 F
Time: 20 sec
Magnification: 250X

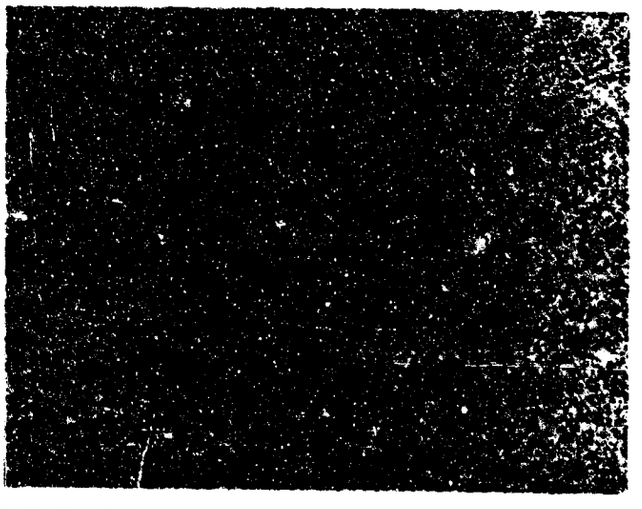
Bond Line

FIGURE 168.
DIFFUSION BONDED JOINT,
Ti-6Al-4V/Ti-5Al-2.5Sn



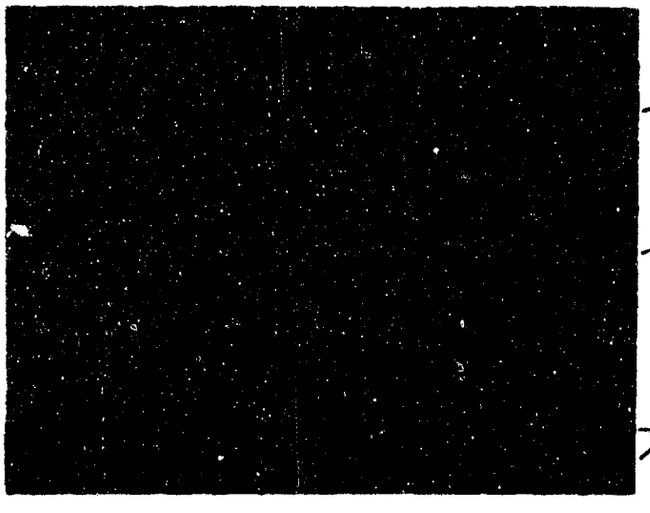
Bond Pressure: 2000 psi
Temperature: 1550 F
Time: 20 sec
Magnification: 250X

FIGURE 169.
DIFFUSION BONDED JOINT,
Ti-6Al-4V/Ti-6Al-4V



Bond Pressure: 1200 psi
Temperature: 1600 F
Time: 20 sec
Magnification: 250X

FIGURE 170.
DIFFUSION BONDED JOINT,
Ti-8Al-1Mo-1V/Ti-8Al-1Mo-1V



Bond Pressure: 600 psi
Temperature: 1650 F
Time: 20 sec
Magnification: 500X

FIGURE 171. DIFFUSION BONDED JOINT, Ti-6Al-4V/Ti-3Al-2.5Sn/Ti-3Al-2.5V

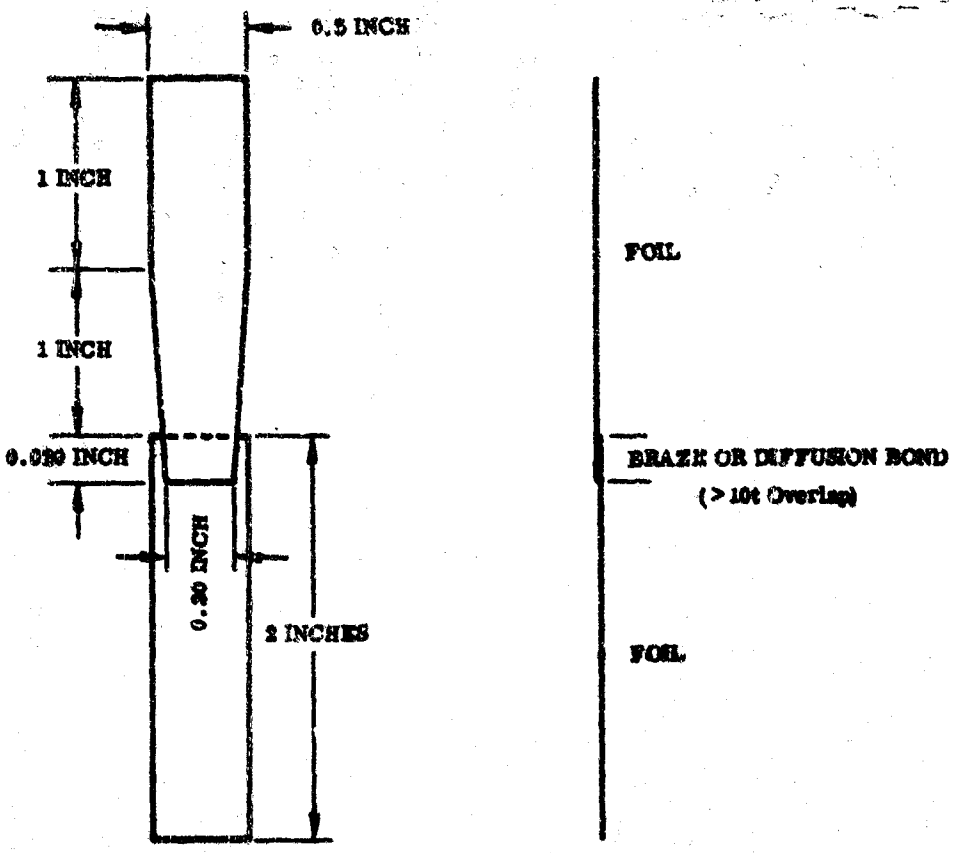
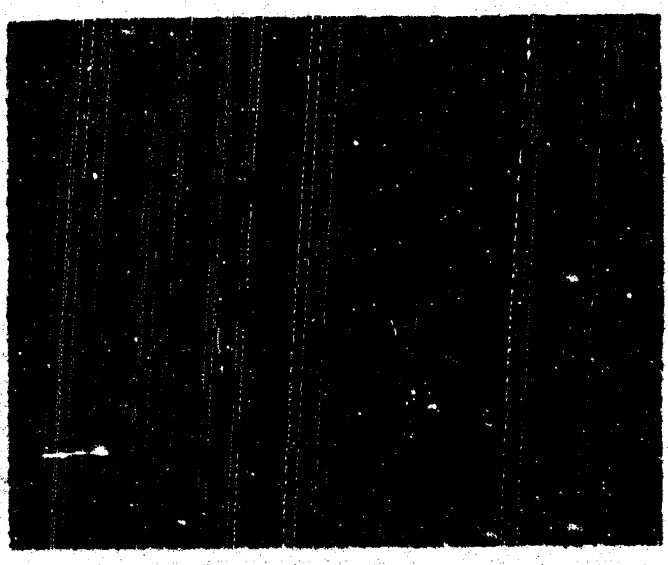


FIGURE 172. TAPERED LAP-JOINT



Bond Pressure: 300 F
Temperature: 1500 F
Time: 20 sec
Magnification: 250X

— Titanium foil 0.5-mil thick as interleaf

FIGURE 173.

DIFFUSION BONDED JOINT, Ti-8Al-1Mo-1V/Ti Interleaf/ Ti-6Al-4V

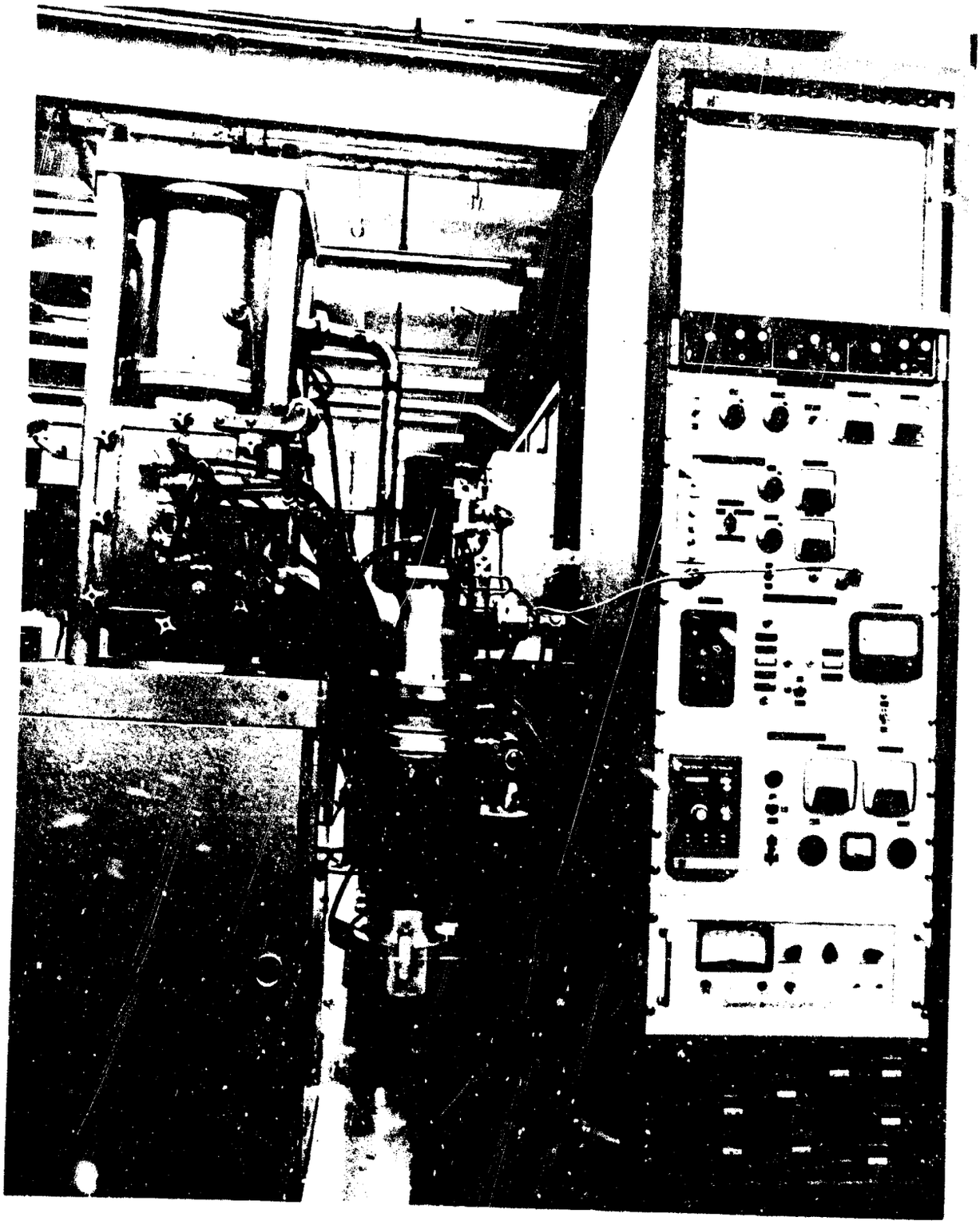


FIGURE 174. ELEVATED TEMPERATURE FOIL TESTER

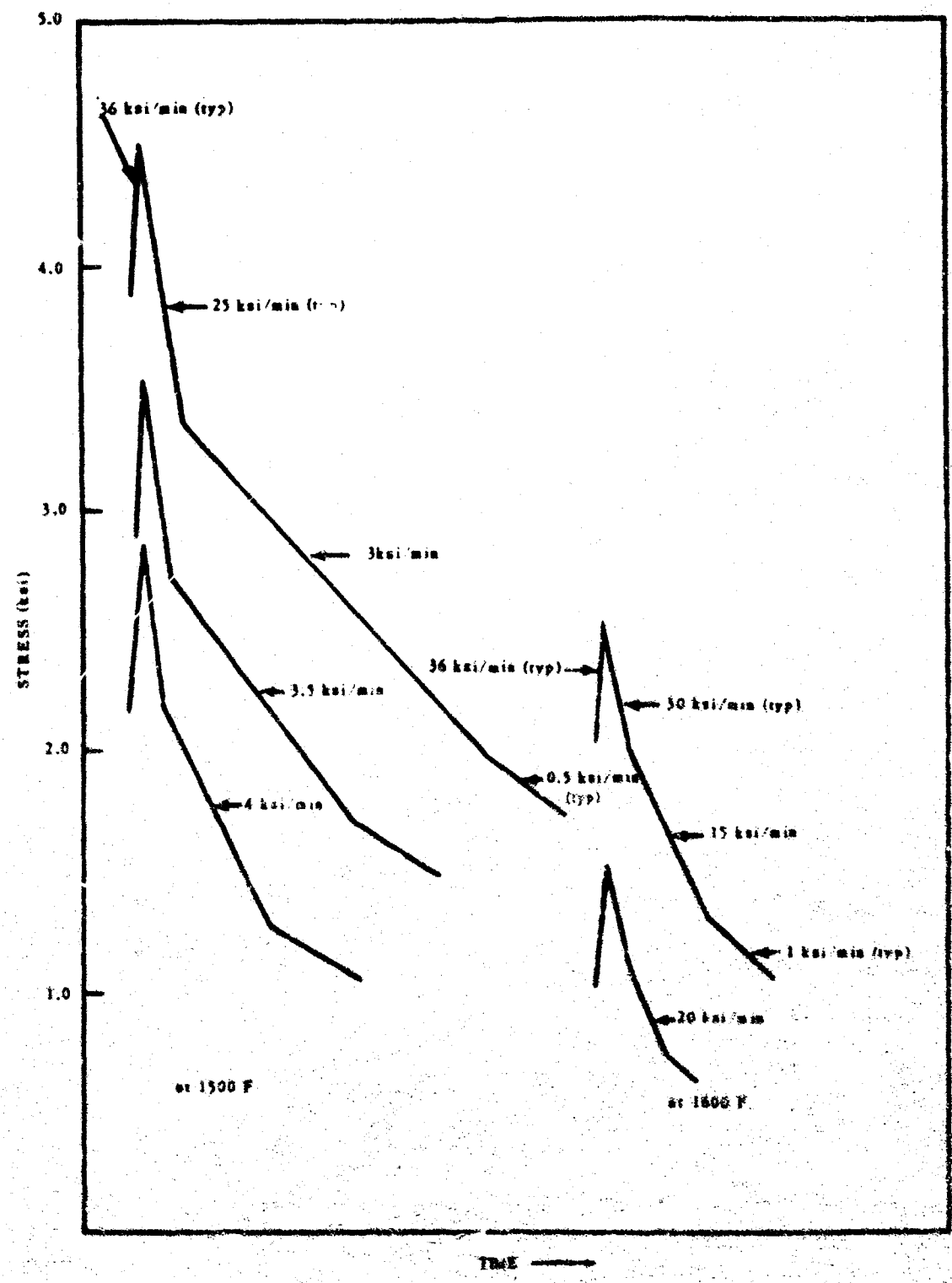
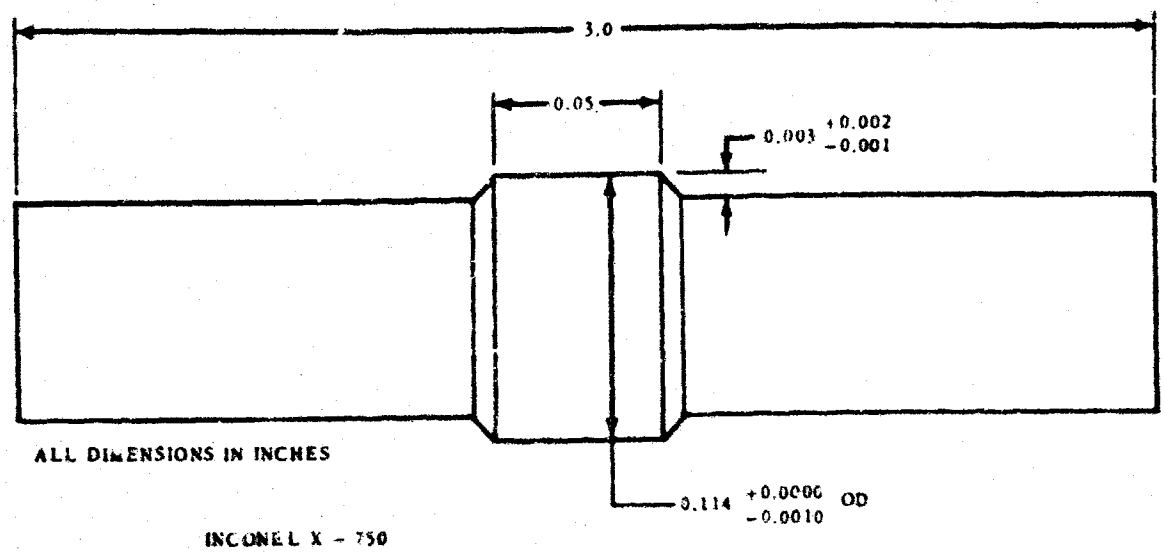


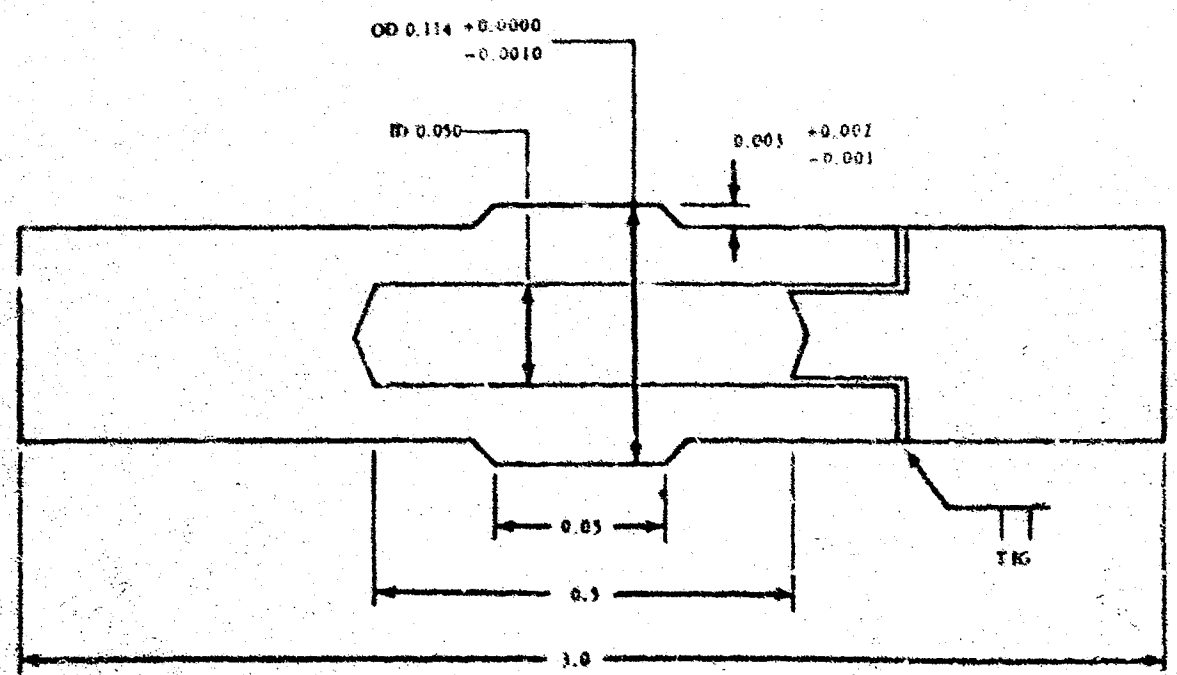
FIGURE 175. STRESS DECAY VERSUS TIME, Ti-6Al-4V Foil



ALL DIMENSIONS IN INCHES

INCONEL X - 750

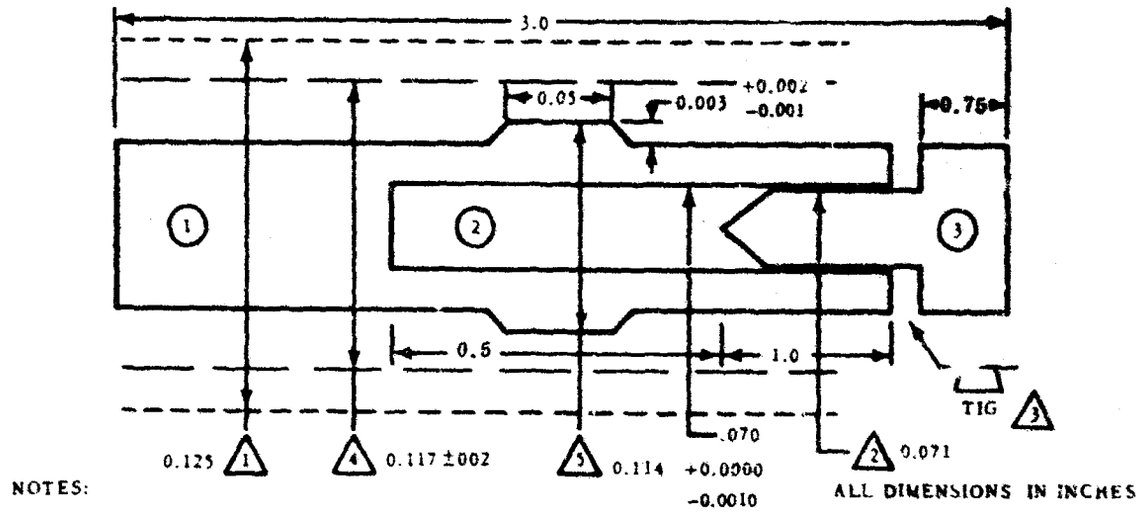
FIGURE 176. SOLID PLUG DESIGN



ALL DIMENSIONS IN INCHES

INCONEL X-750

FIGURE 177. HOLLOW PLUG DESIGN



NOTES:

1. AISI 1010 STEEL PLUG
2. LEAD
3. 321 STAINLESS STEEL PIN
1. ROUGH MACHINE TO 0.125 INCH DIAMETER PACK WITH LEAD AND TAMP SOLID
2. MACHINE 0.001-INCH INTERFERENCE FIT ON (HIGH EXPANSION) 321 STAINLESS STEEL AND DRIVE IN POINT TO EXPAND LEAD
3. WELD IN COPPER CHILL BLOCK COOLED WITH LN_2 (TO AVOID MELTING LEAD).
4. SWAGE TO 0.117 INCH DIAMETER
5. FINISH MACHINE TO 0.114 INCH DIAMETER

FIGURE 178. ENCAPSULATED LIQUID METAL PLUG DESIGN



Component Parts

Assembled

Welded

Swaged

Final Machined

Magnification: Approximately 1X

1/4 Inch Grid

FIGURE 179. STEEL ENCAPSULATED LEAD PLUGS



FIGURE 180.

WELDING THE LEAD-FILLED PLUGS IN A COPPER BLOCK COOLED WITH LIQUID NITROGEN

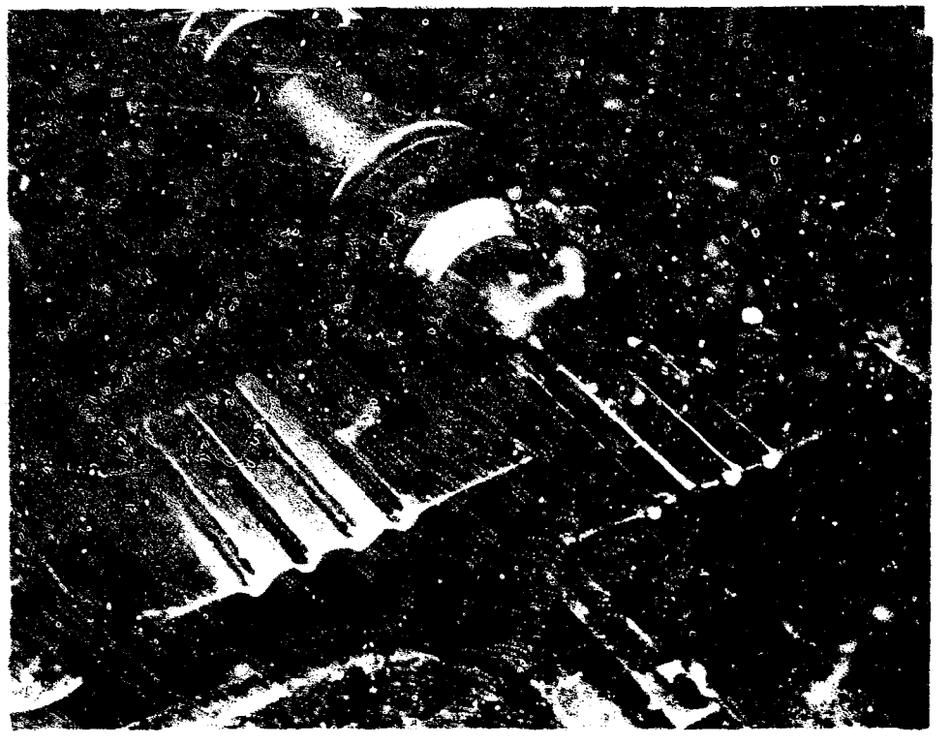
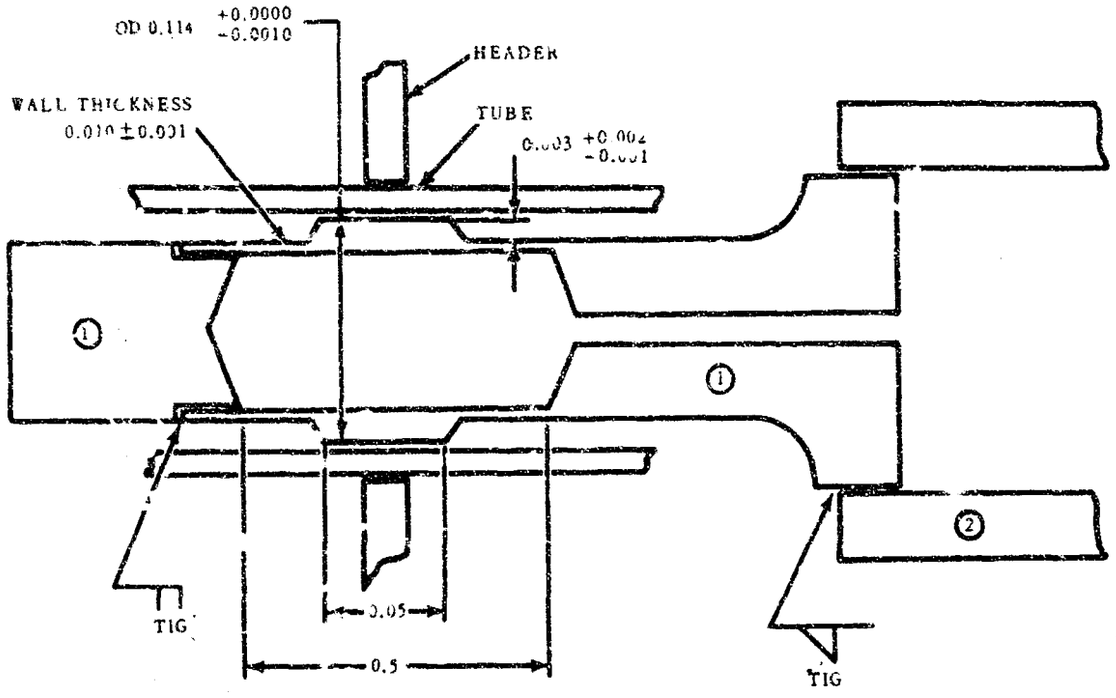


FIGURE 181. LEAD-FILLED PLUG IN BOTTOM DIE OF SWAGING TOOL

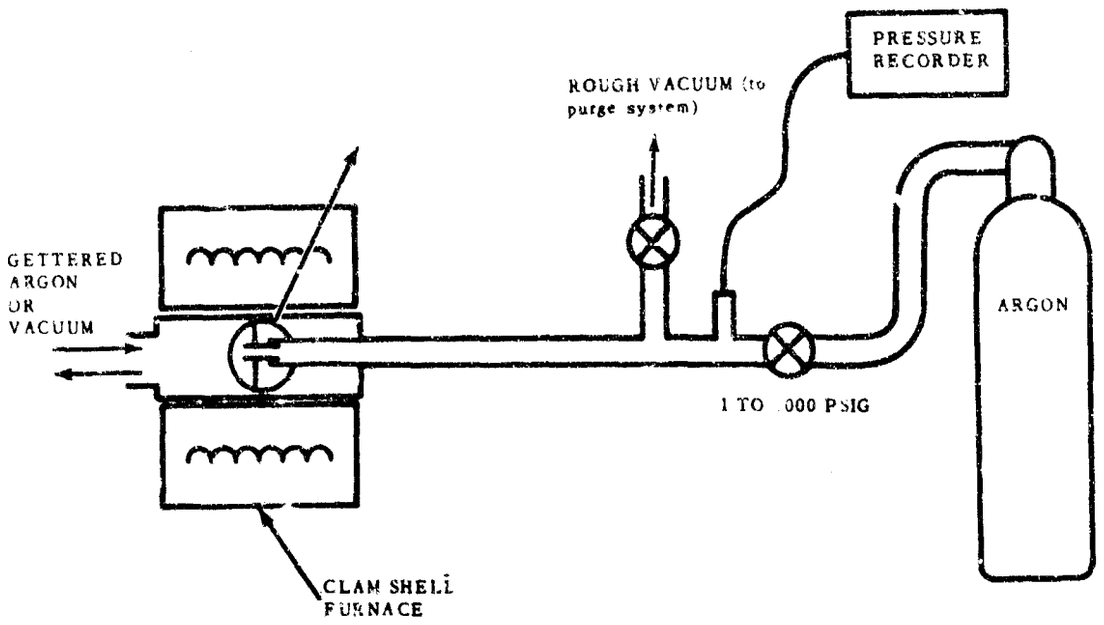


FIGURE 182. SWAGING LEAD-FILLED PLUG WITH PNEUMATIC HAMMER



① INCONEL 600

② N-155 TUBE, 0.375 BY 0.065



ALL DIMENSIONS IN INCH

FIGURE 183. PNEUMATIC EXPANSION PLUG DESIGN AND SYSTEM



As Machined

Welded to Pressure Tube

FIGURE 184.
PNEUMATIC EXPANSION PLUG

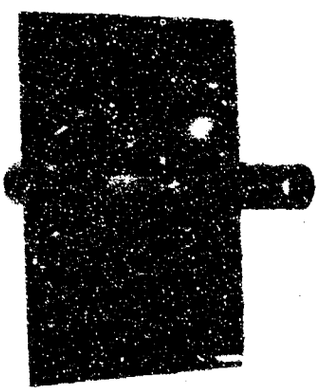


FIGURE 185.
TYPICAL TUBE AND HEADER
TEST SPECIMEN



FIGURE 186.
BEVELED EDGE OF HEADER
HOLE



FIGURE 187.

ASSEMBLING THE TUBE-HEADER JOINT

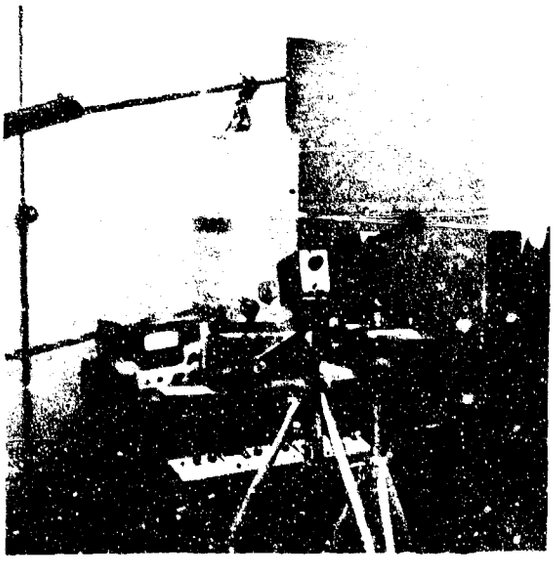


FIGURE 188.

VACUUM FURNACE AND CONTROLS USED FOR ELECTRICAL RESISTANCE HEATING OF EXPANSION PLUGS



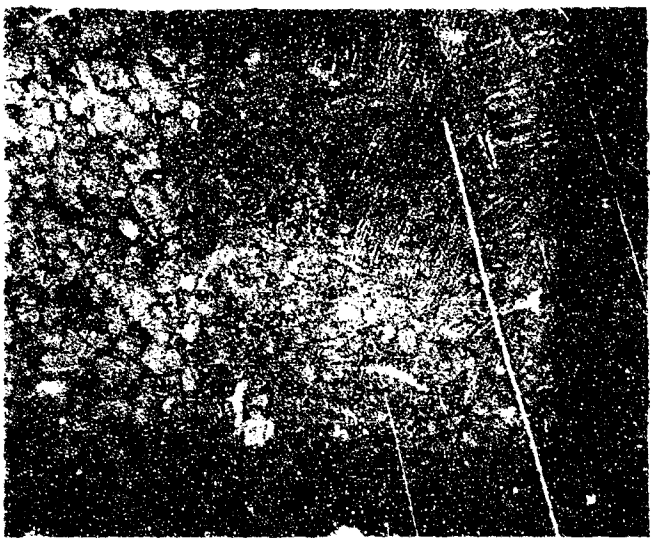
FIGURE 189.

EUTECTIC MELTING OF RESISTANCE-HEATED TUBE AND PLUG



FIGURE 190.

COLD-WALL VACUUM FURNACE



Etchant: Kroll's

Magnification: 400X

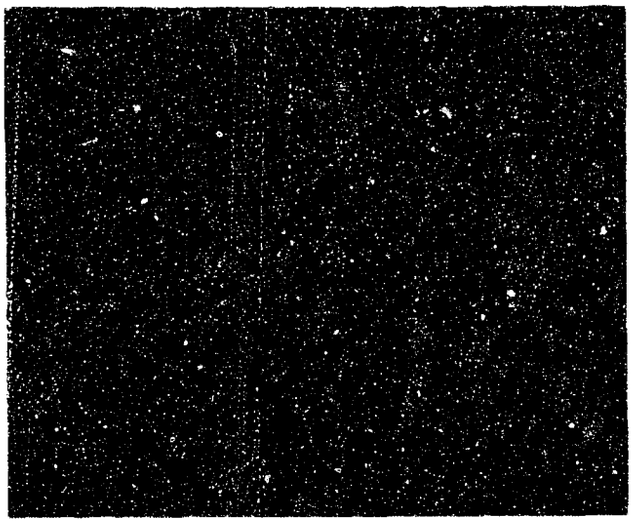
FIGURE 191.

TUBE-TO-HEADER JOINT PRODUCED IN SPECIMEN L4

Ti-6Al-4V Header

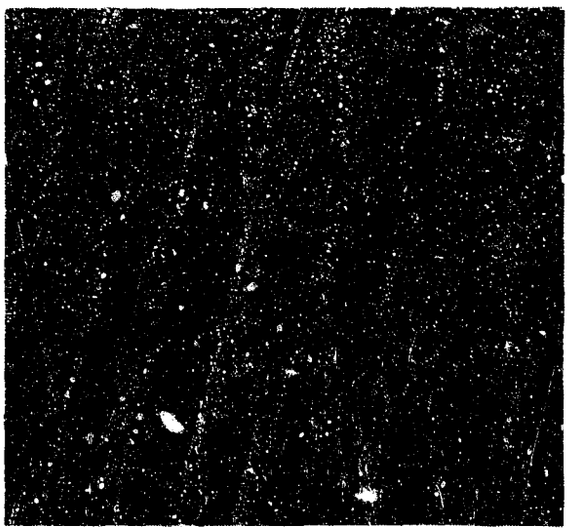
Ti-3Al-2.5Sn Tube

Type 1010 Steel Case of Lead-Filled Plug



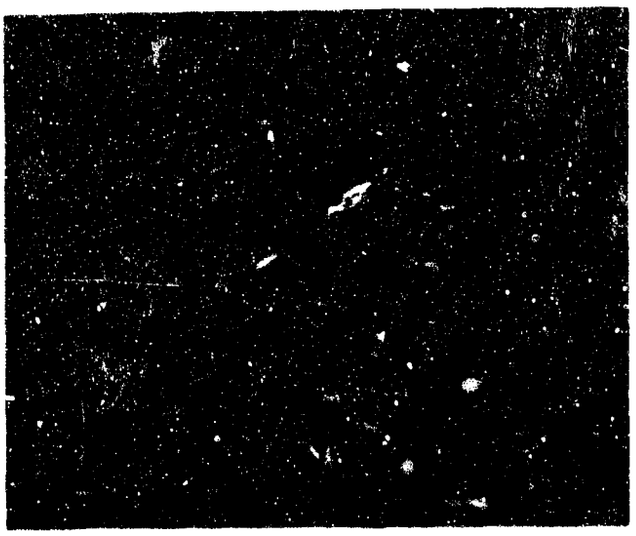
Bonding Temperature: 1650 F
Time: 30 min
Etchant: Kroll's
Magnification: 250X

FIGURE 192.
TUBE-TO-HEADER JOINT PRODUCED IN SPECIMEN L11



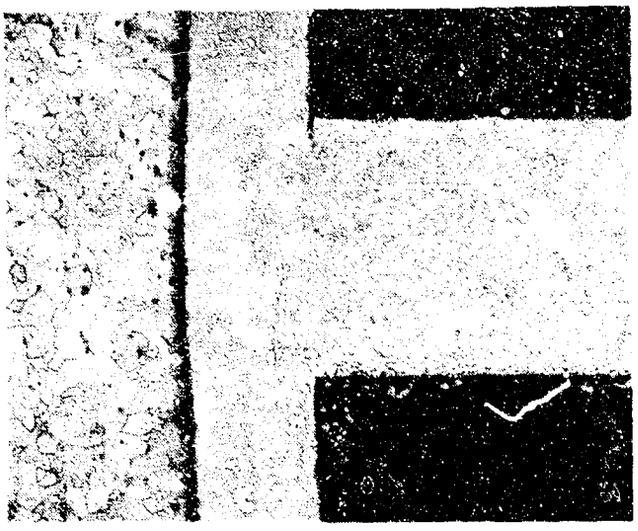
Bonding Temperature: 1650 F
Time: 90 min
Etchant: Kroll's
Magnification: 500X

FIGURE 193.
TUBE-TO-HEADER JOINT PRODUCED IN SPECIMEN L7



Bonding Temperature: 1650 F
Time: 30 min
Etchant: Kroll's
Magnification: 100X

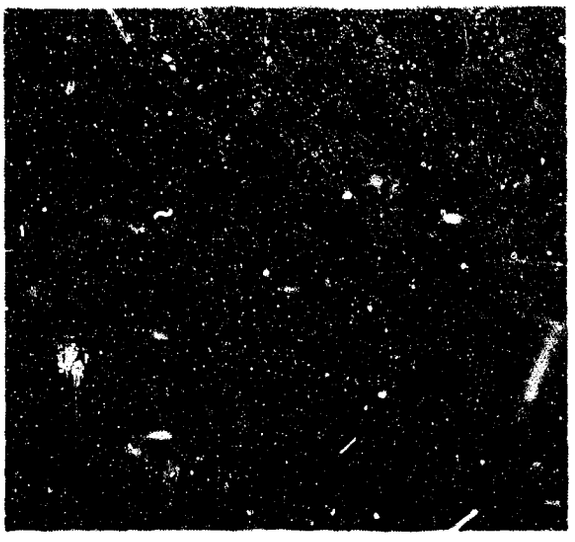
FIGURE 194.
TUBE-TO-HEADER JOINT PRODUCED IN SPECIMEN L10



Bonding Temperature: 1700 F
Time: 30 min
Etchant: Kroll's
Magnification: 100X

FIGURE 195.

TUBE-TO-HEADER JOINT PRODUCED IN SPECIMEN L9



Bonding Temperature: 1800 F
Time: 10 min
Etchant: Kroll's
Magnification: 500X

FIGURE 196.

TUBE-TO-HEADER JOINT PRODUCED IN SPECIMEN L8

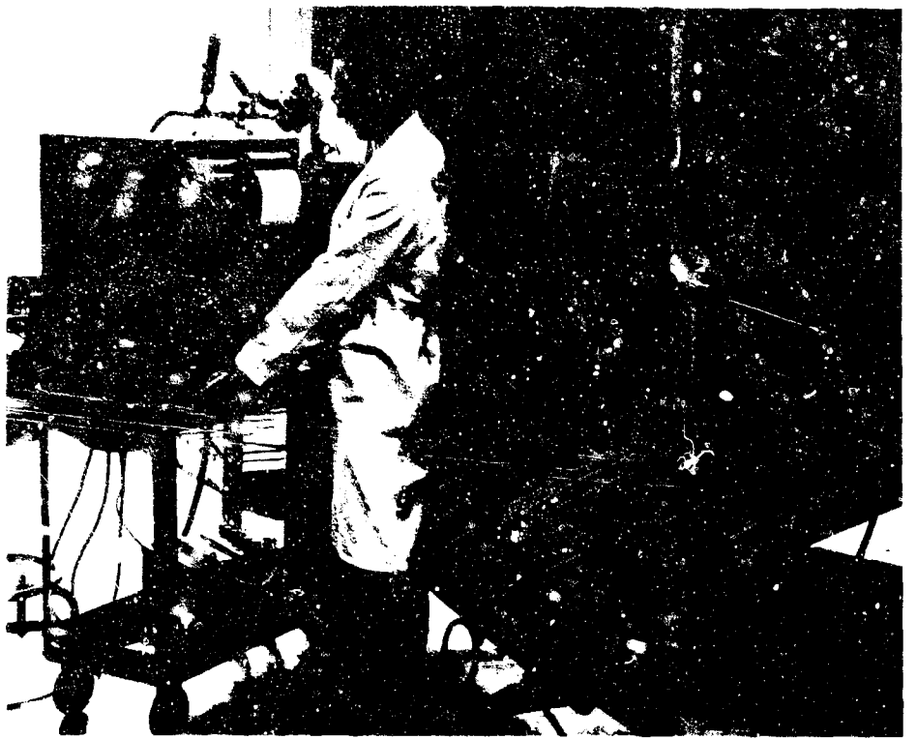


FIGURE 197. PNEUMATIC PRESSURIZATION EQUIPMENT

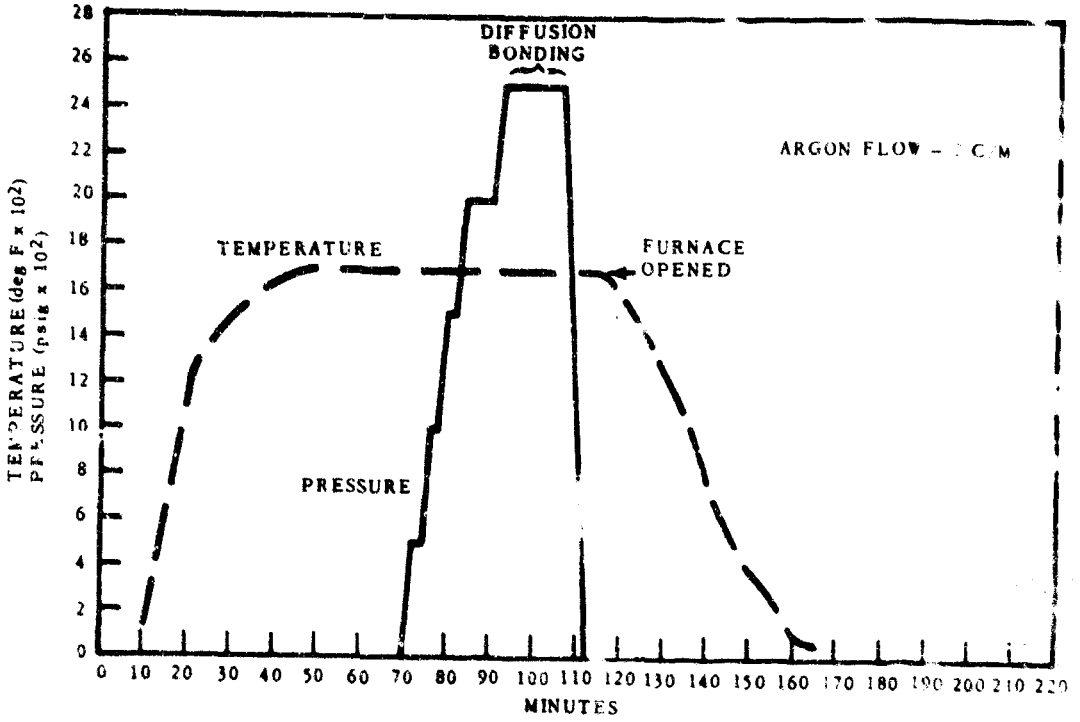


FIGURE 198. PNEUMATIC BONDING CYCLE OF SAMPLE P2; Pressure Applied and Released at Temperature

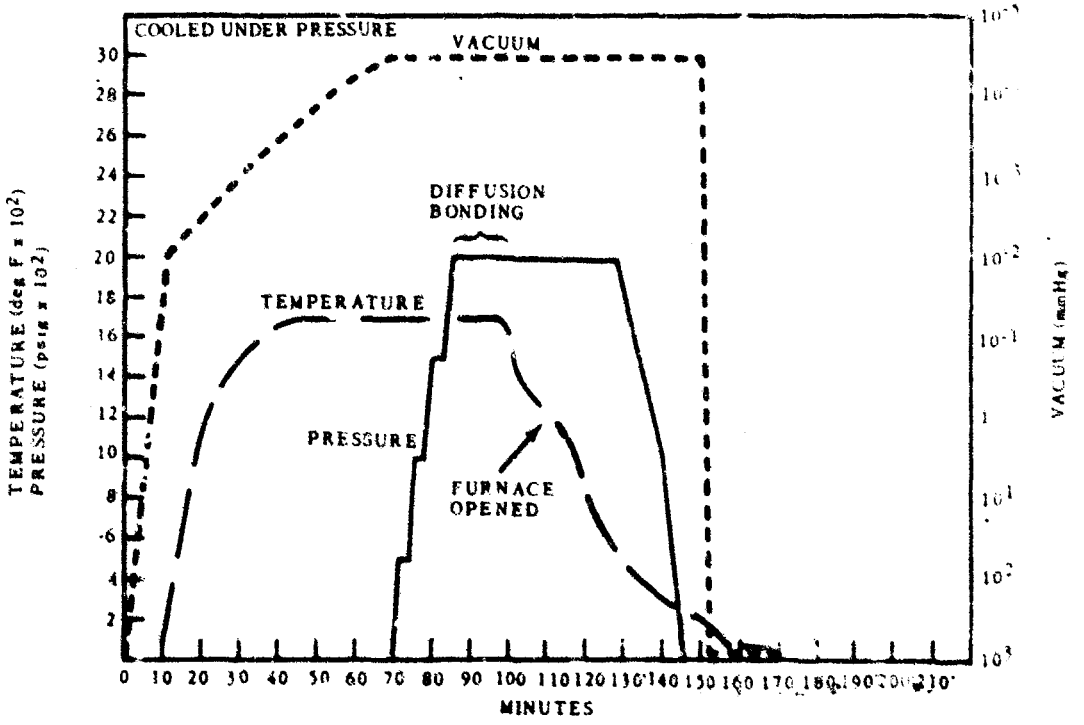


FIGURE 199. PNEUMATIC BONDING CYCLE OF SAMPLE P3, Cooled Under Pressure

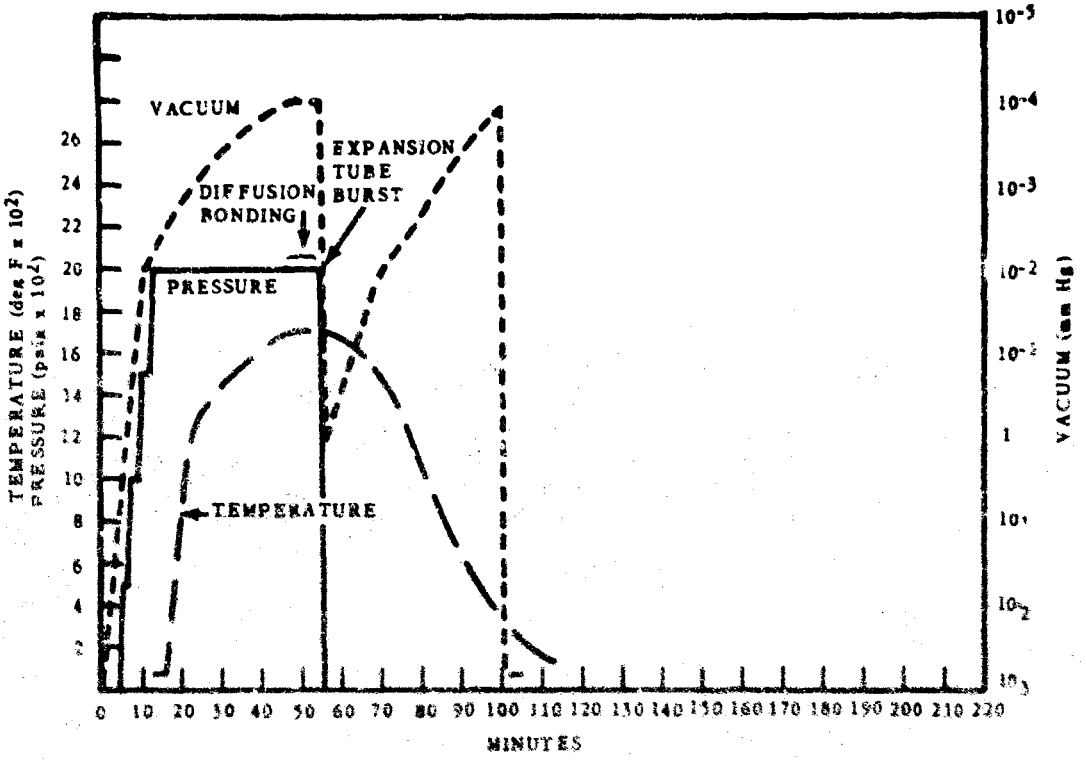
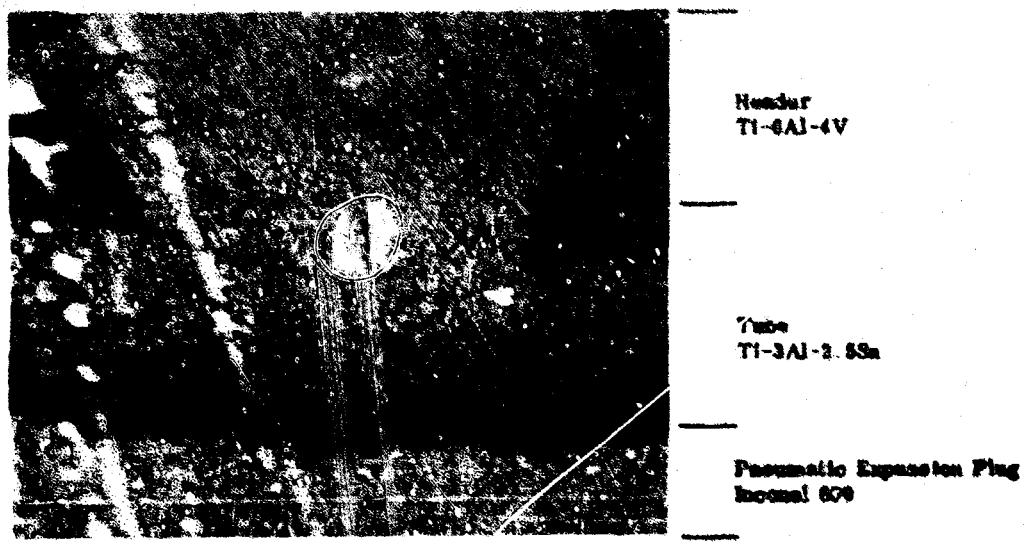


FIGURE 200. PNEUMATIC BONDING CYCLE OF SAMPLE P6, Heated Under Pressure



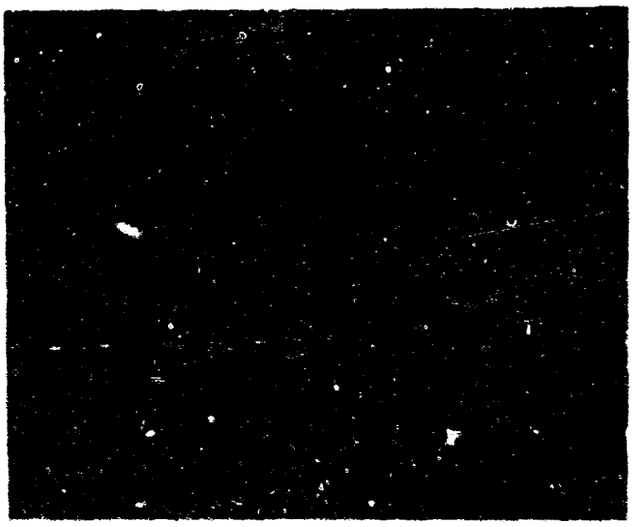
Etchant: Kroll's Magnification: 200X

FIGURE 201. DIFFUSION BOND PRODUCED IN SAMPLE P6 BY PNEUMATIC PRESSURIZATION



Bonding Temperature: 1675 F
Time: 5 min
Etchant: Kroll's
Magnification: 150X

FIGURE 202.
DIFFUSION BOND IN SPECIMEN P7



Bonding Temperature: 1675 F
Time: 5 min
Etchant: Kroll's
Magnification: 150X

FIGURE 203.
DIFFUSION BOND IN SPECIMEN P8



Bonding Temperature: 1675 F
Time: 5 min
Etchant: Kroll's
Magnification: 150X

FIGURE 204.
DIFFUSION BOND IN SPECIMEN P10